

Probing the Adaptation Strategies in the Genus *Xanthomonas*

by

Prabha Dhananjani Liyanapathirana

A dissertation submitted to the Graduate Faculty of
Auburn University
in partial fulfillment of the
requirements for the Degree of
Doctor of Philosophy

Auburn, Alabama
August 7, 2021

Keywords: Genus *Xanthomonas*, *Xanthomonas perforans*, type six secretion system,
epiphytic colonization, *tssM* and experimental evolution

Copyright 2021 by Prabha Dhananjani Liyanapathirana

Approved by

Neha Potnis, Chair, Assistant Professor, Department of Entomology and Plant Pathology
Leonardo De La Fuente, Professor, Department of Entomology and Plant Pathology
Jeffrey J. Coleman, Associate Professor, Department of Entomology and Plant Pathology
Paul Cobine, Professor, Department of Biological Sciences

Abstract

Bacterial species belonging to the genus *Xanthomonas* can infect and cause severe diseases in a wide range of host plants including many economically important crops throughout the world. While the majority of studies investigating the mechanistic basis of pathogenesis of *Xanthomonas* have broadly looked at the contribution of virulence factors towards successful apoplastic growth of the pathogen, mechanisms by which pathogens successfully adapts to the phyllosphere and maintains epiphytic asymptomatic colonization are understudied. Identification of these adaptation factors that contribute to host-pathogen interactions and understanding the evolutionary history and distribution patterns of the bacterial fitness determinants are important to predict the emergence of novel pathogens and mitigate proper disease management strategies. In this study, we explored the adaptation strategies in the genus *Xanthomonas*, using two approaches. As the first step, we studied the recently identified type VI secretion system for its role in crucial points of the *Xanthomonas* life cycle using bacterial leaf spot causing pathogen, *Xanthomonas perforans* as our model system. Findings from this study highlighted the contribution of functional T6SS-i3* towards early events of epiphytic colonization, adaptation in response to epiphytic stress and crucial stages of *Xanthomonas perforans* life cycle, that are considered to be important for mitigation of the pathogen. Since the role of the T6SS in the genus *Xanthomonas* has not been fully understood yet, we studied all the available *Xanthomonas* genomes to describe the evolutionary patterns and distribution of the T6 clusters across the genus. Our findings revealed a possible acquisition of the T6SS by group 2 *Xanthomonas* spp. through an ancient horizontal gene transfer event followed by subsequent losses of the clusters in some of the *Xanthomonas* spp., thus indicating a possible role of T6SS during niche adaptation onto various hosts as pathovars evolved. Furthermore, through bioinformatic analysis we were able to recognize several candidate T6SS-dependent effectors that are not limited to toxins, but rather an adaptation to the host

environment, avoiding host defenses and in nutrient acquisition. As the second step, towards understanding the adaptation strategies in the genus *Xanthomonas*, we conducted an experimental evolution study, using BLS causing *Xanthomonas perforans* as our model system. We were able to reveal a route of host range expansion in the Xp4B passaged on the non-host pepper plants via the loss of the hypersensitive response in resistant pepper variety. Additionally, our phenotypic analysis showed the importance of avoiding the repeated exposure of susceptible as well as resistant host plants to bacterial pathogen, due to the possibility of the emergence of more virulent or novel pathogenic races. Future works combining experimental evolution with genome sequencing will provide useful information that can lead to the identification of specific genetic changes that occurred during the continuous passaging. Overall, these findings provide useful insight into pathogen adaptation strategies, that were not well understood before and understanding these adaptive processes in pathogens are important in understanding risk of emergence of novel or virulent pathogens.

Keywords: Genus Xanthomonas, Xanthomonas perforans, type six secretion system, epiphytic colonization, tssM and experimental evolution

Acknowledgements

First and foremost, I would like to express my heartfelt appreciation and sincere gratitude to my major advisor, Dr. Neha Potnis for her priceless guidance, constant attention and inspiring encouragement throughout this time period. I am grateful to her for believing in me and being patient with me as I tested every possible limit. I would like to express my deepest appreciation to my committee members Dr. Leonardo De La Fuente, Dr. Jeffrey Coleman and Dr. Paul Cobine for their time and detailed feedback. Additionally, I would like to thank my university reader Dr. Timothy Bruce for his constructive suggestions and review of my dissertation. Many thanks to my lab members Dr. Eric Newberry, Rishi Bhandari, Shreya Sadhukhan, Destiny Brokaw, Auston Holland and Dr. Michelle Pena for continuous support, suggestions, encouragement and for a cherished time spent together in the lab. I am grateful for my parents, my sisters, brothers and in-laws whose constant love and encouragement keep me motivated. Without you believing in me, I never would have made it. Most importantly, I owe my deepest gratitude to my dear husband, Kumuditha Hikkaduwa Epa Liyanage, for all the sacrifices you have made in order for me to succeed. Last but not least, my warm and heartfelt thanks to my baby Sayul, for patiently staying next to me while I complete this dissertation. Thank you all for your unwavering support.

Table of Contents

1. CHAPTER ONE.....	2
Introduction	2
References	8
2. CHAPTER TWO.....	14
Type VI secretion system of <i>Xanthomonas perforans</i> contributes to asymptomatic epiphytic phase during pathogenesis on tomato.....	14
Abstract	14
Introduction	15
Materials and Methods	18
Bacterial strains, media and growth conditions.....	18
Plant material and growth conditions	19
Construction of the in-frame deletion mutant AL65 Δ tssM	19
Construction of AL65 Δ tssM complement	20
<i>In planta</i> population study – dip inoculation using individual strains and mixed inoculum	20
<i>In planta</i> population study – infiltration inoculation.....	22
Role of T6SS in <i>X. perforans</i> epiphytic survival under high-humidity conditions.....	22
Effect of T6SS on seed-to-seedling disease transmission	23
Growth of the bacterial strains under <i>in vitro</i> conditions	24
Results	25

Mutation in the <i>Xanthomonas perforans</i> T6SS-i3* core gene, <i>tssM</i> , results in increased virulence	25
Mixed infection does not provide a competitive advantage for the mutant over wild-type in terms of aggressiveness but rather leads to reduced disease severity when compared to individual infection with the mutant.....	26
Mutation in <i>tssM</i> does not contribute to the virulence of the pathogen when directly infiltrated into the apoplast.....	27
AL65Δ <i>tssM</i> displays lower epiphytic survival and reduced transmission compared to the wild type.	27
AL65Δ <i>tssM</i> is highly aggressive on seedlings eliciting more severe symptoms with higher population compared to the wild-type upon vertical transmission from seed to seedling.....	28
<i>X. perforans</i> wild-type exhibited a higher osmotolerance compared to the AL65Δ <i>tssM</i> .	28
Discussion	29
Conclusion.....	36
References	37
3. CHAPTER THREE	62
Phylogenetic distribution and evolution of Type VI secretion system in the genus <i>Xanthomonas</i>	62
Abstract	62
Introduction	63
Methodology	67
Construction of T6 core gene phylogenies	67

Splitstree analysis for homologous recombination visualization	68
Multi-locus sequence analysis	68
Construction of core genome phylogeny	69
Identification of T6SS clusters across genomes of <i>Xanthomonas</i>	69
Identification of T6 effectors	70
Results	70
Distribution of T6 clusters in the genus <i>Xanthomonas</i>	70
Evolutionary history of the i3* cluster in <i>Xanthomonas</i> spp.....	74
Comparison of the <i>Xanthomonas</i> T6 phylogeny to <i>Xanthomonas</i> multi-locus phylogeny	76
T6SS in non-pathogenic and environmental strains	78
Contribution of the T6SS for the evolutionary history of the <i>X. axonopodis</i> complex....	79
Determining the role of T6 effectors for the <i>X. axonopodis</i> complex host specificity.....	81
Discussion	82
Conclusion.....	93
References	94
4. CHAPTER FOUR	121
Investigating the phenotypic variations arising in experimentally passaged <i>Xanthomonas</i> <i>perforans</i> populations.....	121
Abstract	121
Introduction	121
Methodology	126

Bacterial Strains, Plant Material, and Growth Conditions	126
Serial passaging experiment- experimental procedure	127
Individual passages of Xp4B and XpPM1 on Tomato and pepper.....	127
Mixed passages of Xp4B+Xe85-10 and XpPM1+Xe75.3 on tomato and pepper.....	127
Growth chamber pathogenicity assay with 2 nd , 4 th and 6 th passages of Xp4B individual (600) and Xp4B +Xe85-10 (800) mixed passaged on pepper plants.....	129
Hypersensitive response (HR) assay	129
Host swapped experiment.....	130
Statistical analysis.....	130
Results	131
<i>X. perforans</i> 4B strain lost the HR in the resistant host (pepper cv.ECW) and expanded its host range to pepper, when serial passaged six times on pepper plants	131
<i>X. perforans</i> 4B strain shows ascending population density when continuously passaged on its non-host pepper plants, indicating possible host-expansion.....	132
<i>X. perforans</i> PM1 strain does not show a drastic change in the population density when continuously passaged on tomato and pepper plants.....	133
<i>X. perforans</i> 4B and <i>X. perforans</i> PM1 population change is unaffected by the mixed passages with the <i>X. euvesicatoria</i> sister strains	133
Pathogenicity assays reveal a significant decrease in the pathogenicity of Xp4B in tomato plants, when continuously passaged on pepper plants	133
Pathogenicity of XpPM1 is not affected by the serial passaging in tomato and pepper in the absence or presence of the sister strain Xe75.3	135
Discussion	135

Conclusion.....	140
References	141
5. CHAPTER FIVE	170
Summary and Future Directions	170

List of Tables

Table 2-1: Bacterial strains and plasmids used in this study.	46
Table 3-1: Analysis of T6 cluster distribution in genus <i>Xanthomonas</i>	106
Table 3-2: Comparison of T6SS-i3* cluster core genes in <i>Xe85-10</i> and early branching species, <i>X. translucens</i> F5 and identifying the closely related species to <i>X. translucens</i> F5 i3* cluster.....	107
Table 3-3: List of non-pathogenic strains used in the phylogenetic analysis.....	108
Table 3-4: Distribution of the i3* and i3*** clusters in the <i>X. axonopodis</i> complex.	109
Table 3-5: Distribution of the T6 clusters according to the lifestyle of <i>Xanthomonas</i> spp.	110
Table 4-1: Characteristics of the strains used in the experimental evolution study.....	147
Table 4-2: List of treatments in the passaging experiment	148
Table 4-3: List of treatments used in the host swapped experiment	149

List of Figures

Figure 1-1: Diversity of *Xanthomonas* spp. and lineages and their virulence genes. Phylogenetic distribution of *Xanthomonas* spp. based on the core alignment of 198,114 nucleotide sequences using the Roary pipeline (Page et al., 2015). Whole-genome sequences of type strains or completely sequenced genomes representing the *Xanthomonas* spp. available in the National Center for Biotechnology Information (NCBI) database were used for phylogenetic reconstruction. The presence of virulence-associated secretion systems (T3, T2 and T6SS) is shown. This figure was published in Nature Reviews Microbiology 18, no. 8 (2020): 415-427 (Timilsina, Sujan, Neha Potnis, Eric A. Newberry, Prabha Liyanapathiranaige, Fernanda Iruegas-Bocardo, Frank F. White, Erica M. Goss, and Jeffrey B. Jones. "Xanthomonas diversity, virulence and plant–pathogen interactions." Nature Reviews Microbiology 18, no. 8 (2020): 415-427 (Timilsina et al., 2020)..... 13

Figure 2-1: Arrangement of the trays inside the humidity chambers. (a) Chamber 1: Mixed inoculation of AL65^{strep} and AL65Δ*tssM*^{nal} (b) Chamber 2: Mixed inoculation of AL65Δ*tssM*^{nal} and AL65Δ*tssM*(*tssM*)^{km} 48

Figure 2-2: Disease symptom development 4 days after dip-inoculation..... 49

Figure 2-3: Effect of TssM on pathogenicity of *X. perforans* AL65. (a) bacterial population growth individual inoculation, right panel-area under the growth progress curve calculated for each strain growth in individual inoculation (b) bacterial population growth mixed inoculation AL65 + AL65Δ*tssM* , right panel- area under the growth progress curve calculated for each strain growth in mixed inoculation AL65 + AL65Δ*tssM* (c) bacterial population growth mixed inoculation AL65Δ*tssM*(*tssM*) + AL65Δ*tssM*, area under the growth progress curve calculated for each strain growth in mixed inoculation AL65Δ*tssM*(*tssM*) + AL65Δ*tssM* . 4-5-week-old tomato (cv. FL8000) plants inoculated with ~1x 10⁶ cfu/ml of AL65, AL65Δ*tssM* or AL65Δ*tssM*(*tssM*) strains were evaluated for bacterial population growth, every alternate day for 14 dpi on semi-selective media. log₁₀ cfu/cm² values were used to calculate AUGPC values for each corresponding treatment. Lines represent the standard error of the mean. A one-way ANOVA was applied for the statistical analysis of AUGPC and treatments

with different letters are significantly different according to Tukey's test of least significant difference (P<0.05). A one-way ANOVA was applied for the statistical analysis of bacterial population log₁₀ values and treatments with * marks are significantly different according to Tukey's test of least significant difference (P<0.05). 50

Figure 2-4: Effect of TssM on symptom development of *X. perforans* AL65. (a) Disease scale in individual inoculation (b) disease scale in mixed inoculations (c) tomato leaves 14 days after inoculation with each strain. 4-5-week-old tomato (cv. FL8000) plants inoculated with ~1x 10⁶ cfu/ml of AL65, AL65ΔtssM or AL65ΔtssM(tssM) strains were evaluated for disease development, every alternate day for 14 dpi. A one-way ANOVA was applied for the statistical analysis of disease index values on each sampling day separately and treatments with * marks are significantly different according to Tukey's test of least significant difference (P<0.05). 52

Figure 2-5: Effect of TssM on pathogenicity of *X. perforans* AL65 - Infiltration method (a) bacterial population growth (b) area under the growth progress curve calculated for each strain (C) tomato leaves 8 days after inoculation with each strain. A one-way ANOVA was applied for the statistical analysis of AUGPC and treatments with different letters are significantly different according to Tukey's test of least significant difference (P<0.05). A one-way ANOVA was applied for the statistical analysis of bacterial population log₁₀ values and disease severity values on each sampling day separately and treatments with * marks are significantly different according to Tukey's test of least significant difference (P<0.05). 54

Figure 2-6: *X. perforans* survival under high-humidity conditions. (a) bars represent the total population growth inside chamber 1 where AL65^{strep} and AL65ΔtssM^{nal} were mixed inoculated while lines represent the epiphytic population growth inside chamber 1 where AL65^{strep} and AL65ΔtssM^{nal} were mixed inoculated, (b) bars represent the total population growth inside chamber 2 where AL65ΔtssM^{nal} and AL65ΔtssM(tssM)^{km} were mixed inoculated while lines represent the epiphytic population growth inside chamber 2 where AL65ΔtssM^{nal} and AL65ΔtssM(tssM)^{km} were mixed inoculated. (c) Bars represent the total population growth inside chamber 1 where AL65^{strep} and AL65ΔtssM^{nal} were mixed inoculated while lines represent the epiphytic population growth inside chamber 1 where AL65^{strep} and AL65ΔtssM^{nal} were mixed inoculated 28 dpi. (d) Bars represent the total population growth inside

chamber 2 where AL65 Δ tssM^{nal} and AL65 Δ tssM(tssM)^{km} were mixed inoculated while lines represent the epiphytic population growth inside chamber 2 where AL65 Δ tssM^{nal} and AL65 Δ tssM(tssM)^{km} were mixed inoculated 28 dpi. Vertical lines represent the standard error of the mean. T-tests were done on AUGPC and log values on each sampling point separately and treatments with * marks are a significant difference (P<0.05). 57

Figure 2-7: *X. perforans* disease symptom development survival under high-humidity conditions. Percentage of plants that showed disease symptoms (a) inside chamber 1 where AL65^{strep} and AL65 Δ tssM^{nal} were mixed inoculated (b) inside chamber 2 where AL65 Δ tssM^{nal} and AL65 Δ tssM(tssM)^{km} were mixed inoculated. Surface plots were created to show the development of disease severity percentages of each sampling point during the course of the experiment. 59

Figure 2-8: Effect of TssM on seed-to-seedling disease transmission of *X. perforans* AL65 (A) bacterial population growth and (B) disease index in tomato (cv. FL8000) seedlings. Seeds were inoculated with ~1x 10⁶ cfu/ml of AL65, AL65 Δ tssM or AL65 Δ tssM(tssM) strains and seedlings were evaluated 21 days after planting. Bars with standard deviation represent the means of two independent experiments. A one-way ANOVA was applied for the statistical analysis and treatments with different letters are significantly different according to the Tukey’s test of least significant difference (P<0.05). 60

Figure 2-9: Bacterial population growth of AL65, AL65 Δ tssM and AL65 Δ tssM(tssM) strains in XVM2 media amended with different concentrations of NaCl (a) NaCl 0.02M (b) NaCl 0.1M (C) 0.2M NaCl. Lines represent the standard error of the mean. 61

Figure 3-1: Schematic representation of the two genomic T6SS loci (a) i3* and (b) i3*** in *Xanthomonas euvesicatoria* 85-10..... 111

Figure 3-2: Distribution of T6SS in pathogenic *Xanthomonas* spp. Phylogenetic distribution of 43 *Xanthomonas* spp. based on the core alignment of nucleotide sequences using the Roary pipeline (Page et al., 2015). Whole-genome sequences of type strains or completely sequenced genomes representing the *Xanthomonas* spp. available in the National Center for Biotechnology Information (NCBI) database were used for phylogenetic reconstruction. The presence of complete and partial T6 clusters (i3*, i3*** and i4) have shown with different colors in the figure. 112

Figure 3-3: Presence/absence of T6 clusters in genus *Xanthomonas*. Heat maps were generated with T6SS-i3*, i3*** and i4 cluster presence/ absence matrix data obtained from the automlsa pipeline. 113

Figure 3-4: Presence of T6 cluster i3* in *Xanthomonas* spp. with flanking regions. Phylogenetic distribution of 43 *Xanthomonas* spp. based on the core alignment of nucleotide sequences using the Roary pipeline and branch support was determined using 1000 bootstraps (Page et al., 2015). Whole-genome sequences of type strains or completely sequenced genomes representing the *Xanthomonas* spp. available in the National Center for Biotechnology Information (NCBI) database were used for phylogenetic reconstruction. Flanking regions of the T6 clusters were identified using the (IMG/M) (v.6.0) system and genome and microbiome datasets sequenced at DOE's Joint Genome Institute. Presence of all the core genes in the i3* cluster (Red), absence of one or more core genes in the i3* cluster (pink) or the absence of all the core genes (black) have been indicated with different colors and can be found in the middle of up and downstream genes. Genomic environments, similar (blue) and different (purple) genes found in the up and downstream of the T6SS-i3* cluster are represented with colors. Comparisons were done using the *X. vesicatoria* 85-10 as the reference strain. Size of the T6 i3* cluster is mentioned if the cluster is present or the number of CDS or the length of the DNA fragment (*) found in place of the i3* cluster has been included in the last column of the figure. 114

Figure 3-5: Relationship among 1577 *Xanthomonas* genomes. Multi-locus sequence analysis (MLSA) phylogeny of *Xanthomonas* spp. based on the concatenation of partial sequences of housekeeping genes *atpD*, *dnaK*, *efp*, *fusA*, *fyuA*, *gapA*, *glnA*, *gltA*, *gyrB*, *lacF*, *lepA* and *rpoD*. Phylogenetic tree in maximum likelihood (ML) criterion was developed using the IQ-TREE multicore version 2.1.2 COVID-edition and branch support was determined using 1000 bootstraps and 1000 SH-aLRT bootstrap replicates. 115

Figure 3-6: Distribution of T6 clusters in the genus *Xanthomonas*. T6 core gene phylogeny of *Xanthomonas* spp. based on the concatenation of T6 core genes (*tssA*, *tssB*, *tssC*, *tssD* (*hcp*), *tssE*, *tssF*, *tssG*, *tssH*, *tssI* (*vgrG*), *tssJ* (only in i4 cluster), *tssK*, *tssL* and *tssM*). (a) T6SS core gene phylogeny of i3***, i3* and i4 clusters including *hcp* and *vgrG* core genes (b) T6SS core gene phylogeny of i3***, i3* and i4 clusters in the absence of *hcp* and *vgrG* core genes. Phylogeny was generated using the automated multi-locus sequence analysis pipeline (automlsa2). Phylogenetic tree in maximum

likelihood (ML) criterion was developed using the IQ-TREE multicore version 2.1.2 COVID-edition and branch support was determined using 1000 bootstraps and 1000 SH-aLRT bootstrap replicates.

..... 116

Figure 3-7: Split decomposition tree of the selected *Xanthomonas* spp that showed incongruencies between MLSA phylogeny and (a) T6SS-i3* without *hcp* and *vgrG* (b) T6SS-i3*** without *hcp* and *vgrG*. The figure was drawn to scale using Splitstree4. The formation of parallel lines indicates conflicting phylogeny or possible recombination events..... 117

Figure 3-8: Comparison of the core genome phylogeny of *X. axonopodis* subspecies with T6 i3***/ i3* core genome phylogeny to T6SS-i3*/i3*** core gene phylogeny. (a) core gene phylogeny for the strains with i3*** (b) T6SS-i3*** phylogeny (c) core gene phylogeny for the strains with i3* (d) T6SS-i3* phylogeny. Core genome phylogenies were developed based on the core alignment of nucleotide sequences using the Roary pipeline (Page et al., 2015) while T6 phylogenies were generated using the automated multi-locus sequence analysis pipeline (automlsa2). Phylogenetic tree in maximum likelihood (ML) criterion was developed using the IQ-TREE multicore version 2.1.2 COVID-edition and branch support was determined using 1000 bootstraps and 1000 SH-aLRT bootstrap replicates.

..... 118

Figure 3-9: T6 effectors identified using the T6SS effectors using the Bastion6 machine-learning tool (Wang et al., 2018). T6 effectors identified in the (a) i3* cluster and (b) i3*** clusters of *X. axonopodis* subgroups..... 119

Figure 3-10: Organization of the T6SS-i3* clusters in BLS *Xanthomonas*. (a) *XpAL65* (b) *Xe85-10* and (c) *XvLMG911* 120

Figure 4-1: Experimental evolution scheme of *X. perforans* 4B strain through a serial passages experiment on host plant (tomato cv.FL47) and non-host (pepper cv.ECW) in either the presence or absence of closely related *X. euvesicatoria* 85-10 150

Figure 4-2: Experimental evolution scheme of *X. perforans* PM1 strain through a serial passages experiment on host plant (tomato cv.FL47) and non-host (pepper cv.ECW) in either the presence or absence of closely related *X. euvesicatoria* 75.3..... 151

Figure 4-3: Schematic diagram of the host swapped experiment. Pools of the bacterial strains (Xp4B alone on pepper and tomato, Xp4B together with *X. euvesicatoria* 85-10 on pepper and tomato, XpPM1 alone on pepper and tomato and XpPM1 together with *X. euvesicatoria* 75.3 on pepper and tomato) from the passages 0, 6, 10, 15 and 19 were used to inoculate on the original host they were serial passaged or in the swapped host. 152

Figure 4-4: In planta population assay conducted inside the growth chamber after passaging *X. perforans* 4B strain on pepper plants, up to six passages. Four to five weeks old pepper cv. ECW were infiltrated with $\sim 1 \times 10^5$ cfu/ml of bacterial pools taken from passages 2, 4 and 6. Strains were evaluated for bacterial population growth, on the day of inoculation, 4 days after inoculation and 8 days after inoculation on antibiotic (nalidixic) amended media. A one-way ANOVA was applied for the statistical analysis for each tested date and treatments with different letters are significantly different according to the Tukey's test of least significant difference ($P < 0.05$). 153

Figure 4-5: In planta population assay conducted inside the growth chamber after passaging *X. perforans* 4B strain together with *X. euvesicatoria* 85-10 on pepper plants, up to six passages. Four to five weeks old pepper cv. ECW were infiltrated with $\sim 1 \times 10^5$ cfu/ml of bacterial pools taken from passages 2, 4 and 6. Strains were evaluated for bacterial population growth, on the day of inoculation, 4 days after inoculation and 8 days after inoculation on antibiotic (nalidixic) amended media. A one-way ANOVA was applied for the statistical analysis for each tested date and treatments with different letters are significantly different according to the Tukey's test of least significant difference ($P < 0.05$). 154

Figure 4-6: High inoculum infiltrated spots were performed at 10^8 CFU/ml to show the loss of AvrBsT plasmid in the 6th passage of *X. perforans* 4B strain alone and together with *X. euvesicatoria* 85-10 on pepper plants (cv.ECW). Xp 4B ancestor strain and *X. perforans* 4B Δ avrBsT were also used in the assay to compare the symptom development. Plants were kept inside the growth chamber inside open-lid containers to check for the development of HR or water soaking and photographed 3 dpi. 155

Figure 4-7: Density ridgeline plots to visualize the changes in distributions, of population growth, over time in Xp4B strains passaged on (a) tomato and (b) pepper plants. Plots include the distribution of the

4B ancestor strain (Passage 0), Passage 6 and Passages 10-19 on tomato (cv.FL47) and pepper (cv.ECW) plants.....	156
Figure 4-8: Density ridgeline plots to visualize the changes in distributions, of population growth, over time in Xp4B strains passaged on (a) tomato and (b) pepper plants in the presence with <i>X. euvesicatoria</i> 85-10. Plots include the distribution of the 4B ancestor strain (Passage 0), Passage 6 and Passages 10-19 on tomato (cv.FL47) and pepper (cv.ECW) plants.	157
Figure 4-9: Density ridgeline plots to visualize the changes in distributions, of population growth, over time in XpPM1 strains passaged on (a) tomato and (b) pepper plants. Plots include the distribution of the XpPM1 ancestor strain (Passage 0), Passage 6 and Passages 10-19 on tomato (cv.FL47) and pepper (cv.ECW) plants.....	158
Figure 4-10: Density ridgeline plots to visualize the changes in distributions, of population growth, over time in XpPM1 strains passaged on (a) tomato and (b) pepper plants in the presence with <i>X. euvesicatoria</i> 75.3. Plots include the distribution of the XpPM1 ancestor strain (Passage 0), Passage 6 and Passages 10-19 on tomato (cv.FL47) and pepper (cv.ECW) plants.....	159
Figure 4-11: Boxplots to visualize the changes in distributions, of population growth, over time in Xp4B strains passaged on (a) tomato and (b) pepper plants individually and together with Xe85-10. Plots include the distribution of the 4B ancestor strain (Passage 0), Passage 6 and Passages 10-19 on pepper (cv.ECW) and tomato (cv.FL47). A two-way ANOVA was applied for each host for the statistical analysis and treatments with different letters are significantly different according to the Tukey's test of least significant difference ($P<0.05$).	160
Figure 4-12: Boxplots to visualize the changes in distributions, of population growth, over time in XpPM1 strains passaged on (a) tomato and (b) pepper plants individually and together with Xe75.3. Plots include the distribution of the PM1 ancestor strain (Passage 0), Passage 6 and Passages 10-19 on pepper (cv.ECW) and tomato (cv.FL47). A two-way ANOVA was applied for each host for the statistical analysis and treatments with different letters are significantly different according to the Tukey's test of least significant difference ($P<0.05$).	161
Figure 4-13: Comparison of population growth of Xp4B pools taken from the passages 0, 6, 10, 15 and 19. (a) originally passaged on tomato with Xp4B originally passaged on pepper when infiltrated to	

tomato plants (cv.FL47) and (b) Xp4B pools originally passaged on pepper with Xp4B originally passaged on tomato when infiltrated to pepper plants (cv.ECW). Four to five weeks old pepper and tomato plants were infiltrated with $\sim 1 \times 10^5$ cfu/ml of bacterial pools. Strains were evaluated for bacterial population growth, 6 days after inoculation on antibiotic (nalidixic) amended media. A two-way ANOVA was applied for the statistical analysis and treatments with different letters are significantly different according to the Tukey's test of least significant difference ($P < 0.05$). 162

Figure 4-14: Comparison of population growth of the Xp4B population growth when passaged together with Xe85-10. Xp4B pools taken from the passages 0, 6, 10, 15 and 19 (a) originally passaged on tomato with XpPM1 originally passaged on pepper when infiltrated to tomato plants (cv.FL47) and (b) Xp4B pools originally passaged on pepper with Xp4B originally passaged on tomato when infiltrated to pepper plants (cv.ECW). Four to five weeks old pepper and tomato plants were infiltrated with $\sim 1 \times 10^5$ cfu/ml of bacterial pools. Strains were evaluated for bacterial population growth, 6 days after inoculation on antibiotic (nalidixic) amended media A two-way ANOVA was applied for the statistical analysis and treatments with different letters are significantly different according to the Tukey's test of least significant difference ($P < 0.05$). 163

Figure 4-15: Comparison of population growth of XpPM1 pools taken from the passages 0, 6, 10, 15 and 19. (a) originally passaged on tomato with XpPM1 originally passaged on pepper when infiltrated to tomato plants (cv.FL47) and (b) XpPM1 pools originally passaged on pepper with XpPM1 originally passaged on tomato when infiltrated to pepper plants (cv.ECW). Four to five weeks old pepper and tomato plants were infiltrated with $\sim 1 \times 10^5$ cfu/ml of bacterial pools. Strains were evaluated for bacterial population growth, 6 days after inoculation on antibiotic (kanamycin) amended media. A two-way ANOVA was applied for the statistical analysis and treatments with different letters are significantly different according to the Tukey's test of least significant difference ($P < 0.05$). 164

Figure 4-16: Comparison of population growth of the XpPM1 population growth when passaged together with Xe75.3. XpPM1 pools taken from the passages 0, 6, 10, 15 and 19 (a) originally passaged on tomato with XpPM1 originally passaged on pepper when infiltrated to tomato plants (cv.FL47) and (b) XpPM1 pools originally passaged on pepper with XpPM1 originally passaged on tomato when infiltrated to pepper plants (cv.ECW). Four to five weeks old pepper and tomato plants were infiltrated

with $\sim 1 \times 10^5$ cfu/ml of bacterial pools. Strains were evaluated for bacterial population growth, 6 days after inoculation on antibiotic (kanamycin) amended media. A two-way ANOVA was applied for the statistical analysis and treatments with different letters are significantly different according to the Tukey's test of least significant difference ($P < 0.05$). 165

Supplementary figure 4-17: Changes of the bacterial population growth of Xp4B pools taken from the passages 0, 6, 10, 15 and 19. (a) passaged on tomato plants (cv.FL47) and (b) passaged on pepper plants (cv.ECW). Four to five weeks old pepper and tomato plants were infiltrated with $\sim 1 \times 10^5$ cfu/ml of bacterial pools. Strains were evaluated for bacterial population growth, 6 days after inoculation on antibiotic (nalidixic) amended media. A one-way ANOVA was applied for the statistical analysis and treatments with different letters are significantly different according to the Tukey's test of least significant difference ($P < 0.05$). 166

Supplementary figure 4-18: Changes of the Xp4B population growth when passaged together with Xe85.10. Xp4B pools taken from the passages 0, 6, 10, 15 and 19. (a) passaged on tomato plants (cv.FL47) and (b) passaged on pepper plants (cv.ECW). Four to five weeks old pepper and tomato plants were infiltrated with $\sim 1 \times 10^5$ cfu/ml of bacterial pools. Strains were evaluated for bacterial population growth, 6 days after inoculation on antibiotic (nalidixic) amended media. A one-way ANOVA was applied for the statistical analysis and treatments with different letters are significantly different according to the Tukey's test of least significant difference ($P < 0.05$). 167

Supplementary figure 4-19: Changes of the bacterial population growth of XpPM1 pools taken from the passages 0, 6, 10, 15 and 19. (a) passaged on tomato plants (cv.FL47) and (b) passaged on pepper plants (cv.ECW). Four to five weeks old pepper and tomato plants were infiltrated with $\sim 1 \times 10^5$ cfu/ml of bacterial pools. Strains were evaluated for bacterial population growth, 6 days after inoculation on antibiotic (kanamycin) amended media. A one-way ANOVA was applied for the statistical analysis and treatments with different letters are significantly different according to the Tukey's test of least significant difference ($P < 0.05$). 168

Supplementary figure 4-20: Changes of the XpPM1 population growth when passaged together with Xe75.3. XpPM1 pools taken from the passages 0, 6, 10, 15 and 19. (a) passaged on tomato plants (cv.FL47) and (b) passaged on pepper plants (cv.ECW). Four to five weeks old pepper and tomato

plants were infiltrated with $\sim 1 \times 10^5$ cfu/ml of bacterial pools. Strains were evaluated for bacterial population growth, 6 days after inoculation on antibiotic (kanamycin) amended media. A one-way ANOVA was applied for the statistical analysis and treatments with different letters are significantly different according to the Tukey's test of least significant difference ($P < 0.05$)..... 169

1. CHAPTER ONE

Introduction

Genus *Xanthomonas* is a large group constituted by plant associated Gram-negative bacteria. *Xanthomonas* name is made with two Greek words; “*Xantho*-yellow”, “*monas*-entity” and this yellow color is due to the presence of membrane-bound pigment xanthomonadin (Starr and Stephens, 1964). These obligate, aerobic bacteria in the genus *Xanthomonas* are generally rod shaped and consist with a single polar flagellum (An et al., 2020). Genus *Xanthomonas* is belonging to the family *Xanthomonadaceae*, which also includes other important genera such as *Xylella* and *Stenotrophomonas* (Bayer-Santos et al., 2019).

Members in the genus *Xanthomonas* are widespread plant pathogens especially in regions with a warm and humid climate, and cause disease in about 27 plant species, including approximately 400 hosts (124 monocotyledonous -11 families comprising at least 70 genera and 268 dicotyledonous plants -57 families comprising more than 170 genera) (Hayward, 1993; Büttner and Bonas, 2010; Ryan et al., 2011; An et al., 2020). *Xanthomonas* disease outbreaks have been reported from many parts of the world in multiple economically important crop plants such as rice, wheat, *Citrus* spp., crucifers, tomato, pepper, *Manihot esculenta* (cassava), banana and legumes (Ryan et al., 2011; Jacques et al., 2016; Timilsina et al., 2020). Even though the vast majority of the studies are frequently focusing on pathogenic *Xanthomonas* species, the genus *Xanthomonas* is also comprised of several nonpathogenic/environmental *Xanthomonas* strains, including some species that are highly distinct from known species (*X. sontii* and *X. maliensis*) and some species with both known pathogens and nonpathogenic plant associated strains (*X. arboricola*) (Vauterin et al., 1996; Bansal et al., 2020).

Due to the remarkable host and tissue specificities observed with the pathogenic *Xanthomonas* spp., species have been further divided into pathovars, that are defined by not

only the host range but also by tissue specificity (Jacques et al., 2016). For example, *X. oryzae* that are pathogenic on rice include, pv. *oryzae* which is a vascular pathogen that invades the xylem of the vascular system and nonvascular pv. *oryzicola* that invade intercellular spaces of the mesophyll parenchyma tissue of the host (Triplett et al., 2015).

These foliar plant pathogenic *Xanthomonas* spp. usually undergo different stages in the infection cycle including initial leaf surface colonization as epiphytes and invasion of the host intercellular space as endophytes (Lindow and Brandl, 2003). In *Xanthomonas* spp. epiphytic stage is the time between the introduction of the bacteria to the aerial tissues of the new host to the time bacteria enter into the host tissues. Even though the plant surface is a hostile environment for foliar pathogens due to the limited nutrient resources, water scarcity, exposure to severe radiation and competition from resident microflora, *Xanthomonas* spp. have shown the ability to survive as epiphytes for an extended time period from a few weeks to several months (Rigano et al., 2007; Zarei et al., 2018).

Xanthomonas can enter into the host tissue through either entering mesophyll parenchyma via stomata, or through hydathodes or wounds and spread systematically through the vascular system (Ryan et al., 2011). Endophytic stage of this bacterium starts, once the bacteria are inside the host plant. These hemi-biotrophic pathogens will initially feed on living host tissue, but in later infection stages, start the extensive colonization and cause the death of plant cells. Once the bacteria reach high population density inside the plant tissue, they will re-emerge into the leaf surface and get transmitted through wind or rain into a new host/ non-host and start the infection cycle again (Moreira et al., 2014). Even though contaminated seeds are considered as the main route of disease transmission, higher epiphytic *Xanthomonas* populations under high humidity conditions also considered as a significant source of inoculum for dispersal (Christiano et al., 2009; An et al., 2020). Under high humidity, while stomata and hydathodes are opened to maintain water homeostasis, it also provides the opportunity for

Xanthomonas to enter plant tissue and also for the exit of bacteria from the infected tissue (Zeng et al., 2010). *Xanthomonas* spp. can also survive outside of the host as saprophytes on weed plants, decaying organic matter and in the soil or water droplets which can act as a potential source of inoculum for *Xanthomonas* spp. (Gitaitis and Walcott, 2007).

Symptoms caused by *Xanthomonas* include water soaked spots on leaves, wilting, rotting, hypertrophy and hyperplasia and also die back and canker (Rudolph, 1993; Jacques et al., 2016). Despite the phenotypic uniformity, and economic and biological importance of the genus, *Xanthomonas* shows remarkable phylogenetic diversity and has undergone changes in nomenclature in the past 25 years and still under active debate (Timilsina et al., 2020). This genus has been subjected to many taxonomic studies based on conventional molecular techniques as well as recent whole-genome sequencing techniques and currently been categorized into 35 species and is subdivided into subspecies and pathovars (Timilsina et al., 2020). Recombination and horizontal gene transfer have been identified as the main driving forces behind the diversity in the genus *Xanthomonas* and several virulence factors have been identified as important elements for host specificity and bacterial pathogenicity in *Xanthomonas* spp. (Jacques et al., 2016; Timilsina et al., 2019, 2020). Secretion systems—mainly focusing on the T3SS and related effectors, adhesins, EPS, LPS, degradative enzymes, transcriptional factors and TonB-dependent receptors have been frequently described as important virulence factors in the genus *Xanthomonas* (Büttner and Bonas, 2010; Newberry et al., 2019; An et al., 2020; Timilsina et al., 2020).

Bacterial secretion systems are dedicated multiprotein complexes. They play an important role in the successful infection of the host plant, where it gives the ability to the bacteria to secrete protein and/or DNA into the extracellular milieu or directly into the eukaryotic and prokaryotic host cells host and manipulate the plant cellular process or interact

with the resident microflora. Process of transferring these proteins referred to as translocation and proteins that get translocated are designated as effector proteins (Büttner and Bonas, 2010).

With the availability of whole-genome sequence information from diverse *Xanthomonas* spp. and pathovars, heterogeneous distribution of six secretion systems (Systems I, II, III, IV, V and VI) have been described in the genus *Xanthomonas* (Alvarez-Martinez et al., 2020; Timilsina et al., 2020). According to the phylogenetic analysis based on core genome, two major groups are identified within the genus *Xanthomonas* as group 1 and group 2 and at least 5 clades have been identified within group 2 (Timilsina et al., 2020). In the genus *Xanthomonas*, T3SS is also known as the Hrp2 (hypersensitive response and pathogenicity) cluster and is considered the main secretion system responsible for the virulence. Majority of the group 2 *Xanthomonas* have acquired the Hrp2 cluster through a common ancestor (Merda et al., 2017), except for *X. campestris* pv. *campestris* that has independently acquired Hrp2 (Timilsina et al., 2020). Group 1 *Xanthomonas* spp. also have independently acquired the Hrp2 cluster and have an atypical T3SS except for *X. albilineans* which instead carries a SPI-1-family T3SS. Some *Xanthomonas* spp., including *X. cannabis* and nonpathogenic *X. sacchari* and *X. maliensis* are lacking T3SS and all T3 associated effectors (Büttner and Bonas, 2010; Merda et al., 2017; An et al., 2020). These T3 absent strains are scattered throughout the phylogeny and as Merda et al., 2017 have described, these strains might have acquired the Hrp2 cluster during evolution and might have followed a subsequent loss event while getting adapted into the hosts (Merda et al., 2017).

Two types of T2SS are found in the genus *Xanthomonas*: xps and xcs. While xps is conserved throughout the genus, the xcs cluster is also found in the strains belong to clade C, D and E strains and in most clade A and B strains, but is absent from *X. populi*, *X. fragariae* and *X. oryzae* strains. With the exception of *X. translucens*, the xcs cluster is absent from group 1 strains (Alvarez-Martinez et al., 2020; Timilsina et al., 2020). T2SS-xps is responsible for the

secretion of a range of effectors that are related to cell wall degradation activity, thereby directly influencing the virulence (Szczeny et al., 2010). T2SS is proposed to be aiding other secretion systems for the assembly of extracellular appendages such as the Hrp pilus from the T3SS, by initially degrading the plant cell wall (Lu et al., 2008) but also T2SS mediated cell wall degradation products can get recognized by the plant defense system and can lead for the activation of innate plant defense responses (Jha et al., 2007).

T6SS is the most recently identified secretion system in bacteria and was first described in two independent studies that identified a gene cluster responsible for virulence in animal pathogens *P. aeruginosa* and *V. cholerae* (Mougous, 2006; Pukatzki et al., 2006). T6SS are contact-dependent nanomachines that are found in around 25% of Gram-negative bacteria, mostly within the phylum Proteobacterium that includes both pathogenic and nonpathogenic bacteria and have been characterized for their role in injecting effectors into neighboring prokaryotic and eukaryotic cells and thereby provide competitive advantage for the bacteria in different environments (Boyer et al., 2009; Bernal et al., 2018). Random distribution of the three different types of complete and partial T6 clusters in different clades in the genus *Xanthomonas* indicating the importance of the T6SS in the genus *Xanthomonas*, yet few research studies have been conducted to characterize this system in *Xanthomonas* spp.

Among the major disease caused by the genus *Xanthomonas*, bacterial leaf spot of tomato (*Solanum lycopersicum*) and pepper (*Capsicum annuum*) is considered to be an atypical disease due to the ability of four distinct *Xanthomonas* species to cause this disease (Newberry et al., 2019). *X. euvesicatoria*, *X. perforans*, *X. vesicatoria* and *X. cynarae* pv. *gardneri* are the causal agents of the BLS disease (Jones et al., 2004; Timilsina et al., 2018) and these species have been identified in different geographic locations and have been identified to equipped with different mechanisms for pathogenesis (Potnis et al., 2011, 2015). *X. euvesicatoria* and *X. perforans* that have an average nucleotide identity (ANI) of >98%, are currently the

dominant pathogens of pepper and tomato in the southeastern US respectively while *X. cynarae* pv. *gardneri* and *X. vesicatoria* that are more distantly related have not been observed (Newberry et al., 2019). Extensive genetic exchange through recombination and plasmid transfer have been observed between *X. euvesicatoria* and *X. perforans* and related species that occupy the same niche, while recombination has been identified as the major factor that contributes to the diversification observed in BLS pathogen (Newberry et al., 2019; Timilsina et al., 2019). This diversity observed for the groups that cause BLS in tomato and pepper plants make this an excellent model system to study pathogen co-evolution on a common host (Potnis et al., 2011).

The major objective of this study is to understand the adaptation strategies of the genus *Xanthomonas* using BLS *Xanthomonas* as the model system and focusing mainly on identifying the function and distribution of the T6SS. This major objective was studied through focusing on the following specific objectives,

1. Identifying the role of T6SS in the BLS pathogen *Xanthomonas perforans* during different stages of its life cycle.
2. Identifying the phylogenetic distribution and evolution of T6SS in the genus *Xanthomonas*.
3. Investigating the phenotypic variations arising in an experimentally passaged pathogen population.

References

- Alvarez-Martinez, C. E., Sgro, G. G., Araujo, G. G., Paiva, M. R. N., Matsuyama, B. Y., Guzzo, C. R., et al. (2020). Secrete or perish: The role of secretion systems in *Xanthomonas* biology. *Comput Struct Biotechnol J* 19, 279–302. doi:10.1016/j.csbj.2020.12.020.
- An, S.-Q., Potnis, N., Dow, M., Vorhölter, F.-J., He, Y.-Q., Becker, A., et al. (2020). Mechanistic insights into host adaptation, virulence and epidemiology of the phytopathogen *Xanthomonas*. *FEMS Microbiology Reviews* 44, 1–32. doi:10.1093/femsre/fuz024.
- Bansal, K., Kumar, S., and Patil, P. B. (2020). Phylogenomic Insights into Diversity and Evolution of Nonpathogenic *Xanthomonas* Strains Associated with Citrus. *mSphere* 5. doi:10.1128/mSphere.00087-20.
- Bayer-Santos, E., Ceseti, L. de M., Farah, C. S., and Alvarez-Martinez, C. E. (2019). Distribution, Function and Regulation of Type 6 Secretion Systems of *Xanthomonadales*. *Front. Microbiol.* 10, 1635. doi:10.3389/fmicb.2019.01635.
- Bernal, P., Llamas, M. A., and Filloux, A. (2018). Type VI secretion systems in plant-associated bacteria. *Environ Microbiol* 20, 1–15. doi:10.1111/1462-2920.13956.
- Boyer, F., Fichant, G., Berthod, J., Vandenbrouck, Y., and Attree, I. (2009). Dissecting the bacterial type VI secretion system by a genome wide in silico analysis: what can be learned from available microbial genomic resources? *BMC Genomics* 10, 104. doi:10.1186/1471-2164-10-104.
- Büttner, D., and Bonas, U. (2010). Regulation and secretion of *Xanthomonas* virulence factors. *FEMS Microbiol Rev* 34, 107–133. doi:10.1111/j.1574-6976.2009.00192.x.
- Christiano, R. S. C., Dalla Pria, M., Jesus Junior, W. C., Amorim, L., and Bergamin Filho, A. (2009). Modelling the progress of Asiatic citrus canker on Tahiti lime in relation to temperature and leaf wetness. *Eur J Plant Pathol* 124, 1–7. doi:10.1007/s10658-008-9389-8.
- Gitaitis, R., and Walcott, R. (2007). The Epidemiology and Management of Seedborne Bacterial Diseases. *Annu. Rev. Phytopathol.* 45, 371–397. doi:10.1146/annurev.phyto.45.062806.094321.

- Hayward, A. C. (1993). “The hosts of *Xanthomonas*,” in *Xanthomonas*, eds. J. G. Swings and E. L. Civerolo (Dordrecht: Springer Netherlands), 1–119. doi:10.1007/978-94-011-1526-1_1.
- Jacques, M.-A., Arlat, M., Boulanger, A., Boureau, T., Carrère, S., Cesbron, S., et al. (2016). Using Ecology, Physiology, and Genomics to Understand Host Specificity in *Xanthomonas*. *Annual Review of Phytopathology* 54, 163–187. doi:10.1146/annurev-phyto-080615-100147.
- Jha, G., Rajeshwari, R., and Sonti, R. V. (2007). Functional Interplay Between Two *Xanthomonas oryzae* pv. *oryzae* Secretion Systems in Modulating Virulence on Rice. *MPMI* 20, 31–40. doi:10.1094/MPMI-20-0031.
- Jones, J. B., Lacy, G. H., Bouzar, H., Stall, R. E., and Schaad, N. W. (2004). Reclassification of the *Xanthomonads* Associated with Bacterial Spot Disease of Tomato and Pepper. *Systematic and Applied Microbiology* 27, 755–762. doi:10.1078/0723202042369884.
- Lindow, S. E., and Brandl, M. T. (2003). Microbiology of the Phyllosphere. *Appl. Environ. Microbiol.* 69, 1875–1883. doi:10.1128/AEM.69.4.1875-1883.2003.
- Lu, H., Patil, P., Sluys, M.-A. V., White, F. F., Ryan, R. P., Dow, J. M., et al. (2008). Acquisition and Evolution of Plant Pathogenesis–Associated Gene Clusters and Candidate Determinants of Tissue-Specificity in *Xanthomonas*. *PLOS ONE* 3, e3828. doi:10.1371/journal.pone.0003828.
- Merda, D., Briand, M., Bosis, E., Rousseau, C., Portier, P., Barret, M., et al. (2017). Ancestral acquisitions, gene flow and multiple evolutionary trajectories of the type three secretion system and effectors in *Xanthomonas* plant pathogens. *Molecular Ecology* 26, 5939–5952. doi:https://doi.org/10.1111/mec.14343.
- Moreira, L. M., Facincani, A. P., Ferreira, C. B., Ferreira, R. M., Ferro, M., Gozzo, F., et al. (2014). Chemotactic signal transduction and phosphate metabolism as adaptive strategies during citrus canker induction by *Xanthomonas citri*. *undefined*. Available at: /paper/Chemotactic-signal-transduction-and-phosphate-as-by-Moreira-Facincani/54b14404d1700e54b19aba2778e0809948030fa6 [Accessed May 24, 2021].

- Mougous, J. D. (2006). A Virulence Locus of *Pseudomonas aeruginosa* Encodes a Protein Secretion Apparatus. *Science* 312, 1526–1530. doi:10.1126/science.1128393.
- Newberry, E. A., Bhandari, R., Minsavage, G. V., Timilsina, S., Jibrin, M. O., Kemble, J., et al. (2019). Independent Evolution with the Gene Flux Originating from Multiple *Xanthomonas* Species Explains Genomic Heterogeneity in *Xanthomonas perforans*. *Appl. Environ. Microbiol.* 85. doi:10.1128/AEM.00885-19.
- Page, A. J., Cummins, C. A., Hunt, M., Wong, V. K., Reuter, S., Holden, M. T. G., et al. (2015). Roary: rapid large-scale prokaryote pan genome analysis. *Bioinformatics* 31, 3691–3693. doi:10.1093/bioinformatics/btv421.
- Potnis, N., Krasileva, K., Chow, V., Almeida, N. F., Patil, P. B., Ryan, R. P., et al. (2011). Comparative genomics reveals diversity among xanthomonads infecting tomato and pepper. *BMC Genomics* 12, 146. doi:10.1186/1471-2164-12-146.
- Potnis, N., Timilsina, S., Strayer, A., Shantharaj, D., Barak, J. D., Paret, M. L., et al. (2015). Bacterial spot of tomato and pepper: diverse *Xanthomonas* species with a wide variety of virulence factors posing a worldwide challenge. *Molecular Plant Pathology* 16, 907–920. doi:https://doi.org/10.1111/mpp.12244.
- Pukatzki, S., Ma, A. T., Sturtevant, D., Krastins, B., Sarracino, D., Nelson, W. C., et al. (2006). Identification of a conserved bacterial protein secretion system in *Vibrio cholerae* using the *Dictyostelium* host model system. *Proceedings of the National Academy of Sciences* 103, 1528–1533. doi:10.1073/pnas.0510322103.
- Rigano, L. A., Siciliano, F., Enrique, R., Sendín, L., Filippone, P., Torres, P. S., et al. (2007). Biofilm Formation, Epiphytic Fitness, and Canker Development in *Xanthomonas axonopodis* pv. *citri*. *MPMI* 20, 1222–1230. doi:10.1094/MPMI-20-10-1222.
- Rudolph, K. (1993). “Infection of the plant by *Xanthomonas*,” in *Xanthomonas*, eds. J. G. Swings and E. L. Civerolo (Dordrecht: Springer Netherlands), 193–264. doi:10.1007/978-94-011-1526-1_4.
- Ryan, R. P., Vorhölter, F.-J., Potnis, N., Jones, J. B., Van Sluys, M.-A., Bogdanove, A. J., et al. (2011). Pathogenomics of *Xanthomonas*: understanding bacterium–plant interactions. *Nature Reviews Microbiology* 9, 344–355. doi:10.1038/nrmicro2558.

- Starr, M. P., and Stephens, W. L. (1964). Pigmentation and Taxonomy of the Genus *Xanthomonas*. *Journal of Bacteriology* 87, 293–302.
- Szczesny, R., Jordan, M., Schramm, C., Schulz, S., Cogez, V., Bonas, U., et al. (2010). Functional characterization of the Xcs and Xps type II secretion systems from the plant pathogenic bacterium *Xanthomonas campestris* pv *vesicatoria*. *New Phytologist* 187, 983–1002. doi:<https://doi.org/10.1111/j.1469-8137.2010.03312.x>.
- Timilsina, S., Kara, S., Jacques, M. A., Potnis, N., Minsavage, G. V., Vallad, G. E., et al. Reclassification of *Xanthomonas gardneri* (ex Šutič 1957) Jones et al. 2006 as a later heterotypic synonym of *Xanthomonas cynarae* Trébaol et al. 2000 and description of *X. cynarae* pv. *cynarae* and *X. cynarae* pv. *gardneri* based on whole genome analyses. *International Journal of Systematic and Evolutionary Microbiology* 69, 343–349. doi:10.1099/ijsem.0.003104.
- Timilsina, S., Pereira-Martin, J. A., Minsavage, G. V., Iruegas-Bocardo, F., Abrahamian, P., Potnis, N., et al. (2019). Multiple Recombination Events Drive the Current Genetic Structure of *Xanthomonas perforans* in Florida. *Front. Microbiol.* 10. doi:10.3389/fmicb.2019.00448.
- Timilsina, S., Potnis, N., Newberry, E. A., Liyanapathirana, P., Iruegas-Bocardo, F., White, F. F., et al. (2020). *Xanthomonas* diversity, virulence and plant–pathogen interactions. *Nature Reviews Microbiology* 18, 415–427. doi:10.1038/s41579-020-0361-8.
- Triplett, L. R., Verdier, V., Campillo, T., Van Malderghem, C., Cleenwerck, I., Maes, M., et al. (2015). Characterization of a novel clade of *Xanthomonas* isolated from rice leaves in Mali and proposal of *Xanthomonas maliensis* sp. nov. *Antonie van Leeuwenhoek* 107, 869–881. doi:10.1007/s10482-015-0379-5.
- Vauterin, L., Yang, P., Alvarez, A., Takikawa, Y., Roth, D. A., Vidaver, A. K., et al. (1996). Identification of Non-Pathogenic *Xanthomonas* Strains Associated with Plants. *Systematic and Applied Microbiology* 19, 96–105. doi:10.1016/S0723-2020(96)80016-6.

- Zarei, S., Taghavi, S. M., Hamzehzarghani, H., Osdaghi, E., and Lamichhane, J. R. (2018). Epiphytic growth of *Xanthomonas arboricola* and *Xanthomonas citri* on non-host plants. *Plant Pathology* 67, 660–670. doi:10.1111/ppa.12769.
- Zeng, W., Melotto, M., and He, S. Y. (2010). Plant stomata: a checkpoint of host immunity and pathogen virulence. *Current Opinion in Biotechnology* 21, 599–603. doi:10.1016/j.copbio.2010.05.006.

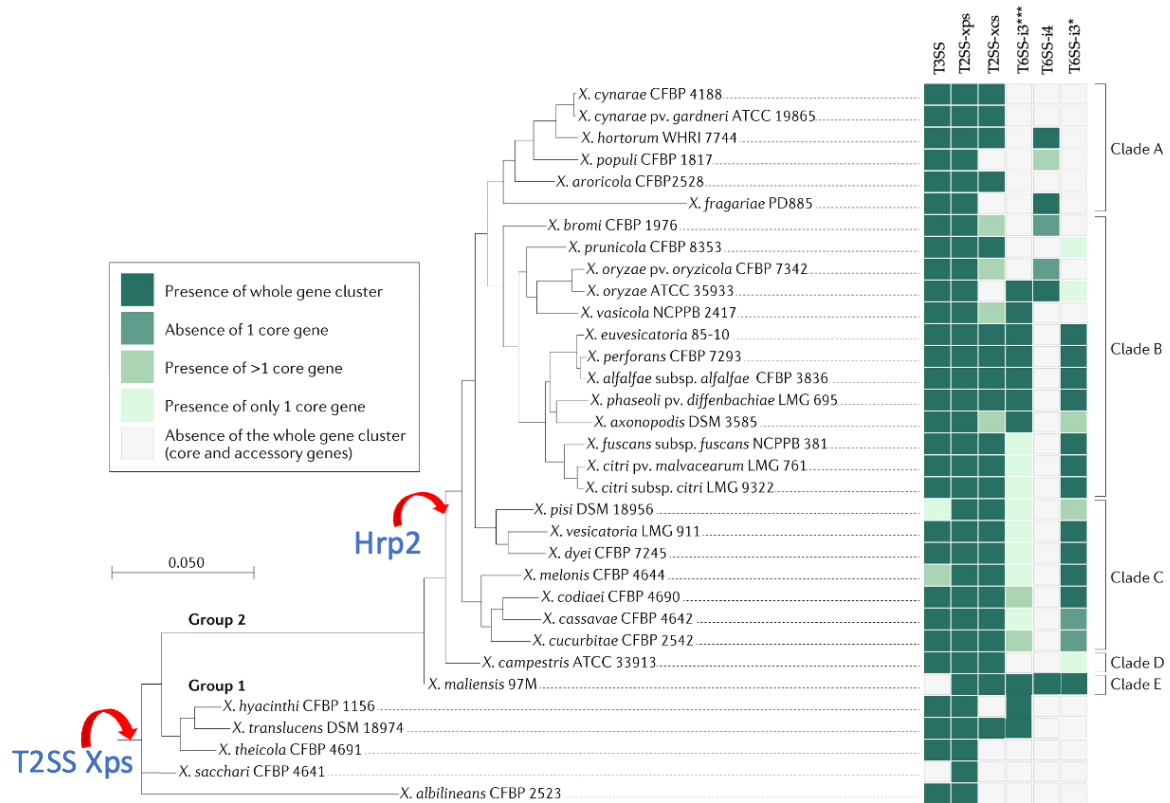


Figure 1-1: Diversity of *Xanthomonas* spp. and lineages and their virulence genes. Phylogenetic distribution of *Xanthomonas* spp. based on the core alignment of 198,114 nucleotide sequences using the Roary pipeline (Page et al., 2015). Whole-genome sequences of type strains or completely sequenced genomes representing the *Xanthomonas* spp. available in the National Center for Biotechnology Information (NCBI) database were used for phylogenetic reconstruction. The presence of virulence-associated secretion systems (T3, T2 and T6SS) is shown. This figure was published in Nature Reviews Microbiology 18, no. 8 (2020): 415-427 (Timilsina, Sujana, Neha Potnis, Eric A. Newberry, **Prabha Liyanapathirana**, Fernanda Iruegas-Bocardo, Frank F. White, Erica M. Goss, and Jeffrey B. Jones. "Xanthomonas diversity, virulence and plant-pathogen interactions." Nature Reviews Microbiology 18, no. 8 (2020): 415-427 (Timilsina et al., 2020).

2. CHAPTER TWO

Type VI secretion system of *Xanthomonas perforans* contributes to asymptomatic epiphytic phase during pathogenesis on tomato.

Abstract

Xanthomonas perforans is a seed-borne hemi-biotrophic pathogen that successfully establishes infection in the phyllosphere of tomato. While the majority of the studies investigating mechanistic basis of pathogenesis have focused on successful apoplastic growth, factors important during epiphytic colonization are not well understood. In this study, we show that type VI secretion system cluster *i3** (T6SS-*i3**) plays a significant role during initial asymptomatic epiphytic colonization at different stages during the life cycle of the pathogen. Mutation in a core gene, *tssM* of T6SS-*i3**, imparted higher aggressiveness to the pathogen, as indicated by higher overall disease severity, higher *in planta* growth as well as shorter latent infection period compared to the wild-type upon dip-inoculation of 4- to 5-week-old tomato plants. Contribution of T6SS-*i3** towards aggressiveness was evident during vertical transmission from seed-to-seedling with wild-type showing reduced disease severity as well as lower *in planta* populations on seedlings compared to the mutant. The role of T6SS-*i3** in maintaining asymptomatic colonization on seedlings was further confirmed in an experimental setup mimicking transplant house condition. Higher epiphytic population in presence of functional T6SS-*i3** was reflected in long-distance dispersal of the pathogen on asymptomatic transplants under high humidity conditions. We showed higher osmotolerance being one mechanism by which T6SS-*i3** confers higher epiphytic fitness. This study highlights the importance of T6SS-*i3** in overall fitness of the pathogen by dictating latent infection period as well as offering adaptive advantage at crucial stages of its life cycle, that are considered to be important for mitigation of the pathogen.

Introduction

Successful infection by bacterial plant pathogens is a result of a complex, multifaceted process mediated by multiple pathogenicity determinants that function across different stages of the infection, asymptomatic, pathogenic and dissemination phase. In case of foliar plant pathogens, adaptation to the phyllosphere environment and successful niche occupancy is a crucial phase during which pathogen successfully overcomes nutritional limitation, water limitation, host defense, competition with the resident microflora and environmental stress. This phase is followed by the pathogenic phase that involves successful apoplastic colonization, suppression of host defense and extensive multiplication. Equipped with the secretion systems that can facilitate the translocation of bacterial effectors outside of the cell membrane into the extracellular environment or directly into the host cell, phytopathogenic bacteria are able to establish successful infection. To date, 10 different secretion systems (systems I - X) have been identified in gram-negative bacteria (Palmer et al. 2020; Meuskens et al. 2019). While these secretion systems have been largely characterized for their importance during pathogenic phase, their role during the initial asymptomatic colonization is an unexplored area. Recent studies with *Pseudomonas syringae* have revealed genetic determinants that allow successful adaptation to an epiphytic vs apoplastic lifestyle of the pathogen. These determinants include genes involved in flagellar, swarming motility, chemosensing, chemotaxis, osmotolerance, and phenylalanine degradation being important for epiphytic colonization and can explain the response of a foliar pathogen to conditions experienced as an epiphyte (Helmann et al. 2019).

During *in planta* screening of a mariner transposon mutant library of *X. perforans* str. 91-118 (also referred to as *X. euvesicatoria* pv. *perforans*) by dip-inoculation of tomato, we identified a transposon mutant disrupting the *tssM* gene of a type VI secretion system cluster i3* (T6SS-i3*) that displayed more aggressive symptoms compared to the wild-type as well as

quicker symptom development. This observation led us to hypothesize that T6SS-i3* plays a role during the asymptomatic epiphytic phase.

T6SS was initially described as nodulation impairment locus (*imp*) in *Rhizobium leguminosarum* and later identified and characterized in *Vibrio cholerae* (Pukatzki et al. 2006) and *Pseudomonas aeruginosa* (Mougous 2006). The genes encoding T6SS are distributed in approximately 25% of the sequenced gram-negative bacteria, mainly in the phylum Proteobacteria including pathogenic, beneficial and commensal bacteria (Boyer et al. 2009; Durand et al. 2014). Among the bacterial species that have a T6SS encoded in their genome, many may contain 1-6 copies of complete T6SS clusters and many more copies of incomplete clusters of individual genes (Boyer et al. 2009). T6SS cluster assemblies have 13 core components, where at least 11 are structural proteins and two structural/ effector proteins (Hcp and VgrG) (Bingle et al. 2008). A subset of these core genes have evolutionary similarities to T4SS components or to bacteriophage and the whole system of T6SS shows structural and functional similarities to contractile bacteriophage cell puncturing device (Boyer et al. 2009; Cascales and Cambillau 2012). This contact-dependent nanomachinery can directly deliver secreted effectors or toxins into diverse neighboring cellular targets including both prokaryotic and eukaryotic organisms (Alcoforado Diniz et al. 2015). Each of these core components are essential for function, and inactivation of any of these 13 core components leads to significant defects in secretion. IcmF family TssM is one of the conserved proteins involved in the assembly of inner membrane-spanning complex of the T6SS that forms a hollow space to allow the inner tube and effectors to travel through. In *Agrobacterium tumefaciens*, TssM has ATP binding and hydrolysis ability to enable the secretion of the known T6 effector hemolysin-coregulated protein (Hcp) (Zoued et al. 2014; Ma et al. 2012). The electron microscopy of this inner membrane complex composed of TssJ, TssL and the important connector protein, TssM, in *E. coli* revealed that trans-envelope structure with double concentric ring like flexible

structure containing 10 TssM and 10 TssJ proteins bound to each other and with arches containing 10 TssL copies (Durand et al. 2015). TssM, being a connector between the inner and outer membrane, can explain how the mutation of the *tssM* (Type six secretion core gene M) inner membrane protein, aborts the secretion of the effector protein Hcp (hemolysin-coregulated protein) (Chow and Mazmanian 2010; Mattinen et al. 2008; Weber et al. 2013; Wang et al. 2021), hence indicating the importance of the uninterrupted core genes for the secretion of type 6 effectors. While known primarily for mediating competition with prokaryotes or unicellular eukaryotes (Ma et al. 2014, Bernal et al. 2018, Hsieh et al. 2019, Bayer-Santos et al. 2018), T6SS has been shown to be important in virulence (Ge et al. 2008; Weber et al. 2013; Shalom et al. 2007), host colonization (Pezoa et al. 2014; de Pace et al. 2011) and intracellular multiplication (Chow and Mazmanian 2010; Parsons and Heffron 2005). In the case of plant pathogenic bacteria, mutation of the T6SS core gene has been associated primarily with impaired virulence as seen with *Agrobacterium tumefaciens* (Wu et al. 2008), *Pseudomonas syringae* pv. *actinidiae*, *Ralstonia solanacearum*, *Erwinia amylovora*, *Xanthomonas oryzae* pv. *oryzae* and *Burkholderia glumae* BGR1 (Zhang et al. 2012; Tian et al. 2017; Wang et al. 2021; Choi et al. 2020; Kim et al. 2020) or not required for full pathogenicity (Montenegro Benavides et al. 2021). Recent research work on *in planta* colonization of rice endophyte *Kosakonia* has reported a significant decrease in rhizoplane and root endosphere colonization by T6SS mutant of *Kosakonia* sp. K0348 (Mosquito et al. 2020)

The role of T6SS appears to be varying depending on the bacterial species, host species and host tissue also the distribution of the T6SS among the commensal as well as phytopathogenic bacteria suggests that the role of T6SS is beyond virulence (Bernal et al. 2018). Potnis et al, described the distribution of the T6SS clusters in bacterial leaf spot *Xanthomonas* spp. where two types of T6SS clusters (type i3*** and i3*) were identified in *X. perforans* and *X. euvesicatoria*, type i3* T6SS cluster in *X. vesicatoria* and no T6SS cluster in

X. gardneri (Potnis et al. 2011). In this study, given our observation of impairment of T6SS resulting in earlier symptom development and increased disease aggressiveness led us to investigate the contribution of T6SS-i3* towards epiphytic phase of pathogen life cycle. We examined crucial points of the bacterial leaf spot *Xanthomonas* life cycle, seed-to-seedling, seedlings at the transplant houses and leaf surfaces of mature plants, which are often control points for disease management. However, these are also control points at which failure of current management practices is noted, likely due to ability of pathogen to maintain asymptomatic colonization. Our findings demonstrate that functional T6SS-i3* contributes towards early events of epiphytic colonization and adaptation in response to epiphytic stress. This asymptomatic colonization in transplants allows successful transmission avoiding artificial selection. Delayed symptom development allows hemi-biotrophic *X. perforans* to prolong its association with the host while minimizing overall disease severity.

Materials and Methods

Bacterial strains, media and growth conditions

Bacterial strains and plasmids used in this study are listed in Table 1. *Xanthomonas perforans* was grown for 24h at 28°C on Nutrient agar (NA) (Difco) and *E.coli* was cultivated in Luria-Bertani (LB) agar or broth at 37°C (Miller 1972). When required antibiotics were added into the media to maintain selection for resistance markers at following working concentration: kanamycin (Km), 50µg/ml; nalidixic (Nal), 50 µg/ml; streptomycin (Strep), 50 µg/ml; rifampicin (Rif), 50 µg/ml, spectinomycin (Spec) 100 µg/ml, tetracycline (Tet) 12.5 µg/ml. All the strains were stored in sterile tap water at room temperature or in 30% glycerol at -80°C or both. Triparental matings were performed on nutrient yeast extract glycerol agar (NYGA) (Turner et al. 1984).

Plant material and growth conditions

Tomato cultivar FL8000 was used in this study. Two weeks old seedlings were transplanted into sterile 4" plastic pots (The HC Companies, OH, USA) with soil-less potting medium (Premier Tech Horticulture, PA, USA). Plants were kept under 16h light per day at 28-30°C under greenhouse conditions up to 4- to 5-week-old.

Construction of the in-frame deletion mutant AL65 Δ *tssM*

X. perforans AL65 strain, isolated from symptomatic pepper plants in Alabama in 2017, was chosen to construct a null mutant since this strain was pathogenic on both tomato and pepper (Newberry et al. 2019), in addition to this strain being recently isolated and comparatively aggressive in relation to other *X. perforans* strains such as *Xp91-118* (data not shown). A 900 bp promoter fragment upstream of the *tssM* (locus tag XPE_14105) ORF (up) (tssMupF-TTGCAGGCGCGTTTGAAC, tssMupR-CTTGCGTAGCAACTGGATCG) and 852bp fragment downstream of the *tssM* ORF (down) (tssMdownF-ATATCGAAGGCCAGCGCTA, tssMdownR- AGATACATCTGGGCGGTGG) were PCR amplified using taq polymerase (Thermo Scientific) according to the manufacturer's instructions. Both of these fragments were individually cloned into pCRTM8/GW/TOPO® (Invitrogen) vector with *attL1/ attL2* sites. Primer sets, M13F/SR (M13F-GTAAAACGACGGCCAG, SR- CGTGCGCCGGCATGCCGTCATTCCCCAGGC) and SF/M13R (SF- GCCTGGGGAATGACGGCATGCCGGCGCACG, M13R-CAGGAAACAGCTATGAC) were used to amplify the upstream and downstream fragments in parallel with the short overlapping ends. Gel purified PCR fragments from the previous parallel reactions were fused together through a single overlap extension PCR reaction. PCR cycling parameters were designed according to the Phusion DNA polymerase guidelines (User Guide: Phusion High-Fidelity DNA Polymerase). Resulting 1100 bp overlapping fragment, representing Δ *tssM* with flanking upstream and downstream regions and the *attL1/attL2* sites

was cloned into pCR™-Blunt II-TOPO. Next, 1100 bp $\Delta tssM$ fragment in pCR™-Blunt II-TOPO was recombined into the suicide vector pLVC18-Rfc (obtained from Mudgett's Lab) by a Gateway LR reaction (Invitrogen) (Atanassov et al. 2009). pLVC18-Rfc ($\Delta tssM$) was moved into AL65 by triparental mating, using *E. coli* helper strain containing pRK2073 plasmid. Single crossover events were selected by growth on NYGA media containing Rif and Tet antibiotics. SacB counter-selectable marker was used to select for a second crossover event by plating previously selected colonies on NYGA media containing 5% sucrose. Several subcultures were conducted to identify the deletion mutants generated through homologous recombination. Strains were selected for growth on NA containing Rif and for loss of growth on NA containing Tet (12.5 ug/ml). A deletion mutant AL65 $\Delta tssM$ was confirmed by PCR using gene specific primers followed by sequence analysis as well as using whole genome sequencing followed by sequence analysis.

Construction of AL65 $\Delta tssM$ complement

Genomic region containing *tssM* promoter (900 bp upstream of the ORF), the *tssM* ORF (4593 bp) and 852 bp downstream of the ORF was PCR amplified from *Xp*AL65 using *tssM*upF and *tssM*downR primers. This DNA fragment (6345 bp) was cloned into expression vector pDSK519. The resulting construct pDSK519 (*tssM*) was introduced into the AL65 $\Delta tssM$ mutant by electroporation (1.8kV/4ms). Complement (AL65 $\Delta tssM$ (*tssM*)) was confirmed by PCR, DNA sequencing and whole-genome sequencing.

***In planta* population study – dip inoculation using individual strains and mixed inoculum**

To determine the role of T6SS in *X. perforans* pathogenicity, 4- to 5-week-old tomato cv. FL8000 plants were dip inoculated (30s) in 600 ml cell suspensions containing $\sim 1 \times 10^6$ cfu/ml of *X. perforans* AL65^{strep}/ AL65 $\Delta tssM$ ^{nal}/ AL65 $\Delta tssM$ (*tssM*)^{km} alone or AL65^{strep} + AL65 $\Delta tssM$ ^{nal} / AL65 $\Delta tssM$ ^{nal} + AL65 $\Delta tssM$ (*tssM*)^{km} mixed in 1: 1 ratio for the mix inoculation study. Inoculum suspensions were amended with 0.0025% (vol/vol) Silwet 77.

Both individual and mixed inoculations were conducted simultaneously so the overall disease severity levels can be compared in individual vs mixed inoculations. Plants dipped in sterile MgSO₄ amended with 0.0025% (vol/vol) Silwet 77 were used as negative controls. The initial inocula were plated onto NA amended with antibiotics to confirm a 1:1 ratio of wild-type and mutant concentrations and complement and mutant concentrations. Wild-type to mutant and complement to mutant initial ratios should be close to one (Macho et al. 2007; Macho et al. 2010). Inoculated plants were placed inside closed boxes and kept in a growth chamber at 25°C with 12h light/dark cycle for 2 days after inoculation to facilitate high humidity. After the initial 48h plants were maintained at high humidity for 12 hours in the dark and at low humidity for 12 hours in light. Middle leaflet samples were taken at every alternate day for 14 days and *in planta* bacterial populations were determined. At each sampling point, ~ 3 cm² area of leaflet tissues were taken from each plant using a sterile cork borer. Using sterile forceps leaf discs were placed inside sterile microcentrifuge tubes containing 1 ml sterile MgSO₄ buffer and macerated using a sterile homogenizer. Ten-fold serial dilutions of the homogenized suspension were plated on antibiotic-amended plates using spiral plater (Neu-tec Group Inc, NY, USA) to estimate the population size of AL65, AL65Δ*tssM*, and AL65Δ*tssM*(*tssM*) in individual inoculations and mixed inoculations. Plates were kept at 28°C for 3 days before quantifying the colony counts. Bacterial populations were determined as colony forming units (cfu) per cm² of leaf area. Bacterial spot severity was recorded using the following scale and mean disease severity was calculated.

Disease scale: 1 = symptomless, 2 = a few necrotic spots on a few leaflets, 3 = a few necrotic spots on many leaflets, 4 = many spots with coalescence on few leaflets, 5 = many spots with coalescence on many leaflets, 6= severe disease and leaf defoliation, and 7= plant dead (Abbasi et al. 2002). This experiment was repeated three times and each treatment

consisted of three replicates and results of a single representative experiment is shown the results section.

Plots of \log_{10} cfu/cm² against time were generated and used to calculate the area under the growth progress curve (AUGPC) using the following formula.

$$\text{AUGPC} = \sum_{i=1}^{n-1} [(Y_{i+1} + Y_i)/2] (X_{i+1} - X_i)$$

Y_i = bacterial population at the i^{th} observation, X_i = time in hours at the i^{th} observation, and n = the total number of observations (Dutta et al. 2014a, 2014b).

***In planta* population study – infiltration inoculation**

Four- to five-week-old tomato cv. FL8000 plants were inoculated with cell suspensions containing $\sim 1 \times 10^5$ cfu/ml of *X. perforans* AL65^{strep}/ AL65 Δ tssM^{nal}/ AL65 Δ tssM(*tssM*)^{km} using a needleless syringe. Plants infiltrated with sterile MgSO₄ were used as negative controls. Inoculated plants were kept in a growth chamber at 25°C with 12h light/dark cycle for 8 days after inoculation. Middle leaflet samples were taken at every alternate day for 8 days and *in planta* bacterial populations were determined as described in the previous section.

Role of T6SS in *X. perforans* epiphytic survival under high-humidity conditions

Humidity chambers were constructed in the greenhouse to mimic conditions inside a seedling transplant house that facilitates conditions conducive for BLS disease development. Each humidity chamber frame was built with PVC pipes and covered with transparent polythene sheets from all sides. Inside each chamber, high relative humidity was maintained by using a sprinkler irrigation system providing overhead irrigation (set to water at 0800 and 1800 h for 1 minute on each occasion each day). As shown in the figure 2-1, six 128-cell trays with two-weeks old seedlings were arranged inside a single chamber. Plants were fertigated two weeks after sowing and every week after that until the end of the trial. To investigate the

role of T6SS on disease transmission, two weeks old tomato cv FL8000 seedlings from the first row of the trays were inoculated with a 1: 1 mixed inoculum of AL65^{step} and AL65 Δ tssM^{nal} or AL65 Δ tssM^{nal} and AL65 Δ tssM(tssM)^{km} at 10⁶ cfu/ml concentration. The leaflets were sampled at 9 sampling points (as shown in figure 2-1) for estimating epiphytic and total population of wild-type, mutant and complement on day 7, 14 and 21 post-inoculation. For estimating epiphytic population, leaf washings were serially diluted and plated on antibiotics amended media using spiral plater (Neu-tec Group Inc, NY, USA). For estimating total population, sampled leaflets were macerated and the homogenate was plated upon serial dilutions on antibiotics amended media. At each sampling point, at each sampling time, the number of tomato seedling that showed BLS symptoms were recorded to calculate proportion infected/symptomless to correlate that to the population of each strain found in different sampling points (Dutta et al. 2014a). Plots of log₁₀ cfu/g against time were generated and used to calculate the area under the growth progress curve (AUGPC) (Dutta et al. 2014a, 2014b). The experiment was repeated at least three times and results of a single representative experiment is shown the results section.

Effect of T6SS on seed-to-seedling disease transmission

To determine the role of T6SS on seed-to-seedling disease transmission, tomato cv. FL8000 seeds were inoculated by immersion in individual cell suspensions containing ~1 X 10⁶ cfu/ml of antibiotic-marked strains of *X. perforans* AL65^{step}, AL65 Δ tssM^{nal} and AL65 Δ tssM(tssM)^{km} for 2 hours. Seeds treated with double-distilled water were used as negative control. Inoculated seeds were then air-dried at room temperature for 24 hours as described previously (Tian et al. 2015). Sterile plastic pots (The HC Companies, OH, USA) with soil-less potting medium (Premier Tech Horticulture, PA, USA) were used to place 3 seeds from each treatment and it served as a single biological replication. Twenty-one day old seedlings were evaluated for BLS severity at the end of the trials based on disease index, as

described previously (Tian et al. 2015). The disease severity scale ranged from ‘0 – 5’; ‘0’- no symptoms: ‘1’ water-soaked lesions on approximately 25% of the cotyledons: ‘2’- water-soaked lesions on approximately 50% of the cotyledons: ‘3’, water-soaked lesions on approximately 75% of the cotyledons: ‘4’, water-soaked lesions spread on 100% of the cotyledons: and ‘5’, total death of the seedling. The disease index (DI) was calculated at the end of the trial based on the following formula, where A is the previously described disease scales and B is the number of plants with water-soaked lesion percentages described in that disease scale per treatment.

$$DI = \frac{\sum (A \times B) \times 100}{\sum B \times 5}$$

Bacterial populations on germinating tomato seedlings were determined by macerating leaves of 21 days old seedlings followed by appropriate serial dilutions of each homogenate replicate on NA plates amended with appropriate antibiotics using spiral plater (Neu-tec Group Inc, NY, USA) and incubated for 2-3 days at 28°C. Colonies were counted and colony-forming units cfu per gram of plant tissue were calculated. The experiment was repeated three times.

Growth of the bacterial strains under *in vitro* conditions

In vitro growth assay was conducted to evaluate if there is any growth defect in the AL65 Δ *tssM* strain due to the mutation. AL65^{step}, AL65 Δ *tssM*^{nal} and AL65 Δ *tssM*(*tssM*)^{km} were grown for 24h on NA media amended with respective antibiotics. Bacterial growth was suspended on XVM2: hrp-inducing minimal medium (Wengelnik et al. 1996) and grew for 24 hours. Bacterial growth was collected by centrifugation and washed twice by XVM2 medium and subcultured twice in the same minimal medium. When the cells reached the late-log phase (0.27-0.3 OD = 10⁸), they were collected by the centrifugation at 5000 X g for 10 minutes. The cell pellets were resuspended in the XVM2 to a final concentration of 10⁸ cfu/ml. Aliquots were transferred to microcentrifuge tubes and diluted to 5X10⁴ cfu/ml with XVM2. Two hundred

microliters of the suspensions were placed on 96 well plate at 28°C at 140rpm and OD₆₀₀ was measured every 12 hours.

Since our observations with previous experiments were showing a role of TssM in epiphytic survival of *Xanthomonas perforans*, we wanted to further test if TssM has any other functions in successful survival in the leaf surface. As water availability is one of the barriers faced by the leaf pathogens, *in vitro* osmotolerance assay was conducted. To conduct this assay bacterial cell pellets collected after the centrifugation were resuspended in the medium lacking NaCl to a final concentration of 10⁸ cfu/ml. Aliquots were transferred to microcentrifuge tubes and diluted to 5X10⁴ cfu/ml with XVM2 with different NaCl concentrations (0M -1M). Two hundred microliters of the suspensions were placed on 96 well plate at 28°C at 140rpm and OD₆₀₀ was measured every 12 hours.

Results

Mutation in the *Xanthomonas perforans* T6SS-i3* core gene, *tssM*, results in increased virulence

In this study, we constructed an in-frame deletion mutant of *tssM* (a null mutant, referred to as AL65Δ*tssM*, hereafter) and a complement by extrachromosomal expression of TssM under the control of the native promoter (referred to as, AL65Δ*tssM*(*tssM*), hereafter). Virulence potential of these constructs was evaluated by dip-inoculating susceptible FL8000 tomato leaves of 4- to 5-week-old plants with a bacterial suspension adjusted to 10⁶ cfu/ml consisting of wild-type (AL65), or a 1:1 ratio of AL65Δ*tssM* or AL65Δ*tssM*(*tssM*), by monitoring growth of these strains and symptom development *in planta* over two weeks. The AL65Δ*tssM* mutant exhibited quicker development of disease symptoms, as early as 3 dpi whereas AL65 and AL65Δ*tssM*(*tssM*) strains showed water-soaking lesions by 4 dpi (Figure 2-2). This delayed symptom development with the AL65 and AL65Δ*tssM*(*tssM*) strains also

directly correlated with the lower titers starting at 4 dpi through 14 dpi. Population of the AL65 Δ *tssM* started to increase rapidly after 2 dpi and maintained ~0.5 to 1 log₁₀ higher population compared to the AL65 and AL65 Δ *tssM*(*tssM*) strains throughout the course of the experiment (Figure 2-3a). These observations on overall symptom development as well as *in planta* growth with AL65 Δ *tssM* were similar to that of our initial observations with the transposon mutation in *tssM* gene identified in Xp91-118 background (data not shown), confirming the similar phenotype of mutation in different strain backgrounds. Next, we compared growth progress curves of these strains. AUGPC value for AL65 Δ *tssM* was significantly higher than those for AL65 and AL65 Δ *tssM*(*tssM*) strains (p<0.05). Even though a significant difference in AUGPC was observed between wild-type and AL65 Δ *tssM*(*tssM*) strains (Figure 2-3a), no significant difference in bacterial growth was observed between them at any sampling day. AL65 Δ *tssM* inoculated leaves had significantly higher disease severity compared to leaves inoculated with AL65 or AL65 Δ *tssM*(*tssM*) strains (Figure 2-4a & c). Overall, AL65 Δ *tssM* was more aggressive on tomato compared to the wild-type and had a comparatively shorter latent period compared to the wild-type.

Mixed infection does not provide a competitive advantage for the mutant over wild-type in terms of aggressiveness but rather leads to reduced disease severity when compared to individual infection with the mutant.

Mixed infection of 4- to 5-week-old tomato plants with a bacterial suspension adjusted to 10⁶ cfu/ml consisting of a 1:1 ratio of either AL65 + AL65 Δ *tssM* or AL65 Δ *tssM*(*tssM*) + AL65 Δ *tssM* did not show significant differences in the AUGPC values of each strain, although the mutant grew to a slightly higher population *in planta* beyond 6 dpi compared to wild-type and complement (Figure 2-3b & c). Despite lack of any differences in overall symptomology, overall disease severity levels were consistently lower in a mixed infection compared to individual infections (Figure 2-4b & c).

Mutation in *tssM* does not contribute to the virulence of the pathogen when directly infiltrated into the apoplast

In the previous experiment we observed contribution of T6SS towards overall pathogen aggressiveness when the dip inoculation method was used and the pathogen was given a chance to establish epiphytic colonization, as it is seen under natural infection conditions. To see whether T6SS has a role during endophytic colonization of the pathogen, we performed an infiltration inoculation assay to artificially introduce AL65, AL65 Δ *tssM* and AL65 Δ *tssM*(*tssM*) strains directly into the apoplast. Water-soaking of lesions were observed by 3 dpi for all three treatments and the degree of severity was uniform among the strains. No significant differences were observed among three treatments at any sampling timepoint for bacterial titers (Figure 2-5a) as well as AUGPC (Figure 2-5b). No difference was observed in the symptom development throughout the course of the experiment between AL65 and AL65 Δ *tssM* (Figure 2-5c).

AL65 Δ *tssM* displays lower epiphytic survival and reduced transmission compared to the wild-type.

Tomato seedlings are usually mass-produced inside high humidity transplant houses prior to the distribution of them to use in field transplantation. We tested the contribution of a functional T6SS towards asymptomatic epiphytic colonization on tomato in transplant house-mimic conditions by enumerating the total (epiphytic and endophytic) population and epiphytic population weekly for up to 28 days. AUGPC values calculated based on weekly enumeration of epiphytic and total populations of AL65, AL65 Δ *tssM*(*tssM*) and AL65 Δ *tssM* up to 28 days revealed similar trends with higher values for AL65 and AL65 Δ *tssM*(*tssM*), beyond sampling point 3 (Figure 2-6a & b). Although total population at the point of inoculation (sampling point 1) and the sampling point 2 was more than 1 log higher for AL65 Δ *tssM* compared to the AL65 strain, we observed higher total population of AL65 beyond 3rd sampling points at 28 dpi (Figure 2-6c). Similar observations were recorded with the complement strain when

AL65 Δ *tssM*(*tssM*) and AL65 Δ *tssM* were co-inoculated in a second humidity chamber (Figure 2-6d). Tomato seedlings were observed for disease symptoms at every 7, 14, 21 and 28 dpi and % of seedlings showing disease symptoms were calculated at each sampling point. Until 14 dpi BLS disease symptoms were only observed in sampling point 1 or 1 and 2 in both of the chambers and the infected plant percentage was less than 30%. There was an absence of obvious symptoms at day 7 and 14 beyond sampling point 2 despite the presence of $\sim 1 \times 10^4$ cfu/g epiphytic population on seedlings. At 28dpi, more than 90% of the seedlings displayed disease symptoms at the 1st and 2nd sampling points in both of the chambers with a gradual reduction in the disease incidence with $< 20\%$ infection beyond sampling point 8 (1.7m) (Figure 2-7a and b).

AL65 Δ *tssM* is highly aggressive on seedlings eliciting more severe symptoms with higher population compared to the wild-type upon vertical transmission from seed to seedling.

With the observations of the previous experiments, we were intrigued to study the role of T6SS in other stages of the disease cycle of BLS caused by *Xanthomonas perforans*. Since this is a seedborne pathogen, seed to seedling disease transmission of *X. perforans* was evaluated after inoculation of tomato seeds with AL65 Δ *tssM*, AL65 and AL65 Δ *tssM*(*tssM*). The AL65 Δ *tssM* strain showed significantly higher mean population growth of $\sim 3 \times 10^9$ cfu/g compared to the AL65 strain and AL65 Δ *tssM*(*tssM*) strain that showed a mean population of $\sim 6 \times 10^8$ cfu/g and $\sim 1 \times 10^8$ cfu/g, respectively, on 21-day-old tomato seedlings (Figure 2-8a). AL65 Δ *tssM* showed significantly higher mean BLS disease severity index of 60%, compared to AL65 and AL65 Δ *tssM*(*tssM*) showing 33.33% disease severity (Figure 2-8b).

***X. perforans* wild-type exhibited a higher osmotolerance compared to the AL65 Δ *tssM*.**

AL65 Δ *tssM* was able to grow as well as the wild-type and the complement in XVM2 medium that mimics the apoplasmic environment, indicating a lack of an inherent growth defect in the mutant (Figure 2-9a). Since osmotolerance is an important trait for epiphytic survival of

the pathogen due to low water availability, we evaluated the tolerance of AL65 and AL65 Δ *tssM* to the osmotic stress during growth in XVM2 with varying concentrations of NaCl. When the NaCl concentration was gradually increased to 0.1M and 0.2M, AL65 exhibited a higher growth dynamic compared to the AL65 Δ *tssM* (Figure 2-9b &c respectively). Growth pattern in the other NaCl concentrations were not showing any different among the tested strains (data not shown).

Discussion

Bacterial leaf spot (BLS) is one of the most destructive diseases of tomato (*Solanum lycopersicum*) and peppers (*Capsicum annuum*) grown in warm and humid climates worldwide. The initial symptoms caused by this disease include small, necrotic lesions on all above-ground plant parts such as leaves, stems and fruits (Potnis et al. 2015). These smaller lesions merge into larger ones and result in a reduction in photosynthetic tissue area and fruit infections that cause major economic losses (Jones and Stall 1991; Kyeon et al. 2016; Roach et al. 2018). BLS pathogens can survive in the seeds for an extended time period (Bashan et al. 1982), hence the contaminated seeds are the most important source of inoculum for long-distance transmission and introduction of the disease into pathogen-free areas (Giovanardi et al. 2018). Despite seed certification programs in place, we continue to see bacterial spot disease outbreaks. Transplant houses are considered to be hot spots for asymptomatic transmission of pathogen on transplants grown for field production (Abrahamian et al. 2019). High temperatures, high humidity, high plant density, and overhead irrigation in commercial transplant house settings favor pathogen spread (Dutta et al. 2014a; Potnis et al. 2015). BLS pathogens can also survive epiphytically on the host as well as non-hosts (Jones 1986). Asymptomatic epiphytic survival of the pathogen has been a major concern due to direct influence on effectiveness of management strategies. Such epiphytic populations have been a culprit in reducing efficacy of bactericides as well as impacting durability of disease resistance

(Pernezny and Collins 1997). While the majority of studies investigating the mechanistic basis of pathogenesis of *Xanthomonas* have broadly looked at the contribution of virulence factors towards successful apoplastic growth of the pathogen, mechanisms by which this hemi-biotrophic pathogen successfully adapts to the phyllosphere and maintains epiphytic asymptomatic colonization are understudied. In this study, we have investigated the role of T6SS-i3* towards latent infection period, an epidemiologically important phase during pathogenesis.

We have noted the overall contribution of T6SS-i3* towards aggressiveness of the pathogen, as measured by two traits, latent infection period (observation of delayed symptom development) and reduced disease severity. In plant pathogens the time between host infection and pathogen sporulation/multiplication due to that infection is referred as the latent period, a crucial life history trait (Lannou 2012; Pariaud et al. 2009). In the case of hemi-biotrophic *Xanthomonas*, the pathogen adapts to the phyllosphere during this epiphytic phase. Our findings of AL65 Δ tssM showing faster symptom development, increased disease severity and higher *in planta* growth compared to the wild-type implied increased aggressiveness in absence of T6SS-i3* in *X. perforans*. This suggested the overall role of functional TssM and in turn, functional T6SS-i3*, in limiting symptom development, during early stages of plant colonization. This is in contrast to typical virulence factors, mutations of which typically lead to reduced virulence or reduced disease severity. A similar phenotype with increased disease severity with T6SS mutant was also observed in case of *Pectobacterium atrosepticum* (Mattinen et al. 2008).

In addition to aggressiveness, we also observed increased *in planta* growth with AL65 Δ tssM. This is indicative of the role of T6SS-i3* in determining threshold *in planta* populations during infection. Similar observation was noted in the case of intracellular animal pathogen *Helicobacter hepaticus*, where mutation of *tssM* and *hcp* led to significantly higher

pathogen titer at 3 and 6 hrs in MODE-K cells. Such limit on intracellular pathogen titers during colonization of a mouse in presence of T6SS was thought to suggest role of T6SS in promoting a symbiotic relationship between *H. hepaticus* and mammals (Chow and Mazmanian 2010). This explanation could also be true with *Xanthomonas*, a hemi-biotrophic pathogen, that maintains colonization within a host to promote its transmission before inducing host cell death. We ruled out a growth defect due to presence or absence of T6SS-i3* under in vitro conditions, i.e., in minimal XVM2 medium, under which T6SS-i3* expression is observed (data not shown). However, we cannot rule out inherent differences in expression patterns observed under in vitro conditions and *in planta* conditions, and thus, cannot completely rule out the explanation of a higher cost associated with expressing T6SS-i3* in wild-type, leading to lower *in planta* titer compared to T6SS-i3* mutant.

We observed the influence of the inoculation method on the T6SS mutant phenotype. Infiltration i.e., artificial inoculation of the pathogen directly into the apoplast failed to show a difference in overall pathogen titers or disease severity ratings between AL65 and the AL65 Δ *tssM*. This observation coincided with the previous finding with mutants (deletion of *tssF*, *G* and *H* genes) in T6SS-i3* of *Xeu* where infiltration experiments in tomato/pepper concluded no role of T6SS in the pathogen virulence (Abendroth et al. 2017). Our findings of the role of T6SS-i3* in limiting virulence of the pathogen using dip-inoculation (mimicking natural infection) suggests the importance of testing different methods of inoculation before inferring the contribution of genes/gene clusters towards pathogenesis. Mixed infection with T6SS-i3* mutant and wild-type did not influence *in planta* population growth, yet lowered disease severity when compared to the mutant alone, indicating expression of T6SS-i3* by wild-type influenced overall pathogen aggressiveness in the mixed infection. This observation can be further tested using different inoculation doses since growth interference typically seen with mixed infections (Macho et al. 2010). Since the influence of the mutant was only evident

upon dip-inoculation, but not infiltration, it is indicative of contribution of the T6SS-i3* towards early colonization period. T6SS activation as early as 3 h after inoculation was observed recently in the case of another hemi-biotrophic foliar pathogen *Pseudomonas syringae* pv. *actinidiae* on kiwifruit (McAtee et al. 2018). Similarly, the upregulation of the T6SS genes was also recorded during the epiphytic growth of the *Xanthomonas citri* pv. *citri* on the host plant citrus while low expression levels were recorded during growth inside plant mesophyll (Ceseti et al. 2019). This study with the citrus canker pathogen also identified temporal induction patterns during epiphytic and endophytic colonization of the pathogens for T6SS and T3SS. These intriguing findings are indicative of a possible regulation or interaction between T6 and T3 secretion systems. This hypothesis is further supported by the previous work with *Ralstonia solanacearum* strain GMI1000 that also identified an increased expression of the T3SS effectors in the *tssM* mutant (Zhang et al. 2012). It is possible that the shortened incubation period and increased aggressiveness observed with the *AL65ΔtssM* is due to regulation between T6SS and other secretion systems such as T3SS. These observations should be further analyzed by conducting a gene expression assay during different stages of disease development.

Being a seed-borne pathogen, a critical control point considered in managing bacterial spot disease is seed-to-seedling transmission (Dutta et al. 2014a). Seedling-grow out assays are commonly used in seed certification programs (Gitaitis and Walcott 2007) . We investigated the role of T6SS-i3* at this important stage of seed-to-seedling transmission. Our results with lower disease severities on seedlings with *AL65* compared to *AL65ΔtssM* indicated that although seed transmission was observed with *AL65*, lower disease severity might be responsible for asymptomatic seedlings. Thus, T6SS-i3* allows successful transmission of *Xanthomonas* to the seedling, yet with lower disease severity. These observations are not in agreement with the evaluation of seed to seedling transmission of *Acidovorax citrulli xjl12* on

melon seeds, where significant reduction in the disease index of melon seedlings inoculated with T6SS mutants $\Delta vasD$, $\Delta impJ$, $\Delta impK$ and $\Delta impF$ was observed compared to wild-type, but no significant difference was observed in disease index with the *impL* mutant (homologous to *tssM*) (Tian et al. 2015). These findings show a differential role of T6SS-i3* in plant pathogenic bacteria, possibly due to differential colonization strategies of these pathogens.

In case of foliar bacterial pathogens such as *Xanthomonas*, or *Pseudomonas*, epiphytic survival of a pathogen without symptom expression in the transplant houses provides ideal conditions for transmission of the pathogen and subsequent growth and allows the pathogen to escape artificial selection. These asymptomatic transplants go undetected and get planted into the field resulting in the outbreaks. In *P. syringae* pv. *tomato*, *hopMI* was identified to have accumulated mutations in order to avoid host recognition during this asymptomatic phase (Badel et al. 2006). Our experiment using conditions mimicking high humidity transplant house conditions revealed that T6SS-i3* has a role in maintaining higher epiphytic bacterial populations and in bacterial dissemination into the longer distances (~2m) while expressing minimal disease symptoms. It is worth noting that no obvious symptoms were visible at day 7 and day 14 beyond sampling point 4, despite the presence of 10^4 cfu/g epiphytic population on the transplant seedlings. Higher epiphytic populations with wild-type allowed pathogen dispersal longer distances while maintaining asymptomatic colonization.

Asymptomatic, epiphytic establishment is vital for a foliar pathogen for its successful colonization as well as for the survival. Low water availability is one of the most adverse obstacles faces by the leaf epiphytic bacteria. Accumulation of solutes on the leaf surface can lead to osmotic stress and thus, osmotolerance is an important trait in bacteria that facilitate successful survival on the leaf surface. We investigated the contribution of T6SS-i3* in osmoadaptation by comparing growth patterns in XVM2 minimal medium in presence of different NaCl concentrations. When subjected to osmotic stress, T6SS-i3* positive strain had

significant advantage in growth. Presence of T6SS-i3* in *Xanthomonas* offers osmotic stress adaptation facilitating epiphytic colonization. Difference in osmoadaptation mechanisms have proven to influence the relative fitness of individual species and strains. For example, *P. syringae* B728a strain that shows superior osmotolerance has shown to be better adapted for epiphytic survival than *P. syringae* DC3000 and 1448A strains. A global transcriptomic analysis of *P. syringae* B728a and *P. syringae* DC3000 strains performed under higher osmotic stress identified upregulation of T3SS and T6SS genes in the *P. syringae* B728a (Freeman et al. 2013). Ten of the 21 genes in the B728a T6SS HSI-I cluster were induced under high osmotic pressure that included *impK*, *clpV*, and *icmF (tssM)* (Freeman et al. 2013). Upregulation of the T6SS genes including *icmF (tssM)*, *impB*, *impH*, and *duf877* as a response to the salt-induced osmotic stress was also recorded in *Acidovorax avenae* subsp. *avenae* RS-1, indicating a possibility of formation of the T6SS structure in response to the salt stress (Cui et al. 2015).

T6SS was first characterized in *Pseudomonas aeruginosa* and *Vibrio cholerae* for its role in contact-dependent interbacterial competition, where tit-for-tat type of interactions were noted (Basler et al. 2013). Such counterattack mediated by T6SS and associated toxins against bacterial or eukaryotic competitors were characterized in multiple animal or human pathogenic bacteria (Russell et al. 2011; MacIntyre et al. 2010; Song et al. 2021; Trunk et al. 2018; Storey et al. 2020). In case of plant pathogens, T6SS-i3* in *Xanthomonas citri* pv. *citri* mediates resistance to predation by amoeba *Dictyostelium discoideum* (Bayer-Santos et al. 2018). While ecological significance of such anti-amoeba interactions remains to be explored, this finding provides interesting questions as to whether T6SS allows bacterial plant pathogens to overcome competition with resident microflora. In *X. oryzae* pv. *oryzicola* GX01, mutation in T6SS i4 cluster resulted in impaired bacterial competition with *Ochrobactrum oryzae*, a rice endophytic bacterium and also with *E. coli* (Zhu et al. 2020). Further studies investigating whether T6SS-mediated manipulation of resident microflora result in altered host susceptibility would help

disentangle the functional profile of T6SS- i3*** not just in the context of virulence but in the context of its ecological significance.

Presence of two T6SS clusters (i3* and i3***, defined based on phylogenetic subclades within clade i3 based on *tssC* gene), hence two *tssM* genes in *Xanthomonas perforans*, raise question about functional redundancy and hence, possible trans-complementation in case of a deletion mutant of a core gene of single T6SS cluster. The two *tssM* genes from cluster i3* and i3*** share only 65% identity at nucleotide level and 45% at amino acid level. In many pathogens carrying multiple T6SS clusters, such sequence divergence reflected different functional profiles and differential regulation (Navarro-Garcia et al. 2019; Pezoa et al. 2014). A strain of *Salmonella enterica* serotype Dublin lacking T6SS_{SPI-6} displayed a strong colonization defect in mice and chickens, like a strain lacking both T6SS_{SPI-6} and T6SS_{SPI-19} clusters. This colonization defect was only reversed by transfer of the T6SS_{SPI-6}, it indicates that these two T6 clusters are not functionally redundant in *Salmonella enterica* serotype Dublin (Pezoa et al. 2014). Similarly in *Aeromonas hydrophila* no functional redundancy was observed for Hcp in influencing motility (Sha et al. 2013). The expression of T6SS₄ in *Yersinia pseudotuberculosis* is differentially thermoregulated than the other three T6SS clusters at 26°C, indicating a differential functional specialization/regulation of each system (Zhang et al. 2011). In *Xanthomonas oryzae* pv. *oryzicola*, T6SS-i3*** cluster was not required for virulence or bacterial competition but i4 cluster played an important role in bacterial killing (Zhu et al. 2020), further indicating that T6SS clusters are not functionally redundant. Further studies with single and double mutants with *tssM* gene deletions in both clusters i3* and i3*** in *X. euvesicatoria* and *X. perforans* would be needed to study phenotype profiles and differential regulation of these multiplied systems.

Conclusion

We present evidence for contribution of T6SS-i3* during some of the crucial stages of the life cycle of the foliar hemi-biotrophic pathogen, seed-to-seedling transmission, transplants and during epiphytic colonization on mature 4- to 5-week-old plants. Interestingly, in all these stages, T6SS-i3* influences a crucial life history trait of the latent infection period. T6SS-i3* dictates the threshold *in planta* population, and thus, is a determinant of aggressiveness of the hemi-biotrophic foliar pathogen, *Xanthomonas*. This study also highlights the importance of T6SS-i3* in overcoming osmotic stress during the initial adaptation period to the phyllosphere. Given the influence of the latent infection period on the overall disease outcome, further studies focused on understanding the regulation of pathogenesis by T6SS-i3* will be crucial.

References

- Abbasi, P. A., Soltani, N., Cuppels, D. A., and Lazarovits, G. (2002). Reduction of Bacterial Spot Disease Severity on Tomato and Pepper Plants with Foliar Applications of Ammonium Lignosulfonate and Potassium Phosphate. *Plant Disease* 86, 1232–1236. doi:10.1094/PDIS.2002.86.11.1232.
- Abendroth, U., Adlung, N., Otto, A., Grüneisen, B., Becher, D., and Bonas, U. (2017). Identification of new protein-coding genes with a potential role in the virulence of the plant pathogen *Xanthomonas euvesicatoria*. *BMC Genomics* 18, 625. doi:10.1186/s12864-017-4041-7.
- Abrahamian, P., Timilsina, S., Minsavage, G. V., Potnis, N., Jones, J. B., Goss, E. M., et al. (2019). Molecular Epidemiology of *Xanthomonas perforans* Outbreaks in Tomato Plants from Transplant to Field as Determined by Single-Nucleotide Polymorphism Analysis. *Appl Environ Microbiol* 85. doi:10.1128/AEM.01220-19.
- Alcoforado Diniz, J., Liu, Y., and Coulthurst, S. J. (2015). Molecular weaponry: diverse effectors delivered by the Type VI secretion system. *Cell Microbiol* 17, 1742–1751. doi:10.1111/cmi.12532.
- Atanassov, I. I., Atanassov, I. I., Etschells, J. P., and Turner, S. R. (2009). A simple, flexible and efficient PCR-fusion/Gateway cloning procedure for gene fusion, site-directed mutagenesis, short sequence insertion and domain deletions and swaps. *Plant Methods* 5, 14. doi:10.1186/1746-4811-5-14.
- Badel, J. L., Shimizu, R., Oh, H.-S., and Collmer, A. (2006). A *Pseudomonas syringae* pv. *tomato* avrE1/hopM1 Mutant Is Severely Reduced in Growth and Lesion Formation in Tomato. *MPMI* 19, 99–111. doi:10.1094/MPMI-19-0099.
- Bashan, Y., Diab, S., and Okon, Y. (1982). Survival of *Xanthomonas campestris* pv. *vesicatoria* in pepper seeds and roots in symptomless and dry leaves in non-host plants and in the soil. *Plant and Soil* 68, 161–170. doi:10.1007/BF02373702.
- Basler, M., Ho, B. T., and Mekalanos, J. J. (2013). Tit-for-Tat: Type VI Secretion System Counterattack during Bacterial Cell-Cell Interactions. *Cell* 152, 884–894. doi:10.1016/j.cell.2013.01.042.

- Bayer-Santos, E., Lima, L. dos P., Ceseti, L. de M., Ratagami, C. Y., Santana, E. S. de, Silva, A. M. da, et al. (2018). *Xanthomonas citri* T6SS mediates resistance to *Dictyostelium* predation and is regulated by an ECF σ factor and cognate Ser/Thr kinase. *Environmental Microbiology* 20, 1562–1575. doi:<https://doi.org/10.1111/1462-2920.14085>.
- Bernal, P., Llamas, M. A., and Filloux, A. (2018). Type VI secretion systems in plant-associated bacteria. *Environmental Microbiology* 20, 1–15. doi:[10.1111/1462-2920.13956](https://doi.org/10.1111/1462-2920.13956).
- Bingle, L. E., Bailey, C. M., and Pallen, M. J. (2008). Type VI secretion: a beginner's guide. *Current Opinion in Microbiology* 11, 3–8. doi:[10.1016/j.mib.2008.01.006](https://doi.org/10.1016/j.mib.2008.01.006).
- Boyer, F., Fichant, G., Berthod, J., Vandenbrouck, Y., and Attree, I. (2009). Dissecting the bacterial type VI secretion system by a genome wide in silico analysis: what can be learned from available microbial genomic resources? *BMC Genomics* 10, 104. doi:[10.1186/1471-2164-10-104](https://doi.org/10.1186/1471-2164-10-104).
- Cascales, E., and Cambillau, C. (2012). Structural biology of type VI secretion systems. *Phil. Trans. R. Soc. B* 367, 1102–1111. doi:[10.1098/rstb.2011.0209](https://doi.org/10.1098/rstb.2011.0209).
- Ceseti, L. M., de Santana, E. S., Ratagami, C. Y., Barreiros, Y., Lima, L. D. P., Dunger, G., et al. (2019). The *Xanthomonas citri* pv. *citri* Type VI Secretion System is Induced During Epiphytic Colonization of Citrus. *Curr Microbiol* 76, 1105–1111. doi:[10.1007/s00284-019-01735-3](https://doi.org/10.1007/s00284-019-01735-3).
- Choi, Y., Kim, N., Mannaa, M., Kim, H., Park, J., Jung, H., et al. (2020). Characterization of Type VI Secretion System in *Xanthomonas oryzae* pv. *oryzae* and Its Role in Virulence to Rice. *Plant Pathol J* 36, 289–296. doi:[10.5423/PPJ.NT.02.2020.0026](https://doi.org/10.5423/PPJ.NT.02.2020.0026).
- Chow, J., and Mazmanian, S. K. (2010). A Pathobiont of the Microbiota Balances Host Colonization and Intestinal Inflammation. *Cell Host & Microbe* 7, 265–276. doi:[10.1016/j.chom.2010.03.004](https://doi.org/10.1016/j.chom.2010.03.004).
- Cui, Z., Jin, G., Li, B., Kakar, K. U., Ojaghian, M. R., Wang, Y., et al. (2015). Gene Expression of Type VI Secretion System Associated with Environmental Survival in *Acidovorax avenae* subsp. *avenae* by Principle Component Analysis. *Int J Mol Sci* 16, 22008–22026. doi:[10.3390/ijms160922008](https://doi.org/10.3390/ijms160922008).

- De Pace, F., Boldrin de Paiva, J., Nakazato, G., Lancellotti, M., Sircili, M. P., Guedes Stehling, E., et al. (2011). Characterization of IcmF of the type VI secretion system in an avian pathogenic *Escherichia coli* (APEC) strain. *Microbiology* 157, 2954–2962. doi:10.1099/mic.0.050005-0.
- Durand, E., Cambillau, C., Cascales, E., and Journet, L. (2014). VgrG, Tae, Tle, and beyond: the versatile arsenal of Type VI secretion effectors. *Trends in Microbiology* 22, 498–507. doi:10.1016/j.tim.2014.06.004.
- Durand, E., Nguyen, V. S., Zoued, A., Logger, L., Péhau-Arnaudet, G., Aschtgen, M.-S., et al. (2015). Biogenesis and structure of a type VI secretion membrane core complex. *Nature* 523, 555–560. doi:10.1038/nature14667.
- Dutta, B., Gitaitis, R., Sanders, H., Booth, C., Smith, S., and Langston, D. B. (2014a). Role of blossom colonization in pepper seed infestation by *Xanthomonas euvesicatoria*. *Phytopathology* 104, 232–239. doi:10.1094/PHYTO-05-13-0138-R.
- Dutta, B., Gitaitis, R., Smith, S., and Langston, D. (2014b). Interactions of Seedborne Bacterial Pathogens with Host and Non-Host Plants in Relation to Seed Infestation and Seedling Transmission. *PLoS One* 9. doi:10.1371/journal.pone.0099215.
- Freeman, B. C., Chen, C., Yu, X., Nielsen, L., Peterson, K., and Beattie, G. A. (2013). Physiological and Transcriptional Responses to Osmotic Stress of Two *Pseudomonas syringae* Strains That Differ in Epiphytic Fitness and Osmotolerance. *J Bacteriol* 195, 4742–4752. doi:10.1128/JB.00787-13.
- Ge, Z., Sterzenbach, T., Whary, M., Rickman, B., Rogers, A., Shen, Z., et al. (2008). *Helicobacter hepaticus* HHGII is a pathogenicity island associated with typhlocolitis in B6.129-IL10tm1Cgn mice. *Microbes Infect* 10, 726–733. doi:10.1016/j.micinf.2008.03.011.
- Giovanardi, D., Biondi, E., Ignjatov, M., Jevtić, R., and Stefani, E. (2018). Impact of bacterial spot outbreaks on the phytosanitary quality of tomato and pepper seeds. *Plant Pathology* 67, 1168–1176. doi:10.1111/ppa.12839.
- Gitaitis, R., and Walcott, R. (2007). The Epidemiology and Management of Seedborne Bacterial Diseases. *Annu. Rev. Phytopathol.* 45, 371–397. doi:10.1146/annurev.phyto.45.062806.094321.

- Helmann, T. C., Deutschbauer, A. M., and Lindow, S. E. (2019). Genome-wide identification of *Pseudomonas syringae* genes required for fitness during colonization of the leaf surface and apoplast. *Proc Natl Acad Sci USA* 116, 18900–18910. doi:10.1073/pnas.1908858116.
- Jones, J. B. (1986). Survival of *Xanthomonas campestris* pv. *vesicatoria* in Florida on Tomato Crop Residue, Weeds, Seeds, and Volunteer Tomato Plants. *Phytopathology* 76, 430. doi:10.1094/Phyto-76-430.
- Jones, J. P., and Stall, R. E. (1991). *Compendium of Tomato Diseases*. 1 edition. , ed. T. A. Zitter St. Paul, Minn., USA: The American Phytopathological Society.
- Keen, N. T., Tamaki, S., Kobayashi, D., and Trollinger, D. (1988). Improved broad-host-range plasmids for DNA cloning in Gram-negative bacteria. *Gene* 70, 191–197. doi:10.1016/0378-1119(88)90117-5.
- Kim, N., Kim, J. J., Kim, I., Mannaa, M., Park, J., Kim, J., et al. (2020). Type VI secretion systems of plant-pathogenic Burkholderia glumae BGR1 play a functionally distinct role in interspecies interactions and virulence. *Molecular Plant Pathology* 21, 1055–1069. doi:https://doi.org/10.1111/mpp.12966.
- Kyeon, M.-S., Son, S.-H., Noh, Y.-H., Kim, Y.-E., Lee, H.-I., and Cha, J.-S. (2016). *Xanthomonas euvesicatoria* Causes Bacterial Spot Disease on Pepper Plant in Korea. *Plant Pathol J* 32, 431–440. doi:10.5423/PPJ.OA.01.2016.0016.
- Lannou, C. (2012). Variation and selection of quantitative traits in plant pathogens. *Annu Rev Phytopathol* 50, 319–338. doi:10.1146/annurev-phyto-081211-173031.
- Ma, L.-S., Hachani, A., Lin, J.-S., Filloux, A., and Lai, E.-M. (2014). *Agrobacterium tumefaciens* Deploys a Superfamily of Type VI Secretion DNase Effectors as Weapons for Interbacterial Competition In Planta. *Cell Host & Microbe* 16, 94–104. doi:10.1016/j.chom.2014.06.002.
- Ma, L.-S., Narberhaus, F., and Lai, E.-M. (2012). IcmF family protein TssM exhibits ATPase activity and energizes type VI secretion. *J Biol Chem* 287, 15610–15621. doi:10.1074/jbc.M111.301630.

- Macho, A. P., Guidot, A., Barberis, P., Beuzón, C. R., and Genin, S. (2010). A Competitive Index Assay Identifies Several *Ralstonia solanacearum* Type III Effector Mutant Strains with Reduced Fitness in Host Plants. *MPMI* 23, 1197–1205. doi:10.1094/MPMI-23-9-1197.
- Macho, A. P., Zumaquero, A., Ortiz-Martín, I., and Beuzón, C. R. (2007). Competitive index in mixed infections: a sensitive and accurate assay for the genetic analysis of *Pseudomonas syringae*–plant interactions. *Molecular Plant Pathology* 8, 437–450. doi:10.1111/j.1364-3703.2007.00404.x.
- MacIntyre, D. L., Miyata, S. T., Kitaoka, M., and Pukatzki, S. (2010). The *Vibrio cholerae* type VI secretion system displays antimicrobial properties. *Proc Natl Acad Sci U S A* 107, 19520–19524. doi:10.1073/pnas.1012931107.
- Mattinen, L., Somervuo, P., Nykyri, J., Nissinen, R., Kouvonen, P., Corthals, G., et al. (2008a). Microarray profiling of host-extract-induced genes and characterization of the type VI secretion cluster in the potato pathogen *Pectobacterium atrosepticum*. *Microbiology* 154, 2387–2396. doi:10.1099/mic.0.2008/017582-0.
- Mattinen, L., Somervuo, P., Nykyri, J., Nissinen, R., Kouvonen, P., Corthals, G., et al. (2008b). Microarray profiling of host-extract-induced genes and characterization of the type VI secretion cluster in the potato pathogen *Pectobacterium atrosepticum*. *Microbiology* 154, 2387–2396. doi:10.1099/mic.0.2008/017582-0.
- McAtee, P. A., Brian, L., Curran, B., van der Linden, O., Nieuwenhuizen, N. J., Chen, X., et al. (2018). Re-programming of *Pseudomonas syringae* pv. *actinidiae* gene expression during early stages of infection of kiwifruit. *BMC Genomics* 19, 822. doi:10.1186/s12864-018-5197-5.
- Meuskens, I., Saragliadis, A., Leo, J. C., and Linke, D. (2019). Type V Secretion Systems: An Overview of Passenger Domain Functions. *Front. Microbiol.* 10, 1163. doi:10.3389/fmicb.2019.01163.
- Miller, J. H. (1972). *Experiments in molecular genetics*. [Cold Spring Harbor, N.Y.]: Cold Spring Harbor Laboratory.
- Montenegro Benavides, N. A., Alvarez B., A., Arrieta-Ortiz, M. L., Rodriguez-R, L. M., Botero, D., Tabima, J. F., et al. (2021). The type VI secretion system of *Xanthomonas*

- phaseoli pv. manihotis is involved in virulence and in vitro motility. *BMC Microbiology* 21, 14. doi:10.1186/s12866-020-02066-1.
- Mosquito, S., Bertani, I., Licastro, D., Compant, S., Myers, M. P., Hinarejos, E., et al. (2020). In Planta Colonization and Role of T6SS in Two Rice *Kosakonia* Endophytes. *MPMI* 33, 349–363. doi:10.1094/MPMI-09-19-0256-R.
- Mougous, J. D. (2006). A Virulence Locus of *Pseudomonas aeruginosa* Encodes a Protein Secretion Apparatus. *Science* 312, 1526–1530. doi:10.1126/science.1128393.
- Navarro-Garcia, F., Ruiz-Perez, F., Cataldi, Á., and Larzábal, M. (2019). Type VI Secretion System in Pathogenic *Escherichia coli*: Structure, Role in Virulence, and Acquisition. *Front. Microbiol.* 10. doi:10.3389/fmicb.2019.01965.
- Newberry, E. A., Bhandari, R., Minsavage, G. V., Timilsina, S., Jibrin, M., Kemble, J., et al. (2019). Independent evolution with the gene flux originating from multiple *Xanthomonas* species explains genomic heterogeneity in *Xanthomonas perforans*. *Appl. Environ. Microbiol.*, AEM.00885-19. doi:10.1128/AEM.00885-19.
- Palmer, T., Finney, A. J., Saha, C. K., Atkinson, G. C., and Sargent, F. (2020). A holin/peptidoglycan hydrolase-dependent protein secretion system. *Molecular Microbiology*.
- Pariaud, B., Robert, C., Goyeau, H., and Lannou, C. (2009). Aggressiveness components and adaptation to a host cultivar in wheat leaf rust. *Phytopathology* 99, 869–878. doi:10.1094/PHYTO-99-7-0869.
- Parsons, D. A., and Heffron, F. (2005). *sciS*, an *icmF* Homolog in *Salmonella enterica* Serovar Typhimurium, Limits Intracellular Replication and Decreases Virulence. *Infect Immun* 73, 4338–4345. doi:10.1128/IAI.73.7.4338-4345.2005.
- Pernezny, K., and Collins, J. (1997). Epiphytic Populations of *Xanthomonas campestris* pv. *vesicatoria* on Pepper: Relationships to Host-Plant Resistance and Exposure to Copper Sprays. *Plant Disease* 81, 791–794. doi:10.1094/PDIS.1997.81.7.791.
- Pezoa, D., Blondel, C. J., Silva, C. A., Yang, H.-J., Andrews-Polymenis, H., Santiviago, C. A., et al. (2014). Only one of the two type VI secretion systems encoded in the *Salmonella*

- enterica serotype Dublin genome is involved in colonization of the avian and murine hosts. *Vet Res* 45, 2. doi:10.1186/1297-9716-45-2.
- Potnis, N., Krasileva, K., Chow, V., Almeida, N. F., Patil, P. B., Ryan, R. P., et al. (2011). Comparative genomics reveals diversity among xanthomonads infecting tomato and pepper. *BMC Genomics* 12, 146. doi:10.1186/1471-2164-12-146.
- Potnis, N., Timilsina, S., Strayer, A., Shantharaj, D., Barak, J. D., Paret, M. L., et al. (2015). Bacterial spot of tomato and pepper: diverse *Xanthomonas* species with a wide variety of virulence factors posing a worldwide challenge. *Molecular Plant Pathology* 16, 907–920. doi:https://doi.org/10.1111/mpp.12244.
- Pukatzki, S., Ma, A. T., Sturtevant, D., Krastins, B., Sarracino, D., Nelson, W. C., et al. (2006). Identification of a conserved bacterial protein secretion system in *Vibrio cholerae* using the *Dictyostelium* host model system. *Proceedings of the National Academy of Sciences* 103, 1528–1533. doi:10.1073/pnas.0510322103.
- Roach, R., Mann, R., Gambley, C. G., Shivas, R. G., and Rodoni, B. (2018). Identification of *Xanthomonas* species associated with bacterial leaf spot of tomato, capsicum and chilli crops in eastern Australia. *Eur J Plant Pathol* 150, 595–608. doi:10.1007/s10658-017-1303-9.
- Russell, A. B., Hood, R. D., Bui, N. K., LeRoux, M., Vollmer, W., and Mougous, J. D. (2011). Type VI secretion delivers bacteriolytic effectors to target cells. *Nature* 475, 343–347. doi:10.1038/nature10244.
- Sha, J., Rosenzweig, J. A., Kozlova, E. V., Wang, S., Erova, T. E., Kirtley, M. L., et al. (2013). Evaluation of the roles played by Hcp and VgrG type 6 secretion system effectors in *Aeromonas hydrophila* SSU pathogenesis. *Microbiology (Reading)* 159, 1120–1135. doi:10.1099/mic.0.063495-0.
- Shalom, G., Shaw, J. G., and Thomas, M. S. (2007). In vivo expression technology identifies a type VI secretion system locus in *Burkholderia pseudomallei* that is induced upon invasion of macrophages. *Microbiology*, 153, 2689–2699. doi:10.1099/mic.0.2007/006585-0.

- Song, L., Pan, J., Yang, Y., Zhang, Z., Cui, R., Jia, S., et al. (2021). Contact-independent killing mediated by a T6SS effector with intrinsic cell-entry properties. *Nature Communications* 12, 423. doi:10.1038/s41467-020-20726-8.
- Storey, D., McNally, A., Åstrand, M., Santos, J. sa-P. G., Rodriguez-Escudero, I., Elmore, B., et al. (2020). *Klebsiella pneumoniae* type VI secretion system-mediated microbial competition is PhoPQ controlled and reactive oxygen species dependent. *PLOS Pathogens* 16, e1007969. doi:10.1371/journal.ppat.1007969.
- Tian, Y., Zhao, Y., Shi, L., Cui, Z., Hu, B., and Zhao, Y. (2017). Type VI Secretion Systems of *Erwinia amylovora* Contribute to Bacterial Competition, Virulence, and Exopolysaccharide Production. *Phytopathology* 107, 654–661. doi:10.1094/PHYTO-11-16-0393-R.
- Tian, Y., Zhao, Y., Wu, X., Liu, F., Hu, B., and Walcott, R. R. (2015). The type VI protein secretion system contributes to biofilm formation and seed-to-seedling transmission of *Acidovorax citrulli* on melon: T6SS contributes to biofilm formation and seed-to-seedling transmission of *Acidovorax citrulli* on melon. *Molecular Plant Pathology* 16, 38–47. doi:10.1111/mpp.12159.
- Trunk, K., Peltier, J., Liu, Y.-C., Dill, B. D., Walker, L., Gow, N. A. R., et al. (2018). The type VI secretion system deploys antifungal effectors against microbial competitors. *Nature Microbiology* 3, 920–931. doi:10.1038/s41564-018-0191-x.
- Turner, P., Barber, C., and Daniels, M. (1984). Behaviour of the transposons Tn5 and Tn7 in *Xanthomonas campestris* pv. *campestris*. *Molecular and General Genetics* MGG 195, 101–107. doi:10.1007/BF00332731.
- Wang, N., Han, N., Tian, R., Chen, J., Gao, X., Wu, Z., et al. (2021). Role of the Type VI Secretion System in the Pathogenicity of *Pseudomonas syringae* pv. *actinidiae*, the Causative Agent of Kiwifruit Bacterial Canker. *Frontiers in Microbiology* 12. doi:10.3389/fmicb.2021.627785.
- Weber, B. S., Miyata, S. T., Iwashkiw, J. A., Mortensen, B. L., Skaar, E. P., Pukatzki, S., et al. (2013). Genomic and Functional Analysis of the Type VI Secretion System in *Acinetobacter*. *PLoS ONE* 8, e55142. doi:10.1371/journal.pone.0055142.

- Wengelnik, K., Marie, C., Russel, M., and Bonas, U. (1996). Expression and localization of HrpA1, a protein of *Xanthomonas campestris* pv. *vesicatoria* essential for pathogenicity and induction of the hypersensitive reaction. *J Bacteriol* 178, 1061–1069.
- Wu, H.-Y., Chung, P.-C., Shih, H.-W., Wen, S.-R., and Lai, E.-M. (2008). Secretome Analysis Uncovers an Hcp-Family Protein Secreted via a Type VI Secretion System in *Agrobacterium tumefaciens*. *J Bacteriol* 190, 2841–2850. doi:10.1128/JB.01775-07.
- Zhang, L., Xu, J., Xu, J., Chen, K., He, L., and Feng, J. (2012a). TssM is essential for virulence and required for type VI secretion in *Ralstonia solanacearum*. *J Plant Dis Prot* 119, 125–134. doi:10.1007/BF03356431.
- Zhang, L., Xu, J., Xu, J., Chen, K., He, L., and Feng, J. (2012b). TssM is essential for virulence and required for type VI secretion in *Ralstonia solanacearum*. *J Plant Dis Prot* 119, 125–134. doi:10.1007/BF03356431.
- Zhang, W., Xu, S., Li, J., Shen, X., Wang, Y., and Yuan, Z. (2011). Modulation of a thermoregulated type VI secretion system by AHL-dependent Quorum Sensing in *Yersinia pseudotuberculosis*. *Arch Microbiol* 193, 351–363. doi:10.1007/s00203-011-0680-2.
- Zhu, P.-C., Li, Y.-M., Yang, X., Zou, H.-F., Zhu, X.-L., Niu, X.-N., et al. (2020). Type VI secretion system is not required for virulence on rice but for inter-bacterial competition in *Xanthomonas oryzae* pv. *oryzicola*. *Res Microbiol* 171, 64–73. doi:10.1016/j.resmic.2019.10.004.
- Zoued, A., Brunet, Y. R., Durand, E., Aschtgen, M.-S., Logger, L., Douzi, B., et al. (2014). Architecture and assembly of the Type VI secretion system. *Biochimica et Biophysica Acta (BBA) - Molecular Cell Research* 1843, 1664–1673. doi:10.1016/j.bbamcr.2014.03.018.

Table 2-1: Bacterial strains and plasmids used in this study.

Strain or plasmid	Relevant characteristics	References or source
<i>Xanthomonas perforans</i>		
strains		
WT/ AL65	XpAL65, Rif ^r , Strep ^r	Laboratory collection (Newberry et al. 2019)
AL65ΔtssM	Strain XpAL65, in-frame deletion in <i>tssM</i> , Nal ^r	This study
AL65ΔtssM(<i>tssM</i>)	Strain XpAL65, Δ <i>tssM</i> mutant complemented with pDSK519(<i>tssM</i>), Km ^r	This study
<i>Escherichia coli</i>		
One Shot™ TOP10	F ⁻ mcrA Δ (mrr-hsdRMS-mcrBC) ϕ 80lacZ Δ M15 Δ lacX74recA1araD139 Δ (a ra-leu) 7697 galU galK rpsL (Str ^r) endA1 nupG λ -	Invitrogen
DH5α	F ⁻ 80dlacZ Δ M15 Δ (lacZYA-argF)U169 endA1 deoR recA1 hsdR17(rK ⁻ mK ⁺) phoA supE44 λ -thi-1 gyrA96 relA1	Life Technologies, Carlsbad, CA
Plasmids		
pCR™8/GW/TOPO®	Topo cloning vector, Spec ^r	Invitrogen

pCRTM-BlunII-TOPO®	Blunt DNA Cloning Vector, Km ^r	Invitrogen
pLVC18-RfC	Tet ^r , Gateway destination suicide vector	Roden et al. 2004
pLVC18-RfC ($\Delta tssM$)	pLVC18 derivative containing fusion of genomic regions upstream and downstream of <i>tssM</i> , Tet ^r	This study
pRK 2073	Helper plasmid	
pDSK519	Km ^r	(Keen et al. 1988)
pDSK519 (<i>tssM</i>)	pDSK19 with genomic region containing coding region of <i>tssM</i> along with upstream and downstream flanking region of <i>tssM</i> ; Km ^r	This study

Rif^r, Strep^r, Km^r, Nal^r Nal^r, Str^r, Spec^r, Tet^r : ^r indicates antibiotic resistance respectively.

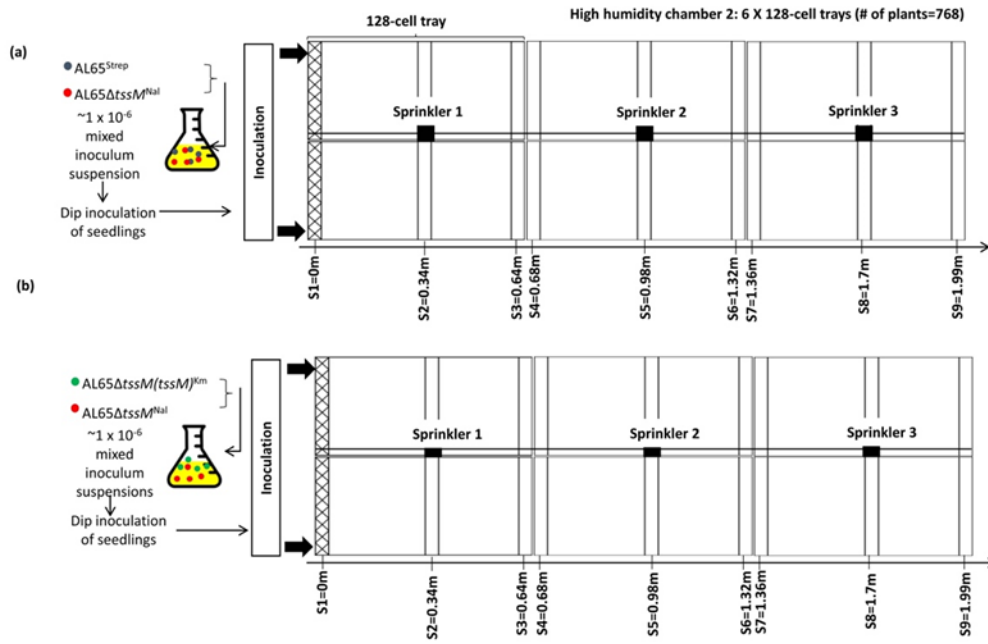


Figure 2-1: Arrangement of the trays inside the humidity chambers. (a) Chamber 1: Mixed inoculation of $AL65^{strep}$ and $AL65\Delta tssM^{nal}$ (b) Chamber 2: Mixed inoculation of $AL65\Delta tssM^{nal}$ and $AL65\Delta tssM(tssM)^{km}$

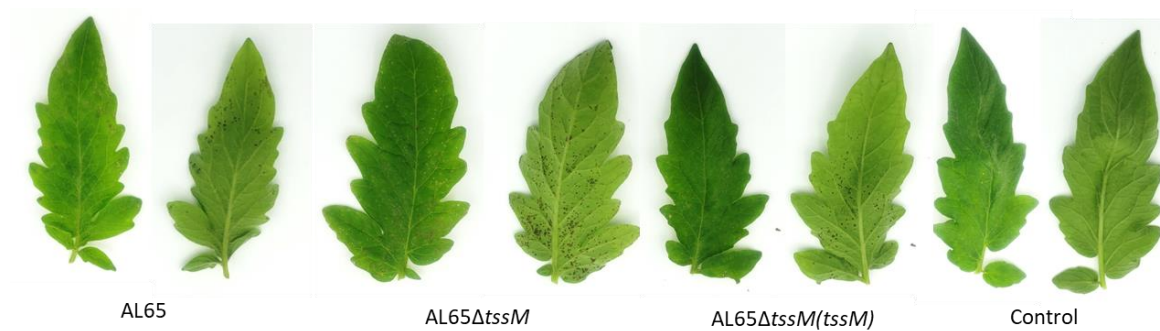


Figure 2-2: Disease symptom development 4 days after dip-inoculation.

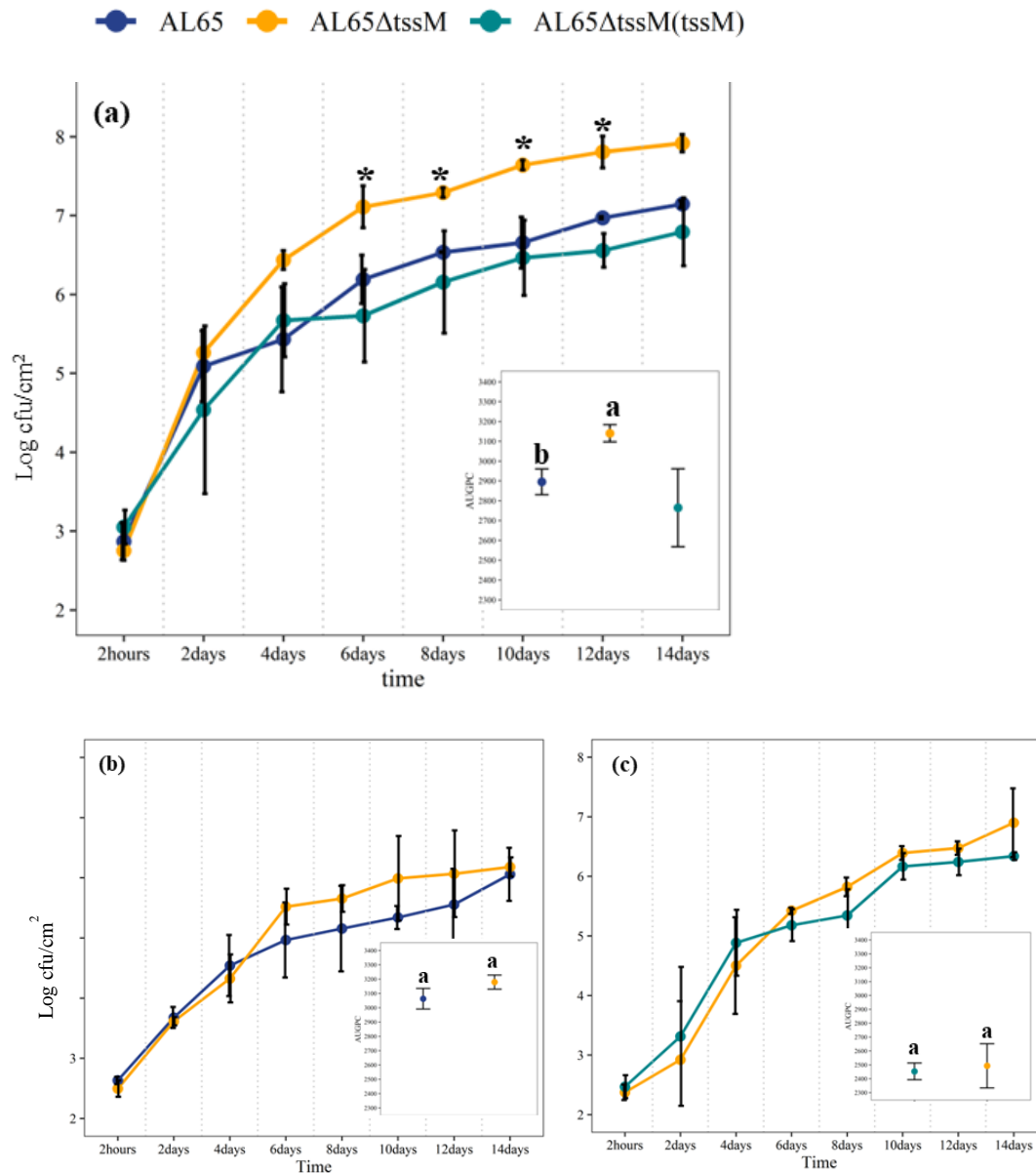


Figure 2-3: Effect of TssM on pathogenicity of *X. perforans* AL65. (a) bacterial population growth individual inoculation, right panel-area under the growth progress curve calculated for each strain growth in individual inoculation (b) bacterial population growth mixed inoculation AL65 + AL65ΔtssM, right panel- area under the growth progress curve calculated for each strain growth in mixed inoculation AL65 + AL65ΔtssM (c) bacterial population growth mixed inoculation AL65ΔtssM(tssM) + AL65ΔtssM, area under the growth progress curve calculated for each strain growth in mixed inoculation AL65ΔtssM(tssM) + AL65ΔtssM. 4- to 5-week-old tomato (cv. FL8000) plants inoculated with $\sim 1 \times 10^6$ cfu/ml of AL65, AL65ΔtssM or

AL65 Δ *tssM*(*tssM*) strains were evaluated for bacterial population growth, every alternate day for 14 dpi on semi-selective media. \log_{10} cfu/cm² values were used to calculate AUGPC values for each corresponding treatment. Lines represent the standard error of the mean. A one-way ANOVA was applied for the statistical analysis of AUGPC and treatments with different letters are significantly different according to Tukey's test of least significant difference (P<0.05). A one-way ANOVA was applied for the statistical analysis of bacterial population \log_{10} values and treatments with * marks are significantly different according to Tukey's test of least significant difference (P<0.05).

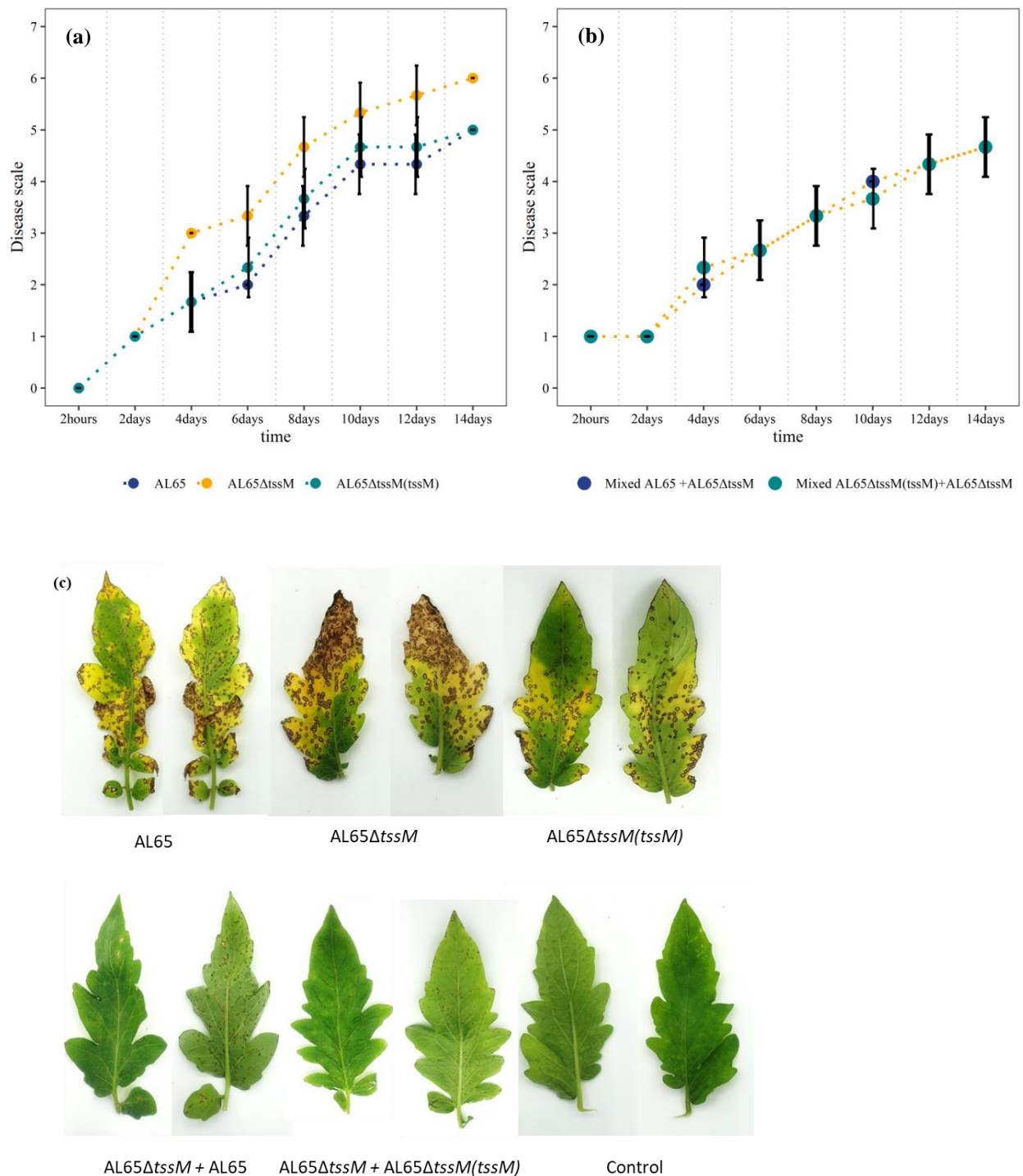


Figure 2-4: Effect of TssM on symptom development of *X. perforans* AL65. (a) Disease scale in individual inoculation (b) disease scale in mixed inoculations (c) tomato leaves 14 days after inoculation with each strain. 4- to 5-week-old tomato (cv. FL8000) plants inoculated with ~1x

10^6 cfu/ml of AL65, AL65 Δ *tssM* or AL65 Δ *tssM*(*tssM*) strains were evaluated for disease development, every alternate day for 14 dpi. A one-way ANOVA was applied for the statistical analysis of disease index values on each sampling day separately and treatments with * marks are significantly different according to Tukey's test of least significant difference ($P < 0.05$).

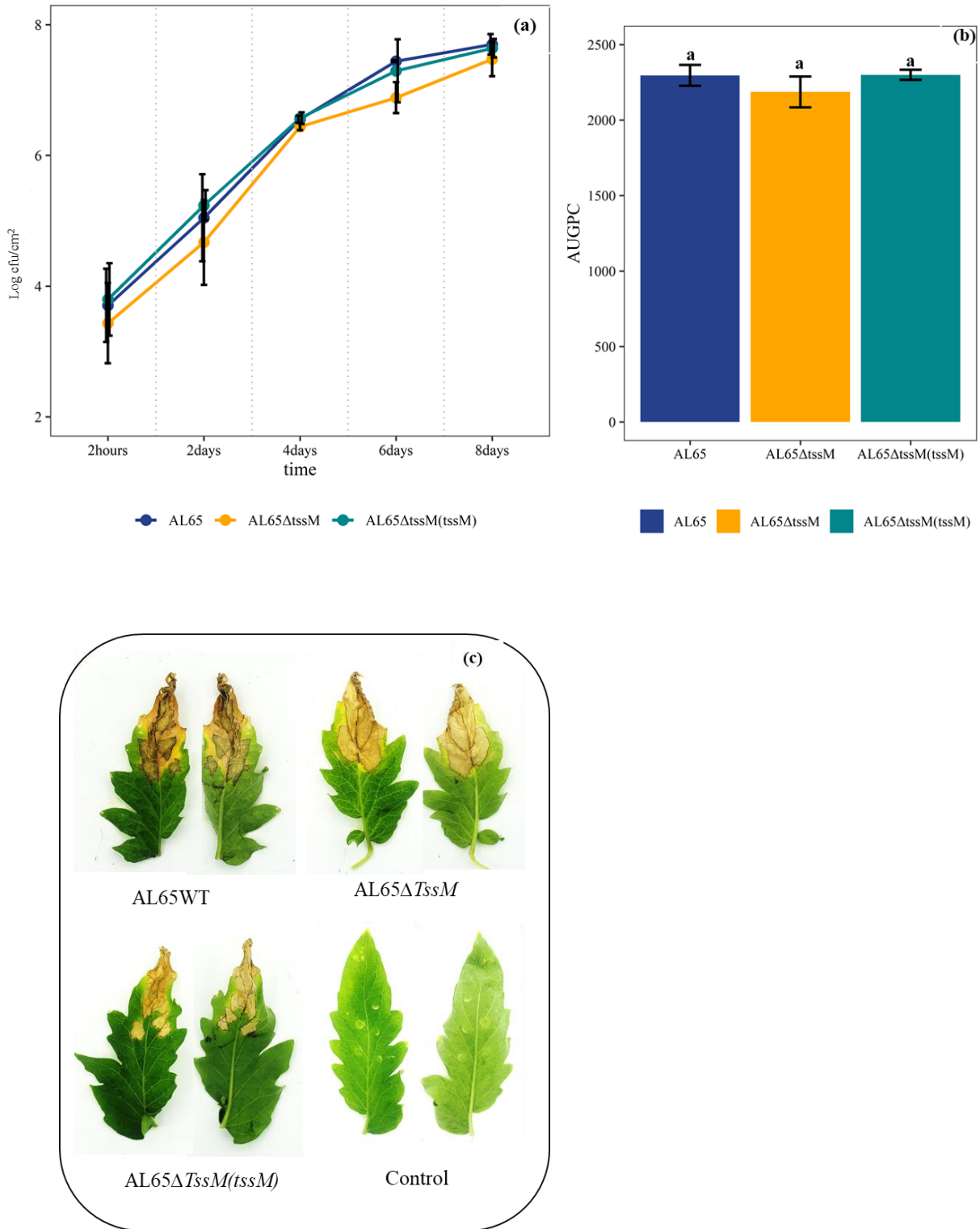
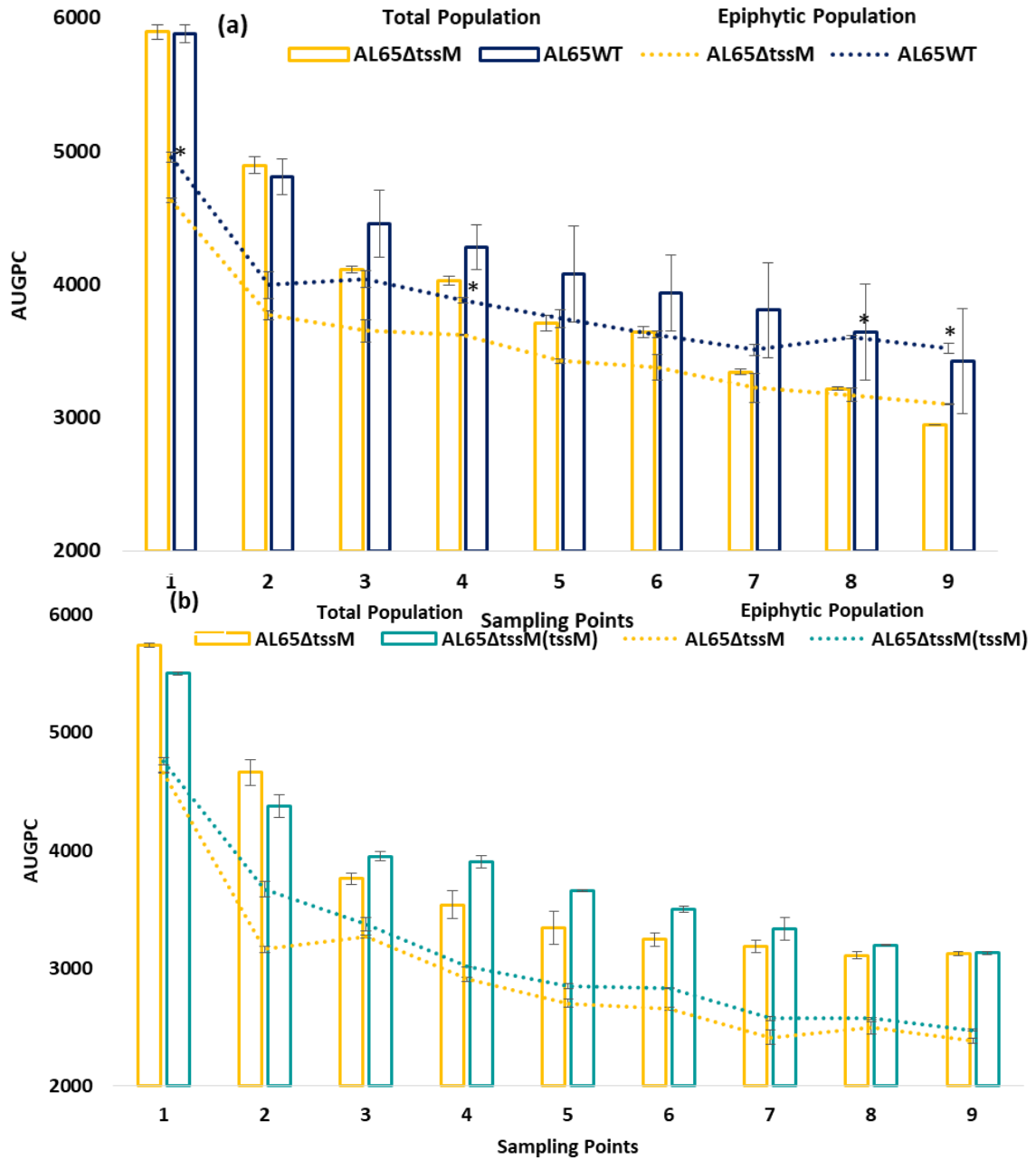


Figure 2-5: Effect of TssM on pathogenicity of *X. perforans* AL65 - Infiltration method (a) bacterial population growth (b) area under the growth progress curve calculated for each strain (c) tomato leaves 8 days after inoculation with each strain. A one-way ANOVA was applied for the statistical analysis of AUGPC and treatments with different letters are significantly

different according to Tukey's test of least significant difference ($P < 0.05$). A one-way ANOVA was applied for the statistical analysis of bacterial population \log_{10} values and disease severity values on each sampling day separately and treatments with * marks are significantly different according to Tukey's test of least significant difference ($P < 0.05$).



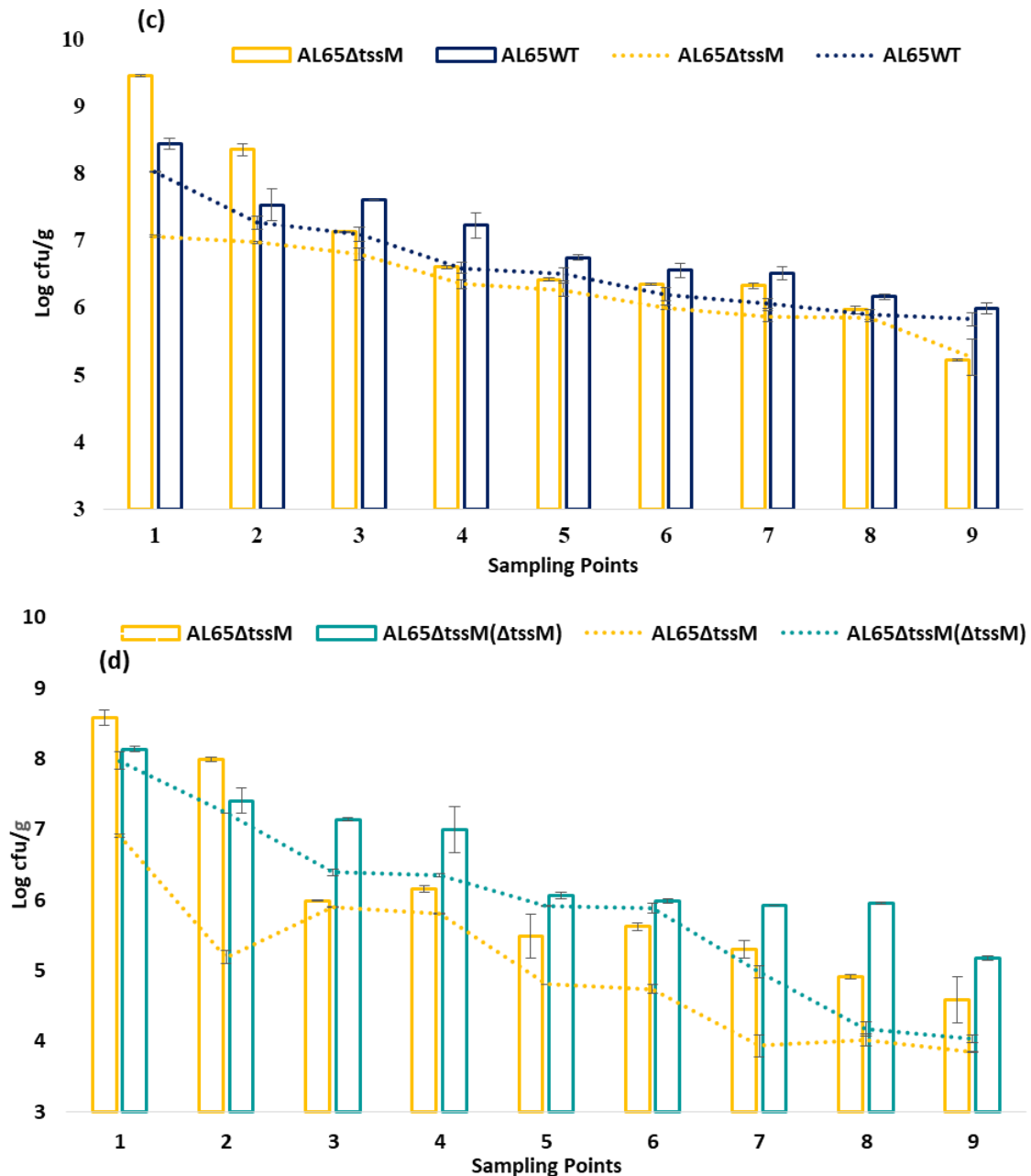


Figure 2-6: *X. perforans* survival under high-humidity conditions. (a) bars represent the total population growth inside chamber 1 where AL65^{strep} and AL65ΔtssM^{nal} were mixed inoculated while lines represent the epiphytic population growth inside chamber 1 where AL65^{strep} and AL65ΔtssM^{nal} were mixed inoculated, (b) bars represent the total population growth inside chamber 2 where AL65ΔtssM^{nal} and AL65ΔtssM(*tssM*)^{km} were mixed inoculated while lines represent the epiphytic population growth inside chamber 2 where AL65ΔtssM^{nal} and AL65ΔtssM(*tssM*)^{km} were mixed inoculated. (c) Bars represent the total population growth inside chamber 1 where AL65^{strep} and AL65ΔtssM^{nal} were mixed inoculated while lines represent the epiphytic population growth inside chamber 1 where AL65^{strep} and AL65ΔtssM^{nal} were mixed inoculated 28 dpi. (d) Bars represent the total population growth inside chamber 2

where $AL65\Delta tssM^{nal}$ and $AL65\Delta tssM(tssM)^{km}$ were mixed inoculated while lines represent the epiphytic population growth inside chamber 2 where $AL65\Delta tssM^{nal}$ and $AL65\Delta tssM(tssM)^{km}$ were mixed inoculated 28 dpi. Vertical lines represent the standard error of the mean. T-tests were done on AUGPC and log values on each sampling point separately and treatments with * marks are a significant difference ($P < 0.05$).

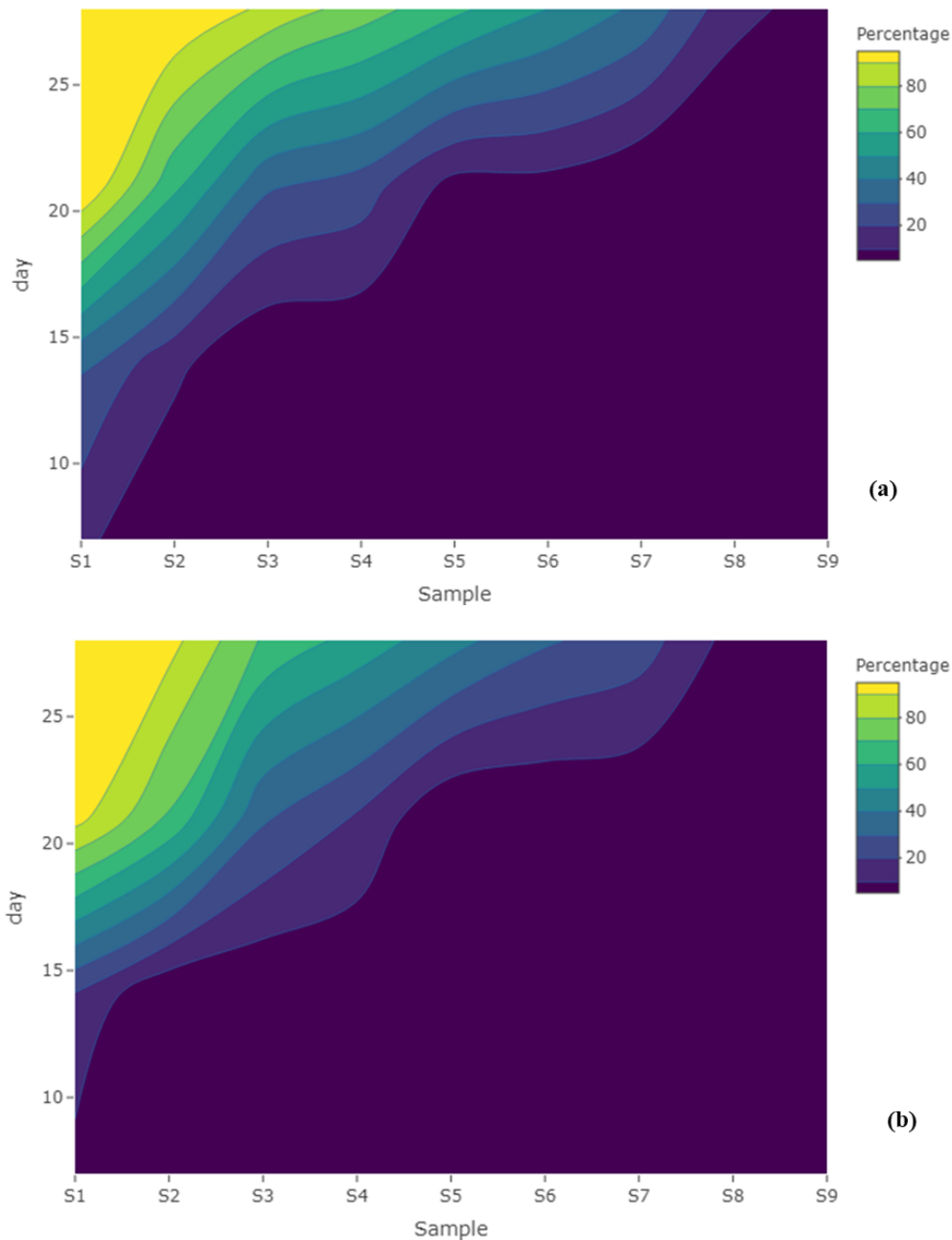


Figure 2-7: *X. perforans* disease symptom development survival under high-humidity conditions. Percentage of plants that showed disease symptoms (a) inside chamber 1 where AL65^{strep} and AL65 Δ *tssM*^{nal} were mixed inoculated (b) inside chamber 2 where AL65 Δ *tssM*^{nal} and AL65 Δ *tssM*(*tssM*)^{km} were mixed inoculated. Surface plots were created to show the development of disease severity percentages of each sampling point during the course of the experiment.

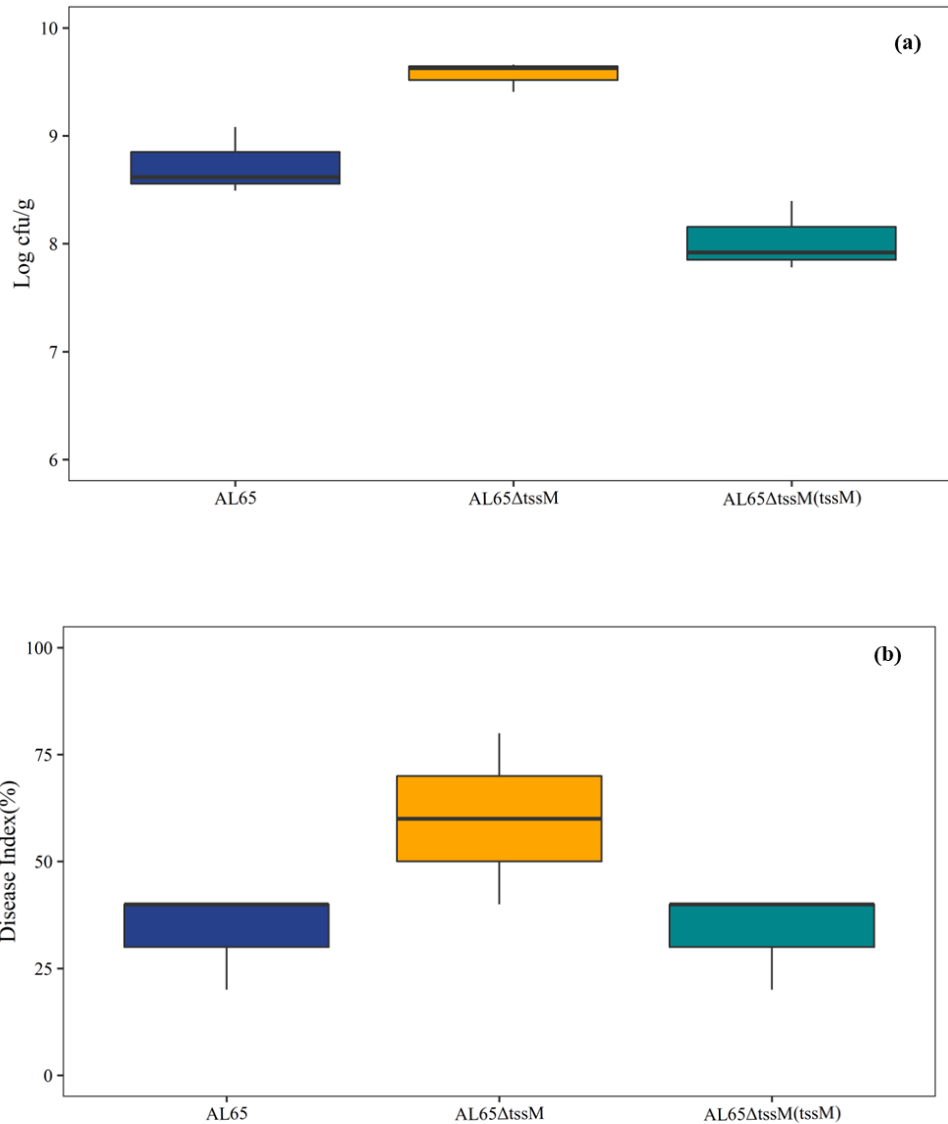


Figure 2-8: Effect of TssM on seed-to-seedling disease transmission of *X. perforans* AL65 (A) bacterial population growth and (B) disease index in tomato (cv. FL8000) seedlings. Seeds were inoculated with $\sim 1 \times 10^6$ cfu/ml of AL65, AL65ΔtssM or AL65ΔtssM(tssM) strains and seedlings were evaluated 21 days after planting. Bars with standard deviation represent the means of two independent experiments. A one-way ANOVA was applied for the statistical analysis and treatments with different letters are significantly different according to the Tukey's test of least significant difference ($P < 0.05$).

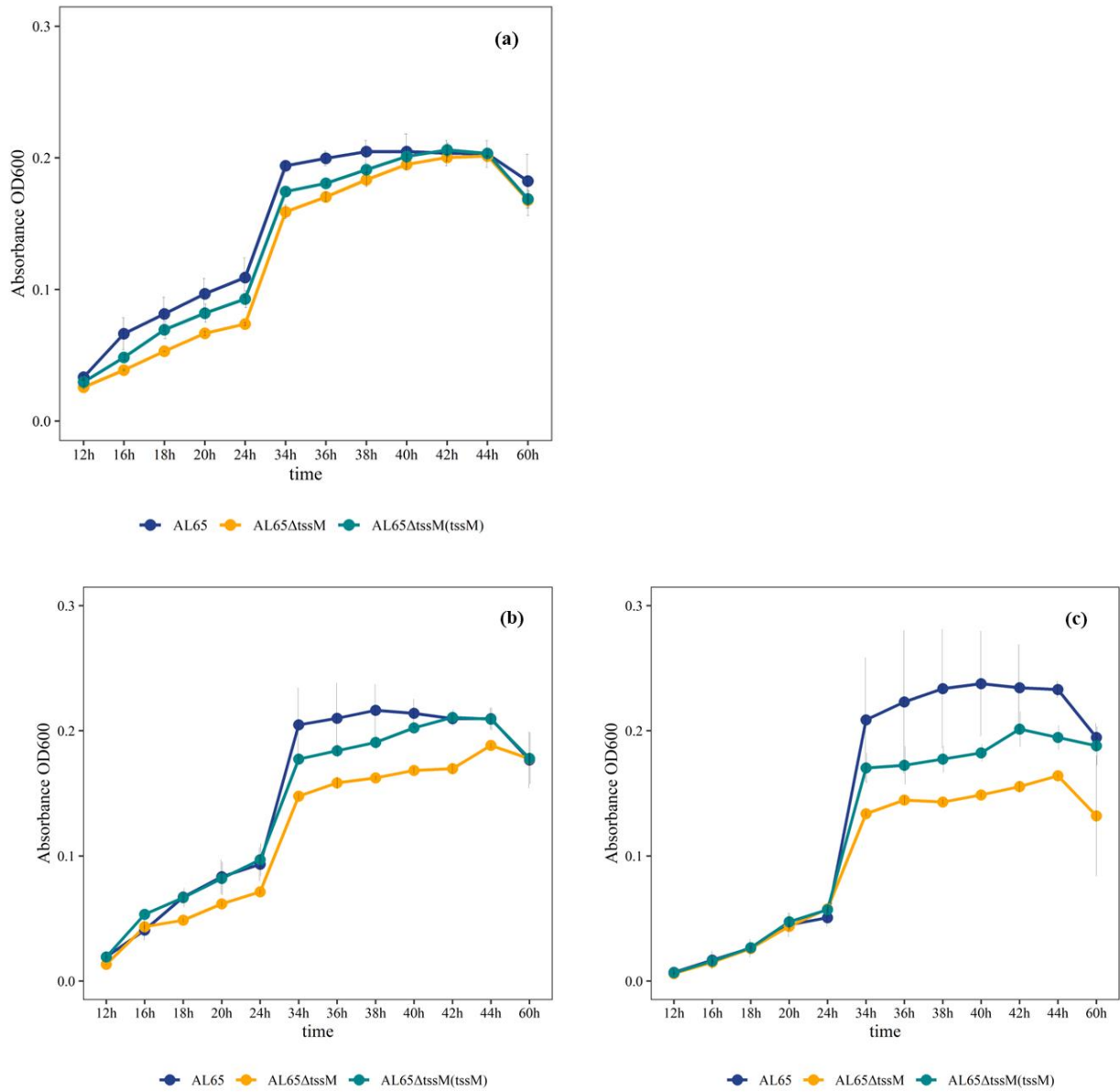


Figure 2-9: Bacterial population growth of AL65, AL65ΔtssM and AL65ΔtssM(*tssM*) strains in XVM2 media amended with different concentrations of NaCl (a) NaCl 0.02M (b) NaCl 0.1M (c) 0.2M NaCl. Lines represent the standard error of the mean.

3. CHAPTER THREE

Phylogenetic distribution and evolution of Type VI secretion system in the genus

Xanthomonas

Abstract

Bacterial species belonging to the genus *Xanthomonas* can infect and cause severe diseases in a wide range of host plants including many economically important crops throughout the world. Understanding the evolutionary history and distribution patterns of the bacterial fitness determinants is important to predict the emergence of novel pathogens and design proper disease management strategies. Our recent work with *Xanthomonas* pathogenic on tomato indicated a role of the type VI secretion system (T6SS) cluster i3* in epiphytic fitness and in turn in dictating hemi-biotrophic lifestyle of the pathogen. T6SS is a contact-dependent apparatus that can directly deliver secreted effectors or toxins into diverse neighboring cellular targets including both prokaryotic and eukaryotic organisms. In this study, we explored the distribution of the three distinguishable T6SS clusters in ~1500 *Xanthomonas* genomes, their conservation, genetic organization and their evolutionary patterns in this genus. Forty four percent of strains contain at least 2 clusters, 0.01% of strains contain all three clusters, 35% contain at least 1 cluster and 22% strains contain none.

Presence of the T6 clusters consistently in group 2 *Xanthomonas* spp. led us to hypothesize that T6SS was acquired by the ancestor of group 2 *Xanthomonas* spp. followed by its conservation or subsequent loss of individual clusters upon diversification into different clades and that individual T6SS clusters and associated effectors provided selective advantage to the species during adaptation onto specific hosts. Certain group 1 *Xanthomonas* spp. seem to have acquired it recently through a horizontal gene transfer event or recombination from members of the *Xanthomonadaceae* family. There appears to be horizontal gene transfer of *hcp* and *vgrG* among different species, which serve a dual role of being a part of T6SS structure as

well as effectors. Bioinformatic analysis recognize the role of several candidate T6SS-dependent effectors not limited to toxins, but rather in adaptation to the host environment, avoiding host defenses and in nutrient acquisition.

Introduction

Genus *Xanthomonas*, that belongs to the gamma subdivision of the phylum Proteobacteria is comprised with ubiquitous Gram-negative plant pathogenic bacteria (Jun et al., 2010). Genus *Xanthomonas* is comprised with more than 35 species, that can cause economically important diseases in more than 400 host plants (Timilsina et al., 2020). Even though a wide host range is observed with *Xanthomonas* spp., individual strains can be tightly restricted to a particular host or host group, hence the *Xanthomonas* spp. are further differentiated into pathovars based on host range and tissue specificity (White et al., 2009; An et al., 2020). To date *Xanthomonas* spp. have been isolated from host plants belonging to 124 monocotyledonous and 268 dicotyledonous species (White et al., 2009; Kyrova et al., 2020). *Xanthomonas* spp. have a higher degree of host tissue specificity and can either invade the vascular tissues or can survive in the intercellular spaces of the mesophyll parenchyma tissue (An et al., 2020). To successfully adapt into the hostile host environment, *Xanthomonas* spp. usually depend on several factors that are important for adherence to the plant surface, to invade the intercellular space of the host tissue, to manipulate plant cellular processes, to acquire nutrients, to counteract plant defense responses and also to compete with other microbes that occupy the same niche (Büttner and Bonas, 2010). Identification of these adaptation factors that contribute to host-pathogen interactions is crucial in implementing future management strategies.

Currently, there are more than 1500 *Xanthomonas* genomes publicly available in the National Center for Biotechnology Information (NCBI) database. With this availability of genome data, comparative studies have been able to identify many potential virulence

mechanisms that can contribute to pathogen virulence and host adaptation and their evolution. Secretion systems that are utilized by the bacteria to translocate proteins/ DNA directly into the host cell or into the extracellular milieu are frequently being identified as such important strategy used by many pathogenic and non-pathogenic bacteria.

In gram-negative bacteria 10 different secretion systems have been identified, but only six secretion systems (I-VI) have been described in the genus *Xanthomonas* (Meuskens et al., 2019; Alvarez-Martinez et al., 2020; Palmer et al., 2020). Even though most of these secretion systems have been extensively studied in the genus *Xanthomonas*, the role, distribution and evolutionary history of the most recently identified T6SS has been described in only a few studies (Bayer-Santos et al., 2018; Bansal et al., 2019, 2020; Bayer-Santos et al., 2019; Ceseti et al., 2019; Alvarez-Martinez et al., 2020; Choi et al., 2020; Zhu et al., 2020; Montenegro Benavides et al., 2021). Most of the above-mentioned studies used representative *Xanthomonas* spp., to derive conclusions regarding the distribution of the T6SS clusters in the whole genus *Xanthomonas*, while the evolutionary history of the T6 clusters in this genus remains unclear.

T6SS is present in about 25% of gram-negative bacteria, mainly within the phylum Proteobacterium and the classes α -, β - and γ -proteobacteria, including pathogenic, beneficial and commensal bacteria, indicating possible functions of this system unrelated to pathogenicity (Boyer et al., 2009a; Durand et al., 2014). T6SS is composed of 15-23 different proteins, including 13 core structural proteins that assemble an injectisome-like structure (Shyntum et al., 2014). Core components are named as Tss (for Type six secretion) A-M and are usually encoded in the same gene cluster (Zoued et al., 2014). Most T6 clusters are also encoded with additional subunits that are referred as Tag (Type six associated genes), and are suggested to be important in the assembly of the T6 system, transcriptional or post-transcriptional regulation of the T6 clusters or as T6 effectors/immunity proteins (Shalom et al., 2007; Boyer et al., 2009a;

Silverman et al., 2011; Coulthurst, 2013). This Tss nomenclature is now widely adopted by many while common names such as Hcp, VgrG and ClpV are also in use.

T6SS is comprised of three major complexes: the trans-membrane complex, the baseplate and the tail and together form a larger machine that extends from bacterial cytoplasm, across the bacterial cell wall and to the target cell (Silverman et al., 2012; Coulthurst, 2013; Durand et al., 2015; Nguyen et al., 2018; and Hernandez et al., 2020). The transmembrane complex made from TssM, TssJ and TssL acts as a docking site for the cytoplasmic baseplate like structure made from TssE, TssF, TssG and TssK. and act as an adaptor between the trans-membrane complex and the tail. The internal tube of the tail component is made with Hcp tubes that are assembled into the central VgrG-PAAR spike and is enclosed by a contractile sheath composed of TssB and TssC. Secretion of effector proteins through the T6SS is a one-step process that is independent of the Sec or Tat secretion machinery and is mediated through contraction of the sheath to propel the Hcp-VgrG-PAAR complex towards the target cell and deliver a cocktail of effectors in each contraction. Unlike other secretion systems, after each firing event T6 tube disassembles and Hcp is lost to the extracellular milieu. AAA + ClpV (TssH) ATPase is recruited to the contracted sheath to disassemble the complex and to recycle the sheath components for the next round of firing. Apart from being core components of the T6SS, Hcp (hemolysin co-regulated protein) and VgrG (valine-glycine repeat protein G) also have been identified as specialized effectors important in antibacterial activity in several pathogen systems (Lien and Lai, 2017; Ma et al., 2017). Effectors that get delivered via the T6SS are either categorized as ‘Cargo’ or ‘specialized’ effectors and interact with the Hcp-VgrG-PAAR complex non-covalently or covalently respectively. ‘True’ T6 effectors or effectors that have no role in the secretion machinery or process (unlike VgrG or Hcp) but dedicated effector proteins are usually found within the T6 cluster or sometimes in the other parts of the genome (Hernandez et al., 2020).

Depending on the 13 core proteins, T6 clusters have been separated into 4 subtypes (T6SS^{i-iv}). The majority of the proteobacteria have T6 clusters belonging to the subtype T6SSⁱ and due to the diversity observed in this subgroup, it has been further subdivided into 5 phylogenetic clades (I-V) (Boyer et al., 2009a). Bacteria belong to the family Xanthomonadaceae harbor three of the subtypes of T6SSⁱ, including clades i1, i3 and i4, while genus *Xanthomonas* only has T6 clusters belong to i3 and i4 clades (Bayer-Santos et al., 2019; Alvarez-Martinez et al., 2020). *Xanthomonas* i3 clade can be further subdivided into two distinct subclades as i3* and i3*** based on the phylogenetic analysis conducted using *tssC* gene (Bayer-Santos et al., 2019). All the *Xanthomonas* species that have i3 T6SS cluster lack *tssJ*, core component in the outer membrane complex in T6 machinery (Alvarez-Martinez et al., 2020). T6SS-i3* and i3*** show differences in their genetic architecture, for example, i3* cluster in *X. euvesicatoria* 85-10 is about 40kb (XCV4202-XCV 4243) while the i3*** cluster is about 20kb (XCV2120 - XCV2143) and the difference in the cluster sizes are due to the presence of genes encoding hypothetical proteins and transcriptional regulators in each cluster (figure 3-1) (Boyer et al., 2009a; Abendroth et al., 2017; Alvarez-Martinez et al., 2020).

Similar to observations with other bacteria, some *Xanthomonas* spp. have both i3* and i3*** or one copy from each of these two subclades together with the i4 cluster or without it (Bingle et al., 2008; Alvarez-Martinez et al., 2020). These multiple copies of T6 gene clusters are believed to be acquired by independent horizontal gene transfer events, indicating the possibility of different roles played by the T6 clusters in different bacteria (Bingle et al., 2008; Blondel et al., 2009; Boyer et al., 2009a). In *X. oryzae* pv. *oryzae*, one T6 cluster is distantly related to the *phaseoli* clade while the second cluster forms a monophyletic clade with i3*** cluster of *X. euvesicatoria* and *X. perforans*, implicating a recent common origin (Montenegro Benavides et al., 2021).

The goal of this study is to harness a large set of publicly available *Xanthomonas* genomes spanning the entire genus *Xanthomonas* with multiple strains of important pathogenic species and study the conservation, genetic organization and evolutionary patterns of multiple clusters of T6SS. We hypothesize that the acquisition of the multiple T6SS clusters occurred as independent events during the adaptation of *Xanthomonas* species on specific hosts as they diverged into various clades. Specific cases of loss or gain events happened in certain clades as an adaptation to vascular or non-vascular lifestyle. Identification of the putative T6 effectors is important to predicting the strategies used by these pathogens for successful adaptation to the host environment.

Methodology

Construction of T6 core gene phylogenies

T6 core gene based phylogeny was generated using the automated multi-locus sequence analysis pipeline (automlsa2) as previously described (Davis et al., 2021). Briefly, T6SS core genes in each cluster were identified according to the previous literature (Potnis et al., 2015; Montenegro Benavides et al., 2021) and reference nucleotide sequences from *X. euvesicatoria* 85-10 (clusters i3* and i3***) and *X. oryzae* pv. *oryzae* str. PXO99 (cluster i4) were used as queries to retrieve homologous sequences from the genomes downloaded from NCBI GenBank dataset on April 07, 2021. A total of 1577 complete genome sequences were retrieved from the NCBI GenBank, were used in the makeblastdb tool to create a local blast DB and used in the BLASTN+ (v. 2.11.0) to identify and extract the sequences. BLASTN analysis was done with slight alterations to the default values, where coverage was set to 30 and identity was changed to 50 while keeping 1e-05 as the e-value. Each sorted output multi-FASTA file was aligned using the MAFFT (v.7.471) (L-ins-I algorithm). Phylogenetic tree in maximum likelihood (ML) criterion was developed using the IQ-TREE multicore version 2.1.2 COVID-edition, using aligned nexus file generated as the output file of the MAFFT. ‘-m MFP’ function was

used for the model selection while ‘--merge rclusterf’ was used for partition finding. Branch support was determined using 1000 bootstraps and 1000 SH-aLRT bootstrap replicates (-B 1000, -alrt 1000). Nodes with the $\geq 80\%$ support with the SH-aLRT and $>80\%$ with normal bootstrap supports, were considered well supported (Davis et al., 2021). The ML tree in NEWICK format was visualized using the tree viewer program: FigTree v1.4.4 (Rambaut et al., 2018).

Splitstree analysis for homologous recombination visualization

To identify and visualize possible conflicting signals, that would suggest possible recombination events and evolutionary relationships within sequence data, phylogenetic networks were developed using the Splits Tree4 (version 4.17.0) (Huson and Bryant, 2006). Concatenated T6 core genes from each cluster were used to generate splitstree files, for a selected subset of genomes using the above-mentioned automlsa pipeline. Resultant splits.nex files were visualized using the Splits Tree4 (version 4.17.0), using rooted equal angle algorithm (Gambette and Huson, 2008). The possibility of recombination events was identified by the branches that form parallelograms (Joseph and Forsythe, 2012).

Multi-locus sequence analysis

Multi-locus sequence analysis using 12 housekeeping genes was performed on the 1577 complete genome sequences retrieved from the NCBI GenBank. Housekeeping genes, *atpD* (ATP synthase β chain), *dnaK* (70-kDa heat shock protein), *efp* (elongation factor P), *fusA* (Translation elongation factor aEF-2), *fyuA* (transmembrane protein; Ton-B-dependent transporter), *gapA* (glyceraldehyde 3-phosphate dehydrogenase), *glnA* (glutamine synthetase I), *gltA* (citrate (Si)-synthase gene), *gyrB* (DNA gyrase β subunit), *lacF* (sugar ABC transporter permease), *lepA* (GTP binding protein) and *rpoD* (RNA polymerase sigma 70 factor) previously described in the literature were used in the MLSA analysis (Young et al., 2008; Fischer-Le Saux et al., 2015; Timilsina et al., 2015). Phylogeny was generated using the

automated multi-locus sequence analysis pipeline (automlsa2), and phylogenetic tree in maximum likelihood (ML) criterion was developed using the IQ-TREE multicore version 2.1.2 COVID-edition using the parameters as described in the previous section. The ML tree in NEWICK format was visualized using the tree viewer program: FigTree v1.4.4 (Rambaut et al., 2018)

Construction of core genome phylogeny

For the reconstruction of the core genome phylogeny Roary was used (Page et al., 2015). All the genomes downloaded from the NCBI GenBank in the .fna format were first annotated using the Prokka (v1.14.5) software tool (Seemann, 2014). After annotating the genome to determine the location and attributes of the genes contained in them, the resultant .gff file in the GFF3 format was used as the input file to perform the pan-genome analysis using Roary. Roary extracted the coding sequences from the input GFF3 files, converted them into protein sequences, removed partial clusters and created pre-clusters. Next Roary performed BLASTP with 95% sequence identity and the sequences were clustered with Markov cluster (MCL) algorithm. As the next step, Roary generated clusters and obtained the true orthologs. Finally Roary identified core genes and generated a concatenated core gene alignment that can be used to generate maximum like hood phylogeny using RAxML (v 8.2.12) (Randomized Axelerated Maximum Likelihood) (Stamatakis, 2014).

Identification of T6SS clusters across genomes of *Xanthomonas*

The NCBI GenBank database was used to identify homologs of the T6 clusters encoded by *X. euvesicatoria* 85-10 (clusters i3* and i3***) and *X. oryzae* pv. *oryzae* str. PXO99 (cluster i4), using the BLASTP and TBLASTN (v2.11.0) with default parameters (Camacho et al., 2009). To confirm the presence of the whole T6 clusters, positive hits from the BLAST search were further analyzed to identify their locus tags to search the neighboring genes. To further confirm the presence of T6 clusters, we used the Integrated Microbial Genomes &

Microbiomes (IMG/M) (v.6.0) system and genome and microbiome datasets sequenced at DOE's Joint Genome Institute (JGI), using the above-mentioned genomes as references (Chen et al., 2021; Mukherjee et al., 2021). Gene Neighborhood tool and IMG genome BLAST options were used to identify gene synteny and cluster organization (Chen et al., 2021).

Identification of T6 effectors

Amino acid sequences of each core and accessory genes in T6 clusters of the selected genomes were used to predict the T6SS effectors using the Bastion6 machine-learning tool, which is a two-layer support-vector machine (SVM) -based ensemble model with optimized parameters (Wang et al., 2018). In the development of this tool, features of the amino acid sequences including, sequence profile (based on three types of sequence-derived features, including amino acid composition (AAC), dipeptide composition (DPC) and Quasi-Sequence-Order descriptors (QSO)), evolutionary information (using the Blocks substitution matrix (BLOSUM), A position-specific scoring matrix (PSSM), S-FPSSM and Pse-PSSM models) and based on physicochemical property (based on CTDT and CTDC, which describe the global composition of the amino acid properties in protein sequences) were taken into the consideration (Wang et al., 2018). We utilized this program to search for T6SS effectors in selected *Xanthomonas* spp., using the amino acid sequences of the T6 gene clusters of each species. Predicted putative effectors were selected based on an ensemble model result score of ≥ 0.5 (Kumar et al., 2020).

Results

Distribution of T6 clusters in the genus *Xanthomonas*

In this study, we analyzed 1577 complete genome sequences, belong to 37 *Xanthomonas* spp. retrieved from the NCBI GenBank. A large proportion of the sequenced genomes belong to the species *X. oryzae* (388 genomes), *X. citri* (194 genomes), *X. phaseoli* (155 genomes), *X. perforans* (149 genomes) and *X. arboricola* (139 genomes). When the

nucleotide sequences of the core genes in the T6SS clusters were used in the BLAST analysis, the presence of three T6 clusters belonging to clade i3 (i3* and i3 ***) and i4 were identified across the genus. Among the 1577 genomes analyzed, T6SS-i3*** was identified in 417 genomes, T6SS-i3* in 608 genomes and 489 genomes had the complete T6SS-i4 cluster.

To further study the sequence cluster organization as well as flanking genes, representative, strains of pathogenic *Xanthomonas* spp. were chosen. Core genome phylogeny was generated for the genus *Xanthomonas* reference strains and used to map the distribution of each T6 cluster (figure 3-2). Complete T6 clusters were identified in 29 genome sequences while only incomplete T6 clusters were observed in 4 of the tested *Xanthomonas* spp. including, *X. campestris* pv. *campestris* ATCC33913, *X. nasturtii* WHRI885, *X. prunicola* CFBP8353, *X. pisi* DSM18956. When considering all the strains belong to *X. campestris* pv. *campestris*, ~58% of the strains were with partial T6 clusters while all the remaining *X. campestris* pv. *campestris* were encoded with either i3* or i3*** complete clusters (table 3-1). Interestingly, all the sequenced *X. nasturtii* and *X. prunicola* strains only encoded with single T6 core genes, *tssA* and *tssB* respectively. Moreover, between the two *X. pisi* strains, DSM 18956 T6SS-i3* cluster was missing *tssK*, *tssL* and *tssM* core genes from the cluster while *X. pisi* CFBP4643 was encoded with a complete T6SS-i3* cluster.

Among early-branching strains, also known as group 1, T6SS-i3*** cluster was identified in *X. hyacinthi* CFBP1156 and *X. translucens* pv. *translucens* DSM18974. Interestingly, according to BLAST results, T6SS-i3*** core genes in *X. hyacinthi* CFBP1156, showed more nucleotide similarity to *Luteibacter rhizovicinus* DSM16549 strain (100% Query cover & ~100% percent identity), than other species in the genus *Xanthomonas*. *Luteibacter rhizovicinus* is a Gammaproteobacterium in the order *Xanthomonadales* isolated from the rhizosphere of barley (*Hordeum vulgare*) (Johansen et al., 2005). Most of the core genes in the *X. translucens* pv. *translucens* DSM 18974 had higher nucleotide similarities to *Lysobacter*

enzymogenes belongs to the *Xanthomonadaceae* family and have identified as a ubiquitous environmental bacterium (Zhao et al., 2017). Interestingly, *X. translucens* F5 non-pathogenic *Xanthomonas* spp. isolated from pepper plants has the T6SS-i3* cluster, this observation gains our attention to the possible acquisition of the T6 clusters by individual strains within the early-branching clade.

The distribution pattern of complete and partial T6 clusters were identified within the group 2 *Xanthomonas* spp. and visualized in figure 3-2. T6 clusters were not identified in group 2 clade A, while all the three T6 clusters were identified in clade B, which consisted of the two strains belong to *X. maliensis*. In the group 2 clade C, distribution of the i3* cluster was identified in all the species, while *X. codiaei* CFBP4690 was also encoded with a partial i3*** cluster. Species belonging to the *X. hortorum* complex were identified in the clade D, and few of the strains in this clade were identified with complete and partial i4 clusters. Among the species clustered together in clade E, *X. bromi* was the only species with the complete i4 cluster while all the other species were encoded with complete and partial i3* cluster. According to the core genome phylogeny, *X. nasturtii* was identified as a separate clade (F), and as mentioned in the previous section, both of the strains belong to *X. nasturtii* were encoded only with *tssA* gene of the i3* cluster. Most of the species that belong to the axonopodis complex (clade F) that is comprised of several leaf associated *Xanthomonas* species including *X. perforans*, *X. euvesicatoria* and a majority of the *X. phaseoli* were encoded with both i3* and i3***, except for *X. axonopodis* DSM3585, *X. citri* pv. *citri* LMG9322. Among the 155 *X. phaseoli* genomes, 98 strains were with the only i3* while 52 strains had both i3* and i3***. Interestingly, in this analysis, we were also able to identify two *X. phaseoli* strains (*X. phaseoli* pv. *phaseoli* NCPPB220 and NCPPB1138) with i4 cluster together with the i3* cluster. The presence of both i3* and i4 clusters were only observed in *X. phaseoli* and 11 *X. citri* species. In *X. citri*, even though the representative strain LMG9322 was only found with a complete i3*

cluster, 12 strains out of 194 strains were found with a complete i4 cluster along with the i3* cluster, while a majority of the strains have a single i3* cluster (table 3-1). Strains belonging to *X. axonopodis* were identified with either complete i3* with partial i3*** cluster or complete i3*** with partial i3* cluster and interestingly *X. axonopodis* LPF_602 was encoded with complete i3* cluster and partial i4 cluster separating it as the only strain with partial i4 cluster in the axonopodis complex. All the strains belonging to the *X. vasicola* were found with either complete or partial i3*** clusters, while *X. oryzae* that share the clade H with *X. vasicola* were mostly encoded with both i3*** and i4 clusters, while only i4 cluster was identified in 69 *X. oryzae* strains. *X. oryzae* cluster i4 was not present as a single cluster, but in two separate genomic loci, and about 20 *vgrG* (*tssI*) genes were dispersed throughout the *X. oryzae* genomes. According to core genome phylogeny, *X. campestris* was found as a separate clade (I) and complete and partial i3* and i3*** clusters identified. To summarize the above findings, i4 cluster was identified in *X. oryzae* species, *X. maliensis* and most of the spp. that belong to the hortorum complex. I3*** cluster was only observed in the axonopodis complex, *X. oryzae*, *X. maliensis* and few early-branching *Xanthomonas* spp. Partial i3*** cluster was observed only in *X. codiae* CFBP4690 (7027 bp) (figure 3-2).

Size of the each T6 clusters were also compared in this study. Most of the species with complete i3* cluster were encoded with 49-60kbp in size, while the i3* cluster in *X. cucurbitae* CFBP2542 was about 70kbp. i3*** clusters with 23-28kbp in size were identified in the analyzed genomes while determining the size of the i4 cluster was not possible due to the presence of the i4 cluster in two loci.

When the T6 cluster distribution in the genus *Xanthomonas* was further analyzed at the species level, it was revealed that within a single species there can be strains with complete single T6 cluster, more than one T6 clusters, partial T6 clusters as well as some strains without T6 clusters.

When we consider *X. phaseoli*, ~96% of the strains encoded at least 1 complete T6 cluster, 0.64% with only partial T6 clusters while in 2.5% of the strains T6 clusters were not identified. On the contrary, in *X. arboricola* only 5% of the strains were with T6 clusters, while 0.2% with partial clusters and ~95% strains were not encoded with any T6 clusters, indicating T6 is not a rule in *X. arboricola* (table 3-1).

Among the analyzed genomes, presence of a single T6 core gene (*tssC*), was observed in the 342 genomes (mostly consisted of *X. phaseoli* and *X. citri*). In *X. phaseoli* 100 genomes were identified with the *tssC* gene in the i3*** clusters while the majority of those genomes were also encoded with a complete i3* cluster. On the contrary, in some of the *Xanthomonas* spp., absence of a single core gene was observed, while other components of the T6 cluster was present. While the *clpV* core gene was absent in the i4 cluster of some of the *X. oryzae* genomes, most of the genomes consisted of a complete set of T6 core genes in the i4 cluster. Partial/incomplete T6 clusters were further observed in *X. pruni*, *X. dyei*, *X. pisi*, *X. sp.*, and *X. massiliensis*, possibly indicating recent loss of the T6 clusters in these strains (table 3-1 and figure 3-3).

Evolutionary history of the i3* cluster in *Xanthomonas* spp.

To study the genomic environments of T6SS-i3* cluster in different *Xanthomonas* spp., we compared the upstream and downstream regions (5 genes up and down) based on the synteny and similarities of the genes (figure 3-4).

As previously described, the T6SS-i3* cluster is present in the early-branching species, *X. translucens* F5, non-pathogenic *Xanthomonas* spp. isolated from pepper plants, while i3* core genes were not identified in any of the other species in the same clade. When we observe the flanking regions of these early-branching *Xanthomonas* spp., we could identify similar and unique flanking genes, immediately up and down stream regions of the i3 synteny (even in the absence of the T6 clusters) in most of the early-branching *Xanthomonas* spp., except for *X.*

translucens F5. The upstream region of the *X. translucens* F5 is similar to several *Xanthomonas* spp. that have the i3* cluster while it showed a unique downstream region, indicating a complete replacement of the downstream region (figure 3-4). With these observations we could assume the i3* cluster might have been independently acquired and insertion of the i3* locus has occurred in the same genomic region in the *X. translucens* F5. This acquisition of the i3* cluster by *X. translucens* F5 could be due to a gene exchange between *Xanthomonas* spp. that reside the pepper plants including *X. perforans* and *X. euvesicatoria* that frequently isolated from the pepper phyllosphere or due to the gene exchange with any other *Xanthomonas* or non-*Xanthomonas* spp. due to the commensal nature of this bacterium. To identify the closely related bacteria to the T6SS-i3* cluster in *X. translucens* F5, each core gene in the cluster was used in BLAST analysis. According to the analysis, T6SS-i3* cluster core genes in *X. translucens* F5 showed 61-97% identity to Xe85-10, while percent identities above 95% resulted with unclassified *Xanthomonas* spp., SI, SS, GW, which have been isolated from the seed microbiome of perennial ryegrass (table 3-2).

Flanking regions of the i3* cluster of most of the *Xanthomonas* spp. were conserved and mostly less than 15 CDS were found between the flanking regions if the i3* cluster was absent, except for *X. fragariae* PD885 and *X. hyacinthi* CFBP1156 that contained 76854 bp and 181557bp genomic regions respectively in between the flanking regions (figure 3-4). As mentioned earlier, species belong to the hortorum complex lack the i3* cluster but when the i3 synteny was further examined, even in the absence of the i3* core genes, presence of two i3* accessory genes (Serine/threonine protein kinase and RNA polymerase sigma factor (TIGR02999 family) was conserved between the flanking regions. Similarly in *X. oryzae* pv. *oryzicola* CFBP7342, in the i3 synteny a Jacalin-like lectin domain-containing protein, which is also an accessory gene commonly found in the i3* locus, was identified in-between the up and downstream flanking regions. Furthermore, it was observed that single i3* core genes or

partial i3* clusters are randomly distributed among the group 2 *Xanthomonas* spp., as observed with *X. prunicola* (only *tssB* gene), *X. campestris* ATCC33913 (only *tssA* gene) and *Xanthomonas pisi* i3* cluster (absence of a couple of core genes in the middle of the cluster). Collectively these observations suggest possible acquisition of the i3* cluster from a common ancestor of *X. axonopodis* and *X. campestris*, which upon subsequent diversification into separate clades experienced loss events by specific strains or clades during niche adaptation.

Comparison of the *Xanthomonas* T6 phylogeny to *Xanthomonas* multi-locus phylogeny

To better explore the evolutionary origin and distribution of the T6SS clusters and to use as a reference to infer the evolutionary patterns in the genus *Xanthomonas*, a robust phylogeny was generated using concatenated 12 housekeeping genes (*atpD*, *dnaK*, *efp*, *fusA*, *fyuA*, *gapA*, *glnA*, *gltA*, *gyrB*, *lacF*, *lepA* and *rpoD*) (figure 3-5). MLSA phylogeny was compared to that of the T6SS-i3^{***}, i3* and i4 core gene phylogenies. Incongruencies among the MLSA phylogeny and that of T6SS-i3* and i3^{***} were noted among *X. perforans* and *X. euvesicatoria* and incongruencies between the MLSA phylogeny and T6SS-i4 cluster phylogeny were also observed in *X. translucens* and *X. fragariae*.

Hcp and VgrG are the components of the T6SS spike complex and can be hypothesized to be highly variable due to their role as effectors. To investigate if the T6 effectors *hcp* and *vgrG* contribute to the incongruencies observed among the above phylogeny comparisons, both of these gene sequences were removed from the concatenated T6 core gene query file and the phylogenies of T6SS core genes without *hcp* and *vgrG* sequences were re-constructed for the T6 clusters (figure 3-6). Incongruencies between T6 core gene phylogeny with and without *vgrG* and *hcp* were observed in *X. perforans*, *X. euvesicatoria*, *X. translucens* and *X. fragariae* strains indicating different evolutionary patterns for *vgrG* and *hcp* compared to that of other core genes. When the phylogeny for the cluster i3^{***} without *hcp* and *vgrG* was compared to that of the MLSA phylogeny, strains belong to the *X. perforans* and *X. euvesicatoria* showed

inconsistent placement. Interestingly, when the i3* phylogeny without *hcp* and *vgrG* was generated and compared to the MLSA phylogeny, previously observed incongruencies between the i3* phylogeny and MLSA phylogeny in *X. perforans* had been resolved, while incongruencies were still visible in *X. euvesicatoria*.

Given our observation of incongruencies among the MLSA phylogeny and T6SS core gene phylogeny without *hcp*, *vgrG*, we hypothesized that there is genetic exchange of the T6 core genes among different strains belonging to different species. We constructed phylogenetic networks using SplitsTree which can demonstrate conflicting signals for phylogenetic placements as reticulation. We observed reticulation at the base of the branches connecting, *X. perforans* NI1, *X. euvesicatoria* CFBP6369, *X. sp* A1809, *X. euvesicatoria* DAR26930, *X. phaseoli* A1962, *X. phaseoli* LMG12749, *X. euvesicatoria* F1, *X. euvesicatoria* LMG12749, *X. euvesicatoria* LMG495, *X. euvesicatoria* CFBP3836, *X. euvesicatoria* CFBP3371, *X. axonopodis* LMG26789, *X. euvesicatoria* NI38, *X. euvesicatoria* CFBP7921, *X. axonopodis* CFBP7922, *X. phaseoli* NCPPB1713, *X. campestris* LMG954, *X. citri* LMG859, *X. citri* Bagalkot, *X. citri* LMG7439, *X. axonopodis* LMG753, *X. campestris* LMG940, *X. axonopodis* LMG9049, *X. campestris* LMG939, *X. axonopodis* LMG9050, *X. citri* 12609, *X. axonopodis* LMG558, *X. campestris* LMG9044, *X. phaseoli* NCPPB1158, *X. citri* NCPPB3660, *X. phaseoli* NCPPB1495, *X. citri* NCPPB1495, *X. citri* NCPPB1056, *X. euvesicatoria* 85-10 and *X. perforans* 91-118 in the split decomposition tree generated for T6SS-i3* without *hcp* and *vgrG* (figure 3-7a). Branches connecting, *X. perforans* NI1, *X. euvesicatoria* CFBP 6369, *X. sp* A1809, *X. euvesicatoria* DAR26930, *X. phaseoli* A1962, *X. phaseoli* LMG12749, *X. euvesicatoria* F1, *X. euvesicatoria* CFBP3371, *X. euvesicatoria* LMG495, *X. euvesicatoria* CFBP3836, *X. campestris* NLP121, *X. campestris* NLP172, *X. campestris* LMCP25, *X. phaseoli* NBC703, *X. axonopodis* CFBP5823, *X. euvesicatoria* 85-10 and *X. perforans* 91-118

in the split decomposition tree generated for T6SS-i3*** without *hcp* and *vgrG* were also showing possible recombination events (figure 3-7b)

T6SS in non-pathogenic and environmental strains

Since the T6 clusters were not identified in all the pathogenic *Xanthomonas* spp., a possible role of this secretion system can be beyond pathogenicity. Furthermore, identification of the T6 clusters in the non-pathogenic or environmental isolates can provide added clarification to the possible unidentified functions of this system. To identify the distribution of T6 clusters in 13 strains collected from rainwater and 16 non-pathogenic *Xanthomonas* collected from tomato, beans, citrus, pepper and rice seed/leaf phyllosphere were included in a core genome phylogenetic analysis (table 3-3). Among the non-pathogenic *Xanthomonas* species, *X. maliensis* strains, previously mentioned early-branching strain *X. translucens* F5 and *X. floridensis* WHRI8848 were having i3* cluster encoded in its genome. Interestingly *X. maliensis* have both i3* and i3 *** clusters and a i4 cluster compared to other non-pathogenic rice leaf associated *Xanthomonas* species such as *X. sontii* and *X. sacchari* R1, that do not have any T6SS cluster encoded in their genome and rice pathogenic *X. oryzae* pv. *oryzae* and *X. oryzae* pv. *oryzicola* that only has i3 *** and i4 cluster, it's interesting to discover all three T6 clusters in non-pathogenic *X. maliensis*. Similarly, non-pathogenic *X. floridensis* WHRI8848, has a complete i3* cluster while watercress pathogenic *X. nasturtii* WHRI8853 only has a single i3* core gene with flanking regions similar to the *X. floridensis*.

Among the *Xanthomonas* strains collected from the rainwater, two *X. arboricola* strains (*X. arboricola* 4461 and 3793) were encoded with T6SS-i3*. When all the *X. arboricola* genomes were further examined, it was identified that some of the strains have a partial *tssB* gene, with some accessory T6SS-i3* genes encoded in the synteny of i3* cluster with similar flanking regions. *tssB* gene in *X. arboricola* pv. *juglandis* CFBP2528 is showing only 27% query cover and 89% identity to the *tssB* gene in *X. euvesicatoria* 85-10, but the gene size of

the *tssB* (621 bp) in *X. arboricola* pv. *juglandis* is bigger than the *tssB* gene in *X. euvesicatoria* 85-10 (510 bp) or the two *X. arboricola* strains that have the complete *i3** clusters. Interestingly, along with the partial *tssB* gene, *X. arboricola* pv. *juglandis* CFBP2528 and several other *X. arboricola* genomes encode a few *i3** accessory genes (Serine/threonine protein kinase and RNA polymerase sigma factor (TIGR02999 family) similar to our observations with *X. horotorum* complex and *X. oryzae* pv. *oryzicola*. tRNA (aspartyl-tRNA (Asn)/glutamyl-tRNA(Gln) amidotransferase subunit A) was also conserved in *X. arboricola* pv. *juglandis* CFBP 2528 and several other *X. arboricola* genomes in the *i3** synteny.

Identifying T6SS clusters in non-pathogenic strains, brings out the question of why bacteria with T6SSs dedicate a vast energy expenditure to the production of T6SS proteins? When the T6 effector profiles of the *X. arboricola* 4461 and 3793 were compared to its closely related *X. pisi* to identify any unique T6 effectors in these non-pathogenic strains, we couldn't identify effectors common to the two *X. arboricola* but were absent in the *X. pisi* CFBP 4643. One of the identified T6 effectors (type 1 glutamine amidotransferase) was common to the compared three strains and a cubico group peptidase and a hypothetical protein (132aa) was unique to the *X. arboricola* 4461 while another hypothetical protein (145aa) was unique to *X. arboricola* 3793 strain. These identified effectors need further study to identify if they have any function related to the non-pathogenic lifestyle of these pathogens.

Contribution of the T6SS for the evolutionary history of the *X. axonopodis* complex

Identification of both *i3** and *i3**** clusters and the conserved synteny in the T6SS-*i3** locus found in the species belong to the *axonopodis* complex, it can be hypothesized that the *axonopodis* complex has acquired the T6 clusters before divergence into different pathovars. Given that *axonopodis* evolutionary history has been recently well studied and the first step of generalist diversification into the *X. axonopodis* subgroups followed by the second step of ecology-driven specialization that favored the emergence of novel pathovars has been well

described (Mhedbi-Hajri et al., 2013), we closely examined the patterns of the evolutionary history of the i3* and i3*** T6 clusters in the *X. axonopodis* complex

In this current study, we hypothesized that T6SS clusters were acquired by the ancestor of Group 2 xanthomonads and upon subsequent diversification into separate clades, individual species either retained or lost T6SS clusters during the process of niche adaptation that provided significant advantage during lifestyle of a vascular vs non-vascular mode and dicot vs monocot pathogens.

When the distribution of the T6 clusters was examined according to the subspecies group they belong to, it was observed that strains belonging to the same subgroup are having a similar distribution of the T6 clusters except for *X. phaseoli* pv. *dieffenbachiae* LMG695 in subgroup 9.4. Strains belonging to subgroup 9.2 and *X. phaseoli* pv. *dieffenbachiae* LMG695 in subgroup 9.4 have both complete clusters while, strains belong to subgroups 9.4, 9.5 and 9.6 have complete i3* clusters. Subgroup 9.3 is only having a complete i3*** cluster, along with an incomplete i3* cluster with 1-3 core genes (table 3-4). Interestingly, 9.3 is the only subgroup that has strains pathogenic only on monocot plants. *X. axonopodis* pv. *axonopodis* belong to subgroup 9.3 are pathogenic on *Axonopus scoparius* while *X. axonopodis* pv. *vasculorum* are pathogenic on *Saccharum officinarum*. All the other subgroups consist of strains that are pathogenic on dicot plants, except for *X. axonopodis* pv. *allii* (9.2) that is pathogenic on *Allium* sp..

To determine if the T6 clusters follow the same evolutionary history as the species belonging to the *X. axonopodis* complex, a phylogeny based on the T6 core genes in i3*/i3*** clusters were compared with the phylogenies generated based on the core genome of stains with either i3* or i3*** core genes encoded in their genomes. According to the core genome phylogeny and i3* or i3*** core genes phylogeny, similar clustering of the subgroupings were observed. This observation confirms the previous hypothesis where we suggested a common

origin of the T6 clusters before the divergence of the pathovars. Interestingly in the phylogeny based on *i3** or *i3**** core genes, clustering of the subgroup clades indicates incongruencies compared to the core gene phylogeny (figure 3-8). Core genome phylogeny clustered subgroups 9.2 and 9.4 in a single clade while *i3**** phylogeny clustered subgroups 9.4 and 9.3 in one clade while *i3** phylogeny indicates an early divergence in the subgroup 9.4. Clustering of subgroups 9.5 and 9.6 shows the same arrangement when core genome phylogeny was compared to the *i3** phylogeny. These difference in the phylogeny hints at a possible evolution pattern in T6 clusters independent of its core genome evolution thus further confirming T6 plays a major role in host adaptations.

We further assessed the distribution of T6 clusters according to the vascular and non-vascular mode of colonization as well as preferred dicot vs monocot host. More of the dicotyledonous species contain T6SS-*i3**, while most of the monocotyledonous host plants infecting *Xanthomonas* contain T6SS-*i3**** cluster (table 3-4). Furthermore, when the T6 cluster distribution was analyzed depending on their lifestyles of vascular vs non-vascular mode, a clear correlation was not observed and T6 clusters are randomly distributed in both vascular and non-vascular *Xanthomonas* spp. (table 3-5).

Determining the role of T6 effectors for the *X. axonopodis* complex host specificity

T6 effectors were identified in each subgroup of *X. axonopodis* to identify if we see any patterns in the effector profile that contributes to the subgrouping of the strains, hence contribute to the divergence of pathovars in the *X. axonopodis* complex.

When the effector profiles were compared, we were able to identify T6 effectors that were commonly found in all the subclades and a few of the effectors that were restricted to few subgroups, few strains or to a single strain (figure 3-9). Some effectors were found in both clusters *i3** and *i3****, including Hcp, VgrG, FHA- forkhead-associated protein and Serine/threonine protein kinase protein.

Hemolysin activator protein (HlyB family), TonB-dependent outer membrane receptor (TBDR), protein with Jacalin-like lectin domain/phosphodiesterase domains from the EEP family (endo/exonuclease/phosphatase) and putative acid phosphatase precursor (Histidine phosphatase superfamily) were identified as effectors unique to the i3* cluster in *X. axonopodis* spp. (figure 3-9a). In *X. axonopodis* i3*** cluster, all the subgroups except for the 9.3, Toll/interleukin-1 receptor (TIR) domain was identified as a T6SS effector (figure 3-9b).

Discussion

In this present study, 1577 *Xanthomonas* genomes obtained from the NCBI website were analyzed to understand the distribution and evolutionary patterns of the T6SS in the genus *Xanthomonas*. With T6 cluster presence/absence analysis we were able to identify the distribution of complete T6 clusters, partial clusters and even single T6 genes belong to i3*, i3***, and i4 subgroups. It was interesting to identify the distribution of incomplete/partial T6 clusters in some *Xanthomonas* spp. Since it has been identified that presence of all the core T6SS genes are required for the functionality of the T6SS (Boyer et al., 2009b), it is intriguing to identify some strains that lack single T6 genes and raise the questions about the possible function of the inactive T6 cluster in that strain. In our analysis, we observed the T6SS locus lacking *clpV* gene in some of the *X. oryzae* strains, and interestingly in previous studies on the distribution of the T6 clusters in *Campylobacter jejuni*, the T6SS locus lacking the *clpV* (*tssH*) gene has been noted (Bönemann et al., 2009; Bleumink-Pluym et al., 2013). Even though ClpV is required for the recycling of the TssB/TssC tubular sheath, the *V. cholerae clpV* mutant was still effective in killing activity towards *E. coli*, thus indicating the possible function of a *clpV* related ClpB family of ATPase encoded from elsewhere compensating for the lack of *clpV* in the T6SS (Pietrosiuk et al., 2011; Zheng et al., 2011).

Distribution of T6SS among *Xanthomonas* spp. does not correlate with host preference, four *Xanthomonas* species that cause BLS in tomato and pepper shows the diverse distribution

of T6 clusters *X. euvesicatoria* and *X. perforans* have both i3* and i3*** clusters while *X. vesicatoria* has i3* cluster, *X. gardneri* doesn't have T6 clusters encoded in its genome (Potnis et al., 2011). Even the three BLS species that have the i3* cluster shows the difference in the cluster organization (figure 3-10).

Few studies conducted in recent years were able to identify the role of T6SS in host adaptation or virulence in the genus *Xanthomonas*. *X. citri* pv. *citri* T6SS- i3*** was the first functionally characterized in the genus and is required for resistance to predation by the bacterivorous amoeba *Dictyostelium discoideum* (Bayer-Santos et al., 2018). In the rice pathogen *X. oryzae* pv. *oryzicola*, T6SS-i4 has been identified for its role in the interbacterial competition, while in *X. oryzae* pv. *oryzae* and *X. phaseoli* pv. *manihotis* reduced virulence and reduced host colonization in presence of T6SS-i3*** (Choi et al., 2020; Zhu et al., 2020; Montenegro Benavides et al., 2021).

When the T6 core gene phylogenies were developed for the *Xanthomonas* spp. that have complete T6 clusters, we were able to clearly identify the distribution of each T6 cluster in major *Xanthomonas* spp.. *X. phaseoli* species shows the most diverse T6SS distribution pattern and identification of two *X. phaseoli* pv. *phaseoli* strains with the i4 cluster was an unusual observation since the *X. phaseoli* strains are part of the *Xanthomonas axonopodis* species complex and only previously known for the harboring i3* and i3*** clusters (Montenegro Benavides et al., 2021). This is indicating the importance of analyzing all the available genomes, before conferring conclusions regarding the group as a whole.

Accumulation of point mutations play a major role in the diversification observed in many pathogen systems and in several studies mutations in the T3SE have been identified as the driving force for diversification (Bogdanove et al., 2011; Merda et al., 2017; Denancé et al., 2018). According to the observations from the T6 core gene phylogenies without the T6 effectors Hcp and VgrG, we could also conclude that T6 effectors also contributes for the

diversification observed in the *Xanthomonas* spp., also further research needs to be done to identify other core genes that are also contributing to the diversification observed even in the absence of Hcp and VgrG.

The distribution of the T6 clusters does not show a clear correlation with its lifestyle and clusters are randomly distributed in both vascular and non-vascular *Xanthomonas* spp., (table 3-4) and this observation is in agreement with previous literature (Bayer-Santos et al., 2019). In the previous research work we were able to identify the role of T6SS-i3* for the epiphytic survival of the BLS *Xanthomonas*. Since most of the vascular *Xanthomonas* spp. initially spend part of its life cycle as a epiphyte before entering the host through natural openings and systematically spread through the vascular system (An et al., 2020), harboring the T6 clusters might be in beneficial for the vascular *Xanthomonas* spp. Interestingly T6 clusters are absent in the xylem limited *X. albilineans*, which also has a reduced genome (3.78 Mb) similar to the genus *Xylella* (2.5 Mb) (Bayer-Santos et al., 2019), both of which are strict vascular pathogens, and shows high degree of host specificity.

Most of the species found as early-branching species at the base of the core genome phylogeny including *X. albilineans*, *X. sacchari*, *X. hyacinthi* and *X. translucens* are infecting monocot hosts except for *X. theicola*, the causal agent of canker on tea plants (Koebnik et al., 2020). According to the literature, the genus *Xanthomonas* first surfaced as a monocot pathogen, and later evolved to become a dicot pathogen (Parkinson et al., 2007). Since the majority of the monocot plants are harboring the i3*** cluster, it is possible that i3*** clusters were first acquired by early-branching strains to successfully survive on monocot hosts and once the host range was expanded into dicots i3* cluster was acquired. Interestingly, *X. perforans*, *X. euvesicatoria* and *X. phaseoli* pv. *dieffenbachiae* LMG695 that have both clusters i3* and i3*** have both mono and dicotyledonous hosts or just known monocotyledonous hosts as seen with *X. phaseoli* pv. *dieffenbachiae* LMG695 (Constantin et al., 2017; Bansal et

al., 2018; Newberry et al., 2019). Hence harboring both clusters i3* and i3*** might be important for determining the host range.

Identification of both i3* and i3*** clusters and an i4 cluster in non-pathogenic *X. maliensis* was interesting since this is the only *Xanthomonas* spp. that have all three T6 clusters found in this analysis and in previous studies (Alvarez-Martinez et al., 2020). *X. maliensis* was found to be associated with healthy rice seeds or leaves in Mali (Triplett et al., 2015). Compared to other non-pathogenic rice leaves associated *Xanthomas* spp. such as *X. sontii* (Bansal et al., 2019) and *X. sacchari* R1 (Fang et al., 2015), that do not have any T6SS cluster encoded in their genome and rice pathogenic *X. oryzae* pv. *oryzae* and *X. oryzae* pv. *oryzicola* that only has i3*** and i4 cluster, it's interesting to discover all three T6 clusters in non-pathogenic *X. maliensis*.

X. floridensis WHRI8848 was first isolated from the diseased leaves of watercress (*Nasturtium officinale*) but later identified as non-pathogenic to watercress and to a range of brassicas (Vicente et al., 2017). Interestingly, *X. nasturtii* WHRI8853, which was identified as a pathogen on watercress in the same study only encodes a single partial T6SS gene (*tssA*). When the flanking regions of this *tssA* gene was further investigated it was found that the gene had a similar flanking gene region similar to most of the *Xanthomonas* spp. that encoded the i3* cluster. Can this non-pathogenic lifestyle of *X. floridensis* WHRI 8848 be related to having the i3* cluster? This observation is similar to the previous observations in BLS *X. gardneri* species which do not have any T6 gene clusters encoded in the genome yet is highly aggressive in tomato grown cooler climatic regions (Potnis et al., 2015).

Another interesting finding, we observed in our analysis is the identification of T6 clusters in rainwater isolates. There are previous records of *X. arboricola* strains found in rainwater but there are no previous records of finding T6 clusters in any of the other sequenced *X. arboricola* strains (Lindow et al., 2014; Cesbron et al., 2015; Alvarez-Martinez et al., 2020).

Presence of insertion sequences (IS) and tRNAs have been previously described as factors that support gene rearrangements (Merda et al., 2017). Presence of this tRNA and partial *i3** cluster in some of the pathogenic and non-pathogenic *X. arboricola* genomes are further supporting our initial hypothesis of the recent loss of T6 in some *Xanthomonas* spp..

Identifying unique T6 effectors involved in this non-pathogenic interaction can be an effective approach in identifying the T6SS mediated interaction (Jani and Cotter, 2010). When we compared the T6 effectors in rainwater *X. arboricola* strains, we didn't observe any specific effector group that might have the potential role in environmental adaptation, but the individual T6 hypothetical effectors might have a function hence further studies are required.

Nonetheless, when looking at the previous literature we could hypothesize that the presence of the T6 clusters might confer a competitive advantage to these non-pathogens to overcome the stress in the leaf phyllosphere. In *Acinetobacter baumannii* clinical strains, selective pressure in favor for silenced T6SS has been recorded while in *V. cholerae* non-pathogenic strains with constitutively active T6SS has been proposed, both of these scenarios are further confirming importance of the T6 clusters for non-pathogenic strains (Lopez et al., 2020).

One important factor that has to be considered when investigating the non-pathogenic strains is how we are differentiating between pathogenic and non-pathogenic interactions. Even though we use pathogenicity on the host of isolation as the major criteria for the differentiation, that can be easily misled by the context and timeframe of the interaction (Jani and Cotter, 2010). Host of isolation might be a temporary or alternative host for the non-pathogen or if the non-pathogen has a longer sit-and-wait latent infection phase to enable transmission, delayed or reduced symptom development can get misinterpreted as non-pathogenic interaction.

However presence of the T6SS and T2SS in non-pathogenic bacteria gives rise to controversy about the definition of virulence factors (Timilsina et al., 2020). Involvement of

secretion systems, focusing mainly on the T6SS might not be limited to virulence but also for functions such as nutrient acquisition, bacterial communication or bacterial-host communication or other factors required for host adaptation.

Our findings on the distribution of the T6 clusters in *Xanthomonas* spp. are in agreement with previous records and identification of i3* in early-branching strains *X. translucens* F5 was remarkable since presence of the i3* cluster in early-branching *Xanthomonas* spp. has not been recorded before (Alvarez-Martinez et al., 2020; Timilsina et al., 2020). In a previous study where evolutionary patterns of the T3SS was explained, random distribution of the strains without T3 clusters, conservation of the flanking regions in T3 positive and negative strains were considered as the signs of a T3SS loss event (Merda et al., 2017). Scattering of strains without T6 clusters in the core genome phylogenetic tree with the presence of it in ancestor strains support the hypothesis of ancestral acquisition of the T6SS by a common ancestor followed by subsequent individual loss events by some of *Xanthomonas* spp. To further follow up with this hypothesis, as suggested by (Merda et al., 2017) flanking regions of the T6 cluster were analyzed in this current study. When referring to previous literature one can hypothesize that, if the strains show similar flanking regions regardless of the presence or absence of each T6 cluster, it can be likely due to the vertical acquisition of T6 clusters by a common ancestor in a single acquisition event (Merda et al., 2017).

When the flanking regions were compared for each T6 cluster, only flanking regions of the i3* cluster of most of the *Xanthomonas* spp. were conserved while clusters i3*** and i4 showing extreme heterogeneity (data not shown). As described in the results, in most of the *Xanthomonas* spp. that didn't have the T6 core genes, presence of the T6 accessory genes were observed. As seen with the hortorum complex, we could identify the presence of two i3* accessory genes (Serine/threonine protein kinase and RNA polymerase sigma factor (TIGR02999 family)) conserved in between the flanking regions. Interestingly, in previous

research, it has been identified that ECF σ factor (EcfK) that acts downstream from a gene encoding a eukaryotic-like Ser/Thr kinase (pknS) has a role in regulating the T6SS at the transcriptional level for the interaction of *X. citri* with soil amoeba *Dictyostelium discoideum* (Bayer-Santos et al., 2018). In *Vibrio parahaemolyticus*, it has been demonstrated that there is a direct phosphorylation of an EcfK homologue by a cognate Ser/thr kinase, that results in the activation of expression of polymyxin-resistant regulon (Iyer et al., 2020). Also, in another recent publication where T6SS gene expression was analyzed in *X. citri* pv. *citri* responsible for Asiatic citrus canker causing, it was identified that T6 genes and ecfK get upregulated during the bacterial epiphytic growth but had lower expression levels once they enter the endophytic stage (Ceseti et al., 2019). It has also been observed that T6SS subgroup 3*** does not contain EcfK/PknS and has other regulators (LysR-type transcriptional regulator and VirA/VirG-like two-component system are involved in the expression of that cluster (Bayer-Santos et al., 2019). This observation of the presence of just Serine/threonine protein kinase and RNA polymerase sigma factor genes, in the absence of the T6 core genes, in several *Xanthomonas* spp. is worthy to explore further in future experiments since these genes might have other functions independent of the T6SS.

When we further observed the flanking regions of the early-branching strains, interestingly in *X. translucens* pv. *translucens* DSM18974 and *X. theicola* CFBP4691 do not have any genes present in between the up and downstream region, indicating no insertion or deletion events in the i3* locus, further supporting the hypothesis of acquisition of T6SS-i3* cluster after the divergence from the ancestral strains. But it's also important to remember that absence of pseudogenes or remnants of the genes between the flanking regions have been also previously observed with T3SS in *Xanthomonas* spp. and non-pathogenic isolates of the plant pathogen *Pseudomonas syringae*, from which the entire cluster has been excised yet proved to have undergone a lost event (Mohr et al., 2008; Merda et al., 2017)

Species belong to the *X. axonopodis* complex are pathogenic on a wide range of crops (VAUTERIN et al., 1995). According to the Rep-PCR, phylogeny based on MLSA, AFLP and DNA: DNA hybridization indicates the presence of six groups named 9.1-9.6 within *X. axonopodis* (Rademaker et al., 2005; Young et al., 2008; Hajri et al., 2009; Mhedbi-Hajri et al., 2013; Bui Thi Ngoc et al., 2000). According to the core genome phylogeny and i3* or i3*** core genes phylogeny in this current study, we observe the same pattern in the way each strain categorize into the subgroupings as explained in the previous literature (Rademaker et al., 2005; Young et al., 2008; Hajri et al., 2009; Mhedbi-Hajri et al., 2013; Bui Thi Ngoc et al.).

Even though this first step of generalist diversification that spanned over the last 25,000 years shows a strong deviation into these subgroups, the nature of this evolutionary process is still unknown and shows no correlation to the host range, tissue specificity or the location of isolation (Mhedbi-Hajri et al., 2013). The second step of ecology-driven specialization that probably occurred in the past two centuries favored the emergence of novel pathovars. This second event of host specialization likely occurred through agricultural intensification and expansion that facilitated genetic exchanges of virulence-associated genes. All of these pathovars are restricted to one of the six subgroups and most of them formed monophyletic (ex; *citri*, *mangiferaeindicae*, *malvacearum*, *begonia* and *manihotis*) clusters while some strains were polyphyletic (ex; *dieffenbachiae*, *glycines*, *phaseoli*) (Hajri et al., 2009; Mhedbi-Hajri et al., 2013). Some strains that belong to the same pathovar can be found in phylogenetically distant clusters. For example, *X. axonopodis* strains that infect legumes can be found in subgroups 9.2, 9.4 and 9.6, mango (*Mangifera indica*) infecting strains were found in subgroups 9.5 and 9.6 and citrus infecting strains were identified in clusters 9.2, 9.5 and 9.6. Similarly, *X. axonopodis* strains that are pathogenic on phylogenetically distant hosts are clustered in the same subgroups, as seen with subgroup 9.5, where citrus, mango, legume and cotton infecting *X. axonopodis* strains are grouped together. This phylogenetic analysis

suggests the host specialization in the *X. axonopodis* strains are due to phylogeny-independent factors and it has been identified that the T3SS effectors and other virulence-associated genes VA genes (Methyl accepting Chemotaxis Proteins-MCPs, adhesins and sensors) might have a role in host specificity (Hajri et al., 2009; Mhedbi-Hajri et al., 2013).

When the T6 cluster distribution was compared to *X. axonopodis* subspecies they belong to, all the species except for *X. phaseoli* pv. *dieffenbachiae* was showing similar distribution. *X. phaseoli* pv. *dieffenbachiae* is polyphyletic and found in subgroups 9.6 (A- *Dieffenbachia* sp.), 9.2 (B- *Philodendron* sp.) and 9.4 (C- *Anthurium* sp.,) according to the *rpoD* sequences analysis and Rep-PCR, this grouping is also dependent on the host of isolation (Hajri et al., 2009; Mhedbi-Hajri et al., 2013). *X. phaseoli* pv. *dieffenbachiae* LMG695 in subgroup 9.4 was found to be carrying extra T3E genes (*avrXccA2*) compared to the other strains of this pathovar, and recombination events have been observed between the ancestor of group 9.6 to the ancestor of genetic lineage C of pathovar *dieffenbachiae*. Since these pathovars infect three different host species it has been suggested that these strains need to be reclassified into different pathovars or species (Rademaker et al., 2005), hence our observation in heterogeneity of the T6 cluster distribution in the subgroup 9.4 can be explained. So, with this analysis we could reaffirm that harboring T6 clusters might have also played a major role in the clustering of the *axonopodis* subgroups. T6SS might have been acquired by a very ancient event of horizontal gene transfer and maintained through evolution, possibly due to the importance of T6 clusters for the adaptation of *Xanthomonas* spp. to their hosts.

Previous studies have shown that, several factors such as TF, LPS, TonB-dependent receptors and specially T3SS and T3Es have a detrimental influence on host specificity and pathogenicity in many *Xanthomonas* spp. (Hajri et al., 2009, 2012; Newberry et al., 2019; Timilsina et al., 2020). Host specialization observed in the *X. axonopodis* strains are due to

phylogeny-independent factors, and harboring T6SS effectors can be an intriguing factor that contributes to the host specialization.

As mentioned in previous sections, Hcp and VgrG are key components of the T6SS and also have been identified as specialized effectors in several pathogen systems (Lien and Lai, 2017; Ma et al., 2017). Hcp and VgrG also shows structural homology to tail proteins of bacteriophages belonging to the *Myoviridae* family, indicating an evolutionary relationship between T6SS and bacteriophages (Montenegro Benavides et al., 2021). VgrGs found in clusters i3* and i3*** are composed of proteins with a N-terminal VgrG domain, while *Xanthomonas* spp. belonging to cluster i4, have VgrG proteins carrying a C-terminal domain of unknown function DUF2345. As mentioned in the introduction section, for the secretion of the effectors through the T6SS, components of the T6 puncturing device, Hcp, VgrG or PAAR need to establish interactions with the effectors (Hernandez et al., 2020). Interestingly, these PAAR proteins are absent in the i3*** cluster and raise questions regarding the functionality of the i3*** cluster. Since the *X. axonopodis* subgroup 9.2 and *X. phaseoli* pv. *dieffenbachiae* LMG695 in subgroup 9.4 have both i3* and i3*** clusters, it might be possible that the PAAR proteins are shared between clusters or the i3*** clusters might be non-functional. Before making conclusions regarding the functionality regarding the i3***, further experiments need to be conducted and *X. axonopodis* subgroup 9.3 which only has a complete i3*** cluster will be a good model system to further explore this hypothesis. FHA protein is absent in the T6SS in more than half of the sequenced genomes (Boyer et al., 2009a), but have been identified to be important in post-translational regulation of the T6SS in *P. aeruginosa*, together with Serine/threonine protein kinase protein (Mougous et al., 2007).

TonB-dependent receptors are bacterial outer membrane transporters that involve in binding and transporting ferric chelates (siderophores), vitamin B₁₂, saccharides and other heavy metals (Pawelek et al., 2006; Shultis et al., 2006; Fujita et al., 2019). TBDRs are a

common trait in the *Xanthomonas* spp. and in *X. euvesicatoria* 85-10, 52 TBDRs have been identified while in *X. axonopodis* pv. *citri* strain 306, there are 68 TBDRs, indicating overexpression of the TBDRs in the genus *Xanthomonas* (Blanvillain et al., 2007). Several recent publications have indicated, T6SS effectors can bind to extracellular ions including manganese, zinc, ferrous and copper and subsequently interact with TBDRs to allow active transport of those metal ions onto the cell (Lin et al., 2017; Si et al., 2017a, 2017b; Han et al., 2019; Hernandez et al., 2020). This effective mode of metal ion scavenging from the extracellular environment is advantageous to bacteria to outcompete other resident microflora and also for the survival in ion limited niche environment. Identification of TBDRs and several hypothetical proteins in the *Xanthomonas* spp. in the *X. axonopodis* complex is suggestive of TBDR-T6SS mediated metal uptake mechanism, thus supporting the hypothesis, harboring the T6SS is not limited to pathogenies but also for successful niche adaptation.

Jacalin-like lectin domain/phosphodiesterase domains from the EEP family (endo/exonuclease/phosphatase) is absent in plants but found in a wide array of microorganism including bacteria and fungi from the phylum Ascomycota and Basidiomycota. Jacalin, is a mannose-binding lectin domain and usually found in the bacterial and fungal cell wall. Since mannose can serve as a microbial associated molecular pattern (MAMP) it can be recognized by the plant immune system, it is possible that T6SS related Jacalin effectors are secreted to outcompete the plant immune receptors by serving as camouflage (Levy et al., 2018)

Bacterial proteins with the TIR domain have been associated with suppressing innate immunity and increasing virulence also as seen with pathogenic *Staphylococcus aureus* they can also induce NAD⁺ loss in mammalian cells (Cirl et al., 2008; Patot et al., 2017; Essuman et al., 2018; Bayer-Santos et al., 2019; Alvarez-Martinez et al., 2020).

Conclusion

Since the role of the T6SS in the genus, *Xanthomonas* has not been fully understood yet, we used all the available *Xanthomonas* genomes to uncover the evolutionary patterns and distribution of the T6 clusters across the genus. We were able to identify the presence and absence of complete/incomplete T6 clusters according to the phylogenetic group they belong to and our observation of the presence of T6 clusters in non-pathogenic and environmental *Xanthomonas* spp., broadens our understanding regarding the possible functions of the T6SS. It was also revealed that the core genome and the T6 gene clusters of species belong to the *X. axonopodis* complex share a common evolutionary history, and the conserved maintenance of the T6 clusters in this group is most likely driven by the host plant-related selective pressure. Identification of T6SS related effectors that have putative functions, not limited to the pathogenicity but also related to gaining competitive advantage in the host environment, further emphasizing a role of T6SS beyond pathogenesis.

References

- Abendroth, U., Adlung, N., Otto, A., Grüneisen, B., Becher, D., and Bonas, U. (2017). Identification of new protein-coding genes with a potential role in the virulence of the plant pathogen *Xanthomonas euvesicatoria*. *BMC Genomics* 18, 625. doi:10.1186/s12864-017-4041-7.
- Alvarez-Martinez, C. E., Sgro, G. G., Araujo, G. G., Paiva, M. R. N., Matsuyama, B. Y., Guzzo, C. R., et al. (2020). Secrete or perish: The role of secretion systems in Xanthomobiology. *Comput Struct Biotechnol J* 19, 279–302. doi:10.1016/j.csbj.2020.12.020.
- An, S.-Q., Potnis, N., Dow, M., Vorhölter, F.-J., He, Y.-Q., Becker, A., et al. (2020). Mechanistic insights into host adaptation, virulence and epidemiology of the phytopathogen *Xanthomonas*. *FEMS Microbiology Reviews* 44, 1–32. doi:10.1093/femsre/fuz024.
- Bansal, K., Kumar, S., and Patil, P. B. (2018). Complete Genome Sequence Reveals Evolutionary Dynamics of an Emerging and Variant Pathovar of *Xanthomonas euvesicatoria*. *Genome Biology and Evolution* 10, 3104–3109. doi:10.1093/gbe/evy238.
- Bansal, K., Kumar, S., and Patil, P. B. (2020). Phylogenomic Insights into Diversity and Evolution of Nonpathogenic *Xanthomonas* Strains Associated with Citrus. *mSphere* 5. doi:10.1128/mSphere.00087-20.
- Bansal, K., Midha, S., Kumar, S., Kaur, A., Sonti, R. V., and Patil, P. B. (2019). Ecological and evolutionary insights into pathogenic and non-pathogenic rice associated *Xanthomonas*. *bioRxiv*, 453373. doi:10.1101/453373.
- Bayer-Santos, E., Ceseti, L. de M., Farah, C. S., and Alvarez-Martinez, C. E. (2019). Distribution, Function and Regulation of Type 6 Secretion Systems of *Xanthomonadales*. *Front. Microbiol.* 10, 1635. doi:10.3389/fmicb.2019.01635.
- Bayer-Santos, E., Lima, L. dos P., Ceseti, L. de M., Ratagami, C. Y., Santana, E. S. de, Silva, A. M. da, et al. (2018). *Xanthomonas citri* T6SS mediates resistance to *Dictyostelium*

- predation and is regulated by an ECF σ factor and cognate Ser/Thr kinase. *Environmental Microbiology* 20, 1562–1575. doi:<https://doi.org/10.1111/1462-2920.14085>.
- Bingle, L. E., Bailey, C. M., and Pallen, M. J. (2008). Type VI secretion: a beginner's guide. *Curr. Opin. Microbiol.* 11, 3–8. doi:[10.1016/j.mib.2008.01.006](https://doi.org/10.1016/j.mib.2008.01.006).
- Blanvillain, S., Meyer, D., Boulanger, A., Lautier, M., Guynet, C., Denancé, N., et al. (2007). Plant Carbohydrate Scavenging through TonB-Dependent Receptors: A Feature Shared by Phytopathogenic and Aquatic Bacteria. *PLoS One* 2. doi:[10.1371/journal.pone.0000224](https://doi.org/10.1371/journal.pone.0000224).
- Bleumink-Pluym, N. M. C., Alphen, L. B. van, Bouwman, L. I., Wösten, M. M. S. M., and Putten, J. P. M. van (2013). Identification of a Functional Type VI Secretion System in *Campylobacter jejuni* Conferring Capsule Polysaccharide Sensitive Cytotoxicity. *PLOS Pathogens* 9, e1003393. doi:[10.1371/journal.ppat.1003393](https://doi.org/10.1371/journal.ppat.1003393).
- Blondel, C. J., Jiménez, J. C., Contreras, I., and Santiviago, C. A. (2009). Comparative genomic analysis uncovers 3 novel loci encoding type six secretion systems differentially distributed in *Salmonella* serotypes. *BMC Genomics* 10, 354. doi:[10.1186/1471-2164-10-354](https://doi.org/10.1186/1471-2164-10-354).
- Bogdanove, A. J., Koebnik, R., Lu, H., Furutani, A., Angiuoli, S. V., Patil, P. B., et al. (2011). Two New Complete Genome Sequences Offer Insight into Host and Tissue Specificity of Plant Pathogenic *Xanthomonas* spp. *Journal of Bacteriology* 193, 5450–5464. doi:[10.1128/JB.05262-11](https://doi.org/10.1128/JB.05262-11).
- Bönemann, G., Pietrosiuk, A., Diemand, A., Zentgraf, H., and Mogk, A. (2009). Remodelling of VipA/VipB tubules by ClpV-mediated threading is crucial for type VI protein secretion. *The EMBO Journal* 28, 315–325. doi:[10.1038/emboj.2008.269](https://doi.org/10.1038/emboj.2008.269).
- Boyer, F., Fichant, G., Berthod, J., Vandenbrouck, Y., and Attree, I. (2009a). Dissecting the bacterial type VI secretion system by a genome wide in silico analysis: what can be learned from available microbial genomic resources? *BMC Genomics* 10, 104. doi:[10.1186/1471-2164-10-104](https://doi.org/10.1186/1471-2164-10-104).

- Boyer, F., Fichant, G., Berthod, J., Vandenbrouck, Y., and Attree, I. (2009b). Dissecting the bacterial type VI secretion system by a genome wide in silico analysis: what can be learned from available microbial genomic resources? *BMC Genomics* 10, 104. doi:10.1186/1471-2164-10-104.
- Bui Thi Ngoc, L., Vernière, C., Jouen, E., Ah-You, N., Lefeuvre, P., Chiroleu, F., et al. Amplified fragment length polymorphism and multilocus sequence analysis-based genotypic relatedness among pathogenic variants of *Xanthomonas citri* pv. *citri* and *Xanthomonas campestris* pv. *bilvae*. *International Journal of Systematic and Evolutionary Microbiology* 60, 515–525. doi:10.1099/ijms.0.009514-0.
- Büttner, D., and Bonas, U. (2010). Regulation and secretion of *Xanthomonas* virulence factors. *FEMS Microbiol Rev* 34, 107–133. doi:10.1111/j.1574-6976.2009.00192.x.
- Camacho, C., Coulouris, G., Avagyan, V., Ma, N., Papadopoulos, J., Bealer, K., et al. (2009). BLAST+: architecture and applications. *BMC Bioinformatics* 10, 421. doi:10.1186/1471-2105-10-421.
- Cesbron, S., Briand, M., Essakhi, S., Gironde, S., Boureau, T., Manceau, C., et al. (2015). Comparative Genomics of Pathogenic and Nonpathogenic Strains of *Xanthomonas arboricola* Unveil Molecular and Evolutionary Events Linked to Pathoadaptation. *Front Plant Sci* 6. doi:10.3389/fpls.2015.01126.
- Ceseti, L. M., de Santana, E. S., Ratagami, C. Y., Barreiros, Y., Lima, L. D. P., Dunger, G., et al. (2019). The *Xanthomonas citri* pv. *citri* Type VI Secretion System is Induced During Epiphytic Colonization of Citrus. *Curr Microbiol* 76, 1105–1111. doi:10.1007/s00284-019-01735-3.
- Chen, I.-M. A., Chu, K., Palaniappan, K., Ratner, A., Huang, J., Huntemann, M., et al. (2021). The IMG/M data management and analysis system v.6.0: new tools and advanced capabilities. *Nucleic Acids Research* 49, D751–D763. doi:10.1093/nar/gkaa939.
- Choi, Y., Kim, N., Mannaa, M., Kim, H., Park, J., Jung, H., et al. (2020). Characterization of Type VI Secretion System in *Xanthomonas oryzae* pv. *oryzae* and Its Role in Virulence to Rice. *Plant Pathol J* 36, 289–296. doi:10.5423/PPJ.NT.02.2020.0026.

- Cirl, C., Wieser, A., Yadav, M., Duerr, S., Schubert, S., Fischer, H., et al. (2008). Subversion of Toll-like receptor signaling by a unique family of bacterial Toll/interleukin-1 receptor domain-containing proteins. *Nature Medicine* 14, 399–406. doi:10.1038/nm1734.
- Constantin, E. C., Haegeman, A., Vaerenbergh, J. V., Baeyen, S., Malderghem, C. V., Maes, M., et al. (2017). Pathogenicity and virulence gene content of *Xanthomonas* strains infecting Araceae, formerly known as *Xanthomonas axonopodis* pv. *dieffenbachiae*. *Plant Pathology* 66, 1539–1554. doi:https://doi.org/10.1111/ppa.12694.
- Coulthurst, S. J. (2013). The Type VI secretion system – a widespread and versatile cell targeting system. *Research in Microbiology* 164, 640–654. doi:10.1016/j.resmic.2013.03.017.
- Davis, E. W., Okrent, R. A., Manning, V. A., and Trippe, K. M. (2021). Unexpected distribution of the 4-formylaminoxyvinylglycine (FVG) biosynthetic pathway in *Pseudomonas* and beyond. *PLoS One* 16. doi:10.1371/journal.pone.0247348.
- Denancé, N., Szurek, B., Doyle, E. L., Lauber, E., Fontaine-Bodin, L., Carrère, S., et al. (2018). Two ancestral genes shaped the *Xanthomonas campestris* TAL effector gene repertoire. *New Phytologist* 219, 391–407. doi:https://doi.org/10.1111/nph.15148.
- Durand, E., Cambillau, C., Cascales, E., and Journet, L. (2014). VgrG, Tae, Tle, and beyond: the versatile arsenal of Type VI secretion effectors. *Trends in Microbiology* 22, 498–507. doi:10.1016/j.tim.2014.06.004.
- Durand, E., Nguyen, V. S., Zoued, A., Logger, L., Péhau-Arnaudet, G., Aschtgen, M.-S., et al. (2015). Biogenesis and structure of a type VI secretion membrane core complex. *Nature* 523, 555–560. doi:10.1038/nature14667.
- Essuman, K., Summers, D. W., Sasaki, Y., Mao, X., Yim, A. K. Y., DiAntonio, A., et al. (2018). TIR Domain Proteins Are an Ancient Family of NAD⁺-Consuming Enzymes. *Current Biology* 28, 421–430.e4. doi:10.1016/j.cub.2017.12.024.
- Fang, Y., Lin, H., Wu, L., Ren, D., Ye, W., Dong, G., et al. (2015). Genome sequence of *Xanthomonas sacchari* R1, a biocontrol bacterium isolated from the rice seed. *Journal of Biotechnology* 206, 77–78. doi:10.1016/j.jbiotec.2015.04.014.

- Fischer-Le Saux, M., Bonneau, S., Essakhi, S., Manceau, C., and Jacques, M.-A. (2015). Aggressive Emerging Pathovars of *Xanthomonas arboricola* Represent Widespread Epidemic Clones Distinct from Poorly Pathogenic Strains, as Revealed by Multilocus Sequence Typing. *Applied and Environmental Microbiology* 81, 4651–4668. doi:10.1128/AEM.00050-15.
- Fujita, M., Mori, K., Hara, H., Hishiyama, S., Kamimura, N., and Masai, E. (2019). A TonB-dependent receptor constitutes the outer membrane transport system for a lignin-derived aromatic compound. *Communications Biology* 2, 1–10. doi:10.1038/s42003-019-0676-z.
- Gambette, P., and Huson, D. H. (2008). Improved Layout of Phylogenetic Networks. *IEEE/ACM Trans. Comput. Biol. Bioinformatics* 5, 472–479. doi:10.1109/tcbb.2007.1046.
- Hajri, A., Brin, C., Hunault, G., Lardeux, F., Lemaire, C., Manceau, C., et al. (2009). A «Repertoire for Repertoire» Hypothesis: Repertoires of Type Three Effectors are Candidate Determinants of Host Specificity in *Xanthomonas*. *PLOS ONE* 4, e6632. doi:10.1371/journal.pone.0006632.
- Hajri, A., Pothier, J. F., Saux, M. F.-L., Bonneau, S., Poussier, S., Boureau, T., et al. (2012). Type Three Effector Gene Distribution and Sequence Analysis Provide New Insights into the Pathogenicity of Plant-Pathogenic *Xanthomonas arboricola*. *Appl. Environ. Microbiol.* 78, 371–384. doi:10.1128/AEM.06119-11.
- Han, Y., Wang, T., Chen, G., Pu, Q., Liu, Q., Zhang, Y., et al. (2019). A *Pseudomonas aeruginosa* type VI secretion system regulated by CueR facilitates copper acquisition. *PLOS Pathogens* 15, e1008198. doi:10.1371/journal.ppat.1008198.
- Hernandez, R. E., Gallegos-Monterrosa, R., and Coulthurst, S. J. (2020). Type VI secretion system effector proteins: Effective weapons for bacterial competitiveness. *Cellular Microbiology* 22, e13241. doi:https://doi.org/10.1111/cmi.13241.
- Huson, D. H., and Bryant, D. (2006). Application of Phylogenetic Networks in Evolutionary Studies. *Molecular Biology and Evolution* 23, 254–267. doi:10.1093/molbev/msj030.

- Iyer, S. C., Casas-Pastor, D., Kraus, D., Mann, P., Schirner, K., Glatter, T., et al. (2020). Transcriptional regulation by σ factor phosphorylation in bacteria. *Nature Microbiology* 5, 395–406. doi:10.1038/s41564-019-0648-6.
- Jani, A. J., and Cotter, P. A. (2010). Type VI Secretion: not just for pathogenesis anymore. *Cell Host Microbe* 8, 2–6. doi:10.1016/j.chom.2010.06.012.
- Johansen, J. E., Binnerup, S. J., Kroer, N., and Mølbak, L. (2005). *Luteibacter rhizovicinus* gen. nov., sp. nov., a yellow-pigmented gammaproteobacterium isolated from the rhizosphere of barley (*Hordeum vulgare* L.). *Int J Syst Evol Microbiol* 55, 2285–2291. doi:10.1099/ijs.0.63497-0.
- Joseph, S., and Forsythe, S. (2012). Insights into the Emergent Bacterial Pathogen *Cronobacter* spp., Generated by Multilocus Sequence Typing and Analysis. *Front. Microbiol.* 3. doi:10.3389/fmicb.2012.00397.
- Jun, S.-R., Sims, G. E., Wu, G. A., and Kim, S.-H. (2010). Whole-proteome phylogeny of prokaryotes by feature frequency profiles: An alignment-free method with optimal feature resolution. *PNAS* 107, 133–138. doi:10.1073/pnas.0913033107.
- Koebnik, R., Burokiene, D., Bragard, C., Chang, C., Saux, M. F.-L., Kölliker, R., et al. (2020). The Complete Genome Sequence of *Xanthomonas theicola*, the Causal Agent of Canker on Tea Plants, Reveals Novel Secretion Systems in Clade-1 Xanthomonads. *Phytopathology*® 111, 611–616. doi:10.1094/PHYTO-07-20-0273-SC.
- Kumar, R., Bröms, J. E., and Sjöstedt, A. (2020). Exploring the Diversity Within the Genus *Francisella* – An Integrated Pan-Genome and Genome-Mining Approach. *Front. Microbiol.* 11. doi:10.3389/fmicb.2020.01928.
- Kyrova, E. I., Dzhililov, F. S., and Ignatov, A. N. (2020). The role of epiphytic populations in pathogenesis of the genus *Xanthomonas* bacteria. *BIO Web Conf.* 23, 03010. doi:10.1051/bioconf/20202303010.
- Levy, A., Gonzalez, I. S., Mittelviehhaus, M., Clingenpeel, S., Paredes, S. H., Miao, J., et al. (2018). Genomic features of bacterial adaptation to plants. *Nat Genet* 50, 138–150. doi:10.1038/s41588-017-0012-9.

- Lien, Y.-W., and Lai, E.-M. (2017). Type VI Secretion Effectors: Methodologies and Biology. *Front Cell Infect Microbiol* 7. doi:10.3389/fcimb.2017.00254.
- Lin, J., Zhang, W., Cheng, J., Yang, X., Zhu, K., Wang, Y., et al. (2017). A *Pseudomonas* T6SS effector recruits PQS-containing outer membrane vesicles for iron acquisition. *Nature Communications* 8, 14888. doi:10.1038/ncomms14888.
- Lindow, S., Olson, W., and Buchner, R. (2014). Colonization of Dormant Walnut Buds by *Xanthomonas arboricola* pv. *juglandis* Is Predictive of Subsequent Disease. *Phytopathology* 104, 1163–1174. doi:10.1094/PHYTO-01-14-0001-R.
- Lopez, J., Ly, P. M., and Feldman, M. F. (2020). The Tip of the VgrG Spike Is Essential to Functional Type VI Secretion System Assembly in *Acinetobacter baumannii*. *mBio* 11. doi:10.1128/mBio.02761-19.
- Ma, J., Pan, Z., Huang, J., Sun, M., Lu, C., and Yao, H. (2017). The Hcp proteins fused with diverse extended-toxin domains represent a novel pattern of antibacterial effectors in type VI secretion systems. *Virulence* 8, 1189–1202. doi:10.1080/21505594.2017.1279374.
- Merda, D., Briand, M., Bosis, E., Rousseau, C., Portier, P., Barret, M., et al. (2017). Ancestral acquisitions, gene flow and multiple evolutionary trajectories of the type three secretion system and effectors in *Xanthomonas* plant pathogens. *Molecular Ecology* 26, 5939–5952. doi:https://doi.org/10.1111/mec.14343.
- Meuskens, I., Saragliadis, A., Leo, J. C., and Linke, D. (2019). Type V Secretion Systems: An Overview of Passenger Domain Functions. *Front. Microbiol.* 10, 1163. doi:10.3389/fmicb.2019.01163.
- Mhedbi-Hajri, N., Hajri, A., Boureau, T., Darrasse, A., Durand, K., Brin, C., et al. (2013). Evolutionary History of the Plant Pathogenic Bacterium *Xanthomonas axonopodis*. *PLoS One* 8. doi:10.1371/journal.pone.0058474.
- Mohr, T. J., Liu, H., Yan, S., Morris, C. E., Castillo, J. A., Jelenska, J., et al. (2008). Naturally Occurring Nonpathogenic Isolates of the Plant Pathogen *Pseudomonas syringae* Lack a Type III Secretion System and Effector Gene Orthologues. *J Bacteriol* 190, 2858–2870. doi:10.1128/JB.01757-07.

- Montenegro Benavides, N. A., Alvarez B., A., Arrieta-Ortiz, M. L., Rodriguez-R, L. M., Botero, D., Tabima, J. F., et al. (2021). The type VI secretion system of *Xanthomonas phaseoli* pv. *manihotis* is involved in virulence and in vitro motility. *BMC Microbiology* 21, 14. doi:10.1186/s12866-020-02066-1.
- Mougous, J. D., Gifford, C. A., Ramsdell, T. L., and Mekalanos, J. J. (2007). Threonine phosphorylation post-translationally regulates protein secretion in *Pseudomonas aeruginosa*. *Nature Cell Biology* 9, 797–803. doi:10.1038/ncb1605.
- Mukherjee, S., Stamatis, D., Bertsch, J., Ovchinnikova, G., Sundaramurthi, J. C., Lee, J., et al. (2021). Genomes OnLine Database (GOLD) v.8: overview and updates. *Nucleic Acids Research* 49, D723–D733. doi:10.1093/nar/gkaa983.
- Newberry, E. A., Bhandari, R., Minsavage, G. V., Timilsina, S., Jibrin, M. O., Kemble, J., et al. (2019). Independent Evolution with the Gene Flux Originating from Multiple *Xanthomonas* Species Explains Genomic Heterogeneity in *Xanthomonas perforans*. *Appl. Environ. Microbiol.* 85. doi:10.1128/AEM.00885-19.
- Nguyen, V. S., Douzi, B., Durand, E., Roussel, A., Cascales, E., and Cambillau, C. (2018). Towards a complete structural deciphering of Type VI secretion system. *Current Opinion in Structural Biology* 49, 77–84. doi:10.1016/j.sbi.2018.01.007.
- Page, A. J., Cummins, C. A., Hunt, M., Wong, V. K., Reuter, S., Holden, M. T. G., et al. (2015). Roary: rapid large-scale prokaryote pan genome analysis. *Bioinformatics* 31, 3691–3693. doi:10.1093/bioinformatics/btv421.
- Palmer, T., Finney, A. J., Saha, C. K., Atkinson, G. C., and Sargent, F. (2020). A holin/peptidoglycan hydrolase-dependent protein secretion system. *Molecular Microbiology*.
- Parkinson, N., Aritua, V., Heeney, J., Cowie, C., Bew, J., and Stead, D. 2007 Phylogenetic analysis of *Xanthomonas* species by comparison of partial gyrase B gene sequences. *International Journal of Systematic and Evolutionary Microbiology* 57, 2881–2887. doi:10.1099/ijs.0.65220-0.
- Patot, S., Imbert, P. R., Baude, J., Simões, P. M., Campergue, J.-B., Louche, A., et al. (2017). The TIR Homologue Lies near Resistance Genes in *Staphylococcus aureus*, Coupling

- Modulation of Virulence and Antimicrobial Susceptibility. *PLOS Pathogens* 13, e1006092. doi:10.1371/journal.ppat.1006092.
- Pawelek, P. D., Croteau, N., Ng-Thow-Hing, C., Khursigara, C. M., Moiseeva, N., Allaire, M., et al. (2006). Structure of TonB in Complex with FhuA, E. coli Outer Membrane Receptor. *Science* 312, 1399–1402. doi:10.1126/science.1128057.
- Pietrosiuk, A., Lenherr, E. D., Falk, S., Bönemann, G., Kopp, J., Zentgraf, H., et al. (2011). Molecular basis for the unique role of the AAA+ chaperone ClpV in type VI protein secretion. *J Biol Chem* 286, 30010–30021. doi:10.1074/jbc.M111.253377.
- Potnis, N., Krasileva, K., Chow, V., Almeida, N. F., Patil, P. B., Ryan, R. P., et al. (2011). Comparative genomics reveals diversity among xanthomonads infecting tomato and pepper. *BMC Genomics* 12, 146. doi:10.1186/1471-2164-12-146.
- Potnis, N., Timilsina, S., Strayer, A., Shantharaj, D., Barak, J. D., Paret, M. L., et al. (2015). Bacterial spot of tomato and pepper: diverse Xanthomonas species with a wide variety of virulence factors posing a worldwide challenge. *Molecular Plant Pathology* 16, 907–920. doi:https://doi.org/10.1111/mpp.12244.
- Rademaker, J. L., Hoste, B., Louws, F. J., Kersters, K., Swings, J., Vauterin, L., et al. Comparison of AFLP and rep-PCR genomic fingerprinting with DNA-DNA homology studies: Xanthomonas as a model system. *International Journal of Systematic and Evolutionary Microbiology* 50, 665–677. doi:10.1099/00207713-50-2-665.
- Rademaker, J. L. W., Louws, F. J., Schultz, M. H., Rossbach, U., Vauterin, L., Swings, J., et al. (2005). A Comprehensive Species to Strain Taxonomic Framework for Xanthomonas. *Phytopathology* 95, 1098–1111. doi:10.1094/PHYTO-95-1098.
- Rambaut, A., Drummond, A. J., Xie, D., Baele, G., and Suchard, M. A. (2018). Posterior Summarization in Bayesian Phylogenetics Using Tracer 1.7. *Syst Biol* 67, 901–904. doi:10.1093/sysbio/syy032.
- Seemann, T. (2014). Prokka: rapid prokaryotic genome annotation. *Bioinformatics* 30, 2068–2069. doi:10.1093/bioinformatics/btu153.

- Shalom, G., Shaw, J. G., and Thomas, M. S. (2007). In vivo expression technology identifies a type VI secretion system locus in *Burkholderia pseudomallei* that is induced upon invasion of macrophages. *Microbiology*, 153, 2689–2699. doi:10.1099/mic.0.2007/006585-0.
- Shultis, D. D., Purdy, M. D., Banchs, C. N., and Wiener, M. C. (2006). Outer Membrane Active Transport: Structure of the BtuB:TonB Complex. *Science* 312, 1396–1399. doi:10.1126/science.1127694.
- Shyntum, D., Venter, S., Moleleki, L., Toth, I., and Coutinho, T. (2014). Comparative genomics of type VI secretion systems in strains of *Pantoea ananatis* from different environments. *BMC Genomics* 15, 163. doi:10.1186/1471-2164-15-163.
- Si, M., Wang, Y., Zhang, B., Zhao, C., Kang, Y., Bai, H., et al. (2017a). The Type VI Secretion System Engages a Redox-Regulated Dual-Functional Heme Transporter for Zinc Acquisition. *Cell Rep* 20, 949–959. doi:10.1016/j.celrep.2017.06.081.
- Si, M., Zhao, C., Burkinshaw, B., Zhang, B., Wei, D., Wang, Y., et al. (2017b). Manganese scavenging and oxidative stress response mediated by type VI secretion system in *Burkholderia thailandensis*. *PNAS* 114, E2233–E2242. doi:10.1073/pnas.1614902114.
- Silverman, J. M., Austin, L. S., Hsu, F., Hicks, K. G., Hood, R. D., and Mougous, J. D. (2011). Separate inputs modulate phosphorylation-dependent and -independent type VI secretion activation: Posttranslational regulation of type VI secretion. *Molecular Microbiology* 82, 1277–1290. doi:10.1111/j.1365-2958.2011.07889.x.
- Silverman, J. M., Brunet, Y. R., Cascales, E., and Mougous, J. D. (2012). Structure and Regulation of the Type VI Secretion System. *Annual Review of Microbiology* 66, 453–472. doi:10.1146/annurev-micro-121809-151619.
- Stamatakis, A. (2014). RAxML version 8: a tool for phylogenetic analysis and post-analysis of large phylogenies. *Bioinformatics* 30, 1312–1313. doi:10.1093/bioinformatics/btu033.
- Timilsina, S., Jibrin, M. O., Potnis, N., Minsavage, G. V., Kebede, M., Schwartz, A., et al. (2015). Multilocus Sequence Analysis of Xanthomonads Causing Bacterial Spot of Tomato and Pepper Plants Reveals Strains Generated by Recombination among Species

- and Recent Global Spread of *Xanthomonas gardneri*. *Appl Environ Microbiol* 81, 1520–1529. doi:10.1128/AEM.03000-14.
- Timilsina, S., Potnis, N., Newberry, E. A., Liyanapathirana, P., Iruegas-Bocardo, F., White, F. F., et al. (2020). *Xanthomonas* diversity, virulence and plant–pathogen interactions. *Nature Reviews Microbiology* 18, 415–427. doi:10.1038/s41579-020-0361-8.
- Triplett, L. R., Verdier, V., Campillo, T., Van Malderghem, C., Cleenwerck, I., Maes, M., et al. (2015). Characterization of a novel clade of *Xanthomonas* isolated from rice leaves in Mali and proposal of *Xanthomonas maliensis* sp. nov. *Antonie van Leeuwenhoek* 107, 869–881. doi:10.1007/s10482-015-0379-5.
- Vauterin, L., Hoste, B., Kersters, K., And Swings, J. Y. 1995 Reclassification of *Xanthomonas*. *International Journal of Systematic and Evolutionary Microbiology* 45, 472–489. doi:10.1099/00207713-45-3-472.
- Vicente, J. G., Rothwell, S., Holub, E. B., and Studholme, D. J. (2017). Pathogenic, phenotypic and molecular characterisation of *Xanthomonas nasturtii* sp. nov. and *Xanthomonas floridensis* sp. nov., new species of *Xanthomonas* associated with watercress production in Florida. *International Journal of Systematic and Evolutionary Microbiology* 67, 3645–3654. doi:10.1099/ijsem.0.002189.
- Wang, J., Yang, B., Leier, A., Marquez-Lago, T. T., Hayashida, M., Rucker, A., et al. (2018). Bastion6: a bioinformatics approach for accurate prediction of type VI secreted effectors. *Bioinformatics* 34, 2546–2555. doi:10.1093/bioinformatics/bty155.
- WHITE, F. F., POTNIS, N., JONES, J. B., and KOEBNIK, R. (2009). The type III effectors of *Xanthomonas*. *Mol Plant Pathol* 10, 749–766. doi:10.1111/j.1364-3703.2009.00590.x.
- Young, J. M., Park, D.-C., Shearman, H. M., and Fargier, E. (2008). A multilocus sequence analysis of the genus *Xanthomonas*. *Systematic and Applied Microbiology* 31, 366–377. doi:10.1016/j.syapm.2008.06.004.
- Zhao, Y., Qian, G., Chen, Y., Du, L., and Liu, F. (2017). Transcriptional and Antagonistic Responses of Biocontrol Strain *Lysobacter enzymogenes* OH11 to the Plant Pathogenic

Oomycete *Pythium aphanidermatum*. *Front. Microbiol.* 8.
doi:10.3389/fmicb.2017.01025.

Zheng, J., Ho, B., and Mekalanos, J. J. (2011). Genetic Analysis of Anti-Amoebae and Anti-Bacterial Activities of the Type VI Secretion System in *Vibrio cholerae*. *PLOS ONE* 6, e23876. doi:10.1371/journal.pone.0023876.

Zhu, P.-C., Li, Y.-M., Yang, X., Zou, H.-F., Zhu, X.-L., Niu, X.-N., et al. (2020). Type VI secretion system is not required for virulence on rice but for inter-bacterial competition in *Xanthomonas oryzae* pv. *oryzicola*. *Res Microbiol* 171, 64–73. doi:10.1016/j.resmic.2019.10.004.

Zoued, A., Brunet, Y. R., Durand, E., Aschtgen, M.-S., Logger, L., Douzi, B., et al. (2014). Architecture and assembly of the Type VI secretion system. *Biochimica et Biophysica Acta (BBA) - Molecular Cell Research* 1843, 1664–1673. doi:10.1016/j.bbamcr.2014.03.018.

Table 3-1: Analysis of T6 cluster distribution in genus *Xanthomonas*

<i>Xanthomonas</i> spp.	Total # of genomes	% with complete T6	% with partial T6 only	% with no T6 clusters	i3***	i3*	i4	i3*** only	i3* only	i4 only	i3***&i3*	i3***&i4	i3* &i4	i3***&i3*&i4
<i>X. oryzae</i>	388	70.4	5.9	23.7	296(92)*	-	365(23)*	-	-	69	-	296	-	-
<i>X. citri</i>	194	98.9	-	1.1	-	192	12	-	181	-	-	-	12	-
<i>X. phaseoli</i>	155	96.7	0.64	2.5	55(100)*	150(5)*	2	-	98	-	52	-	2	-
<i>X. perforans</i>	149	95.9	4.1	0	133(16)*	143(6)*	-	-	-	-	133	-	-	-
<i>X. arboricola</i>	139	5	0.2	94.8	1(6)*	7(25)*	-	-	6	-	1	-	-	-
<i>X. vasicola</i>	99	43	56	0	43(56)*	-	-	43	-	-	-	-	-	-
<i>X. campestris</i>	75	22.6	57.4	0	3(15)*	14(43)*	-	-	14	-	3	-	-	-
<i>X. euvesicatoria</i>	69	92.7	7.3	0	66(3)*	64(5)*	-	-	1	-	68	-	-	-
<i>X. translucens</i>	64	62.6	10.9	26.5	(47)*	(47)*	40(9)*	-	-	40	-	-	-	-
<i>X. fragariae</i>	63	98.4	0	1.58	-	-	62	-	-	62	-	-	-	-
<i>X. sp</i>	53	17	43.4	39.4	1(15)*	8(8)*	1	-	8	-	1	-	-	-
<i>X. hortorum</i>	32	6.25	0	93.75	-	-	2	-	-	2	-	-	-	-
<i>X. axonopodis</i>	17	64.7	35.3	0	6(11)*	11(6)*	(1)*	-	9	-	2	-	-	-
<i>X. albilineans</i>	17	0	0	100	-	-	-	-	-	-	-	-	-	-
<i>X. vesicatoria</i>	15	100	0	0	-	15	-	-	15	-	-	-	-	-
<i>X. sacchari</i>	7	0	0	100	-	-	-	-	-	-	-	-	-	-
<i>X. euroxanthea</i>	4	0	0	100	-	-	-	-	-	-	-	-	-	-
<i>X. dyei</i>	3	66.6	33.3	0	1(2)*	2(1)*	-	-	2	-	1	-	-	-
<i>X. cannabis</i>	3	0	0	100	-	-	-	-	-	-	-	-	-	-
<i>X. prunicola</i>	3	0	100	0	-	(3)*	-	-	-	-	-	-	-	-
<i>X. sontii</i>	3	0	0	100	-	-	-	-	-	-	-	-	-	-
<i>X. maliensis</i>	2	100	0	0	2	2	2	-	-	-	-	-	-	2
<i>X. cissicola</i>	2	100	0	0	(2)*	2	2	-	-	-	-	2	-	-
<i>X. cucurbitae</i>	2	50	50	0	-	1(1)*	-	-	1	-	-	-	-	-
<i>X. pisi</i>	2	50	50	0	-	1(1)*	-	-	1	-	-	-	-	-
<i>X. bromi</i>	2	50	50	0	-	-	1(1)*	-	-	1	-	-	-	-
<i>X. massiliensis</i>	2	0	0	100	-	-	-	-	-	-	-	-	-	-
<i>X. hyacinthi</i>	2	50	0	50	1	-	-	-	-	-	-	-	-	-
<i>X. nasturtii</i>	2	0	100	0	-	(2)*	-	-	-	-	-	-	-	-
<i>X. theicola</i>	2	0	0	100	-	-	-	-	-	-	-	-	-	-
<i>X. alfalfae</i>	1	100	0	0	1	-	-	1	-	-	-	-	-	-
<i>X. cassavae</i>	1	100	0	0	(1)*	1	-	-	1	-	-	-	-	-
<i>X. codiae</i>	1	50	50	0	(1)*	1	-	-	1	-	-	-	-	-
<i>X. floridensis</i>	1	100	0	0	-	1	-	-	1	-	-	-	-	-
<i>X. melonis</i>	1	100	0	0	-	1	-	-	1	-	-	-	-	-
<i>X. populi</i>	1	0	100	0	-	-	(1)*	-	-	-	-	-	-	-
<i>X. retroflexus</i>	1	0	0	100	-	-	-	-	-	-	-	-	-	-
sum	1577				417	608	489	44	340	174	261	398	14	2
								at least with one cluster		with 2 clusters		with 3 clusters		
								558 (35.4%)		675 (42.8%)		2 (0.01%)		
Total number of <i>Xanthomonas</i> downloaded from NCBI	1577													
<i>Xanthomonas</i> with T6	1186 (~78%)													
<i>Xanthomonas</i> without T6	365 (~22%)													

*number of strains with partial T6 clusters are shown inside the parenthesis

Table 3-2: Comparison of T6SS-i3* cluster core genes in Xe85-10 and early-branching species, *X. translucens* F5 and identifying the closely related species to *X. translucens* F5 i3* cluster

Xe85-10 i3* locus tag	Gene name	Percent identity to Xe85-10 (%)	<i>X. translucens</i> F5 i3* cluster Locus tag	Closest match-percent identities (%) according to BLAST results
XCV4202	<i>tssA</i>	66.67	Ga0372549_3941	99% identity to <i>Xanthomonas</i> sp. SI
XCV4209	<i>tssM</i>	68.81	Ga0372549_3934	100% identity to <i>Xanthomonas</i> sp. SI
XCV4210	<i>tssL</i>	71.93	Ga0372549_3933	95.3% identity to <i>Xanthomonas</i> sp. SI
XCV4211	<i>tssK</i>	80.18	Ga0372549_3932	96% identity to <i>Xanthomonas</i> sp. SI
XCV4217	<i>vgrG</i>	61.56	Ga0372549_3929	95% <i>Xanthomonas</i> sp. SS
XCV4236	<i>clpV</i>	84.55	Ga0372549_3921	95% <i>Xanthomonas</i> sp. SS
XCV4237	<i>tssG</i>	72.59	Ga0372549_3920	95.45% <i>Xanthomonas</i> sp. GW
XCV4238	<i>tssF</i>	79.30	Ga0372549_3919	96.04% <i>Xanthomonas</i> sp. GW
XCV4239	<i>tssE</i>	78.44	Ga0372549_3918	97% <i>Xanthomonas</i> sp. SS
XCV4241	<i>hcp</i>	97.01	Ga0372549_3916	97.62% <i>Xanthomonas</i> sp. SI
XCV4242	<i>tssC</i>	93.16	Ga0372549_3915	100% <i>Xanthomonas</i> sp. SI
XCV4243	<i>tssB</i>	93.45	Ga0372549_3914	97.24% <i>Xanthomonas</i> sp. GW

Table 3-3: List of non-pathogenic strains used in the phylogenetic analysis

	Strain Name	Isolation
1	<i>Xanthomonas campestris</i> CFBP7622	Bean leaf washings
2	<i>Xanthomonas arboricola</i> 2955	Rain
3	<i>Xanthomonas arboricola</i> 3640	Rain
4	<i>Xanthomonas campestris</i> CFBP7635	<i>Juglans regia</i> cv. Franquette
5	<i>Xanthomonas arboricola</i> 2974	Rain
6	<i>Xanthomonas arboricola</i> 2949	Rain
7	<i>Xanthomonas campestris</i> 3338	Rain
8	<i>Xanthomonas</i> sp. BRIP62411	<i>Solanum lycopersicum</i>
9	<i>Xanthomonas</i> sp. BRIP62409	<i>Solanum lycopersicum</i>
10	<i>Xanthomonas</i> sp. BRIP62415	<i>Solanum lycopersicum</i>
11	<i>Xanthomonas arboricola</i> 2957	Rain
12	<i>Xanthomonas arboricola</i> F2	<i>Physalis peruviana</i> Ground cherry
13	<i>Xanthomonas arboricola</i> CFBP8152	<i>Phaseolus vulgaris</i>
14	<i>Xanthomonas campestris</i> CFBP8151	bean seed
15	<i>Xanthomonas arboricola</i> 3793	Rain
16	<i>Xanthomonas arboricola</i> 4461	Rain
17	<i>Xanthomonas arboricola</i> 3058	Rain
18	<i>Xanthomonas campestris</i> 3075	Rain
19	<i>Xanthomonas</i> sp. 60	<i>Solanum lycopersicum</i>
20	<i>Xanthomonas</i> sp. F1	citrus orange
21	<i>Xanthomonas</i> sp. 3498	Rain
22	<i>Xanthomonas</i> sp. F4	citrus orange
23	<i>Xanthomonas sacchari</i> F10	citrus orange
24	<i>Xanthomonas arboricola</i> 3307	Rain
25	<i>Xanthomonas translucens</i> F5	pepper-Bell Boy
26	<i>Xanthomonas maliensis</i> LMG27592	Rice
27	<i>Xanthomonas maliensis</i> M97	Rice
28	<i>Xanthomonas floridensis</i> WHRI 8848	watercress
29	<i>Xanthomonas sontii</i> PPL1	Rice

Table 3-4: Distribution of the i3* and i3*** clusters in the *X. axonopodis* complex.

Subgroups	<i>X. axonopodis</i> strains	i3***	i3*
9.1	<i>X. axonopodis</i> pv. <i>begoniae</i> strain CFBP2524		
	<i>X. axonopodis</i> pv. <i>spondiae</i> strain CFBP2623		
9.4	<i>X. phaseoli</i> pv. <i>dieffenbachiae</i> LMG 695	x	x
	<i>X. axonopodis</i> pv. <i>manihotis</i> str. CFBP1851		x
	<i>X. phaseoli</i> pv. <i>phaseoli</i> CFBP6546 GL1		x
9.2	<i>X. axonopodis</i> pv. <i>citrumelo</i> F1	x	x
	<i>X. axonopodis</i> pv. <i>allii</i> CFBP6369	x	x
	<i>X. alfalfae</i> subsp. <i>alfalfae</i> CFBP3836	x	x
	<i>X.campestris euvesicatoria</i> 85-10	x	x
9.3	<i>X. axonopodis</i> pv. <i>axonopodis</i> LMG 982	x	only <i>tssA</i>
	<i>X. axonopodis</i> pv. <i>vasculorum</i> NCPPB900	x	only <i>tssA</i> , <i>tssB</i> and <i>tssC</i>
9.5	<i>X. citri</i> CFBP3369		x
	<i>X. citri</i> pv. <i>glycines</i> CFBP2526		x
	<i>X. citri</i> pv. <i>malvacearum</i> XcmN1003		x
	<i>X. citri</i> pv. <i>mangiferaeindicae</i> CFBP1716		x
9.6	<i>X. citri</i> pv. <i>anacardii</i> CFBP2913	only <i>tssB</i> , <i>tssC</i> partial gens	x
	<i>X. citri</i> pv. <i>phaseoli</i> var. <i>fuscans</i> CFBP6165	only <i>tssB</i> , <i>tssC</i> partial gens	x
	<i>X. citri</i> pv. <i>fuscans</i> CFBP6991 <i>phaseoli</i> GL2	only <i>tssB</i> , <i>tssC</i> partial gens	x
	<i>X. citri</i> pv. <i>fuscans</i> pv. <i>phaseoli</i> GL3 CFBP6996	only <i>tssB</i> , <i>tssC</i> partial gens	x
	<i>X. citri</i> pv. <i>vignicola</i> CFBP7112	only <i>tssB</i> , <i>tssC</i> partial gens	x
	<i>X. citri</i> pv. <i>aurantifolii</i> ICPB 10535	only <i>tssB</i> , <i>tssC</i> partial gens	x

“x” indicates the presence of all the core genes

Table 3-5: Distribution of the T6 clusters according to the lifestyle of *Xanthomonas* spp.

<i>Xanthomonas</i> spp.	Vascular(V)/ Non-vascular (NV)	Host of isolation Mon(M)/ Dicotyledonous(D)	T6 clusters		
			i3***	i3*	i4
<i>X. floridensis</i> WHRI8848	NV	D		x	
<i>X. nasturtii</i> WHRI8853	V	D		x(partial)	
<i>X. vesicatoria</i> LMG911	NV	D		x	
<i>X. citri</i> pv. <i>citri</i> LMG9322	NV	D		x	
<i>X. perforans</i> CFBP7293	NV	D	x	x	
<i>X. euvesicatoria</i> 85-10	NV	D	x	x	
<i>X. fragariae</i> PD885	NV	D			x
<i>X. melonis</i> CFBP4644	NV	D		x	
<i>X. cucurbitae</i> CFBP2542	NV	D		x	
<i>X. phaseoli</i> pv. <i>phaseoli</i> CFBP412	V	D		x	
<i>X. cassavae</i> CFBP4642	V	D		x	
<i>X. codiae</i> CFBP4690	V	D		x	
<i>X. oryzae</i> pv. <i>oryzicola</i> CFBP7342	NV	M	x		x
<i>X. oryzae</i> ATCC35933	V	M	x		x
<i>X. vasicola</i> CFBP2543	V	M	x		
<i>X. vasicola</i> NCPPB2417	V	M	x		
<i>X. phaseoli</i> pv. <i>dieffenbachiae</i> LMG695	V	M	x	x	
<i>X. translucens</i> pv. <i>translucens</i> DSM18974	V	M	x		

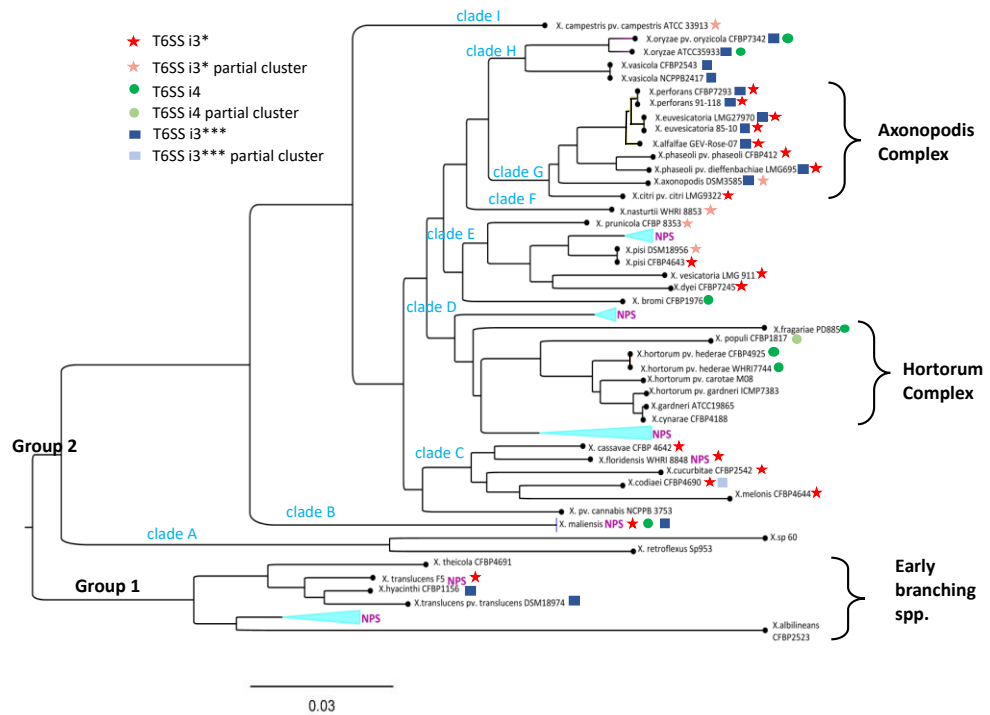


Figure 3-2: Distribution of T6SS in pathogenic *Xanthomonas* spp. Phylogenetic distribution of 43 *Xanthomonas* spp. based on the core alignment of nucleotide sequences using the Roary pipeline (Page et al., 2015). Whole-genome sequences of type strains or completely sequenced genomes representing the *Xanthomonas* spp. available in the National Center for Biotechnology Information (NCBI) database were used for phylogenetic reconstruction. The presence of complete and partial T6 clusters (i3*, i3*** and i4) have shown with different colors in the figure.

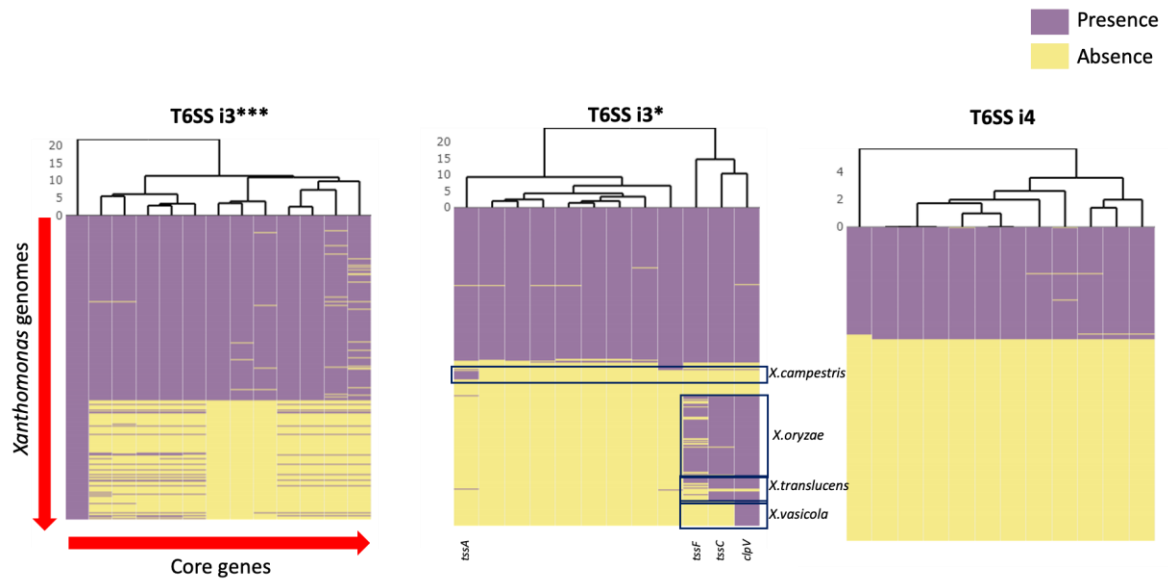


Figure 3-3: Presence/absence of T6 clusters in genus *Xanthomonas*. Heat maps were generated with T6SS-i3*, i3*** and i4 cluster presence/ absence matrix data obtained from the automlsa pipeline.

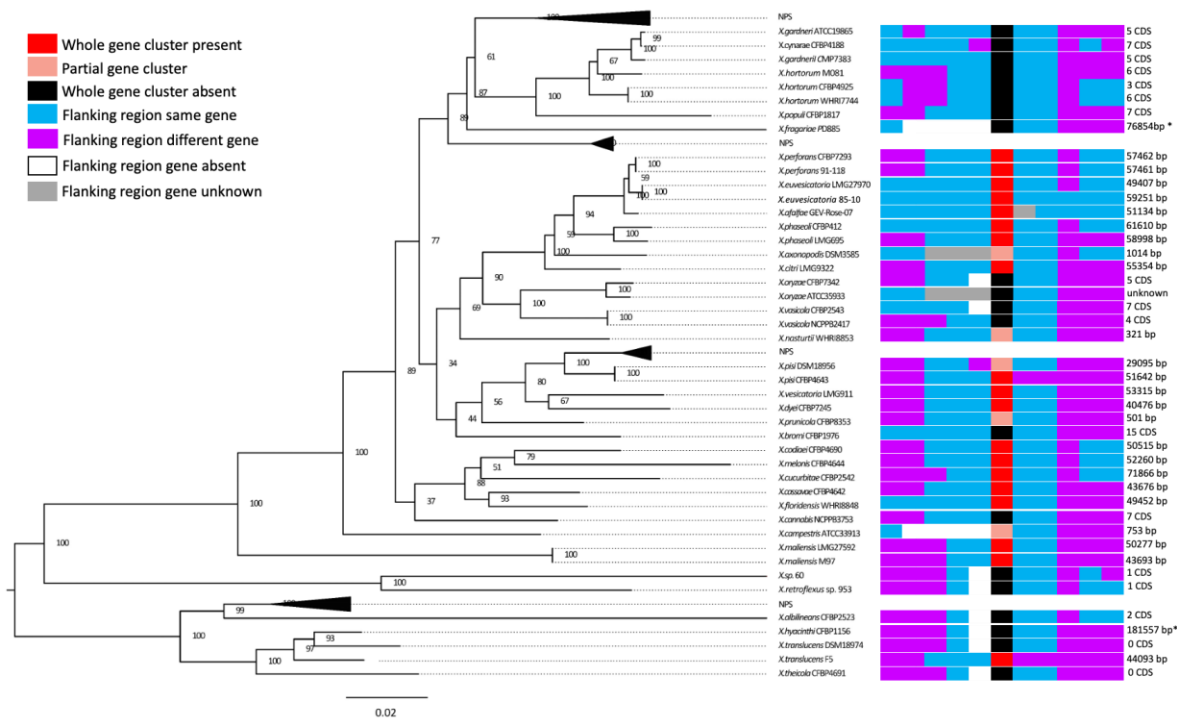


Figure 3-4: Presence of T6 cluster *i3** in *Xanthomonas* spp. with flanking regions. Phylogenetic distribution of 43 *Xanthomonas* spp. based on the core alignment of nucleotide sequences using the Roary pipeline and branch support was determined using 1000 bootstraps (Page et al., 2015). Whole-genome sequences of type strains or completely sequenced genomes representing the *Xanthomonas* spp. available in the National Center for Biotechnology Information (NCBI) database were used for phylogenetic reconstruction. Flanking regions of the T6 clusters were identified using the (IMG/M) (v.6.0) system and genome and microbiome datasets sequenced at DOE's Joint Genome Institute. Presence of all the core genes in the *i3** cluster (Red), absence of one or more core genes in the *i3** cluster (pink) or the absence of all the core genes (black) have been indicated with different colors and can be found in the middle of up and downstream genes. Genomic environments, similar (blue) and different (purple) genes found in the up and downstream of the T6SS-*i3** cluster are represented with colors. Comparisons were done using the *X. vesicatoria* 85-10 as the reference strain. Size of the T6 *i3** cluster is mentioned if the cluster is present or the number of CDS or the length of the DNA fragment (*) found in place of the *i3** cluster has been included in the last column of the figure.

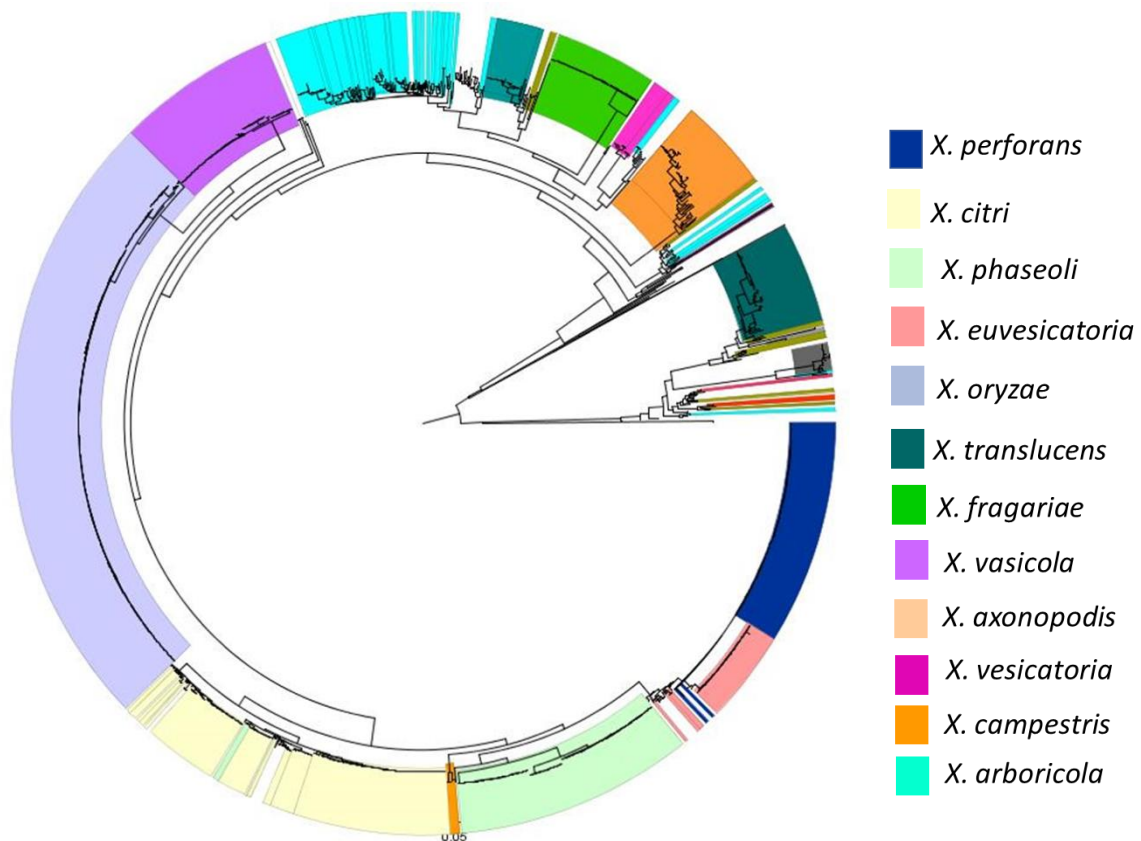


Figure 3-5: Relationship among 1577 *Xanthomonas* genomes. Multi-locus sequence analysis (MLSA) phylogeny of *Xanthomonas* spp. based on the concatenation of partial sequences of housekeeping genes *atpD*, *dnaK*, *efp*, *fusA*, *fyuA*, *gapA*, *glnA*, *gltA*, *gyrB*, *lacF*, *lepA* and *rpoD*. Phylogenetic tree in maximum likelihood (ML) criterion was developed using the IQ-TREE multicore version 2.1.2 COVID-edition and branch support was determined using 1000 bootstraps and 1000 SH-aLRT bootstrap replicates.

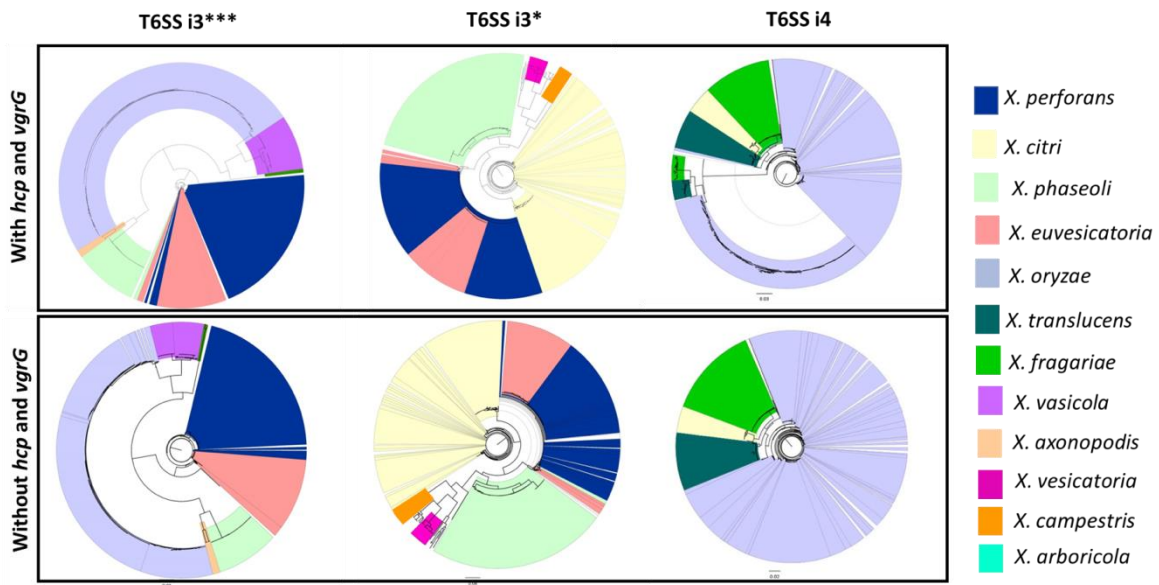


Figure 3-6: Distribution of T6 clusters in the genus *Xanthomonas*. T6 core gene phylogeny of *Xanthomonas* spp. based on the concatenation of T6 core genes (*tssA*, *tssB*, *tssC*, *tssD* (*hcp*), *tssE*, *tssF*, *tssG*, *tssH*, *tssI* (*vgrG*), *tssJ* (only in i4 cluster), *tssK*, *tssL* and *tssM*). (a) T6SS core gene phylogeny of i3***, i3* and i4 clusters including *hcp* and *vgrG* core genes (b) T6SS core gene phylogeny of i3***, i3* and i4 clusters in the absence of *hcp* and *vgrG* core genes. Phylogeny was generated using the automated multi-locus sequence analysis pipeline (automlsa2). Phylogenetic tree in maximum likelihood (ML) criterion was developed using the IQ-TREE multicore version 2.1.2 COVID-edition and branch support was determined using 1000 bootstraps and 1000 SH-aLRT bootstrap replicates.

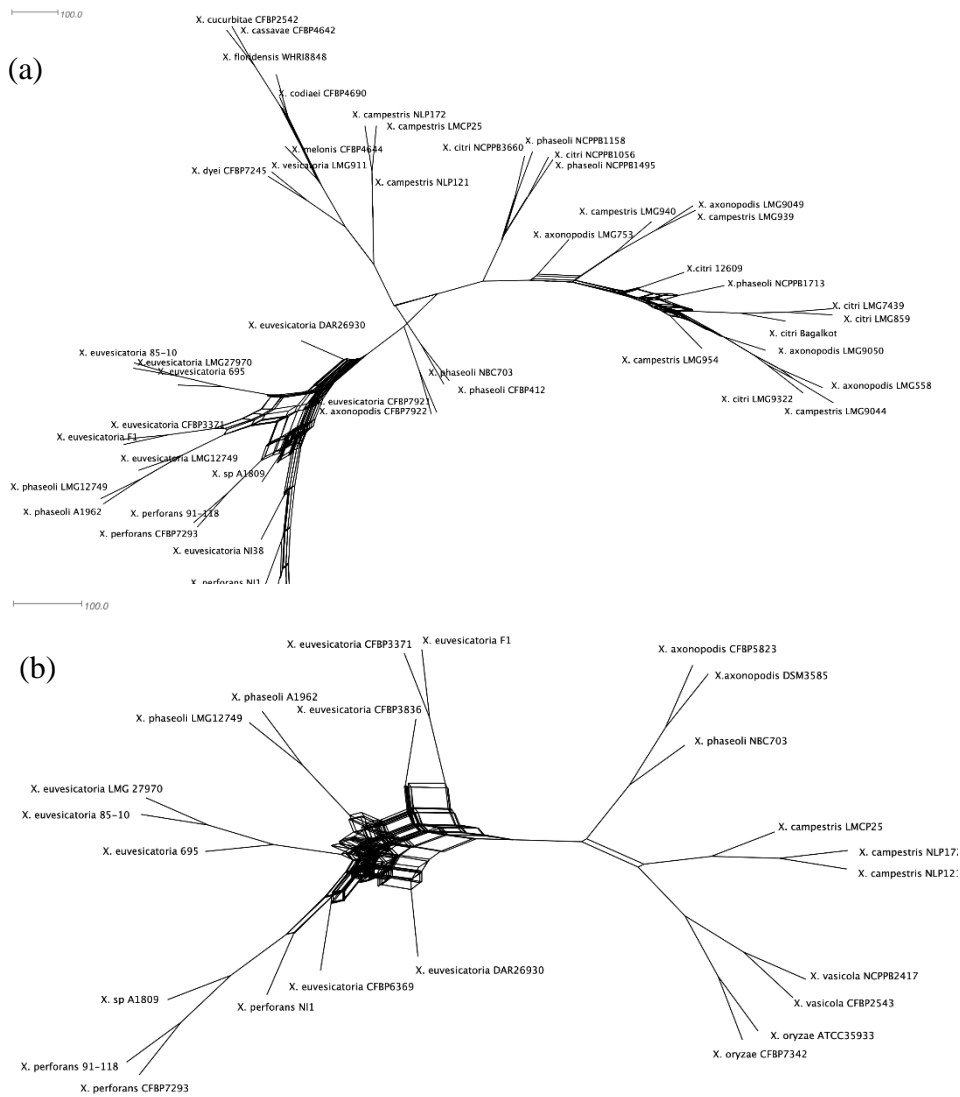


Figure 3-7: Split decomposition tree of the selected *Xanthomonas* spp. that showed incongruencies between MLSA phylogeny and (a) T6SS-i3* without *hcp* and *vgrG* (b) T6SS-i3*** without *hcp* and *vgrG*. The figure was drawn to scale using Splitstree4. The formation of parallel lines indicates conflicting phylogeny or possible recombination events.

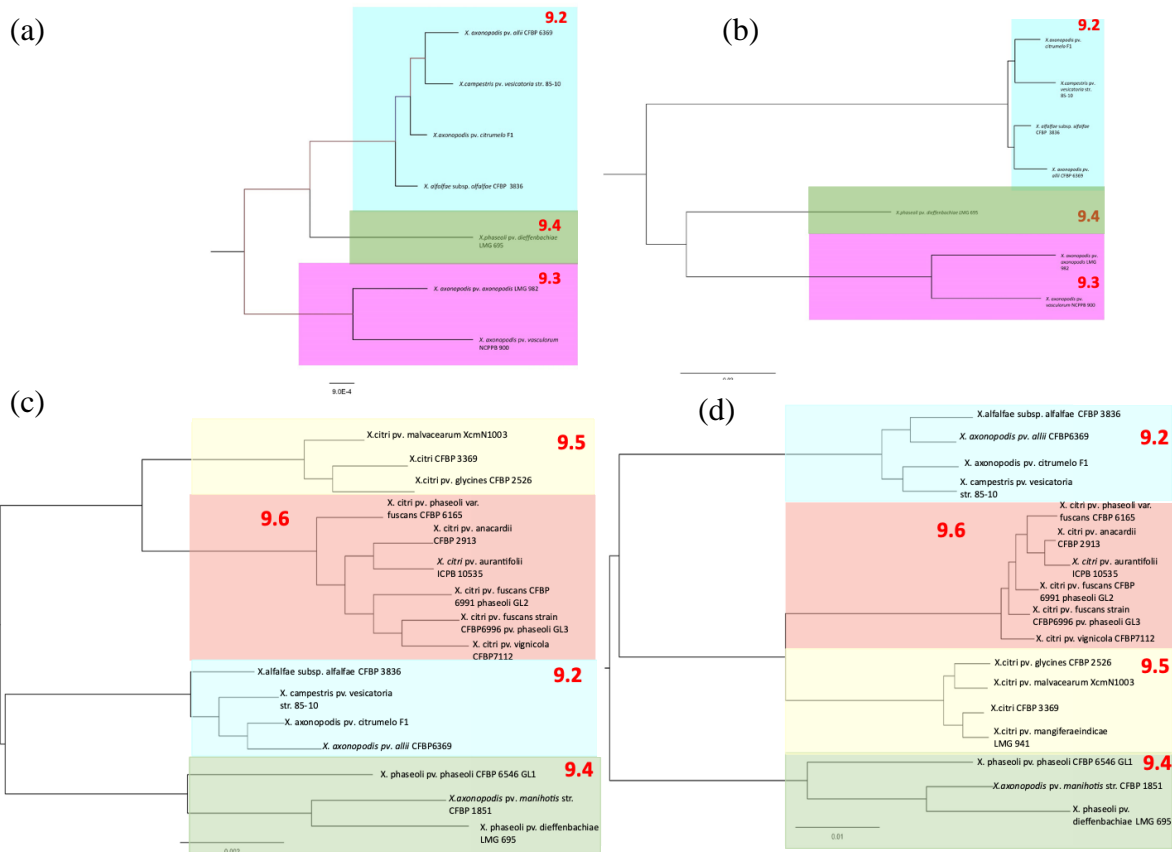


Figure 3-8: Comparison of the core genome phylogeny of *X. axonopodis* subspecies with T6 i3***/ i3* core genome phylogeny to T6SS-i3*/i3*** core gene phylogeny. (a) core gene phylogeny for the strains with i3*** (b) T6SS-i3*** phylogeny (c) core gene phylogeny for the strains with i3* (d) T6SS-i3* phylogeny. Core genome phylogenies were developed based on the core alignment of nucleotide sequences using the Roary pipeline (Page et al., 2015) while T6 phylogenies were generated using the automated multi-locus sequence analysis pipeline (automlsa2). Phylogenetic tree in maximum likelihood (ML) criterion was developed using the IQ-TREE multicore version 2.1.2 COVID-edition and branch support was determined using 1000 bootstraps and 1000 SH-aLRT bootstrap replicates.

(a)

Subgroup	Strains	Cluster	Total #	SMAD/FHA	VgrG	TonB	Endo/exo nuclease	Hcp	Histidine phosphatase	Haemolysin activator	Protein kinase	HP (24Aaa)	DUF4124	HP (236aa)	HP (164aa)	HP (102aa)	HP (71aa)	Pectin lyase fold	Other unique HP
9.2	<i>X. axonopodis</i> pv. <i>citrumelo</i> F1	I3*	11																2
9.2	<i>X. axonopodis</i> pv. <i>allii</i> CFBP 6369	I3*	10																0
9.2	<i>X. alfalfae</i> subsp. <i>alfalfae</i> CFBP 3836	I3*	10																0
9.2	<i>X. campestris</i> pv. <i>vesicatoria</i> str. 85-10	I3*	11																0
9.4	<i>X. phaseoli</i> pv. <i>dieffenbachiae</i> LMG 695	I3*	11																1
9.4	<i>X. axonopodis</i> pv. <i>manihotis</i> str. CFBP 1851	I3*	10																0
9.4	<i>X. phaseoli</i> pv. <i>phaseoli</i> CFBP 6546 GL1	I3*	11																1
9.5	<i>X. citri</i> CFBP 3369	I3*	10																2
9.5	<i>X. citri</i> pv. <i>mangiferae</i> LMG 941	I3*	11																0
9.5	<i>X. citri</i> pv. <i>glycines</i> CFBP 2526	I3*	11																0
9.5	<i>X. citri</i> pv. <i>malvacearum</i> XcmN1003	I3*	11																0
9.6	<i>X. citri</i> pv. <i>anacardii</i> CFBP 2913	I3*	10																0
9.6	<i>X. citri</i> pv. <i>phaseoli</i> var. <i>fuscans</i> CFBP 6165	I3*	10																0
9.6	<i>X. citri</i> pv. <i>fuscans</i> strain CFBP6996 GL3	I3*	10																1
9.6	<i>X. citri</i> pv. <i>vignicola</i> CFBP7112	I3*	9																0
9.6	<i>X. citri</i> pv. <i>aurantifolii</i> ICPB 10535	I3*	11																2
9.6	<i>X. citri</i> pv. <i>phaseoli</i> var. <i>fuscans</i> CFBP 6991 GL2	I3*	10																1

(b)

Subgroup	Strains	Cluster	Total #	serine/threonine kinase	SMAD/FHA	VgrG	Hcp	(TIR)	Deaminase (223aa)	Hp (180aa)	HP (182aa)	Other unique HP
9.2	<i>X. axonopodis</i> pv. <i>citrumelo</i> F1	I3***	7									1
9.2	<i>X. axonopodis</i> pv. <i>allii</i> CFBP 6369	I3***	6									0
9.2	<i>X. alfalfae</i> subsp. <i>alfalfae</i> CFBP 3836	I3***	8									1
9.2	<i>X. campestris</i> pv. <i>vesicatoria</i> str. 85-10	I3***	8									2
9.3	<i>X. axonopodis</i> pv. <i>axonopodis</i> LMG 982	I3***	5									0
9.3	<i>X. axonopodis</i> pv. <i>vasculorum</i> NCPBB 900	I3***	4									0
9.4	<i>X. phaseoli</i> pv. <i>dieffenbachiae</i> LMG 695	I3***	6									1

Figure 3-9: T6 effectors identified using the T6SS effectors using the Bastion6 machine-learning tool (Wang et al., 2018). T6 effectors identified in the (a) i3* cluster and (b) i3*** clusters of *X. axonopodis* subgroups.

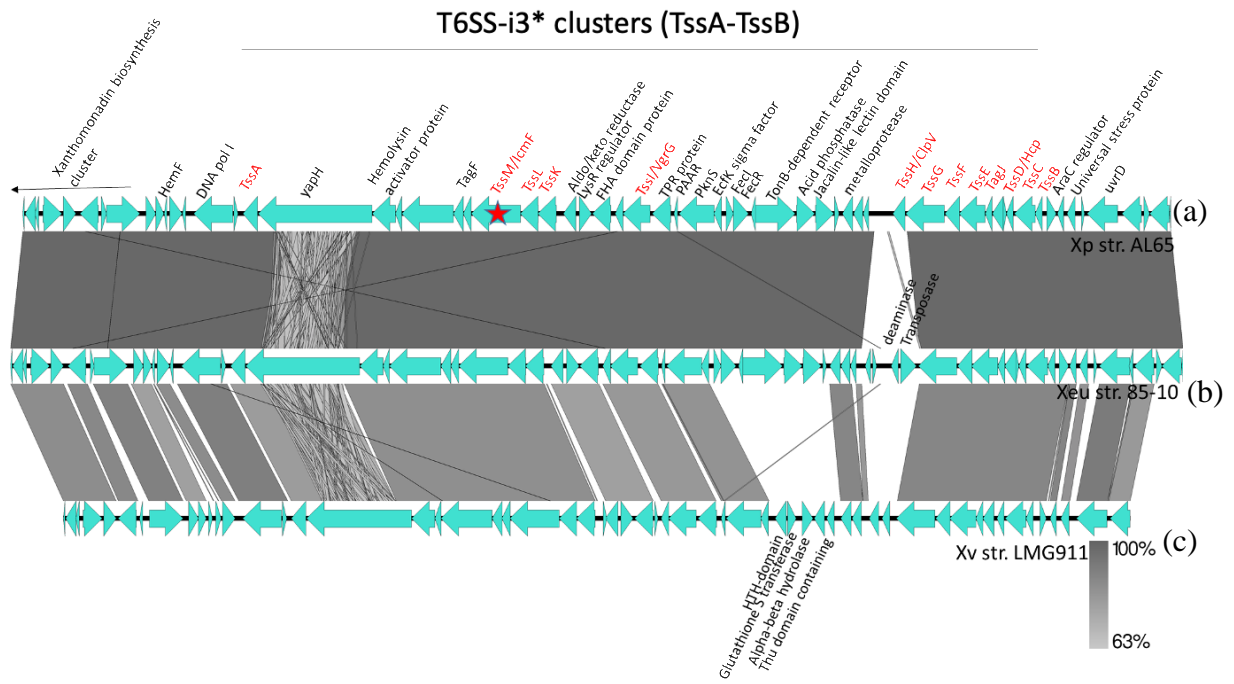


Figure 3-10: Organization of the T6SS-i3* clusters in BLS *Xanthomonas*. (a) *XpAL65* (b) *Xe85-10* and (c) *XvLMG911*

4. CHAPTER FOUR

Investigating the phenotypic variations arising in experimentally passaged

Xanthomonas perforans populations

Abstract

Xanthomonas perforans (Xp) is the predominant, causal agent of the bacterial leaf spot disease in tomatoes. Recent discoveries of naturally occurring Xp in pepper field in the southeastern US indicate a recent shift in the Xp host range. To investigate the genetic basis of host adaptation of Xp, we conducted an experimental evolution study, using BLS causing *Xanthomonas perforans* as our model system. Nineteen rounds of repeated inoculations were conducted on susceptible host tomato (cv. FL47) and resistant host pepper (cv. ECW) either in the presence or absence of *Xanthomonas euvesicatoria*. After 6 rounds of re-inoculations, we detected the loss of the hypersensitive response in the Xp4B passaged on pepper plants, revealing a route of host range expansion by Xp. Phenotypic analysis was able to identify an increase in the bacterial population growth in both tomato and pepper, with a greater magnitude of increment in the non-host pepper plants. We were also able to identify the fitness loss associated with the adaptation of Xp in the pepper plants. Even though XpPM1 (*Xp91-118ΔavrXv3*) strain was also subjected to passaging in tomato and pepper plants, population growth was unaffected by the continuous re-inoculations. Understanding these adaptive processes in pathogens is important in developing effective control measures. Our results also emphasize the importance of preventing the repeated infection of resistant host plants by non-pathogenic strains to avoid the emergence of new pathogenic strains.

Introduction

Bacterial leaf spot (BLS) of tomato (*Solanum lycopersicum*) and pepper (*Capsicum annuum*) is one of the numerous plant diseases caused by the genus *Xanthomonas*, that creates significant crop losses in warm and humid regions worldwide (Potnis et al., 2011). Until the

mid-1990s, bacterial spot in tomato and pepper was considered to be caused by a single species, *Xanthomonas vesicatoria* (Stall et al., 1994; Vauterin et al., 1995). After being reclassified several times, most recently four distinct species, *X. euvesicatoria* (Xe), *X. vesicatoria* (Xv), *X. perforans* (Xp), and *X. gardneri* (Xg) have been identified as the causal agents of the bacterial spot disease in tomato and pepper (Jones et al., 2004). These species display extensive variation according to phenotypic and phylogenetic analyses and also in geographic distribution (Almeida et al., 2010; Stall et al., 1994). Even though all the four species are reported to be extensively distributed worldwide, dramatic changes in the population dynamics have been reported in recent years in the United States (Jones et al., 2004). In the southeast United States, Xp is the predominant BLS causing pathogen in tomatoes, while Xe is in the pepper plants (Horvath et al., 2012; Newberry et al., 2019). In Florida, the emergence of Xp as a dominant tomato pathogen started in the early 1990's while in Ohio and Michigan Xg, which was recently reclassified as of *X. cynarae* emerged as a major pathogen in 2009 (Jones et al., 1998; Stall et al., 2009; Ma et al., 2011; Horvath et al., 2012; Timilsina et al., 2018).

Xp population in Florida has faced species wipeout, race shift and changes in the host specificity in the last two decades. Prior to 1991, only tomato race 1 (T1), Xe strains were reported as the major pathogens on tomato in Florida, but in 1991 the first Xp (tomato race 3, T3) strains were identified in the same fields where Xe T1 strains have existed and Xp T3 became the dominant pathogen in tomato over a single season by displacing Xe. (Jones et al., 2004; Timilsina et al., 2016). This shift in the Xe T1 population to Xp T3 was recognized to be in part due to the production of bacteriocin by Xp T3 strains, that were toxic to Xe T1 strains (Hert et al., 2005). Xp T3 strains also contain *avrXv3* effector genes that elicit a hypersensitive response (HR) in any tomato genotype with *Xv3* gene (Jones et al., 1998). Tomato race 4 (T4) Xp that was identified in 1998 was having null mutations in *avrXv3* gene (XopAF) and became the dominant pathogen causing BLS on tomato in Florida, upon completing the race shift from

T3 to T4 by 2012 (Timilsina et al., 2016). Since AvrXv3 triggers an HR on T3-resistant tomato lines with *Xv3* locus, Xp T4 with mutations in *avrXv3* gene overcomes resistance on these lines (Horvath et al., 2012). Effector profile comparisons between Xp T3 type strain *Xp91-118* with Xp T4 strains have also identified the presence of the *avrBsT* gene in most of the Xp T4 strains, as a notable difference between the two races (Timilsina et al., 2016).

Whole-genome sequence analysis of Xp indicating variations in effector profiles among T4 strains has identified the presence of *avrBsT* effector gene in most of the T4 Xp strains (Timilsina et al., 2016). This self-transmissible, plasmid-borne *avrBsT* effector gene is associated with the hypersensitive response (HR) on most varieties of pepper and present in some strains of Xv and Xe despite not being a core effector (Minsavage et al., 1990; Stall et al., 2009; Kim et al., 2010; Potnis et al., 2011; Schwartz et al., 2015; Timilsina et al., 2016). Interestingly, the *avrBsT* gene from Xp is identical to *avrBsT* gene of Xv LMG919 isolated from Zimbabwe (GCA_001469445.1). Even though it can be hypothesized Xp might have acquired *avrBsT* from Xv through horizontal gene transfer, surprisingly there are no reports of Xv in Florida, so the donor of *avrBsT* to Xp remains unknown. *avrBsT* gene was first recognized in the Xp T4 strain and it was isolated in 1998 in Florida and recent studies have identified *avrBsT* in several Xp T3 strains isolated after 1998 and but not in the Xp T3 collected prior to that including the T3 reference strain *Xp91-118* (Potnis et al., 2011; Timilsina et al., 2016; Abrahamian et al., 2018). So it has been hypothesized that the acquisition of the *avrBsT* might have occurred before or during the race shift by both Xp T3 and T4 strains (Timilsina et al., 2016).

Recent studies on evolutionary dynamics patterns of Xp have identified a genomic flux between Xp and Xe, where Xe is most likely the donor of the recent recombination events (Newberry et al., 2019). Hence Xp is a great model system to further study adaptive evolution mediated by homologous recombination and horizontal gene transfer with other

tomato/pepper-pathogenic strains that occupy the same niche or other closely related *Xanthomonas* species that can infect a wide range of other hosts. With this gene flow observed with BLS *Xanthomonas* spp., we can hypothesize a gain of pepper infectivity by Xp in the presence of a closely related competing pathogen via genes or alleles exchange. To further investigate this hypothesis, an experimental evolution approach can be used to track the changes that arise the Xp population under host selection pressure and in either the presence or absence of closely related Xe.

Experimental evolution is the study of evolutionary changes that occur in populations as a result of experimental conditions imposed by the experimenter, which often involves propagation of microbial populations over many generations in a controlled environment (Kawecki et al., 2012; Hoang et al., 2016). Richard Lenski and collaborators are conducting a Long-Term Evolution Experiment (LTEE), for over 30 years and 70,000 generations of 12 *Escherichia coli* populations in minimal media (Lenski, 2017). Serial passage experiments (SPEs) are a form of experimental evolution, where microbes (or any parasite) can be transferred from one host to another and maintained under defined conditions hence considered as a powerful tool for studying adaptation (Ebert, 1998). Microbes can be transferred artificially or through natural transmission and their evolved populations can be compared with the ancestor at the end of the experiment or during the experiment, since the pooled population of many organisms can be cryogenically preserved (Hoang et al., 2016). Since the environmental conditions can be controlled in experimental evolution experiments, influence of biotic and abiotic factors can be minimalized and trait of interest can be traced, therefore considered as a useful approach in multispecies interaction studies (Hoang et al., 2016). Since parallel evolution or the independent evolution of the same trait across different lineages is unlikely to be a completely random scenario, it delivers strong evidence for adaptive changes and also

provides answers to the concerns regarding the reproducibility of evolutionary changes on independent experiments (Pelosi et al., 2006).

Most of the experimental evolution studies that have been conducted so far are under homogenous (often laboratory) environment conditions in culture media are simplifying the complex conditions in nature. The evolutionary process in nature can proceed differently due to the unidentified biotic and abiotic factors or multiple factors that act in synergy, therefore studying the evolution of a pathogen outside if the host may result in constant selection pressure and function differently than natural environment (Guidot et al., 2014; Hoang et al., 2016). Few of the recent studies have answered this limitation by conducting *in vivo* serial passaging experiments, where pathogens encounter environmental heterogeneity during the interaction with multicellular hosts (Ebert, 1998). Up to date, serial passaging experiments have been conducted in several phytopathogenic bacteria including, evolution studies on *X. citri* subsp. *citri* (Trivedi and Wang, 2014), *Pseudomonas syringae* pv. *phaseolicola* (Pitman et al., 2005), *Pseudomonas syringae* pv. *tomato* (Meaden and Koskella, 2017) and *Ralstonia solanacearum* (Guidot et al., 2014).

In this experimental evolution study, we hypothesized a host expansion in the Xp strains, when the host selection pressure was continuously applied to it, and also relatively faster adaptations in Xp to pepper plants in the presence of the dominant pepper pathogens (Xe sister strains). We used two Xp strains, which represent the ancestral 1990s population of Xp, as parent strains. Xp4B is a tomato race 4 strain that was isolated in 1998, carries a mutation in the *avrXv3* gene and also carries *avrBsT* encoding plasmid hence non-pathogenic on pepper (Schwartz et al., 2015). Xp91-118, isolated in 1991 is a tomato T3 pathogen which carries an avirulence gene, *avrXv3*, that restricts the host range of Xp to tomato, giving HR on pepper (Astua-Monge et al., 2000). Even when there is a mutation in the *avrXv3* gene, Xp91-118 was still non-pathogenic on pepper, indicating the existence of other factors that restrict its host

range on pepper (Astua-Monge et al., 2000; Schwartz et al., 2015). In this study we used the XpPM1 strain, which is a Xp91-118 marker exchange, *avrXv3* mutant, which no longer elicits an HR in pepper (Astua-Monge et al., 2000; Potnis et al., 2011). This study was conducted as two systems, where Xp4B strain was serially passaged individually on tomato and pepper plants and in the presence of closely related Xe85-10 and XpPM1 strain was serially passaged individually on tomato and pepper plants and in the presence of closely related Xe75.3. Characteristics of the strains used in this study are summarized in table 4.1. The experimental design proposed here will allow us to test factorial interactions, namely, effect of host background and presence of sister species on genome plasticity of Xp to influence its ability to expand its host range on pepper. We expect to identify genetic changes (e.g., gene gain/loss) in progeny isolates from the passaging experiments that are associated with an incremental increase in infectivity on pepper.

Methodology

Bacterial Strains, Plant Material, and Growth Conditions

This evolutionary study was conducted as two systems where *Xanthomonas perforans* 4B and *Xanthomonas perforans* PM1 (*Xp91-118ΔavrXv3*) (Potnis et al., 2011) were individually passaged on tomato and pepper plants and Xp4B and XpPM1 were mixed passaged with *Xanthomonas euvesicatoria* (also *Xanthomonas campestris* pv. *vesicatoria*) 85-10 (Xe85-10) and *X. euvesicatoria* 75-3 (Xe75.3) respectively. Nalidixic acid-resistant derivative Xp4B strain and kanamycin-resistant derivative of the XpPM1 strain were used for the plant inoculations. *Xp4BΔavrBsT*, a whole gene knockout strain constructed by Schwartz et al., 2015 using the suicide vector pLVC18 containing 1kb upstream and 1kb downstream fragments flanking the *avrBsT* gene was also used to compare the populations.

X. perforans and *X. euvesicatoria* strains were grown for 24h at 28°C on Nutrient agar (NA) (Difco) and *E. coli* was cultivated in Luria-Bertani (LB) agar or broth at 37°C (Miller,

1972). When required antibiotics were added into the media to maintain selection for resistance markers at following working concentration: kanamycin (Km), 50µg/ml; nalidixic (Nal), 50 µg/ml. All the strains were stored in sterile tap water at room temperature or in 30% glycerol at -80°C or both.

Tomato (*Solanum lycopersicum* cv. FL47) and pepper (*Capsicum annuum* cv. Early Calwonder (ECW) were used in this study. Two weeks old seedlings were transplanted into sterile 4” plastic pots (The HC Companies, OH, USA) with soil-less potting medium (Premier Tech Horticulture, PA, USA). Plants were kept under 16h light per day at 28-30°C under greenhouse conditions. Four- to five-week-old seedlings were used for the inoculations and plants were kept inside the growth chamber at 25°C with 12h light/dark cycle until the end of each trial.

Serial passaging experiment- experimental procedure

Individual passages of Xp4B and XpPM1 on Tomato and pepper

Single colonies from Xp4B^{nalidixic} and XpPM1^{kanamycin} were grown overnight in corresponding antibiotics amended NA at 28°C. Cell suspensions containing ~1 X 10⁵ cfu/ml of Xp4B and XpPM1 were individually inoculated into three leaves (3 reps) of 4- to 5-week-old tomato cv. FL47 and pepper cv. ECW using a needleless syringe.

Mixed passages of Xp4B+Xe85-10 and XpPM1+Xe75.3 on tomato and pepper

Single colonies from Xp4B^{nalidixic}, XpPM1^{kanamycin}, Xe85-10 and Xe75.3 were grown overnight in corresponding antibiotics amended NA or just NA at 28°C. Cell suspensions containing ~1 X 10⁵ cfu/ml of Xp4B^{nalidixic} +Xe85-10 and XpPM1^{kanamycin} + Xe75.3 mixed in 1:1 ratio was used to inoculate three leaves (3 reps) of 4- to-5-week-old tomato cv. FL47 and pepper cv. ECW using a needleless syringe. Table 4-2 summarizes the list of treatments used in this passaging experiment.

Inoculated plants were kept in a growth chamber at 25°C with 12h light/dark cycle after inoculation. After 5 days, inoculated leaves and leaflets were used to recover the inoculated Xp to use in the next round of passaging and to determine the bacterial populations using the below-described procedure.

At 5 days, ~ 3 cm² area of leaflet tissues were taken from each replicate using a sterile cork borer. Using sterile forceps leaf discs were placed inside sterile microcentrifuge tubes containing 1 ml sterile MgSO₄ buffer and macerated using a sterile homogenizer. Ten-fold serial dilutions of the homogenized suspension were plated on kanamycin or nalidixic amended plates using spiral plater (Neu-tec Group Inc, NY, USA) to estimate the population size of XpPM1 and Xp4B in individual inoculations and mixed inoculations. Since the antibiotics were added into the media only the Xp was allowed to grow in the plates in the mix inoculations and this also limits carryover of plant hormones and any other bacteria colonizing the leaves. Plates were kept at 28°C for 2 days before quantifying the colony counts. Bacterial populations were determined as colony forming units (cfu) per cm² of leaf area. Recovered bacterial populations were pooled together to make ~1 X 10⁵ bacterial suspensions of each individual treatments (100, 200, 500 and 600). In the treatments with mixed inoculum (300, 400, 700 and 800), recovered suspensions were mixed in 1:1 ratio with freshly prepared Xe 85-10 or Xe 75.3. These bacterial suspensions were used to inoculate healthy 4- to 5-week-old tomato cv. FL47 and pepper cv. ECW using a needleless syringe and followed the same procedure to recover the bacteria after 5 days. This procedure was followed until 19 passages, which include ~100 days of selection *in planta* and ~40 days of selection on nutrient agar amended with antibiotics. At the end of each passage, 1 ml of the recovered bacterial suspension was also stored in glycerol at -80°C and 1ml was also stored in tap water and stored at room temperature. Each replicate in every treatment were handled individually and labelled accordingly in each passage to track the variations that arise in each replicate in future experiments. These pooled

suspensions were used in the pathogenicity assays and future sequencing experiments. The experimental procedure has been described visually in figures 4-1 and 4-2.

Growth chamber pathogenicity assay with 2nd, 4th and 6th passages of Xp4B individual (600) and Xp4B +Xe85-10 (800) mixed passaged on pepper plants

Pooled suspensions of selected treatments and passages were taken out from the -80°C storage and streaked in the corresponding antibiotics amended NA media. When the serial passages were continued up to 6 passages, we observed a rapid increment in the population growth in two of the treatments: Xp4B individual (600) and Xp4B +Xe85-10 (800) when passaged in pepper plants. To confirm if we see a significant increment in the bacterial population of passage 6, compared to initial passages, we conducted a pathogenicity assay by using passages 2,4 and 6 of Xp4B individual (600) and Xp4B +Xe85-10 (800) treatments. Four- to five-week-old pepper cv. ECW plants were inoculated using a needleless syringe with $\sim 1 \times 10^5$ bacterial suspensions and kept inside the growth chamber at 25°C with 12h light/dark cycle after inoculation. Bacterial populations were calculated at the day of the inoculation, 4 days and 8 days post-inoculation. Bacterial populations were determined as log cfu/cm² as described above.

Hypersensitive response (HR) assay

As we observed an increase in bacterial population growth in 6th passages of Xp4B (600) and Xp4B +Xe85-10 (800) and the *Xp4B Δ avrBsT*, we wanted to further confirm the loss of the AvrBsT plasmid by the Xp4B (600) and Xp4B +Xe85-10 (800) by the 6th passage. Since AvrBsT, has proven to be associated with hypersensitive response (HR) on ECW pepper plants that carries a *Bst* resistance locus (Minsavage et al., 1990), an HR experiment was conducted on 4- to 5-week-old pepper cv. ECW plants using above-motioned *Xanthomonas* spp..

The pepper leaves were inoculated by infiltrating $\sim 1 \times 10^8$ bacterial suspensions into the abaxial leaf surface by using a needleless syringe. Plants infiltrated with sterile MgSO₄ were

used as negative controls. Plants were kept inside the growth chamber at 25°C with 12h light/dark cycle after inoculation for 48 hours and leaves were observed for the symptom development.

Host swapped experiment

After completing 19 passages, by observing the dynamics of the population change in each of the treatments, Passages 6, 10, 15 and 19 were selected to further identify the changes in the population growth with the serial passaging. All the treatments in the above-mentioned passages were taken out of the -80°C storage and streaked on corresponding antibiotic amended media. Four- to five-week-old tomato cv. FL47 and pepper cv. ECW were inoculated with $\sim 1 \times 10^5$ bacterial suspensions and kept inside the growth chamber at 25°C with 12h light/dark cycle for 5 days and bacterial populations were calculated as log cfu/cm² as described above. In the same experiment, we used the prepared inoculum to infiltrate the alternate host for each treatment as well. For example, bacterial suspension of passage 6 of the 4B alone on tomato treatment (500), was used to inoculate both tomato cv. FL47 and pepper cv. ECW plants. Bacterial population values observed from the treatment 500 on pepper plants were compared with the bacterial population values of the treatment 600 (4B alone on pepper). The experimental procedure has been visually illustrated in figure 4-3 and the list of treatments can be found in table 4-3.

Statistical analysis

Difference between the mean values were analyzed using the one-way ANOVA when a single factor was considered, and two-way ANOVA test was performed when two factors (treatment and passage) were compared. Tukey's post-hoc test of least significant difference ($P < 0.05$) was used for the mean comparisons. All the analysis were performed, and Bar charts, boxplots and Density ridgeline plots were generated using the R statistical software.

Pathogenicity experiments were repeated twice, and statistical analysis shows data from a single representative trial.

Results

***X. perforans* 4B strain lost the HR in the resistant host (pepper cv. ECW) and expanded its host range to pepper, when serially passaged six times on pepper plants**

Experimental evolution of two *X. perforans* strains (Xp4B and XpPM1) was conducted on their host of isolation tomato and non-host pepper plants. When the passages were continued up to six passages, an increment of the number of bacterial colonies re-isolated from the infected pepper plants was observed with a treatment, where Xp4B was mixedly passaged with Xe85-10 on pepper plants. To confirm if this increase in the population number is significantly higher than initial passages, a pathogenicity assay was conducted inside the growth chamber. Treatments 600 and 800 from passages 2, 4 and 6 were used in the assay and bacterial population values were calculated on the day of inoculation, 4 dpi and 8 dpi.

As shown in figure 4-4, when the selected passages of the treatment 600 (Xp4B alone on pepper) were compared, on the day of inoculation significantly higher bacterial population was observed in passage 4 compared to passage 6. On day 4 there was no significant difference in the population values among the passages. Eight days post-inoculation, Xp4B passaged on pepper up to 6 passages shows significantly higher mean population values compared to passage 2 and 4.

Similarly, when the bacterial population values of 2nd, 4th and 6th passages of the treatment 800 (Xp4B+ Xe85-10 mixed passage on pepper) were compared, significantly higher population values were observed for passage 6 at day 8 compared to the other two passages ($p < 0.05$) (figure 4-5).

Since AvrBsT was proven to be associated with hypersensitive response (HR) induced programmed cell death on ECW pepper plants that carries a *Bst* resistance locus (Minsavage et

al., 1990), loss of the AvrBst was phenotypically assed by conducting a HR test using Xp4B strains passaged on pepper in the absence and presence of the Xe85-10. When the symptom development was observed 48hpi, Xp4B ancestor strain exhibited the tissue death while mild disease symptoms were observed with the *Xp4BΔavrBsT* strain and the 6th passage, of 4B alone and 4B mixed passaged with Xe85-10, phenotypically confirming the loss of AvrBsT plasmid by the Xp4B strain when passaged on the non-host pepper plants up to 6 passages (figure 4-6).

***X. perforans* 4B strain shows ascending population density when continuously passaged on its non-host pepper plants, indicating possible host-expansion**

When the Xp4B strain was passaged on tomato, initial drop in the population was observed by the 6th passage and this gradual decrease in the population was observed up to the 12th passage, while between passages 13-19, population distribution of the Xp4B gradually increased. By the 19th passage the population distribution of the Xp4B on tomato plants were approximately similar to the population of the ancestor strain (figure 4-7a). Similarly, when the Xp4B was passaged together with Xe85-10 on tomato plants, a similar trend in the population density distribution was observed, except for passage 10, where a ~1log drop of the population distribution was observed between passages 6 and 10 (figure 4-8a). In the presence or absence of the sister strain Xe85-10, XP4B shows approximately similar trend in the population density dynamics on its host of isolation.

Population distribution of the Xp4B passaged on pepper in the presence or absence of the Xe85-10, indicates a continuous gradual increment in most of the passages (figures 4-7b & 4-8b). In passage 15 of Xp4B alone on pepper treatment, population distribution indicated a ~2 log difference within the replicates, indicating possible individual evolution within replicates. Population distribution of the Xp4B ancestral strain (passage 0) ranges in the 4-5 log cfu/cm² while by the 19th passage in both treatments 600 (Xp4B alone pepper) and 800 (Xp4B+Xe85-10) population distribution of Xp4B was increased up to 7-8 log cfu/cm².

***X. perforans* PM1 strain does not show a drastic change in the population density when continuously passaged on tomato and pepper plants**

As shown in the figures 9 and 10, when XpPM1 was passaged on tomato and pepper up to 19 passages in absence or presence of the sister strain Xe75.3, population density distribution was not moved. In the host of isolation, tomato, population distribution ranged from 6-8 log cfu/cm² when XpPM1 was passaged individually or together with Xe75.3 (figures 4-9a & 4-10a). Population distribution of the XpPM1 on pepper plants ranged from 2-4 log cfu/cm² and this 2-log range was greatly determined by the heterogeneity in the population numbers within the replicates of these treatments (figures 4-9b and 4-10b).

***X. perforans* 4B and *X. perforans* PM1 population change is unaffected by the mixed passages with the *X. euvesicatoria* sister strains**

Passaged populations of Xp4B and XpPM1 passaged alone on tomato and pepper plants were compared with their mixed passages with Xe85-10 and Xe75.3 respectively, to identify the effect of the presence of sister strain for the population dynamics of Xp passaged on host and non-host. No significant difference was observed in the population values between individual and mixed inoculation on both tomato and pepper plants and in any of the passages, except in the Xp4B mixed passaged on pepper at the 6th passage vs Xp4B individual passage on pepper at the 6th passage (Figures 4-11 & 4-12).

Pathogenicity assays reveal a significant decrease in the pathogenicity of Xp4B in tomato plants, when continuously passaged on pepper plants

After considering the population distribution patterns (drastic increment or drop or heterogeneity in the population distribution among replicates) observed with each passage in all the treatments, passages 0, 6, 10, 15 and 19 were selected as representative passages to conduct pathogenicity assays in the original host they were passaged and also after swapping the host.

When above mentioned passages of the Xp4B tomato treatment were used to inoculate tomato plants in the pathogenicity assay, between the ancestor strain and passage 6 a significant drop in the population values were observed. By the 10th passage bacterial population values significantly increased compared to the passage 0 and 6 and population numbers remained high until the 19th passage ($p < 0.05$) (supplementary figure 4-1a). In the Xp4B pepper treatment, when the population values were compared, significant increment in the population growth was observed by the 10th passage ($p < 0.05$) and by the 19th passage population values reached up to ~8 log, demonstrating a ~4 log increment in the population since the beginning of this evolution study (supplementary figure 4-1b).

When the hosts were swapped, and Xp4B passaged on pepper (treatment 200) was used to inoculate tomato plants and when the population values were compared with the Xp4B continuously passaged on tomato plants, a significantly higher population value was observed with Xp4B passaged on tomato compared to Xp4B passaged on pepper on tomato plants by the 19th passage ($p < 0.05$) (figure 4-13a). Interestingly, population values of the Xp4B passaged on pepper (treatment 200), did not indicate any significant improvement in the population when compared to the ancestor Xp4B on tomato plants ($p < 0.05$). On the contrary, when the Xp4B passaged on tomato was used to inoculate pepper plants and when pathogenicity was compared with the Xp4B continuously passaged on pepper, a significant difference between the population values were not observed in any of the passages ($p < 0.05$) (figure 4-13b). Even though Xp4B showed significant improvement in the population when serial passaged on pepper (supplementary figure 4-1b), this host swapped assay provides evidence that suggests passaging Xp4B on pepper is improving host specificity while passaging Xp4B on tomato is not limiting its host range to tomato but rather facilitating it to expand its host range.

When Xp4B was passaged on tomato plants together with Xe85-10, population values were not significantly different in any of the tested passage (supplementary figure 4-2a), while

on pepper plants passaging Xp4B in the presence of Xe85-10, was showing a ~3log improvement in the population values between passage 0 and 19 ($p < 0.05$) (supplementary figure 4-2b). Regardless to presence or absence of Xe85-10, Xp4B showed the same level of bacterial population growth when the pepper and tomato plants were inoculated using the initial inoculum from selected passages and compared them after switching the hosts (figure 4-14).

Pathogenicity of XpPM1 is not affected by the serial passaging in tomato and pepper in the absence or presence of the sister strain Xe75.3

XpPM1 passaged on both tomato and pepper individually or in the presence of Xe75.3, indicated an initial drop in the population growth followed by a gradual increment in the population values in later passages (supplementary figures 4-3& 4-4). Similar to what was previously observed in the density ridge plots (figures 4-9& 4-10) in both of these tested hosts population values of the XpPM1 passages distributed closer to the values of the ancestor strain even at the 19th passage. Switching the hosts to compare the population growth on XpPM1 passaged on tomato and pepper on alternate hosts, yielded no significant difference between treatments in any of the passages in the absence or presence of the sister strain Xe75.3. ($p < 0.05$) (figures 4-15 & 4-16).

Discussion

In this current study we conducted a serial experimental passaging experiment, to understand the phenotypic variation arising in the Xp populations when they are continuously exposed to the host environment (tomato) and to a non-host (pepper). We hypothesized host expansion in the Xp strains, when the host selection pressure was continuously applied to it, and relatively faster adaptation in Xp to pepper plants in the presence of the dominant pepper pathogens (Xe sister strains). Bacterial evolution and fitness was defined in this study by bacterial population values calculated for each passage, in each host using *in planta* pathogenicity assays in the presence or absence of the Xe strains and compared to the ancestral

strains. The SPE showed that Xp4B evolved on the resistant host (pepper cv. ECW) displayed a higher population gain with >2 log difference with the ancestral strain, while Xp4B evolved on its host tomato plants showed only <1 log increment in the population compared to the ancestor, after 19 passages. Hence, Xp4B has gained a higher fitness on its resistant host compared to the host. This finding is in agreement with previous theoretical prediction models of adaptive evolution, where pathogen population is initially less adapted to new host, but typically shows quicker fitness gain when colonizing a distant host and finally the trend decelerate over time (Elena and Lenski, 2003; Guidot et al., 2014).

As proposed by previous literature, if we consider the theory explained in the zig-zag model by (Jones and Dangl, 2006) mutations in effectors are the major factors that contribute to the escape from host-defense system yet contributing to the host expansion. In an experimental evolution study on *Xanthomonas citri* subsp. *citri* (Xcc), mutations in a few type three secretion system effectors were identified after 55 rounds of repeated reinoculations in the resistant host kumquat (Trivedi and Wang, 2014). These identified effectors such as *avrXacE1*, *pthA2*, *avrXacE3* and *pthA4* are known to elicit HR in resistant hosts and trigger virulence and pathogenicity in compatible interactions (Boch and Bonas, 2010, 3).

In bacterial BLS *Xanthomonas* spp., host expansion of Xp from tomato to pepper have been partially explained by the absence of the *AvrBsT* plasmid (Schwartz et al., 2015). Until the isolation of Xp2010 strain from pepper plants in Florida, it was believed that the host range of this pathogen was limited to tomato (Parkinson et al., 2009). *avrBsT* gene is absent from this strain and it does not induce HR on pepper cv. Early CalWonder (ECW) plants that carry the *BsT* locus but has the ability to create foliar disease spots (Kim et al., 2010). Furthermore, in recent surveys of the Xp population in Alabama, pepper pathogenic Xp strains lacking the *avrBsT* homologous have been identified, indicating a recent shift in the Xp host range and an emerging threat to pepper production (Newberry et al., 2019). Similar observations on host

range expansion of Xp has been observed with naturally infected pepper samples in Taiwan as well (Burlakoti et al., 2018). Hence, when this current serial passaging experiment was designed, we hypothesized the loss of the AvrBsT plasmid in Xp4B strain after a couple of serial passages in the resistant host. An increase in the population levels were observed in the passage 6, with Xp4B passaged together with Xe85-10 treatment, when the pathogenicity assays were conducted to compare population levels in the initial passages to the population levels of the 6th passage on pepper plants.

Even though population levels and HR test are indicative of possible loss of the AvrBsT plasmid, significant increment in the population level in the Xp4B 6th passage on pepper being significantly higher than the ancestral strain can't be completely explained. This is in agreement with the previous experiments, where host expansion of Xp to pepper was only partially explained by the loss of the AvrBsT plasmid (Schwartz et al., 2015), indicating the presence of other unknown factors contribute to the host expansion. However, rapid pathogen increment in the population levels of by the 6th passage, on the Xp4B passaged together with Xe85-10 compared to the Xp4B passaged alone on pepper can be due to the evolution of other mutations in the presence of the favored phenotype or due to the gene exchange between the two species facilitated by the strong selection pressure imposed by the “new host stress” (Ebert, 1998; Newberry et al., 2019). Due to the lack of phenotypic differences in the Xp4B +Xe85-10 mixed passages, beyond the 6th passage on pepper plants, suggest Xe85-10 had a little impact on the bacterial population levels of Xp4B after the initial increase in the fitness and might have experienced deceleration of the fitness trend over time when continuously passaged up to 19 passages (supplementary figure 2) (Elena and Lenski, 2003). Interestingly, beyond the 6th passage, Xp4B individual passages, reach the same population levels as the Xp4b +Xe85-10 mixed populations (figure 11b), indicating possible evolutionary response by the Xp4B occurred independently the repeated co inoculations with the Xe85-10 in each passage.

Similarly, when *Pseudomonas syringae* pv. *tomato* was co-inoculated with high titers of Lytic bacteriophage viruses into its native tomato host and an alternative host, *Arabidopsis*, no significant was observed due to the co-inoculation, even though phages have been repeatedly shown to be key selective factors on bacterial populations (Meaden and Koskella, 2017).

When Xp4B was passaged on tomato in the absence of the Xe85-10 strain, slight significant increment in the population growth was observed by the 10th passage, following a significant drop in the populations by the 6th passage, and when Xp4B was mixed passaged with Xe85-10, no significant difference in the population growth was observed in tomato plants. This increment in the population growth was less than 1log, compared to the ancestral strains. Similarly, when *Xanthomonas citri* subsp. *citri* (Xcc) was passaged for 55 passages, on the susceptible host grapefruits, population growth showed a trend identical to the parental strain and *Pseudomonas syringae* pv. *tomato*, passaged on to its native tomato showed lesser within-host bacterial densities in tomato than in alternative host *Arabidopsis*.

In our second pathogen system, where XpPM1 was serial passaged on tomato in the presence or absence of Xe75.3, showed no significant difference compared to the ancestral strain, while on pepper plants drastic initial reduction in population growth was observed. Interestingly, the three replicates in the XpPM1 passaged strains, showed heterogeneity in individual and mixed passages on both hosts. As previously observed in other experimental evolution studies, this changes in the populations in the replicates of the same treatment can be likely due to independent evolution by each replicate. To further confirm this hypothesis, it is important to identify the mutations accumulated in each of this replicate, to confirm if the mutilations are due to random drift or selection pressure or if we can identify any parallel evolution among individual replicates (Brockhurst et al., 2011; Dettman et al., 2012; Trivedi and Wang, 2014). Since the mutations accumulated in the passaging stains have to outcompete the ancestral strain to become dominant population, observation of recurrent mutations in the

same genes in independent replicates will be a strong signal for adaptive evolution (Li et al., 2021). Pathogen adaptation to original or novel host is also determined by the host characteristics (Gandon et al., 2013). When XpPM1 was mixed inculcated with Xe75.3, AvrBsT mediated host resistance is likely to be activated in the resistant host pepper cv. ECW, due to the presence of *avrBsT* gene in the Xe75.3 strain. Due to the activation of the AvrBsT mediated HR, possibly the population growth of both XpPM1 and Xe75.3 is getting restricted, hence the reduction in the bacterial population can affect the pool of adaptive mutations available for selection in the original and novel host (Gandon and Michalakis, 2002; Filippov et al., 2011; Meaden and Koskella, 2017).

As discussed in several other studies, evolutionary adaptation to a novel host or novel selective conditions can result in attenuated virulence and diminished growth in the original host (Ebert, 1998; Trivedi and Wang, 2014). Our results from the host swap study, are also in accordance with these previous studies, since we observed a reduced growth in the Xp4B on tomato after re-passaging in pepper for 19 times (figure 13a). In particular, this phenomenon can be identified as a fitness trade-off between generalism and specialism, that might have generated due to the antagonistic pleiotropy, where mutations that are beneficial in one host being deleterious in an alternative host (Benmayor et al., 2009; Elena, 2017). However, many studies on viruses have identified a similar fitness in generalists compared to specialists (Elena et al., 2009). Continuous exposure of Xp4B passaged on pepper to the tomato, might reverse this attenuated growth, as the genotypes favorable in the ancestral hosts are most likely reattain in the population (Ebert, 1998).

Since majority of the Xp T4 strains carry the *avrBsT* gene, it has been suggested that acquisition of the *avrBsT* gene is providing a fitness advantage to the pathogens. This is further supported by the higher *in planta* titers observed with XvBv5-4a strain with *avrBsT* on tomato compared to the strains lacking it (Kim et al., 2010). Furthermore, Abrahamian et al., 2018

have demonstrated the ability of the Xp GEV872 and GEV1001 wild-type strains to spread long distances in the tomato fields compared to the *avrBsT* mutant strains. These findings collectively suggest a role of functional AvrBsT for the fitness of Xp for successful survival in tomato plants, so losing the AvrBsT plasmid to expand the host range to pepper is associated with a fitness penalty for the pathogen.

Conclusion

Understanding the evolution of plant-pathogenic bacteria is an ongoing challenge, since the bacterial pathogenicity to plants is evolving through an arms race. Gene-for-gene based recognition of bacterial effectors by resistant plants, commonly fail in the long run due to the emergence of virulent strains of the pathogens that no longer get recognized by the R genes. One powerful tool that can be utilized to predict the pathogen adaptations in varying environmental conditions, is through experimental evolution. Current serial passaging experiment was able to identify the loss of the AvrBsT plasmid in Xp4B strain after 6 passages in the resistant pepper cv. ECW, hence indicating the possibility of the emergence of naturally occurring Xp T4 strains, lacking the AvrBsT plasmid, with the ability to infect the pepper plants. Our results support the previous hypothesis that bacteria undergo stronger selection pressure in resistant host than in the susceptible host, thus result in fixed mutations that are biased toward effector genes. Combination of experimental evolution with genome sequencing, will provide useful information that can lead to identification of specific genetic changes that occurred during the continuous passaging, thus can postulate precise association between phenotypes and genotypes.

References

- Abrahamian, P., Timilsina, S., Minsavage, G. V., Kc, S., Goss, E. M., Jones, J. B., et al. (2018). The Type III Effector AvrBsT Enhances *Xanthomonas perforans* Fitness in Field-Grown Tomato. *Phytopathology*® 108, 1355–1362. doi:10.1094/PHYTO-02-18-0052-R.
- Almeida, N. F., Yan, S., Cai, R., Clarke, C. R., Morris, C. E., Schaad, N. W., et al. (2010). PAMDB, A Multilocus Sequence Typing and Analysis Database and Website for Plant-Associated Microbes. *Phytopathology*® 100, 208–215. doi:10.1094/PHYTO-100-3-0208.
- Astua-Monge, G., Minsavage, G. V., Stall, R. E., Davis, M. J., Bonas, U., and Jones, J. B. (2000). Resistance of Tomato and Pepper to T3 Strains of *Xanthomonas campestris* pv. *Vesicatoria* Is Specified by a Plant-Inducible Avirulence Gene. *MPMI* 13, 911–921. doi:10.1094/MPMI.2000.13.9.911.
- Benmayer, R., Hodgson, D. J., Perron, G. G., and Buckling, A. (2009). Host Mixing and Disease Emergence. *Current Biology* 19, 764–767. doi:10.1016/j.cub.2009.03.023.
- Boch, J., and Bonas, U. (2010). *Xanthomonas* AvrBs3 Family-Type III Effectors: Discovery and Function. *Annual Review of Phytopathology* 48, 419–436. doi:10.1146/annurev-phyto-080508-081936.
- Brockhurst, M. A., Colegrave, N., and Rozen, D. E. (2011). Next-generation sequencing as a tool to study microbial evolution. *Molecular Ecology* 20, 972–980. doi:10.1111/j.1365-294X.2010.04835.x.
- Burlakoti, R. R., Hsu, C., Chen, J., and Wang, J. (2018). Population Dynamics of *Xanthomonads* Associated with Bacterial Spot of Tomato and Pepper during 27 Years across Taiwan. *Plant Disease* 102, 1348–1356. doi:10.1094/PDIS-04-17-0465-RE.
- Crute, I., and Pink, D. (1996). Genetics and Utilization of Pathogen Resistance in Plants. *Plant Cell* 8, 1747–1755.
- Dettman, J. R., Rodrigue, N., Melnyk, A. H., Wong, A., Bailey, S. F., and Kassen, R. (2012). Evolutionary insight from whole-genome sequencing of experimentally evolved microbes. *Molecular Ecology* 21, 2058–2077. doi:10.1111/j.1365-294X.2012.05484.x.

- Ebert, D. (1998). Experimental Evolution of Parasites. *Science* 282, 1432–1436. doi:10.1126/science.282.5393.1432.
- Elena, S. F. (2017). Local adaptation of plant viruses: lessons from experimental evolution. *Molecular Ecology* 26, 1711–1719. doi:10.1111/mec.13836.
- Elena, S. F., Agudelo-Romero, P., and Lalić, J. (2009). The Evolution of Viruses in Multi-Host Fitness Landscapes. *Open Virol J* 3, 1–6. doi:10.2174/1874357900903010001.
- Elena, S. F., and Lenski, R. E. (2003). Evolution experiments with microorganisms: the dynamics and genetic bases of adaptation. *Nat Rev Genet* 4, 457–469. doi:10.1038/nrg1088.
- Filippov, A. A., Sergueev, K. V., He, Y., Huang, X.-Z., Gnade, B. T., Mueller, A. J., et al. (2011). Bacteriophage-Resistant Mutants in *Yersinia pestis*: Identification of Phage Receptors and Attenuation for Mice. *PLOS ONE* 6, e25486. doi:10.1371/journal.pone.0025486.
- Gandon, S., Hochberg, M. E., Holt, R. D., and Day, T. (2013). What limits the evolutionary emergence of pathogens? *Philos Trans R Soc Lond B Biol Sci* 368. doi:10.1098/rstb.2012.0086.
- Gandon, S., and Michalakis, Y. (2002). Local adaptation, evolutionary potential and host–parasite coevolution: interactions between migration, mutation, population size and generation time. *Journal of Evolutionary Biology* 15, 451–462. doi:10.1046/j.1420-9101.2002.00402.x.
- Guidot, A., Jiang, W., Ferdy, J.-B., Thébaud, C., Barberis, P., Gouzy, J., et al. (2014). Multihost Experimental Evolution of the Pathogen *Ralstonia solanacearum* Unveils Genes Involved in Adaptation to Plants. *Molecular Biology and Evolution* 31, 2913–2928. doi:10.1093/molbev/msu229.
- Hert, A. P., Roberts, P. D., Momol, M. T., Minsavage, G. V., Tudor-Nelson, S. M., and Jones, J. B. (2005). Relative Importance of Bacteriocin-Like Genes in Antagonism of *Xanthomonas perforans* Tomato Race 3 to *Xanthomonas euvesicatoria* Tomato Race 1 Strains. *Appl Environ Microbiol* 71, 3581–3588. doi:10.1128/AEM.71.7.3581-3588.2005.

- Hoang, K. L., Morran, L. T., and Gerardo, N. M. (2016). Experimental Evolution as an Underutilized Tool for Studying Beneficial Animal–Microbe Interactions. *Front. Microbiol.* 7. doi:10.3389/fmicb.2016.01444.
- Horvath, D. M., Stall, R. E., Jones, J. B., Pauly, M. H., Vallad, G. E., Dahlbeck, D., et al. (2012). Transgenic Resistance Confers Effective Field Level Control of Bacterial Spot Disease in Tomato. *PLOS ONE* 7, e42036. doi:10.1371/journal.pone.0042036.
- Jones, J. B., Bouzar, H., Somodi, G. C., Stall, R. E., Pernezny, K., El-Morsy, G., et al. (1998). Evidence for the Preemptive Nature of Tomato Race 3 of *Xanthomonas campestris* pv. *vesicatoria* in Florida. *Phytopathology*® 88, 33–38. doi:10.1094/PHYTO.1998.88.1.33.
- Jones, J. B., Bouzar, H., Stall, R. E., Almira, E. C., Roberts, P. D., Bowen, B. W., et al. Systematic analysis of xanthomonads (*Xanthomonas* spp.) associated with pepper and tomato lesions. *International Journal of Systematic and Evolutionary Microbiology* 50, 1211–1219. doi:10.1099/00207713-50-3-1211.
- Jones, J. B., Lacy, G. H., Bouzar, H., Stall, R. E., and Schaad, N. W. (2004). Reclassification of the Xanthomonads Associated with Bacterial Spot Disease of Tomato and Pepper. *Systematic and Applied Microbiology* 27, 755–762. doi:10.1078/0723202042369884.
- Jones, J. D. G., and Dangl, J. L. (2006). The plant immune system. *Nature* 444, 323–329. doi:10.1038/nature05286.
- Kawecki, T. J., Lenski, R. E., Ebert, D., Hollis, B., Olivieri, I., and Whitlock, M. C. (2012). Experimental evolution. *Trends in Ecology & Evolution* 27, 547–560. doi:10.1016/j.tree.2012.06.001.
- Kim, N. H., Choi, H. W., and Hwang, B. K. (2010). *Xanthomonas campestris* pv. *vesicatoria* Effector AvrBsT Induces Cell Death in Pepper, but Suppresses Defense Responses in Tomato. *MPMI* 23, 1069–1082. doi:10.1094/MPMI-23-8-1069.
- Lenski, R. E. (2017). Experimental evolution and the dynamics of adaptation and genome evolution in microbial populations. *ISME J* 11, 2181–2194. doi:10.1038/ismej.2017.69.

- Li, E., Zhang, H., Jiang, H., Pieterse, C. M. J., Jousset, A., Bakker, P. A. H. M., et al. (2021). Experimental evolution-driven identification of *Arabidopsis* rhizosphere competence genes in *Pseudomonas protegens*. *bioRxiv*, 2020.12.01.407551. doi:10.1101/2020.12.01.407551.
- Ma, X., Lewis Ivey, M. L., and Miller, S. A. (2011). First Report of *Xanthomonas gardneri* Causing Bacterial Spot of Tomato in Ohio and Michigan. *Plant Disease* 95, 1584–1584. doi:10.1094/PDIS-05-11-0448.
- Meaden, S., and Koskella, B. (2017). Adaptation of the pathogen, *Pseudomonas syringae*, during experimental evolution on a native vs. alternative host plant. *Molecular Ecology* 26, 1790–1801. doi:10.1111/mec.14060.
- Miller, J. H. (1972). *Experiments in molecular genetics*. [Cold Spring Harbor, N.Y.]: Cold Spring Harbor Laboratory.
- Minsavage, G. V., Dahlbeck, D., Whalen, M. C., Kearney, B., Bonas, U., Staskawicz, B. J., et al. (1990). Gene-for-gene relationships specifying disease resistance in *Xanthomonas campestris* pv. *vesicatoria* - pepper interactions. *Molecular Plant-Microbe Interactions* 3, 41–47.
- Newberry, E. A., Bhandari, R., Minsavage, G. V., Timilsina, S., Jibrin, M. O., Kemble, J., et al. (2019). Independent Evolution with the Gene Flux Originating from Multiple *Xanthomonas* Species Explains Genomic Heterogeneity in *Xanthomonas perforans*. *Appl. Environ. Microbiol.* 85. doi:10.1128/AEM.00885-19.
- Parkinson, N., Cowie, C., Heeney, J., and Stead, D. 2009 Phylogenetic structure of *Xanthomonas* determined by comparison of *gyrB* sequences. *International Journal of Systematic and Evolutionary Microbiology* 59, 264–274. doi:10.1099/ijs.0.65825-0.
- Pelosi, L., Kühn, L., Guetta, D., Garin, J., Geiselmann, J., Lenski, R. E., et al. (2006). Parallel Changes in Global Protein Profiles During Long-Term Experimental Evolution in *Escherichia coli*. *Genetics* 173, 1851–1869. doi:10.1534/genetics.105.049619.
- Pitman, A. R., Jackson, R. W., Mansfield, J. W., Kaitell, V., Thwaites, R., and Arnold, D. L. (2005). Exposure to Host Resistance Mechanisms Drives Evolution of Bacterial Virulence in Plants. *Current Biology* 15, 2230–2235. doi:10.1016/j.cub.2005.10.074.

- Potnis, N., Krasileva, K., Chow, V., Almeida, N. F., Patil, P. B., Ryan, R. P., et al. (2011). Comparative genomics reveals diversity among xanthomonads infecting tomato and pepper. *BMC Genomics* 12, 146. doi:10.1186/1471-2164-12-146.
- Schwartz, A. R., Potnis, N., Timilsina, S., Wilson, M., Patanã©, J., Martins, J., et al. (2015). Phylogenomics of Xanthomonas field strains infecting pepper and tomato reveals diversity in effector repertoires and identifies determinants of host specificity. *Front. Microbiol.* 6. doi:10.3389/fmicb.2015.00535.
- Sharma, S., and Bhattarai, K. (2019). Progress in Developing Bacterial Spot Resistance in Tomato. *Agronomy* 9, 26. doi:10.3390/agronomy9010026.
- Stall, R. E., Beaulieu, C., Bouzar, H., Jones, J. B., Alvarez, A. M., and Benedict A. A (1994). Two Genetically Diverse Groups of Strains Are Included in Xanthomonas campestris pv. vesicatoriaj-. *INT. J. SYST.BACTERIOL.*, 7.
- Stall, R. E., Jones, J. B., and Minsavage, G. V. (2009). Durability of Resistance in Tomato and Pepper to Xanthomonads Causing Bacterial Spot. *Annual Review of Phytopathology* 47, 265–284. doi:10.1146/annurev-phyto-080508-081752.
- Timilsina, S., Abrahamian, P., Potnis, N., Minsavage, G. V., White, F. F., Staskawicz, B. J., et al. (2016). Analysis of Sequenced Genomes of Xanthomonas perforans Identifies Candidate Targets for Resistance Breeding in Tomato. *Phytopathology*® 106, 1097–1104. doi:10.1094/PHYTO-03-16-0119-FI.
- Timilsina, S., Kara, S., Jacques, M. A., Potnis, N., Minsavage, G. V., Vallad, G. E., et al. Reclassification of Xanthomonas gardneri (ex Šutič 1957) Jones et al. 2006 as a later heterotypic synonym of Xanthomonas cynarae Trébaol et al. 2000 and description of X. cynarae pv. cynarae and X. cynarae pv. gardneri based on whole genome analyses. *International Journal of Systematic and Evolutionary Microbiology* 69, 343–349. doi:10.1099/ijsem.0.003104.
- Trivedi, P., and Wang, N. (2014). Host immune responses accelerate pathogen evolution. *ISME J* 8, 727–731. doi:10.1038/ismej.2013.215.

Vauterin, L., Hoste, B., Kersters, K., And Swings, J. Y. 1995 Reclassification of Xanthomonas. *International Journal of Systematic and Evolutionary Microbiology* 45, 472–489. doi:10.1099/00207713-45-3-472.

Zhan, J., Thrall, P. H., and Burdon, J. J. (2014). Achieving sustainable plant disease management through evolutionary principles. *Trends in Plant Science* 19, 570–575. doi:10.1016/j.tplants.2014.04.010.

Table 4-1: Characteristics of the strains used in the experimental evolution study

Strain	Year of isolation	Host of isolation	Tomato race	<i>avrXv3</i>	<i>avrBsT</i>	HR on pepper cv. ECW
<i>Xp91-118</i>	1991	Tomato	T3	√	X	√
<i>Xp2010</i>	2010	Pepper	T4	IS mutation	X	X
<i>Xe85-10</i>	1985	Tomato	T1	x	X	X
<i>Xe75.3</i>	1975	Tomato	T1	x	√	√
<i>Xp4B</i>	1998	Tomato	T4	Pseudogene	√	√
<i>Xp4BΔavrBsT</i>	(Schwartz et al., 2015)			Pseudogene	X	X
<i>PM1(Xp91-118ΔavrXv3)</i>	(Potnis et al., 2011)			Transposon mutation	X	X

Table 4-2: List of treatments in the passaging experiment

Code number	Treatment	Host	List of replicates
100	XpPM1 ^{kanamycin}	Tomato	101, 102, 103
200	XpPM1 ^{kanamycin}	Pepper	201, 202, 203
300	XpPM1 ^{kanamycin} + Xe75.3	Tomato	301, 302, 303
400	XpPM1 ^{kanamycin} + Xe75.3	Pepper	401, 402, 403
500	Xp4B ^{nalidixic}	Tomato	501, 502, 503
600	Xp4B ^{nalidixic}	Pepper	601, 602, 603
700	Xp4B ^{nalidixic} +Xe85-10	Tomato	701, 702, 703
800	Xp4B ^{nalidixic} +Xe85-10	Pepper	801, 802, 803

Table 4-3: List of treatments used in the host swapped experiment

Code number	Treatment	Host	List of replicates
100	XpPM1 ^{kanamycin}	Tomato-Original host	101, 102, 103
100	XpPM1 ^{kanamycin}	Pepper-Alternate host	101, 102, 103
200	XpPM1 ^{kanamycin}	Pepper-Original host	201, 202, 203
200	XpPM1 ^{kanamycin}	Tomato-Alternate host	201, 202, 203
300	XpPM1 ^{kanamycin} + Xe75.3	Tomato-Original host	301, 302, 303
300	XpPM1 ^{kanamycin} + Xe75.3	Pepper-Alternate host	301, 302, 303
400	XpPM1 ^{kanamycin} + Xe75.3	Pepper-Original host	401, 402, 403
400	XpPM1 ^{kanamycin} + Xe75.3	Tomato-Alternate host	401, 402, 403
500	Xp4B ^{nalidixic}	Tomato-Original host	501, 502, 503
500	Xp4B ^{nalidixic}	Pepper-Alternate host	501, 502, 503
600	Xp4B ^{nalidixic}	Pepper-Original host	601, 602, 603
600	Xp4B ^{nalidixic}	Tomato-Alternate host	601, 602, 603
700	Xp4B ^{nalidixic} +Xe85-10	Tomato-Original host	701, 702, 703
700	Xp4B ^{nalidixic} +Xe85-10	Pepper-Alternate host	701, 702, 703
800	Xp4B ^{nalidixic} +Xe85-10	Pepper-Original host	801, 802, 803
800	Xp4B ^{nalidixic} +Xe85-10	Tomato-Alternate host	801, 802, 803

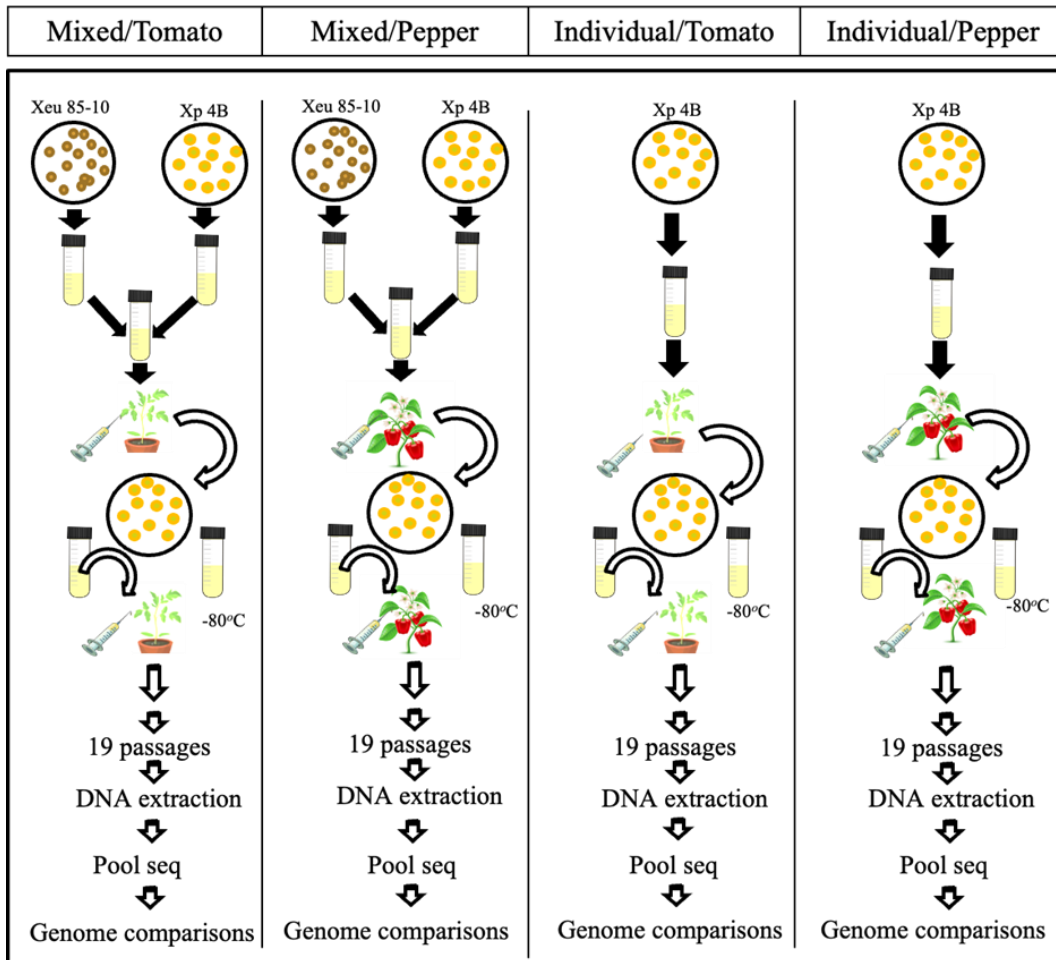


Figure 4-1: Experimental evolution scheme of *X. perforans* 4B strain through a serial passaging experiment on host plant (tomato cv. FL47) and non-host (pepper cv. ECW) in either the presence or absence of closely related *X. euvesicatoria* 85-10

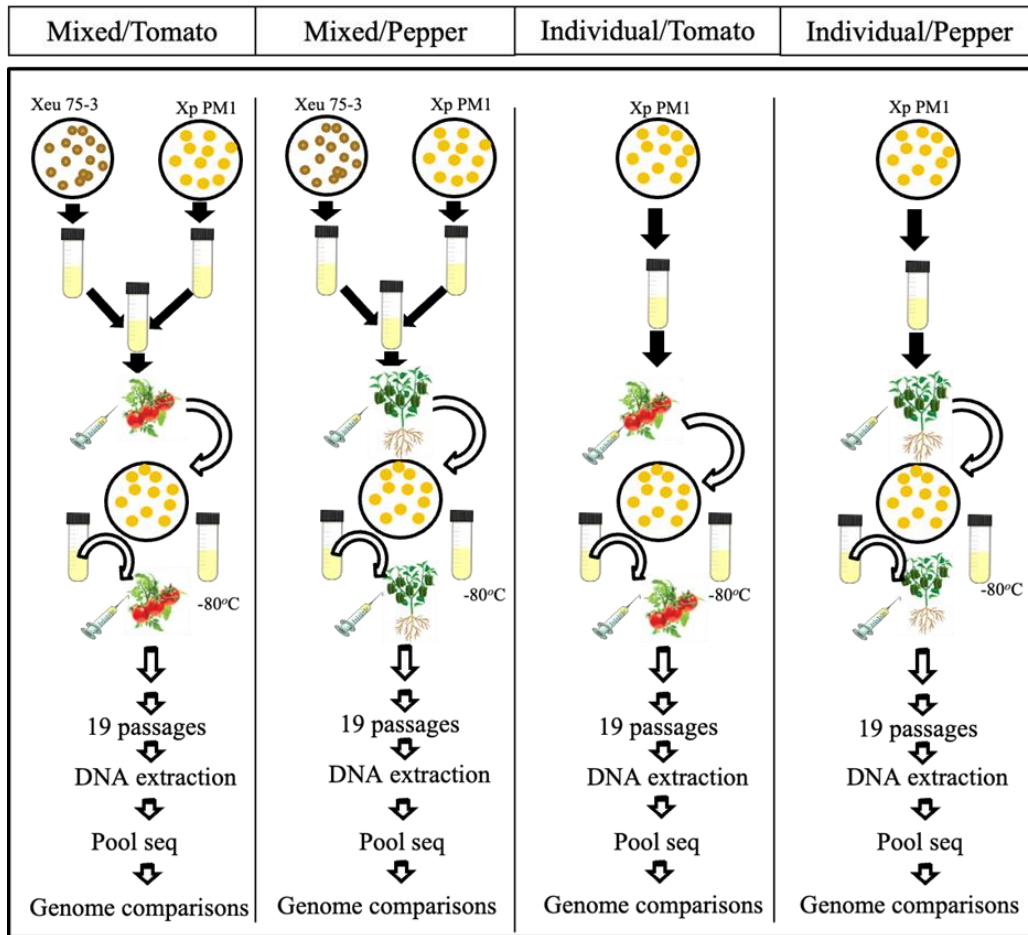


Figure 4-2: Experimental evolution scheme of *X. perforans* PM1 strain through a serial passaging experiment on host plant (tomato cv. FL47) and non-host (pepper cv. ECW) in either the presence or absence of closely related *X. euvesicatoria* 75.3

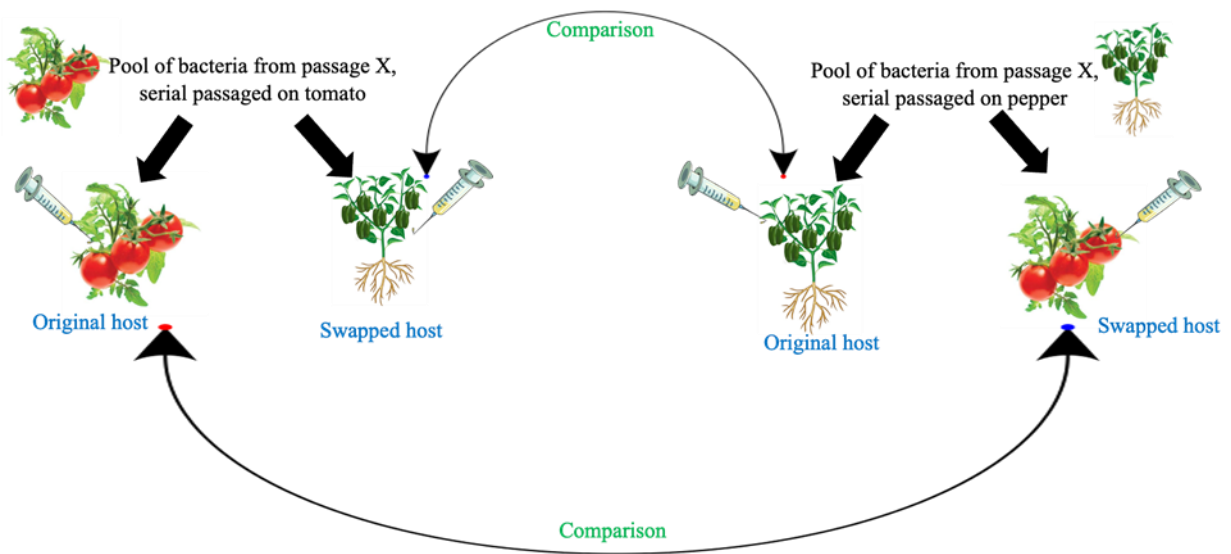


Figure 4-3: Schematic diagram of the host swapped experiment. Pools of the bacterial strains (Xp4B alone on pepper and tomato, Xp4B together with *X. euvesicatoria* 85-10 on pepper and tomato, XpPM1 alone on pepper and tomato and XpPM1 together with *X. euvesicatoria* 75.3 on pepper and tomato) from the passages 0, 6, 10, 15 and 19 were used to inoculate on the original host they were serial passed or in the swapped host.

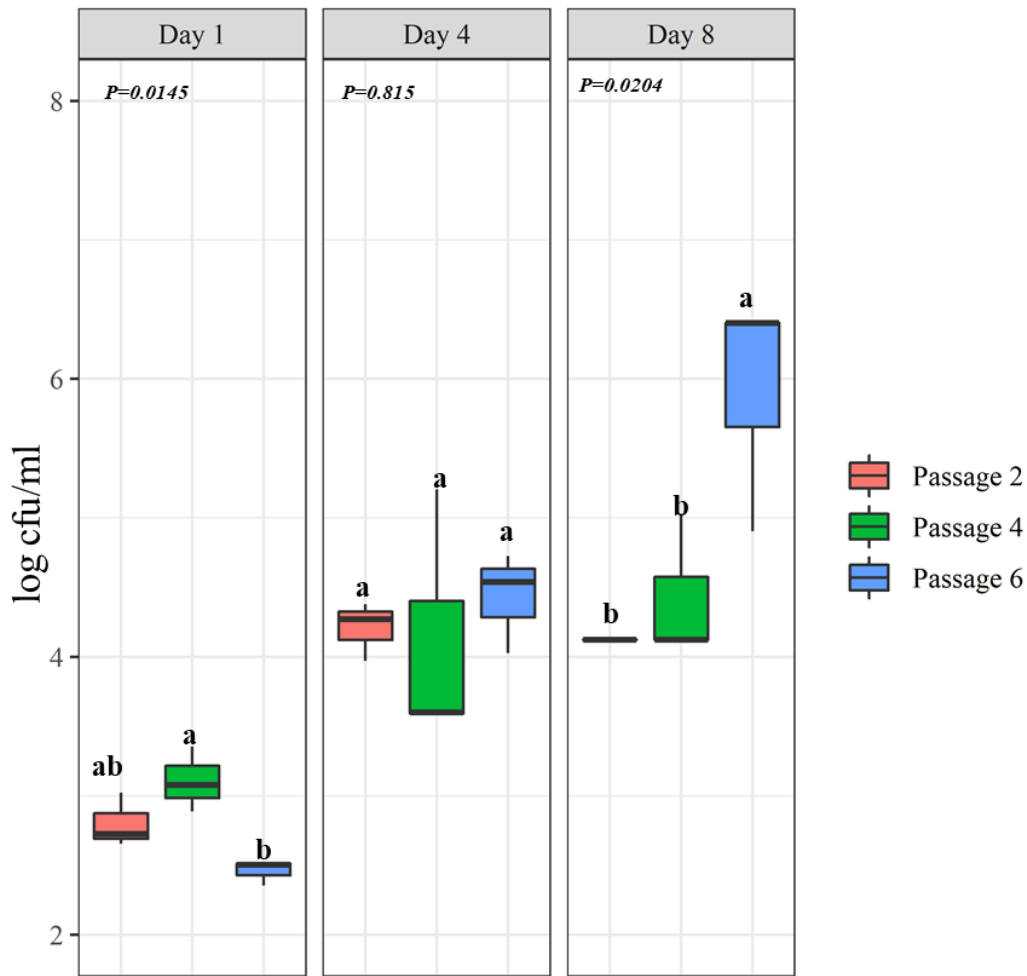


Figure 4-4: *In planta* population assay conducted inside the growth chamber after passaging *X. perforans* 4B strain on pepper plants, up to six passages. Four- to five-week-old pepper cv. ECW were infiltrated with $\sim 1 \times 10^5$ cfu/ml of bacterial pools taken from passages 2, 4 and 6. Strains were evaluated for bacterial population growth, on the day of inoculation, 4 days after inoculation and 8 days after inoculation on antibiotic (nalidixic) amended media. A one-way ANOVA was applied for the statistical analysis for each tested date and treatments with different letters are significantly different according to the Tukey's test of least significant difference ($P < 0.05$).

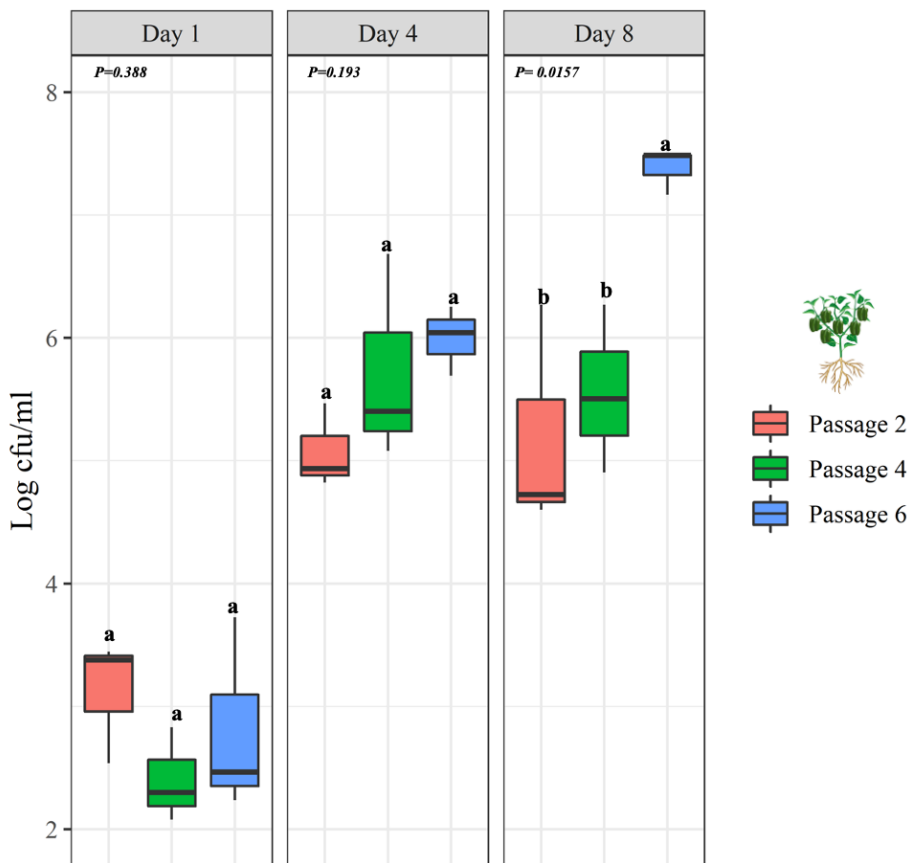


Figure 4-5: *In planta* population assay conducted inside the growth chamber after passaging *X. perforans* 4B strain together with *X. euvesicatoria* 85-10 on pepper plants, up to six passages. Four- to five-week-old pepper cv. ECW were infiltrated with $\sim 1 \times 10^5$ cfu/ml of bacterial pools taken from passages 2, 4 and 6. Strains were evaluated for bacterial population growth, on the day of inoculation, 4 days after inoculation and 8 days after inoculation on antibiotic (nalidixic) amended media. A one-way ANOVA was applied for the statistical analysis for each tested date and treatments with different letters are significantly different according to the Tukey's test of least significant difference ($P < 0.05$).

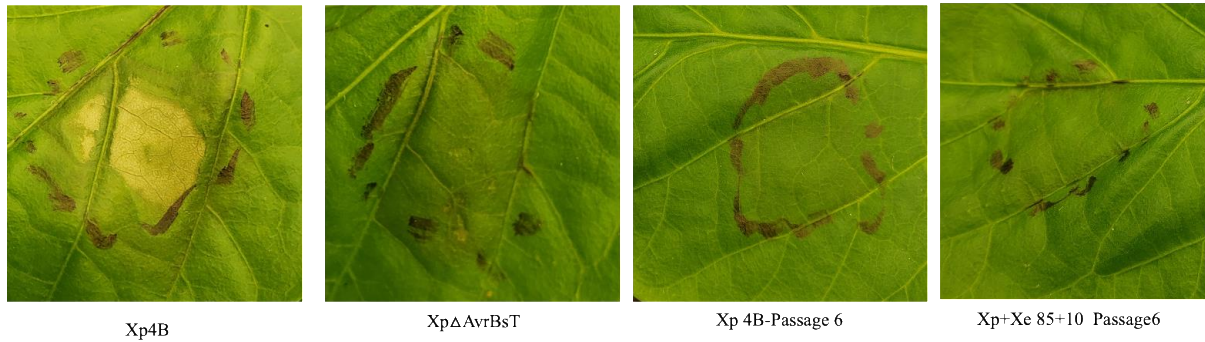


Figure 4-6: High inoculum infiltrated spots were performed at 10^8 cfu/ml to show the loss of AvrBsT plasmid in the 6th passage of *X. perforans* 4B strain alone and together with *X. euvesicatoria* 85-10 on pepper plants (cv. ECW). Xp 4B ancestor strain and *X. perforans* 4B Δ avrBsT were also used in the assay to compare the symptom development. Plants were kept inside the growth chamber inside open-lid containers to check for the development of HR or water-soaking and photographed 3 dpi.

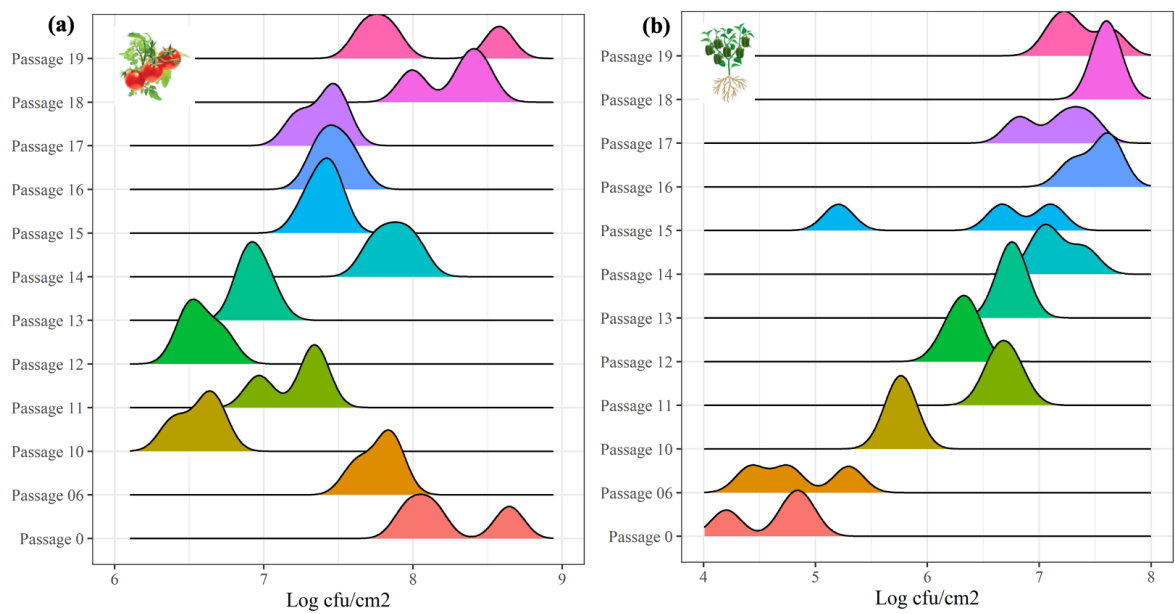


Figure 4-7: Density ridgeline plots to visualize the changes in distributions, of population growth, over time in Xp4B strains passaged on (a) tomato and (b) pepper plants. Plots include the distribution of the 4B ancestor strain (Passage 0), Passage 6 and Passages 10-19 on tomato (cv. FL47) and pepper (cv. ECW) plants.

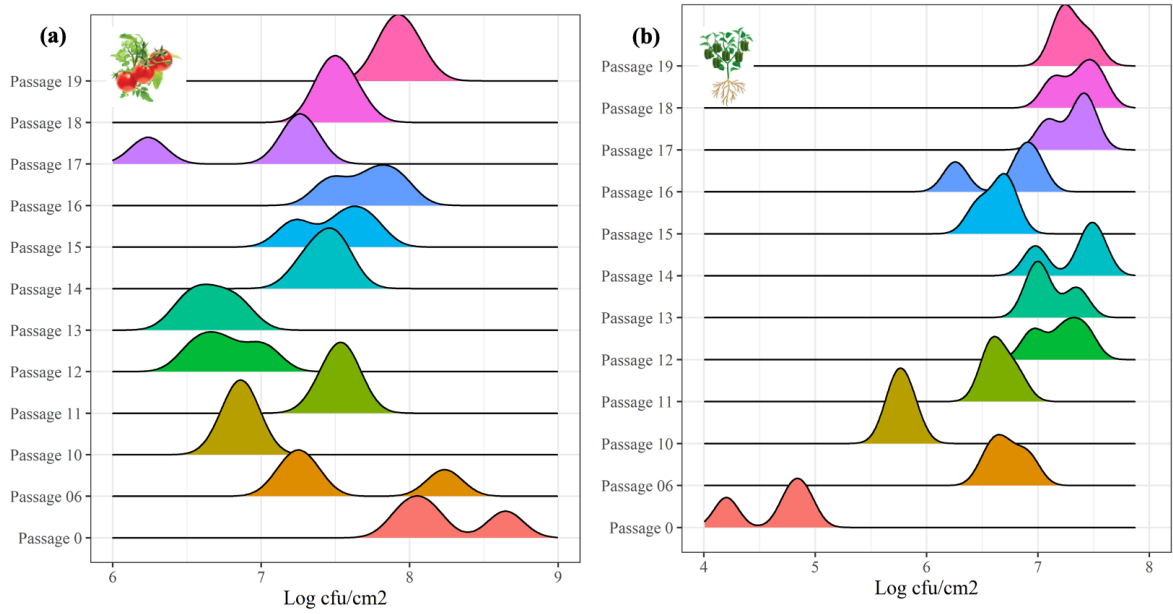


Figure 4-8: Density ridgeline plots to visualize the changes in distributions, of population growth, over time in Xp4B strains passaged on (a) tomato and (b) pepper plants in the presence with *X. euvesicatoria* 85-10. Plots include the distribution of the 4B ancestor strain (Passage 0), Passage 6 and Passages 10-19 on tomato (cv. FL47) and pepper (cv. ECW) plants.

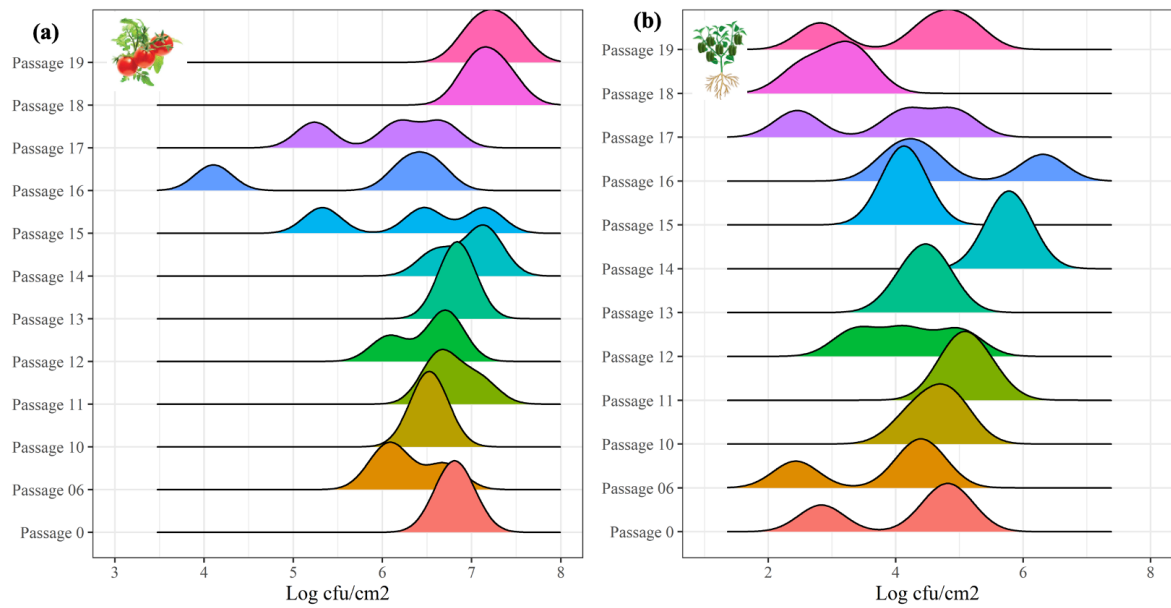


Figure 4-9: Density ridgeline plots to visualize the changes in distributions, of population growth, over time in XpPM1 strains passaged on (a) tomato and (b) pepper plants. Plots include the distribution of the XpPM1 ancestor strain (Passage 0), Passage 6 and Passages 10-19 on tomato (cv. FL47) and pepper (cv. ECW) plants.

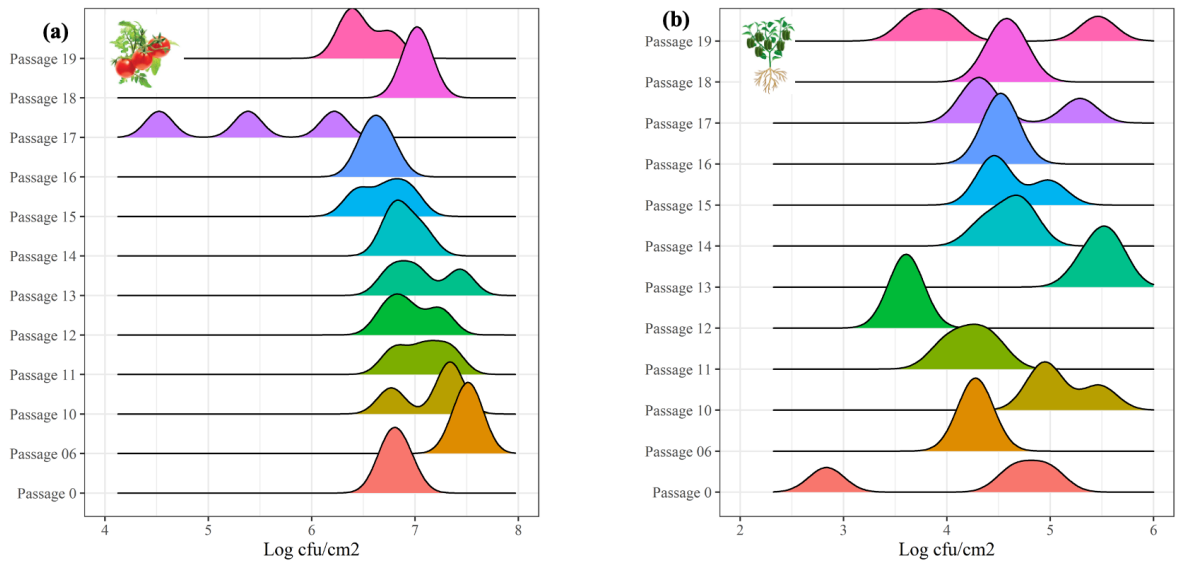


Figure 4-10: Density ridgeline plots to visualize the changes in distributions, of population growth, over time in XpPM1 strains passaged on (a) tomato and (b) pepper plants in the presence with *X. euvesicatoria* 75.3. Plots include the distribution of the XpPM1 ancestor strain (Passage 0), Passage 6 and Passages 10-19 on tomato (cv. FL47) and pepper (cv. ECW) plants.

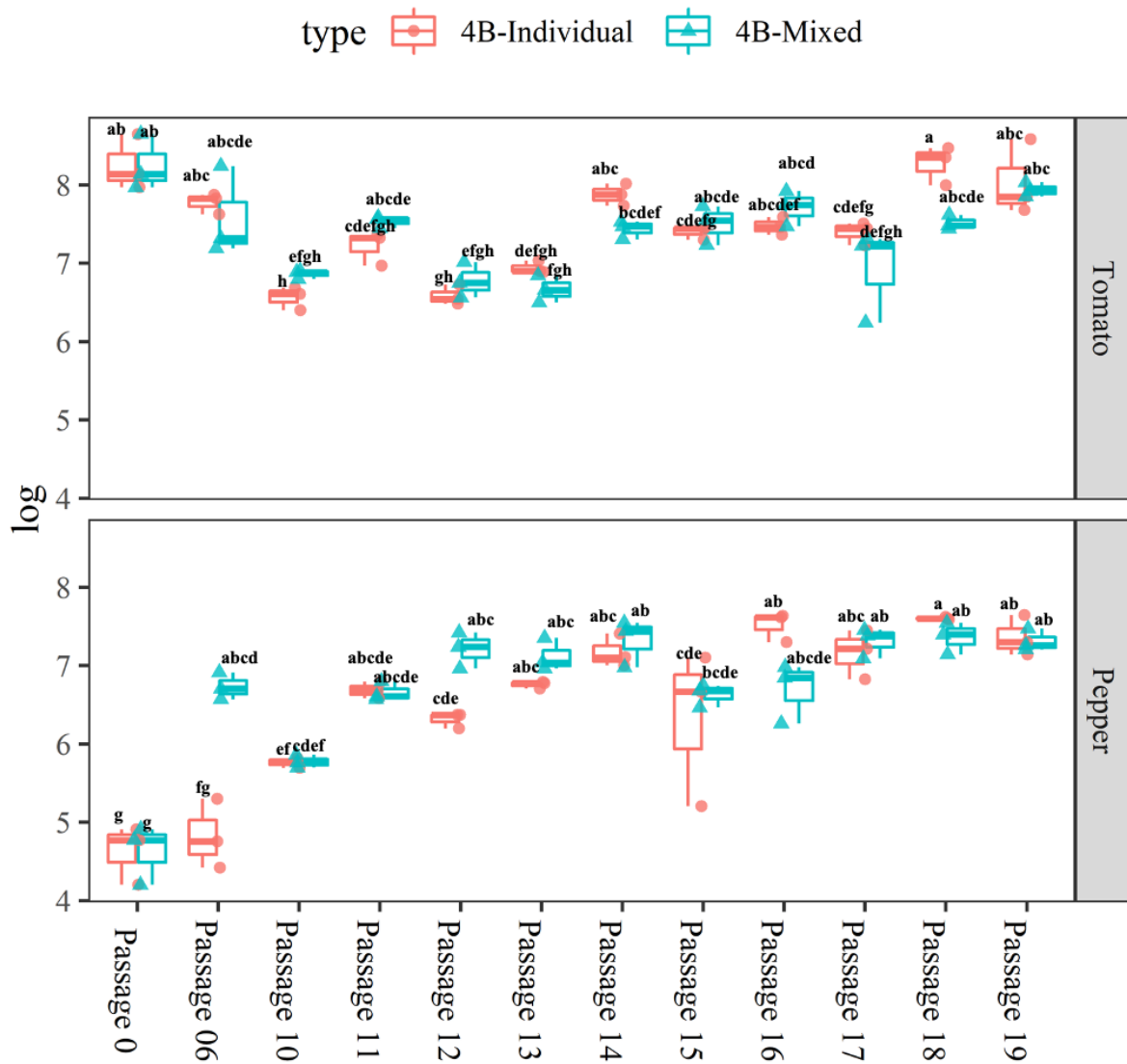


Figure 4-11: Boxplots to visualize the changes in distributions, of population growth, over time in Xp4B strains passaged on (a) tomato and (b) pepper plants individually and together with Xe85-10. Plots include the distribution of the 4B ancestor strain (Passage 0), Passage 6 and Passages 10-19 on pepper (cv. ECW) and tomato (cv. FL47). A two-way ANOVA was applied for each host for the statistical analysis and treatments with different letters are significantly different according to the Tukey's test of least significant difference ($P < 0.05$).

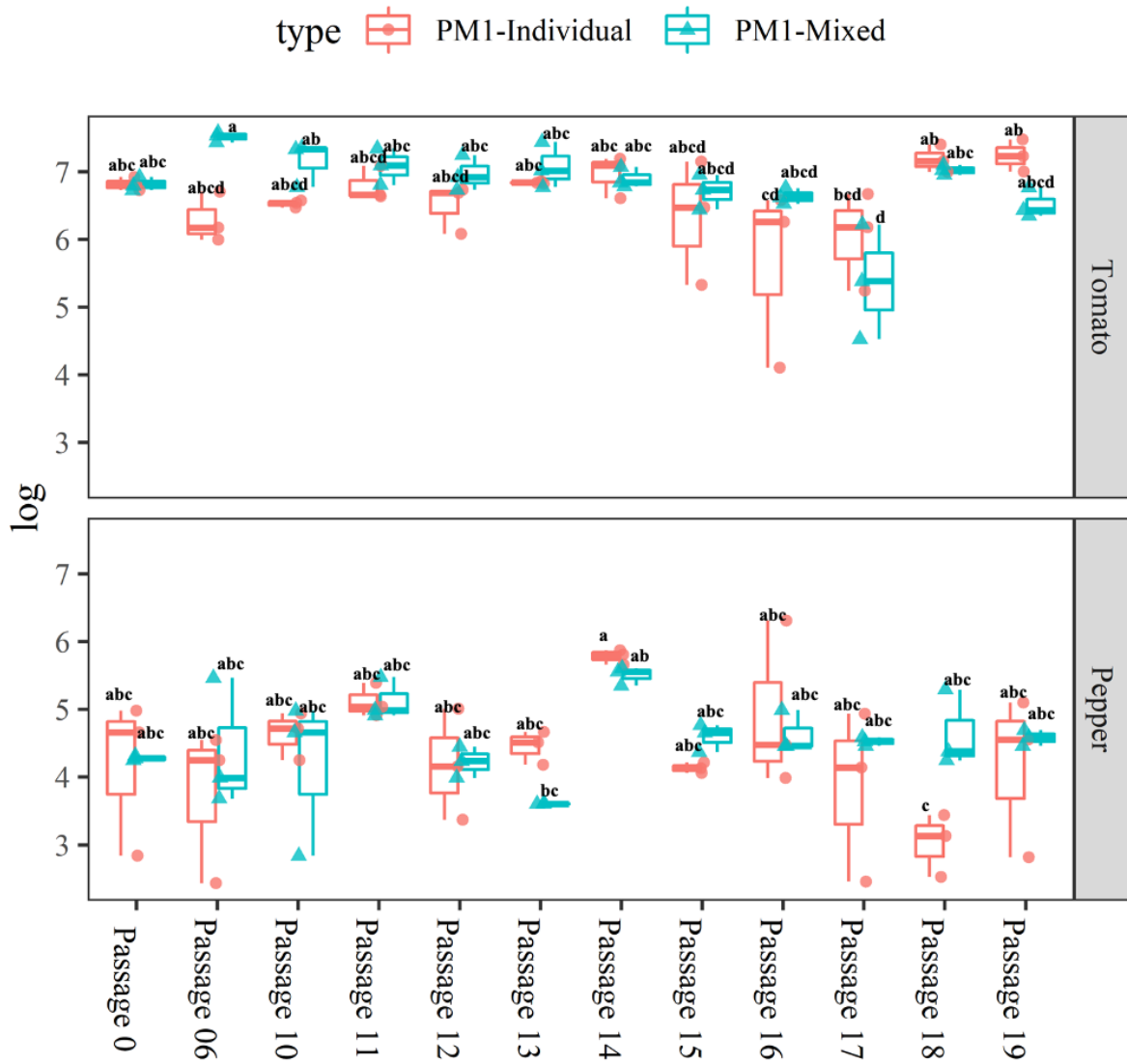


Figure 4-12: Boxplots to visualize the changes in distributions, of population growth, over time in XpPM1 strains passaged on (a) tomato and (b) pepper plants individually and together with Xe75.3. Plots include the distribution of the PM1 ancestor strain (Passage 0), Passage 6 and Passages 10-19 on pepper (cv. ECW) and tomato (cv. FL47). A two-way ANOVA was applied for each host for the statistical analysis and treatments with different letters are significantly different according to the Tukey's test of least significant difference ($P < 0.05$).

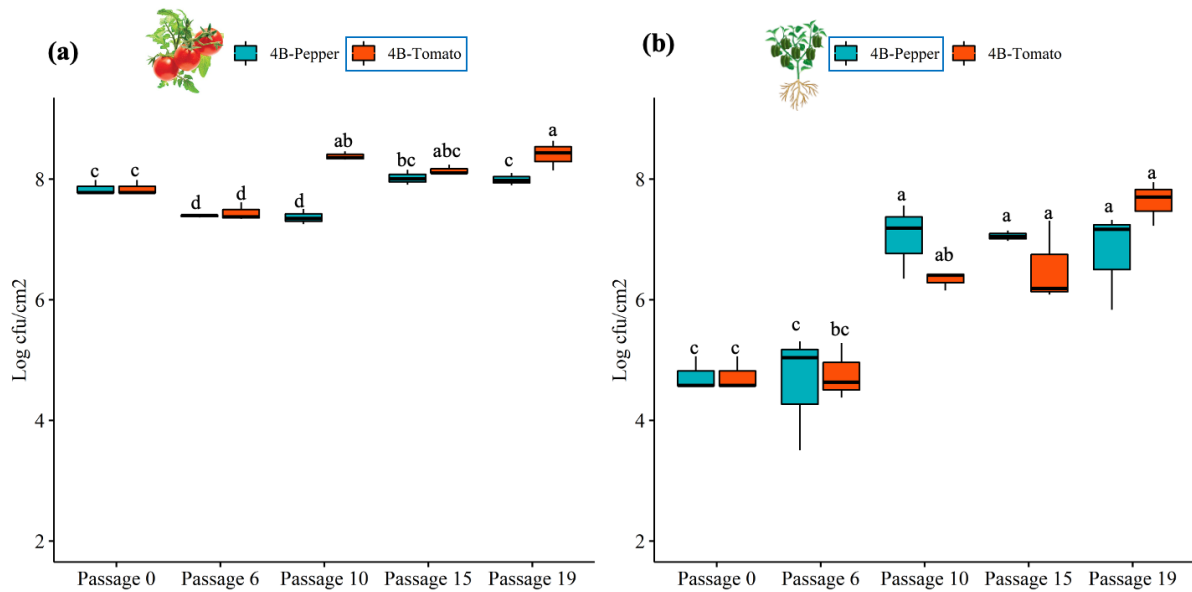


Figure 4-13: Comparison of population growth of Xp4B pools taken from the passages 0, 6, 10, 15 and 19. (a) originally passed on tomato with Xp4B originally passed on pepper when infiltrated to tomato plants (cv. FL47) and (b) Xp4B pools originally passed on pepper with Xp4B originally passed on tomato when infiltrated to pepper plants (cv. ECW). Four- to five-week-old pepper and tomato plants were infiltrated with $\sim 1 \times 10^5$ cfu/ml of bacterial pools. Strains were evaluated for bacterial population growth, 6 days after inoculation on antibiotic (nalidixic) amended media. A two-way ANOVA was applied for the statistical analysis and treatments with different letters are significantly different according to the Tukey's test of least significant difference ($P < 0.05$).

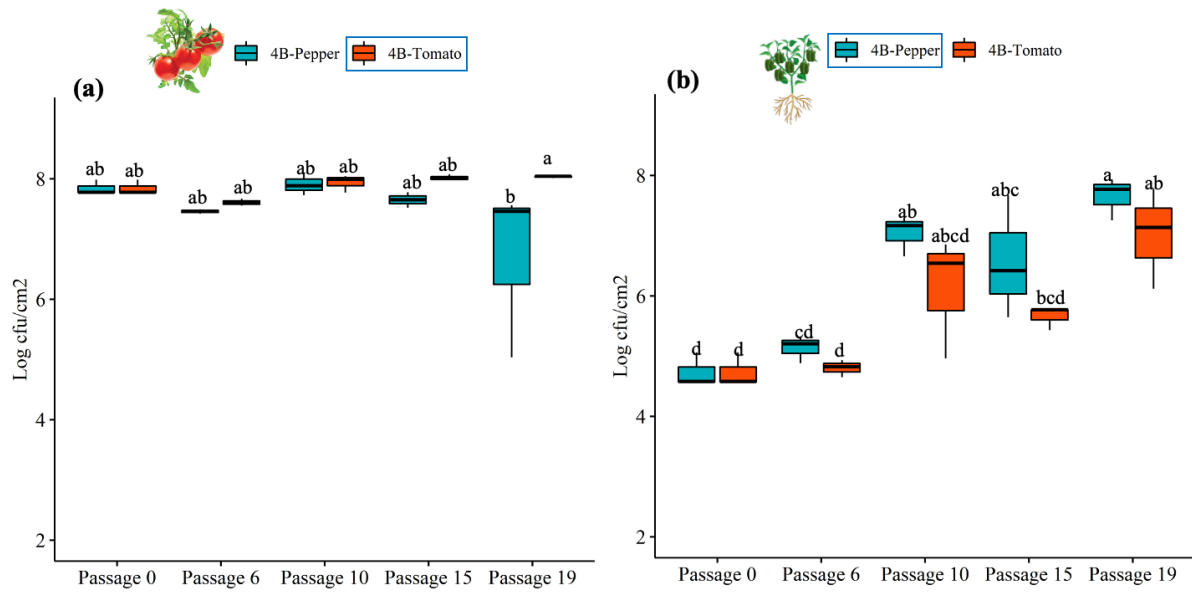


Figure 4-14: Comparison of population growth of the Xp4B population growth when passaged together with Xe85-10. Xp4B pools taken from the passages 0, 6, 10, 15 and 19 (a) originally passaged on tomato with XpPM1 originally passaged on pepper when infiltrated to tomato plants (cv. FL47) and (b) Xp4B pools originally passaged on pepper with Xp4B originally passaged on tomato when infiltrated to pepper plants (cv. ECW). Four- to five-week-old pepper and tomato plants were infiltrated with $\sim 1 \times 10^5$ cfu/ml of bacterial pools. Strains were evaluated for bacterial population growth, 6 days after inoculation on antibiotic (nalidixic) amended media. A two-way ANOVA was applied for the statistical analysis and treatments with different letters are significantly different according to the Tukey's test of least significant difference ($P < 0.05$).

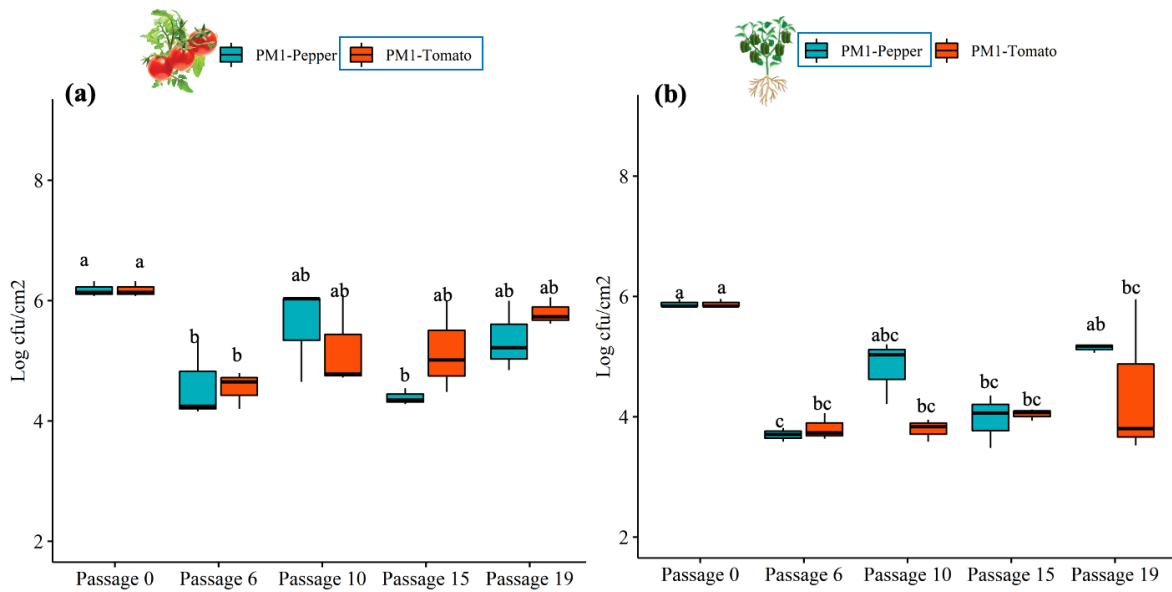


Figure 4-15: Comparison of population growth of XpPM1 pools taken from the passages 0, 6, 10, 15 and 19. (a) originally passaged on tomato with XpPM1 originally passaged on pepper when infiltrated to tomato plants (cv. FL47) and (b) XpPM1 pools originally passaged on pepper with XpPM1 originally passaged on tomato when infiltrated to pepper plants (cv. ECW). Four- to five-week-old pepper and tomato plants were infiltrated with $\sim 1 \times 10^5$ cfu/ml of bacterial pools. Strains were evaluated for bacterial population growth, 6 days after inoculation on antibiotic (kanamycin) amended media. A two-way ANOVA was applied for the statistical analysis and treatments with different letters are significantly different according to the Tukey's test of least significant difference ($P < 0.05$).

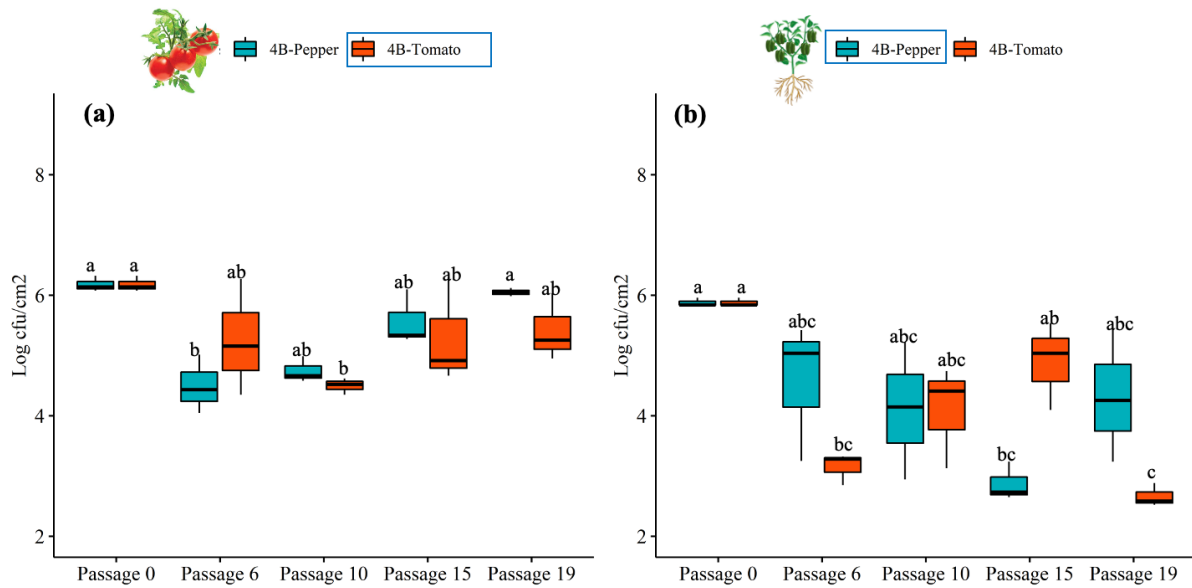
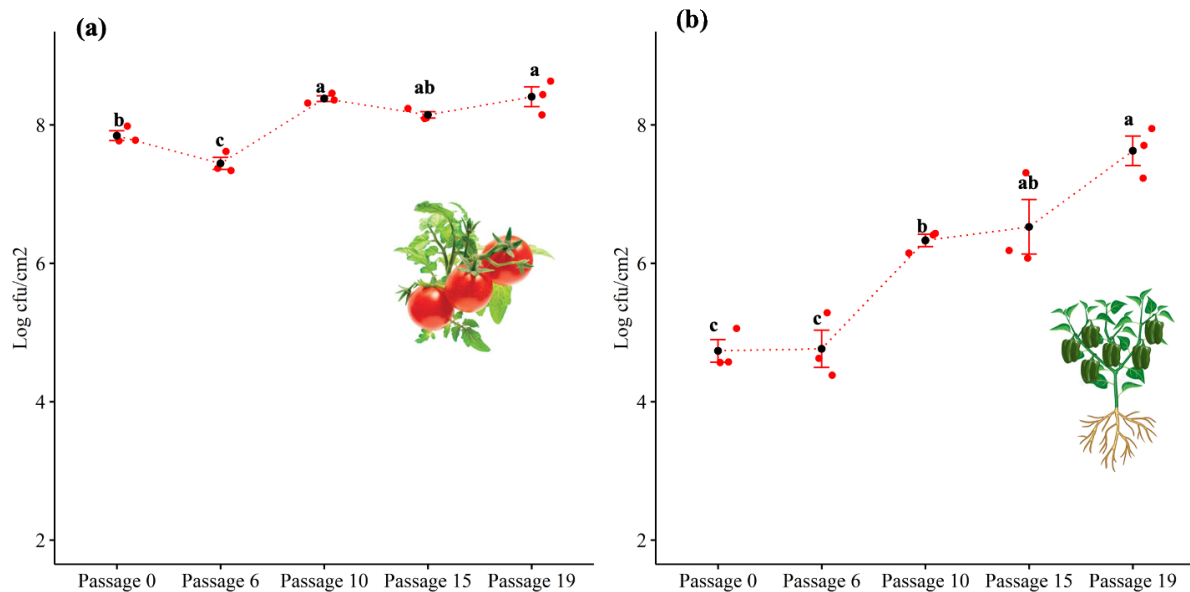
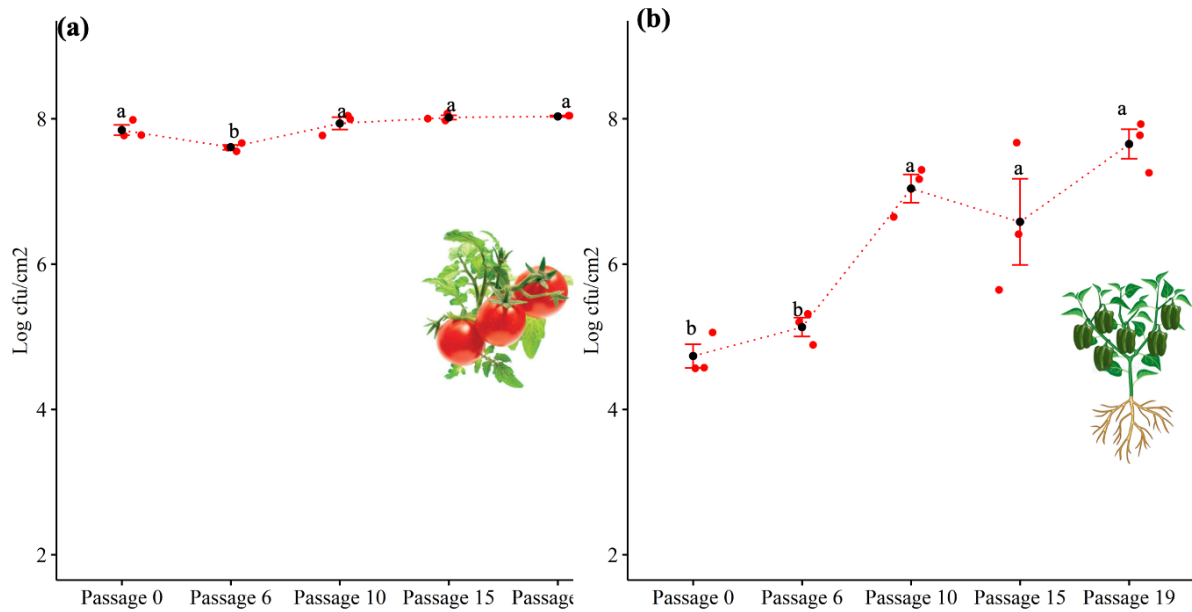


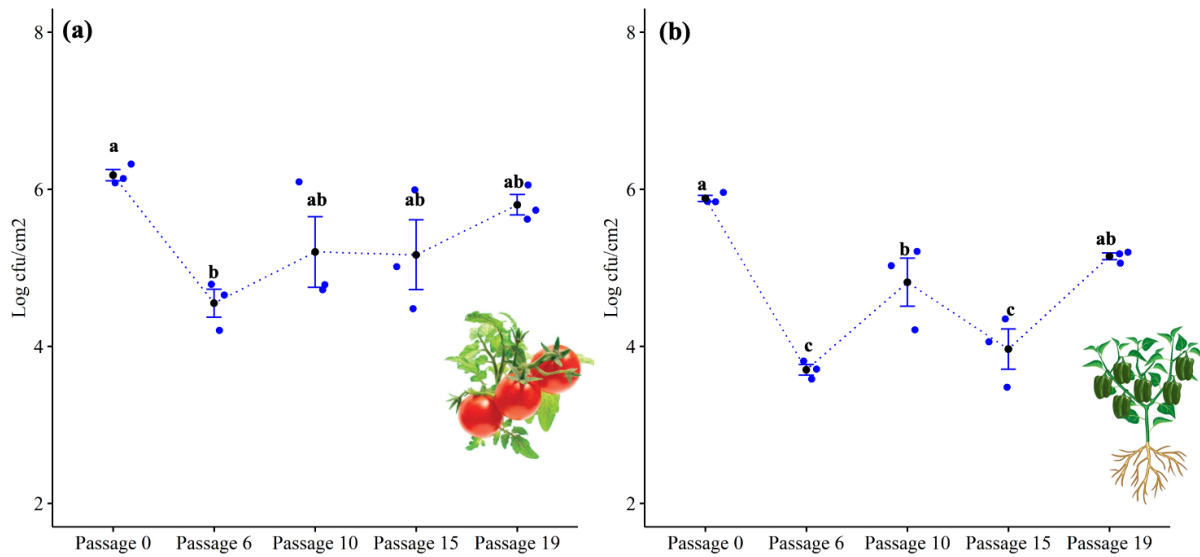
Figure 4-16: Comparison of population growth of the XpPM1 population growth when passaged together with Xe75.3. XpPM1 pools taken from the passages 0, 6, 10, 15 and 19 (a) originally passaged on tomato with XpPM1 originally passaged on pepper when infiltrated to tomato plants (cv. FL47) and (b) XpPM1 pools originally passaged on pepper with XpPM1 originally passaged on tomato when infiltrated to pepper plants (cv. ECW). Four- to five-week-old pepper and tomato plants were infiltrated with $\sim 1 \times 10^5$ cfu/ml of bacterial pools. Strains were evaluated for bacterial population growth, 6 days after inoculation on antibiotic (kanamycin) amended media. A two-way ANOVA was applied for the statistical analysis and treatments with different letters are significantly different according to the Tukey's test of least significant difference ($P < 0.05$).



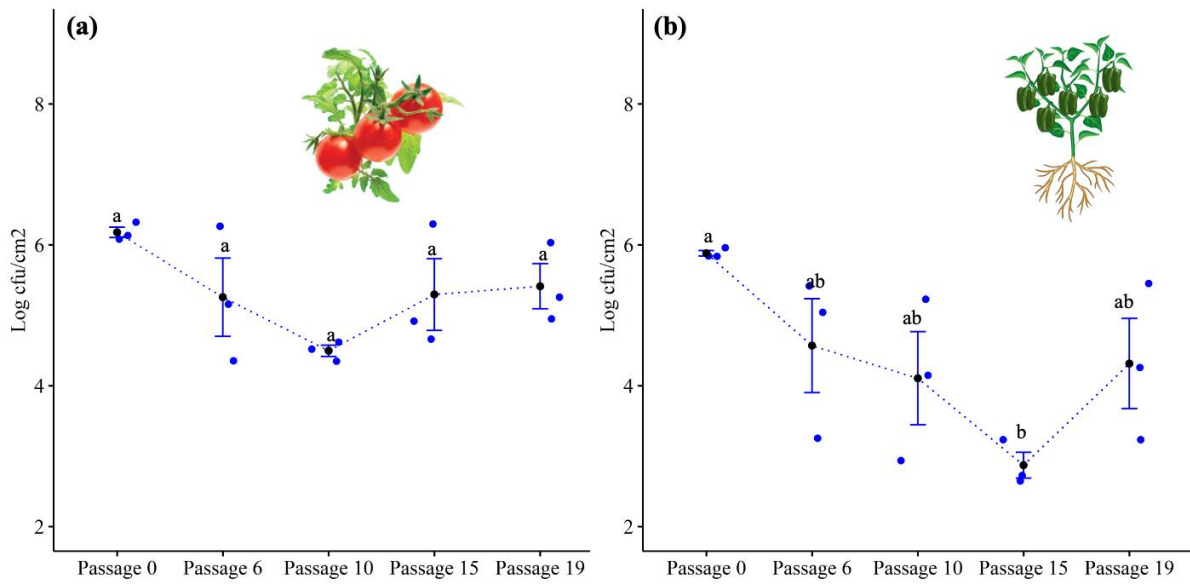
Supplementary figure 4-17: Changes of the bacterial population growth of Xp4B pools taken from the passages 0, 6, 10, 15 and 19. (a) passaged on tomato plants (cv. FL47) and (b) passaged on pepper plants (cv. ECW). Four- to five-week-old pepper and tomato plants were infiltrated with $\sim 1 \times 10^5$ cfu/ml of bacterial pools. Strains were evaluated for bacterial population growth, 6 days after inoculation on antibiotic (nalidixic) amended media. A one-way ANOVA was applied for the statistical analysis and treatments with different letters are significantly different according to the Tukey's test of least significant difference ($P < 0.05$).



Supplementary figure 4-18: Changes of the Xp4B population growth when passaged together with Xe85.10. Xp4B pools taken from the passages 0, 6, 10, 15 and 19. (a) passaged on tomato plants (cv. FL47) and (b) passaged on pepper plants (cv. ECW). Four- to five-week-old pepper and tomato plants were infiltrated with $\sim 1 \times 10^5$ cfu/ml of bacterial pools. Strains were evaluated for bacterial population growth, 6 days after inoculation on antibiotic (nalidixic) amended media. A one-way ANOVA was applied for the statistical analysis and treatments with different letters are significantly different according to the Tukey's test of least significant difference ($P < 0.05$).



Supplementary figure 4-19: Changes of the bacterial population growth of XpPM1 pools taken from the passages 0, 6, 10, 15 and 19. (a) passaged on tomato plants (cv. FL47) and (b) passaged on pepper plants (cv. ECW). Four- to five-week-old pepper and tomato plants were infiltrated with $\sim 1 \times 10^5$ cfu/ml of bacterial pools. Strains were evaluated for bacterial population growth, 6 days after inoculation on antibiotic (kanamycin) amended media. A one-way ANOVA was applied for the statistical analysis and treatments with different letters are significantly different according to the Tukey's test of least significant difference ($P < 0.05$).



Supplementary figure 4-20: Changes of the XpPM1 population growth when passaged together with Xe75.3. XpPM1 pools taken from the passages 0, 6, 10, 15 and 19. (a) passaged on tomato plants (cv. FL47) and (b) passaged on pepper plants (cv. ECW). Four- to five-week-old pepper and tomato plants were infiltrated with $\sim 1 \times 10^5$ cfu/ml of bacterial pools. Strains were evaluated for bacterial population growth, 6 days after inoculation on antibiotic (kanamycin) amended media. A one-way ANOVA was applied for the statistical analysis and treatments with different letters are significantly different according to the Tukey's test of least significant difference ($P < 0.05$).

5. CHAPTER FIVE

Summary and Future Directions

Plant pathogenic bacteria belong to the genus *Xanthomonas* can cause diseases in many economically important crop plants throughout the world. Comparative analyses of sequenced genomes from many *Xanthomonas* species have identified a large number of potential adaptation mechanisms. Among these strategies, bacterial secretion systems have been widely discussed for their role in facilitating successful adaptation of the bacteria to its host environment.

In this dissertation, we studied the recently identified type VI secretion system for its role in crucial points of the *Xanthomonas* life cycle using bacterial leaf spot causing pathogen, *Xanthomonas perforans* as our model system and was discussed as the first objective. Findings from this study, highlighted the contribution of functional T6SS-i3*, *tssM* gene towards early events of epiphytic colonization and adaptation in response to epiphytic stress of *Xanthomonas perforans* life cycle. Even though there are previous literature, that have identified the upregulation of the T6 clusters in foliar pathogens upon establishing as epiphytes, this is the first study that provides evidence for the importance of the T6SS-i3*, *tssM* in this this crucial life stage.

Since two T6SS clusters (T6SS-i3* and T6SS-i3***) are present in the *Xanthomonas perforans*, one can hypothesize the mutation in the T6SS-i3*, *tssM*, being complemented by the T6SS-i3***, *tssM* gene. To understand the possibility of this trans-complementation, western-blot technique can be followed to confirm the aborted Hcp effector secretion, due to the T6SS-i3*, *tssM* gene mutation. To recognize if both T6SS clusters are functional in *X. perforans*, qRT-PCR assay can be performed under *in vitro* conditions where upregulation of the T6SS-i3*, *tssM* was previously observed. Furthermore, these phenotypic variations observed in the *X. perforans* upon the mutation of the T6SS-i3*, *tssM* gene, can also be

independent of T6SS. RNA-Seq assay can be performed to understand the regulation among T6SS/*tssM* gene with other bacterial systems. Enhanced epiphytic survival by the *X. perforans* wild-type strain compared to the *tssM* mutation, was partially explained in this study by the osmoadaptation exhibited by the wild-type strain. We can also hypothesize that the factors such as bacterial swimming motility, EPS production, biofilm formation are contributing to the epiphytic survival of the pathogen, yet further experiments on these aspects will be able support this hypothesis. Experiments designed to determine the role of T6SS in manipulating the resident microbiota, will be further useful in deriving conclusions about the function of the T6SS/*tssM* in epiphytic survival. Due to the prolonged incubation period observed by the wild-type strain we can hypothesize a temporal downregulation of the T3SS upon initiation of the epiphytic colonization of the pathogen on the leaf surface, facilitated by the upregulation of the T6SS. To further test on this hypothesis, *in planta* RNA-seq assay can be performed where, leaf samples need to be collected at initial time points as early as 3 hours post inoculation (hypothesized activation of the T6SS) to possibly up to 96 hours post inoculation (symptom development by the wild-type) to understand the temporal regulation at each stage of leaf colonization by this pathogen.

As the second objective, when a comparative genomic analysis was conducted using 1577 *Xanthomonas* genomes, we were able to identify the evolutionary patterns and distribution of the T6 clusters across the genus *Xanthomonas*. Our findings revealed a possible acquisition of the T6SS by group 2 *Xanthomonas* spp. through an ancient horizontal gene transfer event followed by subsequent losses of the clusters in some of the *Xanthomonas* spp.. This knowledge on distribution patterns of the T6 clusters with regards to their evolutionary backgrounds is indicating possible role of T6SS during niche adaptation onto various hosts. Additionally, our findings of T6SS-dependent effectors that are not limited to toxins, but rather

an adaptation to the host environment, further support the findings from the first objectives, where we identified the bacterial utilization of T6SS was beyond pathogenicity.

Future experiments in characterizing these predicted T6SS effectors will provide insight into the T6 mediated bacterial adaptation strategies in different groups of *Xanthomonas*. Identification of the TonB-dependent receptor as a T6SS effector in several *X. axonopodis* spp., was an interesting finding in this study. Since a role of a TonB-dependent receptor, as a T6SS effector can't be fully explained, a western-blot assay would be able to identify if this protein is getting secreted into the supernatant. Further studies can also be conducted on TonB-dependent receptor mediated survival of *X. perforans* in nutrient limiting conditions using the wild-type and the *tssM* mutant strains generated in the previous objective. Furthermore, identification of the Jacalin-like lectin domain/phosphodiesterase domain as a T6SS effector is indicative of T6SS mediated camouflage of the plant immune receptors. Since callose deposition, is a known marker for plant defense responses, to follow up on the above hypothesis, callose deposits staining assay followed by UV fluorescence microscopy, can be conducted.

As the third objective of the dissertation, experimental evolution assay was conducted using BLS causing *Xanthomonas perforans* as a model system. This study was able to identify the host expansion of Xp4B when continuously passaged on resistant host, by evading the *avrBsT* mediated recognition by pepper cv. ECW with *Bst* resistance locus after 6 passages. Findings of this study also emphasize the importance of preventing the repeated infection of Xp strains in both tomato and pepper plants, due to the possibility of the emergence of more virulent or novel pathogenic races. Analyzing the genome sequences to measure genetic differentiation due to continuous passaging, will provide useful information regarding the adaptation strategies of this pathogen when repeatedly exposed to host and non-host environments.

In this experimental evolution study, since infiltration inoculation was performed to introduce strains in each round of passaging, variations arise in the population are indicative of adaptation strategies acquired during the endophytic colonization stage. When designing future experimental evolution studies using the dip/spray inoculation method to introduce the pathogens to the leaf surface, will facilitate the epiphytic colonization of the pathogens in each round of passaging. Furthermore, extending the time period pathogen spends *in planta* during a single passage will also be beneficial in understanding the variations arise in a pathogen population during the epiphytic, endophytic and also dissemination stage of the pathogen life cycle. In this current experimental evolution study, we collected bacterial pools after growing them in the nutrient agar medium to prepare the inoculum for the next round of passaging, as well as when performing pathogenicity assays with selected passages. When selecting pool populations, there is an incline toward continuous selection of traits that are over-represented in the population, hence low frequency traits can be undetected. In future experiments, along with pool population, selected single colonies should also be used to conduct population studies, as well as in DNA extraction.

With the observation of objectives 1 and 2 we were able to understand the bacterial utilization of a secretion system to prolong asymptomatic colonization while outcompeting the adverse conditions in the leaf surface. This ability of pathogen to prolong its successful colonization in the crop plants is emphasizing the importance of advancing disease detection methods utilized in the transplant house conditions, prior to the distribution of seedlings to the field conditions to prevent disease outbreaks. Findings from the experimental evolution study is suggestive of possibility of the emergence of *X. perforans* as a threat to the pepper production, thus indicates the importance of preventing the continuous re-introduction of these pathogens to susceptible as well as resistant hosts.